



"Novel paths from special functions to scattering amplitudes"

Marzucca, Robin

ABSTRACT

In this thesis we are investigating the mathematical dependence of scattering amplitudes on kinematical invariants. In particular, we are analyzing the underlying geometries of scattering amplitudes in order to predict the resulting function space. We then use this knowledge of the function space to find suitable, more efficient ways to perform the computation of scattering amplitudes. First, we consider the forward-scattering limit of amplitudes in N=4 supersymmetric Yang-Mills theory (SYM), where scattering amplitudes can be written as linear combinations of building blocks that can be expressed in terms of single-valued multiple polylogarithms. Further, we introduce a novel mathematical formalism for the computation of these building blocks exploiting their single-valuedness that allows us to compute scattering amplitudes very efficiently. Finally, we find relations among building blocks for different numbers of external particles, generalizing the factorization of scattering amplitudes...

CITE THIS VERSION

Marzucca, Robin. *Novel paths from special functions to scattering amplitudes*. Prom. : Duhr, Claude <http://hdl.handle.net/2078.1/222558>

Le dépôt institutionnel DIAL est destiné au dépôt et à la diffusion de documents scientifiques émanant des membres de l'UCLouvain. Toute utilisation de ce document à des fins lucratives ou commerciales est strictement interdite. L'utilisateur s'engage à respecter les droits d'auteur liés à ce document, principalement le droit à l'intégrité de l'œuvre et le droit à la paternité. La politique complète de copyright est disponible sur la page [Copyright policy](#)

DIAL is an institutional repository for the deposit and dissemination of scientific documents from UCLouvain members. Usage of this document for profit or commercial purposes is strictly prohibited. User agrees to respect copyright about this document, mainly text integrity and source mention. Full content of copyright policy is available at [Copyright policy](#)



Institut de recherche
en mathématique et physique

Novel Paths From Special Functions to Scattering Amplitudes

Doctoral dissertation presented by

ROBIN MARZUCCA

in fulfilment of the requirement for the degree of Doctor of Sciences.

Thesis Committee

Prof. C. DUHR (<i>Advisor</i>)	CERN/UCLouvain
Prof. J. GOVAERTS (<i>President</i>)	UCLouvain
Prof. V. DEL DUCA	ETH Zürich
Prof. M. GRAN	UCLouvain
Prof. F. MALTONI	UCLouvain
Prof. O. SCHLOTTERER	Uppsala University

2019

Contents

1	Background	11
1.1	Scattering Amplitudes	11
1.2	Feynman Integrals	13
1.3	Gauge Theories	15
2	Special Functions and Relations	27
2.1	Iterated Integrals	28
2.2	Multiple Polylogarithms	30
2.3	Elliptic Multiple Polylogarithms	43
2.4	Iterated Integrals of Modular Forms	52
3	The Multi-Regge Limit of Planar $\mathcal{N} = 4$ SYM	61
3.1	Multi-Regge-Kinematics	63
3.2	The Ratio \mathcal{R}_N at Finite Coupling	68
3.3	The Ratio \mathcal{R}_N at Weak Coupling	70
3.4	The Convolution-Formalism for MRK Amplitudes	74
3.5	The Structure of Scattering Amplitudes	84

4	Transcendentality Properties of the BFKL Ladder	87
4.1	The BFKL Equation	88
4.2	The BFKL ladder at leading logarithmic accuracy	91
4.3	The BFKL ladder at next-to-leading logarithmic accuracy	92
4.4	Analytic results for the BFKL ladder at NLLA in QCD	98
4.5	Transcendental weight properties of the BFKL ladder at NLLA	102
5	The Banana Integral	109
5.1	Integral Families and How to Compute Them	110
5.2	The Banana Graph	119
5.3	The Equal-Mass Banana Graph and Modular Forms for $\Gamma_1(6)$	124
	Conclusion and Outlook	131
	Acknowledgements	135
	Appendices	137
A	De Rham Periods and Symbols	139
B	MRK and the moduli space $\mathfrak{M}_{0,N-2}$	143
C	The BFKL Building Blocks	147
D	Soft Limits and the Contour of Integration	149
E	Symmetries and Soft Limits of Perturbative Coefficients	151
F	Deforming the Contour of Integration	155
G	Proof of the Factorisation Theorem	159
G.1	Proof of the Factorization Theorem	159
H	The Banana Integral in Terms of eMPLs	169

Introduction

The field of physics is one of the oldest academic fields in the history of research. Already in ancient Greek times, physicists have aimed to explain the inner workings of nature itself and to understand the reasons behind the world they observed. Since then a lot of progress has been made and the field has grown to extents where there are hundreds of fields of research aiming to explain phenomena at various frontiers of our knowledge that make up the entirety of physics in the modern age. In the course of history it has become apparent that mathematics and physics are deeply intertwined, and the combined efforts of mathematicians and physicists have sparked a golden age of progress in the research of the universe and its fundamental laws. Physical processes can naturally be described in the language of mathematics and the developments in the fields of mathematics have led to advancement in the fields of physics. Conversely, observations of nature and mathematical descriptions of processes therein have shone new lights on mathematical research and have contributed to the advancements in mathematics.

In this thesis, we will use this symbiosis between these two disciplines in the field of particle physics. Already in early Greek times some philosophers believed that all matter was made up of small, 'uncuttable' particles, the atoms. While the idea was purely philosophical at the time, it is common knowledge today that these Greek philosophers were (partly) right. While we, and all things around us, are indeed made of atoms, they are not 'uncuttable' but are themselves made up of smaller particles. These smallest (elementary) particles and their behaviour are the very matter of interest of particle physics. In order to learn about the fundamental laws underlying their interactions we try to create environments in which two single particles can interact with as little interference from the vast amounts of particles around them as possible.

This is usually done by accelerating elementary particles to very high energies, shooting them at one another and measuring the resulting particles. The strongest such experiment is currently being conducted at the large hadron collider (LHC), where protons are being accelerated to up to 7 TeV before they take part in a collision with another proton. Due to the high energies of the particles involved in the collision it is possible to observe very heavy and equally short-lived particles that we cannot otherwise observe in nature. Mathematically, these interactions are expressed in terms of so-called scattering amplitudes. Scattering amplitudes encode the probability of a set of particles in a given quantum state to evolve into another defined quantum state and are often represented in the form of graphs with several external lines that are related to the prepared and measured particles (c.f. fig. 1).

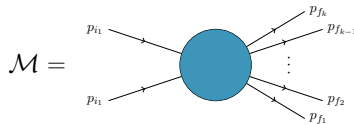


Figure 1: Scattering amplitude for the collision of two particles with momenta p_{i_1} and p_{i_2} decaying into particles with momenta $p_{f_1} \dots p_{f_k}$.

While the external lines relate to physical particles, and hence to the experimental side of particles physics, the blob in the center connecting the external lines represent the scattering event, i.e. the interactions among the external particles and, in a way, the theory side of particle physics. The properties of particles and the way they interact are studied by assuming a set of 'rules', computing a scattering amplitude according to these rules and comparing the result with the outcome of the experiment. If the set of rules represents the laws of nature then the experimental measurement and the theoretical prediction will agree to arbitrary accuracies. The set of rules underlying these computations corresponds to a mathematical model of the physical theory under consideration and consists of a set of particles that are assumed to take part in the interaction as well as the specific way each of these particles interacts with the others. The theory that contains all particles that have, to date, been observed directly as well as their interactions is called the *standard model of particle physics*.

So far the standard model has been an enormous success and even after years of experimental measurements no significant discrepancy between the predictions from computations assuming the standard model and experimental observations has been registered. From astronomical experiments, however, it is clear

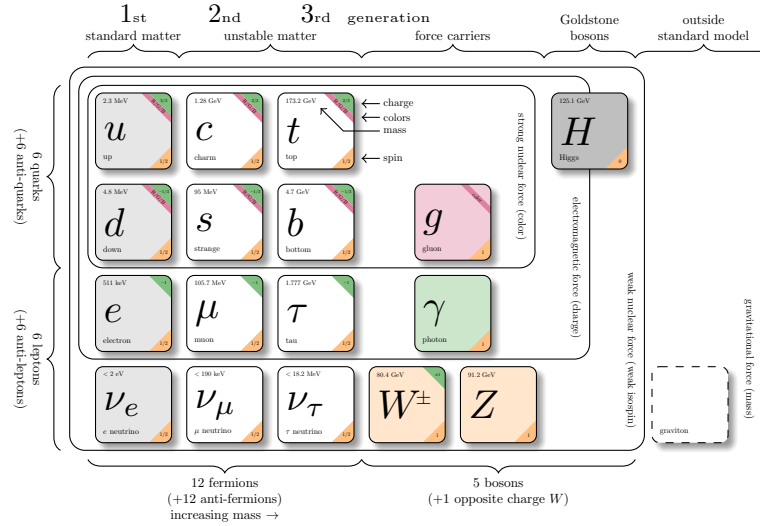


Figure 2: The standard model of particle physics. [Carsten Burgard]

that the standard model cannot be the final answer. There, the gravitational effects of large masses have been observed without the presence of visible matter made out of particles in the standard model. This puts us in a conundrum: The standard model appears to describe the laws of nature to such a high accuracy that we have not been able to observe any significant discrepancies while also knowing that it can not capture the whole picture of particle physics. The only way out of this conundrum seems to be to increase the accuracy in our measurements and our theoretical predictions so that we will hopefully be able to find a mismatch between the two. At the moment, theoretical predictions and experimental measurements are in agreement with one another and hence it will not be enough to increase the accuracy of only one of them. While the LHC continues to collect more and more data, thereby reducing statistic uncertainties, reducing theoretical uncertainties is achieved by performing more and more complicated calculations. In general these calculations are very hard and cannot be performed exactly. Instead, scattering amplitudes are expanded in the *coupling constants*, (small) parameters in the model of the theory that encode the strength of interactions. If the coupling constants are small enough, the first few terms of this *perturbative* expansion will describe the amplitude very well.

State of the art calculations of scattering amplitudes in quantum field theory can often take years and the complexity of the problem scales factorially with the perturbative order. It is therefore clear that we can not simply brute-force these computations. Instead we have to develop new mathematical tools to perform them. Many such tools to reduce the complexity of computations have been established over the last decade and are considered common praxis today. Thanks to these, we have been able to push the perturbative order at which many scattering amplitudes can be computed, we did however also encounter scattering amplitudes with more and more complicated functional dependences. Usually, these functional dependences are given in terms of integrals and it is desirable to solve the integral analytically in terms of functions that can be evaluated efficiently. As the integrands of these integrals get more and more complicated with each perturbative order, so do the functions they evaluate to and many integrals have been encountered to date that we have not been able to solve. It is therefore essential to study the geometry described by the integrand and to find the space of functions associated with integrals over these geometries. In this work we will demonstrate how a good knowledge of the function space and the algebraic properties of these functions can facilitate the computation of scattering amplitudes.

This thesis is structured as follows. In chapter 1, we will introduce the notion of scattering amplitudes. We will show how they depend on the theory under consideration and how they can be computed in terms of Feynman integrals. Finally, we will introduce the theories considered in this work and give the basic structure of scattering amplitudes in these theories. In chapter 2 we will give a detailed review of the function spaces relevant for this work. We will introduce three classes of iterated integrals, multiple polylogarithms, elliptic multiple polylogarithms and iterated integrals of modular forms. We also review some very useful algebraic properties of these functions as well as special linear combinations and relations among them. In chapter 3 we will consider scattering amplitudes in the high-energy limit of $\mathcal{N} = 4$ SYM. We will define the multi-Regge limit and give an all-order description of scattering amplitudes in this limit in an auxiliary space. We show how to use this description of scattering amplitudes and the properties of the function space to define a novel way to perform computations in this kinematical limit. In chapter 4 we will extend the algorithm developed in the previous chapter to the computation of scattering amplitudes in generic Yang-Mills theories. We give a similar description of scattering amplitudes in the high-energy limit in an auxiliary space and use our mathematical framework to compute scattering amplitudes. We then analyse the transcendentality properties of the results and find conditions for a theory to be maximally transcendental. In chapter 5 we consider a class of Feynman

integrals associated to the banana graph and show that it can be written in terms of the same functions as a similar integral that had already been computed. We then use this knowledge to compute solutions for the whole integral family in terms of these functions.

This work is based on the publications [1–6],

- V. Del Duca, S. Druc, J. Drummond, C. Duhr, F. Dulat, R. Marzucca, G. Papathanasiou, and B. Verbeek, *Multi-Regge kinematics and the moduli space of Riemann spheres with marked points*, JHEP 08 (2016) 152,
- V. Del Duca, C. Duhr, R. Marzucca, and B. Verbeek, *The analytic structure and the transcendental weight of the BFKL ladder at NLL accuracy*, JHEP 10 (2017) 001,
- V. Del Duca, S. Druc, J. Drummond, C. Duhr, F. Dulat, R. Marzucca, G. Papathanasiou, and B. Verbeek, *The seven-gluon amplitude in multi-Regge kinematics beyond leading logarithmic accuracy*, JHEP 06 (2018) 116,
- R. Marzucca, and B. Verbeek, *The Multi-Regge Limit of the Eight-Particle Amplitude Beyond Leading Logarithmic Accuracy*, JHEP 07 (2019) 039,
- J. Broedel, C. Duhr, F. Dulat, R. Marzucca, B. Penante, and L. Tancredi *An analytic solution for the equal-mass banana graph*, arXiv:1907.03787,
- V. Del Duca, S. Druc, J. Drummond, C. Duhr, F. Dulat, R. Marzucca, G. Papathanasiou, and B. Verbeek, *In preparation*,

as well as the proceedings [7, 8]

- V. Del Duca, S. Druc, J. Drummond, C. Duhr, F. Dulat, R. Marzucca, G. Papathanasiou, and B. Verbeek, *Multi-Loop Amplitudes in the High-Energy Limit in $N = 4$ SYM*, PoS LL2018 (2018) 026,
- V. Del Duca, S. Druc, J. Drummond, C. Duhr, F. Dulat, R. Marzucca, G. Papathanasiou, and B. Verbeek, *Amplitudes in the Multi-Regge Limit of $N = 4$ SYM*, arXiv:1811.10588.

I have provided major contributions to all of the publications listed above. In particular, I have computed and cross-checked all published results with the exception of the five-loop perturbative coefficient in [1] and the four-loop perturbative coefficients in [3]. I have further determined and proved the possible

leading-coefficients of non-MHV amplitudes at leading-logarithmic accuracy in the multi-Regge limit of $\mathcal{N} = 4$ supersymmetric Yang-Mills theory as well as contributed to all other parts of the publications with exception of the proof of factorization in [1] and the computation of the next-to-leading order central emission block.

Chapter 1

Background

1.1 Scattering Amplitudes

In this section we will introduce scattering amplitudes, the central object of many calculations in particle physics. A scattering amplitude encodes the probability of a set of particles $\{\phi_{i_j}\}$ (with certain boundary conditions), called the *initial state* to evolve over time into a second set of particles $\{\phi_{f_j}\}$ (with certain boundary conditions), called the *final state*. The 'rules' by which they behave, i.e. the mathematical model of the theory in consideration, can be described by a Lagrangian \mathcal{L} . More precisely, the Lagrangian contains information on how individual particles propagate through time and space and on how particles interact with each other. A simple example for such a model is given by the Lagrangian

$$\mathcal{L}_{\phi^4} = \frac{1}{2}(\partial_\mu\phi)^2 - \frac{1}{2}m^2\phi^2 - \frac{\lambda}{4!}\phi^4, \quad (1.1)$$

which describes a theory containing only one type of field, ϕ . The dimensionless quantity λ is called the coupling constant and encodes the strength of the corresponding interaction. The Lagrangian can be divided up into two parts, the free part $\mathcal{L}_{\text{free}} = \frac{1}{2}(\partial_\mu\phi)^2 - \frac{1}{2}m^2\phi^2$ and the interacting part $\mathcal{L}_1 = -\frac{\lambda}{4!}\phi^4$. Due to the interacting part of the Lagrangian it is difficult to define the notion of a single particle, as its time evolution will be influenced by other particles around it.

In collider experiments, we want to observe the collision of two particles ϕ_{i_1} and ϕ_{i_2} which in turn result in a measurement of particles $\phi_{f_1} \dots \phi_{f_k}$. Math-

ematically, this is described by the overlap $\langle \phi_{f_1} \dots \phi_{f_k} | \phi_{i_1} \phi_{i_2} \rangle$ of the initial states, prepared by the experiment and the measured final states. As we have mentioned before, it is difficult to define individual particles in an interacting theory. We will therefore define the particles 'in the far past', where they were isolated from other particles and can therefore be defined by the free theory only. We will then evolve that state over time to the point of the collision. This time evolution is given by an infinite-dimensional unitary matrix called the S -Matrix, whose rows and columns correspond to the numbers of particles and their states. It can be computed from the Lagrangian of the theory, and we define

$$\langle \phi_{f_1} \dots \phi_{f_k} | \phi_{i_1} \phi_{i_2} \rangle \equiv {}_{\text{free}} \langle \phi_{f_1} \dots \phi_{f_k} | S | \phi_{i_1} \phi_{i_2} \rangle_{\text{free}} . \quad (1.2)$$

Naturally, there is a possibility that the particles just pass each other without interacting at all. Therefore, the S -matrix can be written as the identity plus a term due to interactions, and we write

$$S = \mathbf{1} + iT . \quad (1.3)$$

The interesting part for us is the interacting part T of the S -matrix, as it allows us to gather information about the interplay of different particles and hence to gather information about the theory. Factoring out overall energy-momentum conservation, we can define the *scattering amplitude* $\mathcal{M}(\phi_{i_1} \phi_{i_2} \rightarrow \phi_{f_1} \dots \phi_{f_k})$ as

$${}_{\text{free}} \langle \phi_{f_1} \dots \phi_{f_k} | iT | \phi_{i_1} \phi_{i_2} \rangle_{\text{free}} = (2\pi)^4 \delta^{(4)} \left(p_{i_1} + p_{i_2} - \sum_{j=1}^k p_{f_j} \right) i\mathcal{M} , \quad (1.4)$$

where p_x is the momentum of particle ϕ_x , and where we have dropped the information on the particles on the right hand side for compactness. Scattering amplitudes are often represented diagrammatically, as can be seen in fig. 1, where the corresponding diagram for the scattering of two (identical) particles into k (identical) particles is shown.

This scattering amplitude encodes the probability of the two initial particles ϕ_{i_1} and ϕ_{i_2} to decay into the the particles $\phi_{f_1} \dots \phi_{f_k}$, and it is related to the measurable *cross section* $\sigma(\phi_{i_1} \phi_{i_2} \rightarrow \phi_{f_1} \dots \phi_{f_k})$ via

$$\sigma(\phi_{i_1} \phi_{i_2} \rightarrow \phi_{f_1} \dots \phi_{f_k}) = \mathcal{N} \int d\Pi_k |\mathcal{M}|^2 , \quad (1.5)$$

where

$$\int d\Pi_k = \left(\prod_{j=1}^k \frac{d^3 p_{f_j}}{(2\pi)^3} \frac{1}{2E_j} \right) (2\pi)^4 \delta^{(4)} \left(p_{i_1} + p_{i_2} - \sum_{j=1}^k p_{f_j} \right) , \quad (1.6)$$

is the phase-space integration over all allowed final state momenta, $E_j = p_{f_j}^0$ is the energy of the particle ϕ_{f_j} and \mathcal{N} is a normalization constant.

Finding efficient ways to compute these scattering amplitudes, both perturbatively and non-perturbatively, remains one of the central aspects of research in particle physics. One of the most popular ways to perform these computations is via Feynman diagrams, which we will introduce in the following section.

1.2 Feynman Integrals

In the previous section we have introduced scattering amplitudes, the central object of interest in quantum field theory computations for collider experiments. We have seen how they relate to the S -Matrix, which in turn can be computed from the Lagrangian of the theory. In this section, we give a more detailed glance into the S -Matrix and introduce a powerful tool for the perturbative computation of scattering amplitudes, Feynman integrals. The proper mathematical derivation of the relations outlined in this section in all its details is a very tedious task and has been covered in most of the standard textbooks for particle physics. We will therefore only motivate and outline these relations and refer the reader to those textbooks for a detailed discussion of these topics.

As we have mentioned in the previous section, the S -Matrix corresponds to the unitary time evolution of the particle states involved in the scattering process to the far past or far future respectively, where they can be described by the free theory. As in quantum mechanics, this time evolution is given by the exponential of the Hamiltonian H of the theory, which in turn can be computed from the Lagrangian \mathcal{L} , and the interacting part T of the S -matrix is due to the interacting part of the Lagrangian \mathcal{L}_I

Let us at this point introduce a graphical notation that will be very useful to express the perturbative expansion of the matrix element (1.2). We will symbolize the propagation of a particle ϕ in space time between a point x and a point y with a line connecting the points x and y . Then a vertex connecting three or more lines symbolises an interaction among the corresponding particles. In this language, the interacting part of the Lagrangian \mathcal{L}_I in (1.1) corresponds to the diagram

$$\mathcal{L}_I \propto \begin{array}{c} \diagup \\ \times \\ \diagdown \end{array}, \quad (1.7)$$

and every vertex appearing in a diagram is proportional to the coupling constant λ . Ultimately the lines connecting to a vertex must either be connected

to another vertex or to 'a point in the far future (past)' corresponding to a free particle in either the initial or the final state. For a given matrix element $\langle \phi_{f_1} \dots \phi_{f_k} | S | \phi_{i_1} \phi_{i_2} \rangle$, the external lines of each contributing diagram must correspond to the particles $\phi_{i_1}, \phi_{i_2}, \phi_{f_1}, \dots, \phi_{f_k}$.

The perturbative expansion of an S -matrix element can then be obtained as the expansion in powers of the coupling constant λ , or, equivalently in terms of our graphical representation, in the number of vertices in our diagrams. Since the number of external lines is fixed for any matrix element, the only way we can add more vertices to our diagrams is by drawing closed loops. Correspondingly, tree diagrams, i.e. diagrams with no closed loops, are called leading order (LO) contributions, those with one loop are called next-to-leading order (NLO) contributions, etc. For the propagation of a particle in space time, for example we find the expansion

$$\text{---} + \lambda \text{---} \bigcirc \text{---} + \lambda^2 \left(\text{---} \bigcirc \text{---} + \dots \right) + \mathcal{O}(\lambda^3), \quad (1.8)$$

where we have made the factors of λ explicit and have ignored other prefactors of the diagrams. As expected, the leading order contribution is the free propagator and all corrections come with additional loops in the diagrams.

The individual diagrams are called *Feynman diagrams* and a numerical value can be associated to each of them. These numerical values are most conveniently computed in momentum space and the prescriptions to connect a diagram to its numerical value are referred to as Feynman rules. Loosely speaking, we associate to each line of the diagram a momentum and impose energy-momentum conservation at each vertex. The momenta of the external lines correspond to the momenta of the external particles, and we associate a non-physical momentum, called loop momentum to each closed loop. A simple example is the scalar one-loop bubble integral depicted in 1.1. Finally, to get

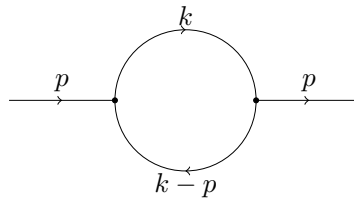


Figure 1.1: The bubble diagram with external momentum p and loop momentum k .

a numerical value, we replace each particle line with the corresponding free

propagator and integrate over all possible configurations of loop momenta. For the bubble integral with two different masses m_i , for example we get

$$\text{---} \bigcirc \text{---} = \int \frac{d^d k}{\pi^{d/2}} \frac{1}{(k^2 - m_1^2)((k-p)^2 - m_2^2)}. \quad (1.9)$$

As we can see in the integration measure, we consider all momenta to be d -dimensional, even though we are interested in scattering amplitudes in four dimensions. The reason for that is that the integrals associated to Feynman graphs do not always converge in four dimensions and need to be regularized. A regularization procedure that has proved to be very effective for the computation of Feynman integrals is the so-called *dimensional regularization*, where we perform all integrals in $d = 4 - 2\epsilon$ dimensions for some small regulator ϵ . Then all Feynman integrals converge and we get a Laurent series in ϵ . Finally, after combining all Feynman diagrams contributing to an observable, all poles in ϵ in the final cross-section must cancel so we can take the limit $\epsilon \rightarrow 0$.

The divergences exhibited by Feynman integrals are usually grouped in one of two sets: Infrared (IR) divergences and ultraviolet (UV) divergences. While the details of these divergences are not essential for this work, it is useful to know the distinction between UV and IR divergences. UV divergences are due to the loop momenta becoming very large. In this case, a possible divergence of the integral can easily be identified by simple power-counting of loop momenta in the numerator and denominator of the integrand. IR divergences on the other hand appear for finite loop momenta and are due to massless propagators $\frac{1}{q^2}$ in the integrand.

We have introduced the notion of Feynman integrals and have seen how they are relevant for the computation of scattering amplitudes in quantum field theory, the only theory we have seen so far, however, was ϕ^4 theory. This theory, while being very simple and well-suited to introduce scattering amplitudes and Feynman integrals, is not realized in nature. In the next section we will turn to theories that are more relevant for the description of particle scattering in nature.

1.3 Gauge Theories

So far we have seen how to mathematically describe the scattering of two particles into other particles of the theory and how to compute the associated probability amplitudes. In this section we will introduce gauge theories, a class of theories that has been very successful in describing the scattering of real

particles. The standard model of particle physics, which is widely accepted to be the current state of the art theory to describe the interactions of elementary particles, is a unification of three theories—electro-magnetism, electro-weak theory and the theory of strong interactions—each of which in itself can be described as a gauge theory. A gauge theory is a theory whose Lagrangian is invariant under certain (local) transformations of the fields. These so-called symmetries of the Lagrangian are often described by a corresponding Lie group. Mathematically, these symmetries are implemented through the appearance of an additional field called the *gauge field* which can be interpreted as mediators of the corresponding force of nature (e.g. the strong force).

In this thesis, we will study the gauge theory described by the special unitary group $SU(N_C)$ for some $N_C \in \mathbb{N}$. These theories are commonly known as Yang-Mills theories and for $N_C = 3$ we find the theory of strong interactions. The reasons for studying this theory over for example $U(1)$ theory describing electromagnetism or $U(1) \times SU(2)$ describing electro-weak interactions are twofold. The most powerful experimental tool to analyse the scattering of elementary particles today is the LHC and the reactions taking place in these collisions are dominated by strong interactions. On the other hand, at energy levels achieved in collider experiments, the coupling constant of strong interactions is much larger than the coupling constants of other interactions. In order to achieve a certain accuracy in our predictions, we need to compute the perturbative expansion of scattering processes involving strong interactions to much higher orders than in other theories. Accordingly, the computations necessary to achieve the same accuracy will be much more involved.

1.3.1 Yang-Mills Theory

Quantum chromodynamics, the theory of strong interactions, describes the interactions of quarks and gluons that make up all hadrons. As such, QCD is at the heart of the description of scattering processes at the LHC. Mathematically, QCD is described by an $SU(3)$ invariant Lagrangian for the quarks ψ and gluons A_μ . Let us now consider the slightly more general Yang-Mills theory, defined by the $SU(N_C)$ invariant Lagrangian

$$\mathcal{L}_{\text{YM}} = \bar{\psi}(i\gamma^\mu D_\mu - m)\psi - \frac{1}{4}G_a^{\mu\nu}G_{\mu\nu}^a, \quad (1.10)$$

where

$$D_\mu = \partial_\mu - igA_\mu \quad (1.11)$$

is the gauge covariant derivative, g is the coupling constant,

$$G_{\mu\nu}^a = \partial_\mu A_\nu^a - \partial_\nu A_\mu^a + g f^{abc} A_\mu^b A_\nu^c \quad (1.12)$$

is the field-strength tensor of the gauge boson A_μ^a , usually referred to as gluon, and the f^{abc} are the structure constants of $SU(N_C)$. The index a of the gluon is its color-index and A_μ^a denotes the component multiplying the corresponding $SU(N_C)$ generator T^a ,

$$A_\mu = A_\mu^a T^a. \quad (1.13)$$

$SU(N_C)$ is generated by $N_C^2 - 1$ generators and we normalize them such that

$$\text{Tr}(T^a T^b) = \frac{1}{2} \delta_{ab}. \quad (1.14)$$

The structure constants of the theory are given by the commutators of the generators and we have

$$[T^a, T^b] = i f^{abc} T^c. \quad (1.15)$$

The Lagrangian (1.10) is invariant under the symmetry transformations

$$\psi \rightarrow U(x)\psi \equiv e^{i\theta^a(x)T^a} \psi \quad (1.16)$$

$$A_\mu \rightarrow U(x)A_\mu U^\dagger(x) + \frac{i}{g}U(x)\partial_\mu U^\dagger(x). \quad (1.17)$$

Now that we know how to compute scattering amplitudes perturbatively and have introduced Yang-Mills theory, we could in principle start calculating scattering amplitudes. It turns out, however, that this is still a very difficult endeavour and that it can take very long to improve theoretical accuracies of scattering amplitudes by brute-forcing the computations. While numerous mathematical tricks for the computation of scattering amplitudes have been developed, it is often helpful to slightly simplify the problem at first and then try and generalize the solution.

1.3.2 $\mathcal{N} = 4$ Supersymmetric Yang-Mills Theory

In this section we will give a brief introduction to $\mathcal{N} = 4$ supersymmetric Yang-Mills theory (SYM) with a focus on the planar limit. Supersymmetry is a global symmetry that assigns to every particle another particle, often referred to as *superpartner*, with a spin differing by $\pm 1/2$. Starting from the highest spin particle in our theory, the gauge boson, we can act, in turn, with up to

four different supersymmetry generators, at which point we would get a particle with spin -1 . Acting with any more than four supersymmetry generators would necessarily require us to consider particles with spins > 1 , and hence $\mathcal{N} = 4$ is the largest number of supersymmetry generators we can add to our gauge theory. Since the particles of all allowed spins in our theory are generated as superpartners of the gauge boson, the particle content of $\mathcal{N} = 4$ SYM is completely constrained by supersymmetry. Starting from the gauge boson we get four different fermions by acting with the four different supergenerators. The square of a supersymmetry generator vanishes and hence we get six distinct pairs of generators corresponding to the six scalars of the theory. The remaining particles with negative spins correspond to the chiral partners of the gauge boson and the fermions, and hence we have one gauge boson, four fermions and six scalar particles. Since all particles of the theory are derived from the gauge boson by the action of the supersymmetry generators, their interactions are equally constrained and share the same coupling constant g .

Supersymmetric theories are often simpler than unconstrained theories while still sharing some of the desired properties and can therefore constitute interesting toy models to consider. In the case of $\mathcal{N} = 4$ SYM, the degree of symmetry in the theory is especially high and its planar limit is considered a candidate for a quantum field theory in four dimensions that can be solved exactly [9]. One of the symmetries that $\mathcal{N} = 4$ SYM exhibits is conformal symmetry. $\mathcal{N} = 4$ SYM is conformally invariant to all orders in perturbation theory and as such must, among other transformations, be invariant under rescaling of coordinates. This implies that there can be no mass scale in the theory and all particles are therefore massless. It also implies that the β -function vanishes to all orders in perturbation theory [10–12]. Due to the large amount of symmetry that scattering amplitudes have to obey in $\mathcal{N} = 4$ SYM they are substantially easier to compute than those in QCD, which makes $\mathcal{N} = 4$ super Yang-Mills theory a nice testing-ground for new computational techniques. As a candidate for an integrable theory, computations in $\mathcal{N} = 4$ SYM also serve as way-signs for the search of an exact solution to the theory.

Due to the invariance of scattering amplitudes in $\mathcal{N} = 4$ supersymmetric Yang-Mills theory under supersymmetry, we can relate scattering amplitudes involving different particles in their final state. While the scattering amplitude must be invariant under the action of supersymmetry generators, we can also use those generators to change one of the external particles defining the scattering amplitude. It is therefore possible to restrict ourselves to the computation of scattering amplitudes \mathcal{A}_n , involving only n external gluons and no other external particles. The scattering of other particles can then be inferred from these using supersymmetry.

Gluon-scattering amplitudes depend on the helicities $h_i \in \{\pm 1\}$ of the external gluons, their momenta p_i as well as their color structure a_i ,

$$\mathcal{A}_n \equiv \mathcal{A}_n^{h_1 \dots h_n}(p_1, \dots, p_n; a_1, \dots, a_n), \quad (1.18)$$

we will however drop the explicit dependence on either of these quantities when it is not essential to the equation. Another thing we can learn from invariance of scattering amplitudes under supersymmetry is that n -gluon amplitudes vanish if all gluons or all but one of the gluons have the same helicity,

$$\mathcal{A}_n^{+\dots+} = \mathcal{A}_n^{-\dots-} = 0. \quad (1.19)$$

The first non-zero amplitudes, namely those with two flipped helicities are called *maximally helicity violating* (MHV) amplitudes

$$\mathcal{A}_n^{-+\dots+}, \mathcal{A}_n^{+ - \dots +}, \dots \quad (1.20)$$

Amplitudes with three flipped helicities are dubbed next-to-maximally helicity violating (NMHV) and the counting continues accordingly. Those amplitudes where all but two helicities are minus are also called $\overline{\text{MHV}}$ and hence for four and five external gluons all non-vanishing amplitudes are either MHV or $\overline{\text{MHV}}$.

Let us now take a closer look at the color structure of the amplitudes \mathcal{A}_n . Generally, color dependence is encoded in the $SU(N_C)$ generators T^a and the structure constants f^{abc} . Using equations (1.14) and (1.15), we can rewrite all appearances of structure constants by traces of $SU(N_C)$ generators,

$$f^{abc} = -2i \text{Tr}([T^a, T^b]T^c). \quad (1.21)$$

In addition, making the matrix-structure of the generators $T^a \equiv T_{ij}^a$ explicit, all fundamental indices i, j must be contracted, and hence all generators must appear inside a trace. This trace-structure can be simplified using the Fierz identity

$$2T_{ij}^a T_{kl}^a = \delta_{il} \delta_{jk} - \frac{1}{N_C} \delta_{ij} \delta_{kl}, \quad (1.22)$$

and we can use it to eliminate all $SU(N_C)$ generators T^a whose color index a does not correspond to an external gluon. Note that one of the terms in the Fierz identity is suppressed by N_C compared to the other, allowing us to expand the amplitude \mathcal{A}_n in powers of N_C . Doing so, we find that the leading term always only contains a single trace, and we write the ℓ -loop amplitude as

$$\begin{aligned} \mathcal{A}_{h_1 \dots h_n}^{(\ell)}(p_1, \dots, p_n; a_1, \dots, a_n) = \\ N_C^\ell \sum_{\sigma} \text{Tr}[T^{a_{\sigma(1)}} \dots T^{a_{\sigma(n)}}] A_{h_1 \dots h_n}^{(\ell)}(p_1, \dots, p_n) + \mathcal{O}(N_C^{\ell-1}), \end{aligned} \quad (1.23)$$

where the sum runs over all non-cyclic permutations and the *partial amplitudes* $A^{(\ell)}$ depend only on the helicities and the momenta of the external gluons. The Feynman graphs contributing to the leading term in this expansion are all planar graphs, and hence we can formally define the *planar limit* of $\mathcal{N} = 4$ SYM by letting the number of colors N_C go to infinity. More precisely, the planar limit, or *'t Hooft limit* [13], is defined by

$$N_C \rightarrow \infty \qquad g \rightarrow 0 \qquad a \equiv \frac{N_C g^2}{8\pi^2} = \text{finite}. \quad (1.24)$$

In this limit, the trace in eq. (1.23) induces a natural ordering of the external momenta p_i and we call those amplitudes *color ordered*. We can make overall energy-momentum conservation of the amplitude manifest by introducing *dual coordinates* x_i through the relation

$$x_i - x_{i-1} = p_i. \quad (1.25)$$

If we express the amplitude A_n in terms of these coordinates, we will find that its integrand is also conformally invariant in the x_i . In fact, planar $\mathcal{N} = 4$ super Yang-Mills theory is *dual-conformally invariant* on the integrand level [14–19], i.e. it is conformally invariant in the dual coordinates x_i as well as in the momenta p_i , and dual conformal invariance is only broken by the IR structure of the integrated amplitude. Luckily, the infrared structure of scattering amplitudes in planar $\mathcal{N} = 4$ SYM can be predicted at every order in perturbation theory and it is possible to rewrite the amplitude in terms of an IR divergent bit and a finite bit which preserves dual conformal invariance at the integral level. More precisely, it is possible to factor out the IR structure of the amplitude to all orders in perturbation theory and we write [20, 21]

$$A_n = A_n^{(\text{BDS})} \mathcal{R}_n. \quad (1.26)$$

The so-called BDS-Ansatz $A_n^{(\text{BDS})}$, due to Bern, Dixon and Smirnov [21], captures the IR structure of the amplitude and is determined to all orders in perturbation theory by the corresponding tree-level and one-loop amplitudes, and the term $\mathcal{R}_n \equiv A_n/A_n^{(\text{BDS})}$ is finite and dual conformally invariant. The ratio \mathcal{R}_n is closely related to the *remainder function* R_n defined for MHV amplitudes, and we have

$$\mathcal{R}_n^{\text{MHV}} = e^{R_n}. \quad (1.27)$$

For four and five external particles, the BDS ansatz captures the entire amplitude, $A_n = A_n^{(\text{BDS})}$ for $n = 4, 5$, and hence the ratio \mathcal{R}_n is trivial. In the following, we will consider the BDS-Ansatz to be known for all considered cases

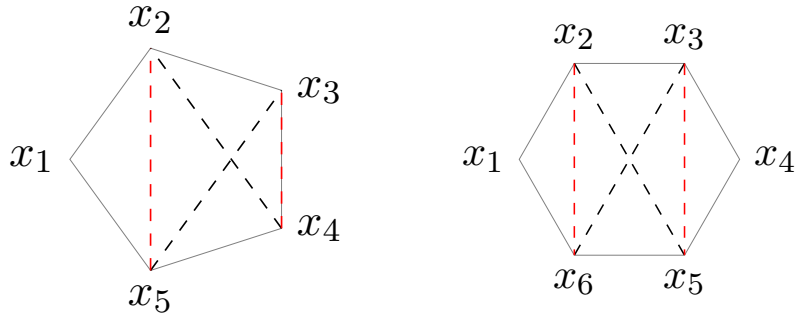


Figure 1.2: Figures displaying two cross ratios in the five- and six-particle case. The dashed lines represent the factors x_{ij}^2 in the numerator and denominator. Note that for five particles, one of the dashed lines will always correspond to an external line.

and focus on the computation of the remainder function. In the next section we will review some mathematical properties of the remainder function and its functional dependence.

The Functional Dependence of \mathcal{R}_n

As we have mentioned before, the ratio \mathcal{R} is finite and dual-conformally invariant. As a consequence, its kinematical dependence can be completely expressed in terms of the dual-conformally invariant *cross ratios*

$$U_{ijkl} = \frac{x_{ij}^2 x_{kl}^2}{x_{ik}^2 x_{jl}^2}, \quad (1.28)$$

where $x_{ij} = x_i - x_j$. Since the difference of two adjacent dual coordinates corresponds to an external momentum (c.f. eq. (1.25)), and since all external momenta are lightlike, we can only define non-trivial cross-ratios if we have six or more external momenta. Indeed, this matches the observation that the ratio \mathcal{R} is trivial for four- and five-point amplitudes and hence they are completely described by the BDS-Ansatz.

In four dimensions, and for n external gluons, only $3n - 15$ of the U_{ijkl} are independent and a possible basis of cross ratios is given by [22, 23]

$$\begin{aligned} u_{1i} &= \frac{x_{i+1,i+5}^2 x_{i+2,i+4}^2}{x_{i+1,i+4}^2 x_{i+2,i+5}^2}, & u_{2i} &= \frac{x_{N,i+3}^2 x_{1,i+2}^2}{x_{N,i+2}^2 x_{1,i+3}^2}, \\ u_{3i} &= \frac{x_{1,i+4}^2 x_{2,i+3}^2}{x_{1,i+3}^2 x_{2,i+4}^2}, \end{aligned} \quad (1.29)$$

for $i = 1, \dots, N - 5$.

Let us now make explicit that all external momenta p_i are lightlike. We can express any momentum p^μ in terms of 2×2 matrices through the relation

$$p_{a\dot{a}} = \sigma_{a\dot{a}}^\mu p_\mu, \quad (1.30)$$

where σ^i , $1 \leq i \leq 3$ are the Pauli matrices and $\sigma^0 = \mathbb{1}$ is the identity matrix. Then the square of a vector p corresponds to the determinant of the respective matrix,

$$p^2 = \det(p_{a\dot{a}}). \quad (1.31)$$

We see that the matrix corresponding to a lightlike momentum p must have a vanishing determinant and hence it is degenerate. This allows us to write it as a product

$$p_{a\dot{a}} = \lambda_a \bar{\lambda}_{\dot{a}}, \quad (1.32)$$

where $\lambda_a, \bar{\lambda}_{\dot{a}}$ are two spinors, which are defined up to a rescaling $\lambda_a \mapsto t\lambda_a$ and $\bar{\lambda}_{\dot{a}} \mapsto t^{-1}\bar{\lambda}_{\dot{a}}$.

Let us now introduce the so-called *momentum twistors* [24], which allow us to restrict the functional dependence of the remainder function even further. Since the external momenta p_i are null, we can express them in terms of twistor variables Z_i as¹

$$Z_i^A = (\lambda_{i+1}^\alpha, \mu_{i+1}^{\dot{\alpha}}), \quad (1.33)$$

with $\mu_i^{\dot{\alpha}}$ and $\lambda_{i\alpha}$ fulfilling the incidence relation

$$\mu_i^{\dot{\alpha}} = x_i^{\alpha\dot{\alpha}} \lambda_{i\alpha}. \quad (1.34)$$

Since λ_a is defined up to a scaling, and since the incidence relation (1.34) is homogenous, the momentum twistors Z_i describe equivalence classes under

¹The the shift in the indices in the definition of the twistors Z_i renders common but competing conventions consistent with each other.

scalar multiplication that are represented in complex projective space \mathbb{CP}^3 . The complex projective space \mathbb{CP}^n can be thought of as the set of all lines in \mathbb{C}^{n+1} passing through the origin. Let us introduce the *twistor four-brackets* $\langle ijkl \rangle$ as the determinant of the 4×4 matrix formed out of the corresponding twistors,

$$\langle ijkl \rangle = \det(Z_i Z_j Z_k Z_l) \equiv \epsilon_{IJKL} Z_i^I Z_j^J Z_k^K Z_l^L, \quad (1.35)$$

where ϵ_{IJKL} denotes the Levi-Civita tensor. Then we can express the kinematical invariants x_{ij}^2 in terms of momentum twistors as

$$x_{ij}^2 = \frac{\langle i-1 i j-1 j \rangle}{\langle i-1 i I \rangle \langle j-1 j I \rangle}, \quad (1.36)$$

where I denotes the so-called *infinity twistor* which corresponds to a null cone at infinity. The infinity twistor breaks conformal invariance, this is however not a problem because the squared differences x_{ij}^2 are not dual conformally invariant either. The cross ratios (1.28) on the other hand are dual conformally invariant and must be independent of the infinity twistor. Indeed, we have

$$U_{ijkl} = \frac{\langle i-1 i j-1 j \rangle \langle k-1 k l-1 l \rangle}{\langle i-1 i k-1 k \rangle \langle j-1 j l-1 l \rangle}. \quad (1.37)$$

This set-up allows us to express the color-ordered partial amplitudes in planar $\mathcal{N} = 4$ SYM by a configuration of n points in \mathbb{CP}^3 [25]. The set of all such configurations, $\text{Conf}_n(\mathbb{CP}^3)$ is closely related to the Grassmannian $\text{Gr}(4, n)$, the space of all four-dimensional linear subspaces of \mathbb{C}^n ,

$$\text{Conf}_n(\mathbb{CP}^3) \simeq \text{Gr}(4, n)/(\mathbb{C}^*)^{n-1}, \quad (1.38)$$

and each Grassmannian can naturally be equipped with a *cluster algebra* [26–30]. It is worth studying these cluster algebras because they are related to the singularities of scattering amplitudes in planar $\mathcal{N} = 4$ super Yang-Mills theory [25]. Let us make this more clear by looking at the cluster algebra attached to the Grassmannian $\text{Gr}(4, n)$.

A cluster algebra is a set of different quivers, that can all be constructed from a single initial quiver under the action of an operation called ‘mutation’. A quiver can be represented as a directed graph, and an initial quiver for the Grassmannian $\text{Gr}(4, n)$ is given in fig. 1.3, where the nodes in boxes are called *frozen nodes* and all other nodes are considered *unfrozen nodes* and each node is labelled with so-called Plücker coordinates $\langle ijkl \rangle$. The mutations used to construct the other quivers of the cluster algebra alter both the labels of the nodes as well as the arrows of the graph. From each quiver in the cluster

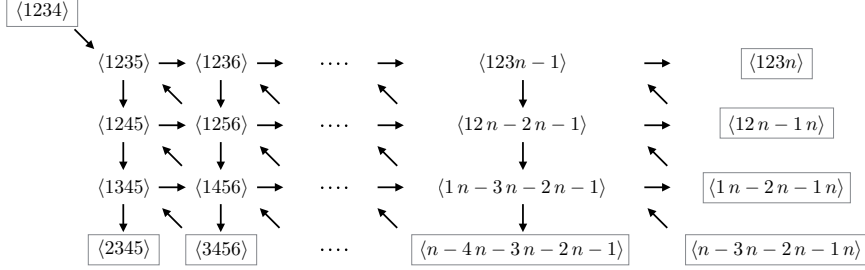


Figure 1.3: The \mathcal{A} -coordinates for the initial quiver for $\text{Gr}(4, n)$ with frozen nodes in boxes.

algebra we can extract so-called \mathcal{X} coordinates [25] and we find for the initial quiver 1.3

$$\begin{aligned}
 \mathcal{X}_{1j} &= \frac{\langle 123j+3 \rangle \langle 12j+4j+5 \rangle}{\langle 123j+5 \rangle \langle 12j+3j+4 \rangle}, \\
 \mathcal{X}_{2j} &= \frac{\langle 123j+4 \rangle \langle 12j+2j+3 \rangle \langle 1j+3j+4j+5 \rangle}{\langle 123j+3 \rangle \langle 12j+4j+5 \rangle \langle 1j+2j+3j+4 \rangle}, \\
 \mathcal{X}_{3j} &= \frac{\langle 12j+3j+4 \rangle \langle 1j+1j+2j+3 \rangle \langle j+2j+3j+4j+5 \rangle}{\langle 12j+2j+3 \rangle \langle 1j+3j+4j+5 \rangle \langle j+1j+2j+3j+4 \rangle}.
 \end{aligned} \tag{1.39}$$

The $3n - 15$ \mathcal{X} -coordinates of any given quiver, including the initial quiver shown above, form a complete set of coordinates for the kinematical dependence of n -gluon amplitudes in $\mathcal{N} = 4$ SYM. The cluster algebras associated to the Grassmannians $\text{Gr}(4, n)$ for $n = 6, 7$ are finite, meaning that there are only finitely many diagrams that can be generated by mutation, while the cluster algebras for $n \geq 8$ are infinite. More precisely, any cluster algebra whose unfrozen nodes, correspond to a Dynkin diagram, possibly after applying a sequence of mutations, is finite.

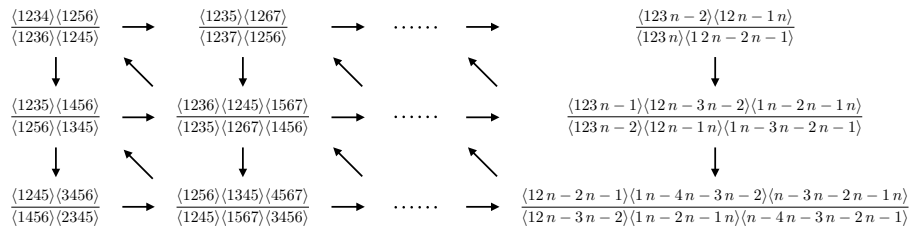


Figure 1.4: The \mathcal{X} -coordinates for the initial quiver for $\text{Gr}(4, n)$.

Chapter 2

Special Functions and Relations

In the previous section we have introduced the notion of scattering amplitudes and have seen how to compute them perturbatively in terms of Feynman integrals. These Feynman integrals are generally still very difficult and are known to give rise to various classes of functions from polylogarithms [31–34], over elliptic generalizations thereof [35–38] to integrals over so-called Calabi-Yau manifolds [39], whose solutions are yet to be fully analysed, and many more classes of functions are expected to appear. Among the mentioned functions, (multiple) polylogarithms are without a doubt the once that have been best understood. It is a reflection of this fact that a lot of progress in the computation of scattering amplitudes has been made in cases where we could write them in terms of (multiple) polylogarithms. In contrast, progress was usually brought to a halt for many years when scattering amplitudes exhibited Feynman integrals evaluating to elliptic generalizations of polylogarithms and few such integrals have been tediously computed. Due to recent developments in the study of iterated integrals over elliptic curves, progress in this area has sped up and more and more Feynman integrals evaluating to iterated elliptic integrals are being solved.

The aim of this thesis is to highlight exactly this connection. We demonstrate how careful analysis of the underlying geometry of the integration as well as good knowledge of the function space of the result can be utilized to efficiently compute scattering amplitudes. Consequently, we will introduce in this chapter various types of iterated integrals as well as special combinations of these functions that are relevant for the scattering amplitudes considered in this thesis. In particular, we are going to consider multiple polylogarithms

(MPLs) [40, 41], elliptic multiple polylogarithms (eMPLs) [42, 43] and iterated integrals of modular forms (IMFs) [44, 45]. Multiple polylogarithms and their underlying algebraic structures have been well studied and understood, and tools for their analytic and numeric treatment are available [46–49]. In the recent years, their elliptic counterparts have gained more and more attention and it has been possible to extend many of the algebraic properties of MPLs to eMPLs [42, 50–52], there are however as of yet no tool-kits for their treatment available. We will start this chapter by reviewing some well-known properties of iterated integrals, which naturally arise during the computation scattering amplitudes by Feynman diagrams.

2.1 Iterated Integrals

In this section we will consider generic (homotopy invariant) iterated integrals of one-forms¹ and review some useful properties that all iterated integrals share. A detailed analysis and proofs can be found in ref. [48]. Let ω_i be differential one-forms defined on some smooth manifold M , $\gamma : [0, 1] \rightarrow M$ denote a path on M and let $\omega_i = f_i dt$, where t parametrizes the path γ , then we define the iterated integral $\int_{\gamma} \omega_1 \dots \omega_k$ as

$$\int_{\gamma} \omega_1 \dots \omega_k = \int_{0 \leq t_1 \leq \dots \leq t_k \leq 1} f_1(t_1) dt_1 \dots f_k(t_k) dt_k. \quad (2.1)$$

Products of two iterated integrals with the same path naturally form a shuffle algebra,

$$\begin{aligned} \int_{\gamma} \omega_1 \dots \omega_k \int_{\gamma} \omega_{k+1} \dots \omega_n &= \sum_{\sigma \in \Sigma(k, n-k)} \int_{\gamma} \omega_{\sigma(1)} \dots \omega_{\sigma(n)} \\ &= \int_{\gamma} \omega_1 \dots \omega_k \sqcup \omega_{k+1} \dots \omega_n, \end{aligned} \quad (2.2)$$

where $\Sigma(k, l)$ denotes the set of all shuffles of $\{1, \dots, k\}$ and $\{k+1, \dots, n\}$, i.e. all permutations of $\{1, \dots, n\}$ that preserve the relative orderings within each set, and \sqcup denotes the shuffle product. If we decompose the path $\gamma = \gamma_1 \gamma_2$ into two parts γ_1 and γ_2 such that $\gamma_2(1) = \gamma_1(0)$,² we have

$$\int_{\gamma} \omega_1 \dots \omega_n = \sum_{k=0}^n \int_{\gamma_1} \omega_1 \dots \omega_k \int_{\gamma_2} \omega_{k+1} \dots \omega_n. \quad (2.3)$$

¹For our purpose it is enough to think of differential one-forms as elements $f(x_i) dx_j$ for some coordinates x_i on a manifold.

²Note that we have implicitly rescaled the parameters t_1, t_2 such that both γ_1 and γ_2 are parametrized by $t_i \in [0, 1]$.

Integrating over the inverted path $\gamma^{-1}(t) = \gamma(1-t)$, i.e. integrating over path γ in the opposite direction, corresponds, up to a sign, to an integral over the reversed sequence of one-forms,

$$\int_{\gamma^{-1}} \omega_1 \dots \omega_n = (-1)^n \int_{\gamma} \omega_n \dots \omega_1. \quad (2.4)$$

Let us now turn to the question when iterated integrals are homotopy invariant, i.e. when the integral does not depend on the specific parametrization γ of the path but only on the endpoints $\gamma(0), \gamma(1)$. It is possible to find so-called *integrability conditions* on the integrand that guarantee exactly that. It is for example easy to see that any integral over an exact one-form $\omega = df$ is homotopy invariant and we have

$$\int_{\gamma} df = f(\gamma(1)) - f(\gamma(0)). \quad (2.5)$$

More generally, this is true for any one-form that is closed $d\omega = 0$. The conditions on iterated integrals are slightly more involved. Let us start by defining the notion of *words* of differential forms ω_i (not necessarily one-forms) as sequences $[\omega_1 | \dots | \omega_k] \in B_k$ and let

$$B = \bigoplus_{k=0}^{\infty} B_k \quad (2.6)$$

denote the space of all words of differential forms of arbitrary length, where $B_0 = \mathbb{F}$ is defined as the field \mathbb{F} over which the vector space of differential forms is defined. Formally, B_k corresponds to the k -fold tensor product of the vector space of differential forms. Together with the shuffle product

$$[\omega_1 | \dots | \omega_k] \sqcup [\omega_{k+1} | \dots | \omega_n] = \sum_{\sigma \in \Sigma(k, n-k)} [\omega_{\sigma(1)} | \dots | \omega_{\sigma(n)}], \quad (2.7)$$

B has the structure of a Hopf algebra. Setting the empty word $[]$ equal to one, the coproduct is given by the deconcatenation of words,

$$\Delta_{\text{dec}}[\omega_1 | \dots | \omega_n] = \sum_{k=0}^n [\omega_1 | \dots | \omega_k] \otimes [\omega_{k+1} | \dots | \omega_n], \quad (2.8)$$

and the antipode is given by

$$\mathcal{S}([\omega_1 | \dots | \omega_n]) = (-1)^n [\omega_n | \dots | \omega_1]. \quad (2.9)$$

It is evident that the basic properties of iterated integrals (2.2), (2.3) and (2.4) are inherited from these operations on Hopf algebras.

Let us now focus on words of one-forms and define the maps $D_1, D_2 : B \rightarrow B$ as

$$D_1([\omega_1 | \dots | \omega_k]) = - \sum_{i=1}^k [\omega_1 | \dots | \omega_{i-1} | d\omega_i | \omega_{i+1} | \omega_k] \quad (2.10)$$

$$D_2([\omega_1 | \dots | \omega_k]) = - \sum_{i=1}^{k-1} [\omega_1 | \dots | \omega_{i-1} | \omega_i \wedge \omega_{i+1} | \omega_{i+2} | \omega_k]. \quad (2.11)$$

Then we can define the differential $D = D_1 + D_2$ on B , which allows us to define integrable words of one-forms. D has the usual properties of a differential, i.e. it fulfils a Leibniz rule with respect to the shuffle product, and we have $D^2 = 0$. We stress that this definition only applies to words of one-forms and not to words of arbitrary differential forms. While it is possible to define a similar map for words of differential forms in general, the definition we give here is sufficient within the scope of this thesis and takes a simpler form.

Let ω be a linear combination of words of one-forms, then we call ω integrable if it lies in the kernel of D , and ω defines a homotopy invariant integral [53].

2.2 Multiple Polylogarithms

Many Feynman integrals can be expressed in terms of multiple polylogarithms [41], in particular it was shown that all one-loop integrals in four dimensions can be expressed in terms of MPLs [13]. In this section we will summarize a few useful properties of multiple polylogarithms and will introduce special, single-valued combinations of them. Multiple polylogarithms are defined [40] by the recursion

$$G(a_1, \dots, a_n; z) = \int_0^z \frac{dt}{t - a_1} G(a_2, \dots, a_n; t), \quad (2.12)$$

where the recursion starts with $G(; z) \equiv 1$. The number of integrations n is called the weight of the multiple polylogarithm. In the case where all $a_i = 0$ we define

$$G(\underbrace{0, \dots, 0}_{n \text{ times}}; z) = \frac{1}{n!} \log^n z. \quad (2.13)$$

As can easily be seen from this definition, MPLs diverge for $z = a_1$. MPLs with the same argument form a *shuffle algebra* which allows us to rewrite a

product of two MPLs as

$$\begin{aligned} G(a_1, \dots, a_k; z)G(a_{k+1}, \dots, a_{k+l}; z) \\ = \sum_{\sigma \in \Sigma(k,l)} G(a_{\sigma(1)}, \dots, a_{\sigma(k+l)}; z). \end{aligned} \quad (2.14)$$

This property follows naturally from their definition as iterated integrals. Note that the shuffle product preserves the weight and hence the product of two MPLs of weight k and l is a linear combination of MPLs of weight $k + l$. The shuffle product is consistent with eq. (2.13) and we find, similarly, in the case where all $a_i = a \neq 0$ are equal

$$G(\underbrace{a, \dots, a}_{n \text{ times}}; z) = \frac{1}{n!} \log^n \left(1 - \frac{z}{a} \right). \quad (2.15)$$

Considering the vector space of MPLs modulo $i\pi$, i.e. modulo their branch cuts, it forms a Hopf algebra [41, 54]. A Hopf algebra H is a bialgebra, i.e. it is both an algebra and a coalgebra such that the two are compatible with each other. More precisely, the coproduct Δ and counit η of the coalgebra are both algebra morphisms (or equivalently, the product μ and unit ε of the algebra are both coalgebra morphisms). Furthermore, H is equipped with a map S called the antipode, which is an endomorphism on H such that

$$\mu \circ (\text{id}_H \otimes S) \circ \Delta = \mu \circ (S \otimes \text{id}_H) \circ \Delta = \eta \circ \varepsilon. \quad (2.16)$$

For the space of MPLs modulo $i\pi$, the coproduct is given by

$$\Delta_G(G(\vec{a}; z)) = \sum_{\vec{b} \subseteq \vec{a}} G(\vec{b}; z) \otimes G_{\vec{b}}(\vec{a}; z), \quad (2.17)$$

where we sum over all order preserving subsets $\vec{b} \subseteq \vec{a}$. The functions $G_{\vec{b}}(\vec{a}; z)$ are defined as the iterated integral with the same integrand as $G(\vec{a}; z)$ but integrated over a contour that encircles, in order, all poles in \vec{b} . This is equivalent to taking the residues in these points without multiplying by $2\pi i$. Let us demonstrate this at some simple examples. For MPLs of weight one there are only two terms and the only residue we have to take is

$$G_a(a; z) = \text{Res}_{z=a} \frac{1}{z-a} = 1. \quad (2.18)$$

Hence we get

$$\Delta_G G(a; z) = G(a, z) \otimes 1 + 1 \otimes G(a; z). \quad (2.19)$$

For a polylogarithm of length two, we have to compute the residues

$$\begin{aligned} G_{a,b}(a,b;z) &= \operatorname{Res}_{w=a} \frac{1}{w-a} \operatorname{Res}_{z=b} \frac{1}{z-b} = 1 \\ G_a(a,b;z) &= \operatorname{Res}_{z=a} \frac{1}{z-a} G(b;z) = G(b;a) \\ G_b(a,b;z) &= \int_b^z dw \frac{1}{w-a} \operatorname{Res}_{z=b} \frac{1}{z-b} = G(a;z) - G(a;b). \end{aligned} \quad (2.20)$$

Note that the lower integration boundary after taking a residue is given by the point at which we took the residue. The reason for this is that we encircle the pole in the integrand and then continue our integration from there. Finally, this yields the coproduct

$$\begin{aligned} \Delta_G G(a,b;z) &= G(a,b;z) \otimes 1 + G(a;z) \otimes G(b;a) \\ &\quad + G(b;z) \otimes (G(a;z) - G(a;b)) + 1 \otimes G(a,b;z) \end{aligned} \quad (2.21)$$

The functions $G_{\vec{b}}(\vec{a};z)$ are linear combinations of (products of) MPLs of weight $|\vec{a}| - |\vec{b}|$, where $|\vec{v}|$ denotes the cardinality of \vec{v} .

The coproduct is coassociative,

$$(\operatorname{id} \otimes \Delta_G) \otimes \Delta_G = (\Delta_G \otimes \operatorname{id}) \otimes \Delta_G, \quad (2.22)$$

and can be lifted to a coaction on the full space of MPLs by setting

$$\Delta_G(i\pi) = i\pi \otimes 1, \quad (2.23)$$

where, by abuse of notation, we denote both the coaction and the coproduct by Δ_G . This asymmetry in the definition of the coaction is also reflected in the way the coaction commutes with taking discontinuities or derivatives. In particular, we have

$$\Delta_G \operatorname{Disc} = (\operatorname{Disc} \otimes \operatorname{id}) \Delta_G \quad \text{and} \quad \Delta_G \partial_z = (\operatorname{id} \otimes \partial_z) \Delta_G. \quad (2.24)$$

Let us quickly comment on the MPLs appearing on the r.h.s. of (2.17). Since we have not imposed any restrictions on the $a_i \in \vec{a}$, we could potentially encounter divergent polylogarithms of the form $G(z, a_2, \dots; z)$. These divergencies can be regularized using the shuffle product. We can formally rewrite any $G(a_1, \dots, a_n; z)$ with $a_i = z$ for $1 \leq i \leq k$ and $k \leq n$ as [48]

$$G(a_1, \dots, a_n; z) = \sum_{i=0}^k G(z; z)^i f_{n-i}(z), \quad (2.25)$$

where the $f_k(z)$ are linear combinations of MPLs $G(b_1, \dots, b_k; z)$ of weight k with $b_1 \neq z$. Then we define

$$G^{\text{Reg}}(a_1, \dots, a_n; z) = f_n(z). \quad (2.26)$$

For the polylogarithm $G(z, a; z)$ for example this yields

$$G(z, a; z) = G(z; z)G(a; z) - G(a, z; z), \quad (2.27)$$

and hence

$$G^{\text{Reg}}(z, a; z) = -G(a, z; z). \quad (2.28)$$

Similarly, we find

$$G(z, z, a; z) = \frac{1}{2}G(z; z)^2G(a; z) - G(z; z)G(a, z; z) + G(a, z, z; z), \quad (2.29)$$

which gives

$$G^{\text{Reg}}(z, z, a, z) = G(a, z, z; z). \quad (2.30)$$

Regularized MPLs have the same algebraic properties as their unregularized versions, in particular they preserve multiplication (and subsequently also the shuffle algebra)

$$\left[G(\vec{a}; z)G(\vec{b}; z) \right]^{\text{Reg}} = G^{\text{Reg}}(\vec{a}; z)G^{\text{Reg}}(\vec{b}; z). \quad (2.31)$$

All MPLs appearing in the r.h.s. of (2.17) are to be understood as their regularised versions.

The coproduct raises the space of MPLs to a bialgebra, graded by the weight, that can be promoted to a Hopf algebra by endowing it with an antipode S . The antipode is determined recursively in the weight through

$$\mu(S \otimes \text{id})\Delta(G(\vec{a}; z)) = \mu(\text{id} \otimes S)\Delta(G(\vec{a}; z)) = 0, \text{ if } |\vec{a}| \geq 1, \quad (2.32)$$

where $\mu(a \otimes b) = a \cdot b$ denotes the multiplication. At weight one, for example, we have

$$S(G(a; z)) + G(a; z) = 0, \quad (2.33)$$

which uniquely determines the antipode of MPLs of weight one. At weight two we similarly find

$$\begin{aligned} 0 &= S(G(a, b; z)) + S(G(a; z))G(b; a) \\ &\quad + S(G(b; z))[G(a; z) - G(a; b)] + G(a, b; z) \\ &= S(G(a, b; z)) - G(a; z)G(b; a) \\ &\quad - G(b; z)[G(a; z) - G(a; b)] + G(a, b; z), \end{aligned} \quad (2.34)$$

where we used (2.33), defining the result for the antipode of a MPL of weight one. We see that $S(G(a, b; z))$ is uniquely determined by eq. (2.34). This process can be repeated for higher weights to uniquely determine the antipode recursively through the coproduct. The antipode is an involution, $S^2 = \text{id}$, and it preserves multiplication and the coproduct,

$$S(a \cdot b) = S(b) \cdot S(a) \quad \text{and} \quad \Delta S = (S \otimes S)\tau\Delta, \quad (2.35)$$

with $\tau(a \otimes b) = b \otimes a$.

2.2.1 The Symbol of MPLs

Another useful operation on MPLs that is closely related to the coproduct is the *symbol*. To define the symbol, let us introduce some useful notation. The coproduct Δ_G splits a polylogarithm of weight n into tensor products of polylogarithms whose combined weight is n . Let us define $\Delta_{G,ij}$ as the component of the coproduct that consists of tensor products of functions of weights i and j respectively. In the case of a polylogarithm of weight 3, for example, we have

$$\begin{aligned} \Delta_G(G(0, 1, 1; z)) &= 1 \otimes G(0, 1, 1; z) + G(1; z) \otimes G(0, 1, z) \\ &\quad + G(1, 1; z) \otimes G(0; z) + G(0, 1, 1; z) \otimes 1, \end{aligned} \quad (2.36)$$

and

$$\begin{aligned} \Delta_{G,03}(G(0, 1, 1; z)) &= 1 \otimes G(0, 1, 1; z) \\ \Delta_{G,30}(G(0, 1, 1; z)) &= G(0, 1, 1; z) \otimes 1 \\ \Delta_{G,12}(G(0, 1, 1; z)) &= G(1; z) \otimes G(0, 1, z) \\ \Delta_{G,21}(G(0, 1, 1; z)) &= G(1, 1; z) \otimes G(0; z). \end{aligned} \quad (2.37)$$

By iteratively applying the coproduct $(k-1)$ -times we can equivalently define $\Delta_{G,i_1 \dots i_k}$ and the uniqueness of the expression is assured by coassociativity.

Then we define the symbol \mathcal{S} of a polylogarithm of weight n as

$$\mathcal{S}(G(\vec{a}; z)) = \Delta_{G, \underbrace{1 \dots 1}_{n\text{-times}}}(G(\vec{a}; z)). \quad (2.38)$$

Since all components of the symbol are ordinary logarithms it is conventional to represent them as $a_1 \otimes \dots \otimes a_n$ instead of $\log a_1 \otimes \dots \otimes \log a_n$.

An equivalent³ definition of the symbol can be derived from the total differential. This definition is often found in the physics literature and will be useful

³This definition is equivalent for MPLs and pure functions of MPLs.

later on. Let us consider a function F_n of transcendental weight n whose total differential can be cast in the form

$$dF_n = \sum_i F_{n-1,i} d \log R_i, \quad (2.39)$$

where the $F_{n-1,i}$ are functions of transcendental weight $n-1$ and the R_i are algebraic functions. Then the symbol of the function F_n is defined by the recursion

$$\mathcal{S}(F_n) = \sum_i \mathcal{S}(F_{n-1,i}) \otimes R_i, \quad \mathcal{S}(F_0) = F_0. \quad (2.40)$$

In order for this recursion to terminate, it is obvious that the differential equation (2.39) must have a trivial homogeneous part. This definition of the symbol therefore only makes sense for so-called *pure* functions. The total differential of a MPL takes the form [40]

$$dG(a_1, \dots, a_n; z) = \sum_{i=1}^n G(a_1, \dots, \hat{a}_i, \dots, a_n; z) d \log \frac{a_{i-1} - a_i}{a_{i+1} - a_i}, \quad (2.41)$$

with $a_0 \equiv z$, and therefore has the form (2.39). The equivalence of the two definitions (2.38) and (2.40) is easy to see from the action of derivatives on the coproduct (2.24).

The symbol map is not injective as can easily be checked. We have, for example,

$$\mathcal{S}(G(1, 0, 1; 1-z)) = z \otimes (1-z) \otimes z = \mathcal{S}(G(0, 1, 0; z)), \quad (2.42)$$

while [49]

$$G(1, 0, 1; 1-z) = G(0, 1, 0; z) - \zeta_2 G(0; z) - 2\zeta_3. \quad (2.43)$$

The coaction on the other hand contains more information, and allows us to find certain relations among MPLs. Let us illustrate this process by deriving the relation (2.43) using only the coaction and the symbol map. Given (2.42), a good starting point for our endeavour is the MPL $G(0, 1, 0; z)$. We know that the difference $G(1, 0, 1; 1-z) - G(0, 1, 0; z)$ lies in the kernel of \mathcal{S} and hence the first entry of $\Delta_{G;21}(G(1, 0, 1; 1-z) - G(0, 1, 0; z))$ must lie in the kernel of \mathcal{S} as well. Indeed we find

$$\Delta_{G;21}(G(1, 0, 1; 1-z) - G(0, 1, 0; z)) = -\zeta_2 \otimes G(0; z). \quad (2.44)$$

The difference $G(1, 0, 1; 1-z) - (G(0, 1, 0; z) - \zeta_2 G(0; z))$ must lie in the kernel of both \mathcal{S} and $\Delta_{G;21}$ and must therefore be a constant. As we have seen before, this is indeed true, and we find

$$G(1, 0, 1; 1-z) - (G(0, 1, 0; z) - \zeta_2 G(0; z)) = -2\zeta_3. \quad (2.45)$$

It is often enough to analyse the components $\Delta_{G;k_1\dots k_1}$ to recursively compute relations among different MPLs and this procedure will be important in the remainder of this thesis.

2.2.2 Special Combinations of MPLs

In this section we will introduce special combinations of MPLs that will be useful in later parts of this thesis. In particular, we will introduce two variants of single-valued combinations of MPLs, the *single-valued multiple polylogarithms* (SVMPLs), \mathcal{G} , and the *generalized single-valued multiple polylogarithms* (gSVMPLs), \mathcal{G} . As we will see in the following, the former are actually contained in the latter. The reason for treating them separately is that we can find a simpler, more direct approach to computing SVMPLs compared to gSVMPLs.

Single-Valued Multiple Polylogarithms

In this section we will introduce the map \mathbf{s} which maps any polylogarithm $G(\vec{a}; z)$ to its single-valued analogue $\mathcal{G}(\vec{a}; z)$ such that $\mathcal{G}(\vec{a}; z)$ fulfils the same holomorphic differential equation as $G(\vec{a}; z)$. This construction is inspired by the work done in [55, 56] on multiple zeta values as well as [57] and relies on the Hopf algebra structure of MPLs. It was first presented in [1] and we refer the reader to that paper for proofs and another description of the single-valued map derived from a Picard-Fuchs equation.

Let L_Σ be the shuffle algebra of MPLs with singularities at $\sigma_i \in \Sigma$, \bar{L}_Σ its complex conjugate and $L_\Sigma \bar{L}_\Sigma \simeq L_\Sigma \otimes \bar{L}_\Sigma$. Then each of these algebras is a Hopf algebra for the coproduct (2.17). Let us further define the map

$$\tilde{S} : L_\Sigma \rightarrow \bar{L}_\Sigma; \quad G(\vec{a}; z) \mapsto (-1)^{|\vec{a}|} \bar{S}(G(\vec{a}; z)), \quad (2.46)$$

where \bar{S} denotes the complex conjugate of the antipode. Like S , \tilde{S} is an involution and it satisfies

$$\tilde{S}(a \cdot b) = \tilde{S}(b) \cdot \tilde{S}(a) \quad \text{and} \quad \Delta \tilde{S} = (\tilde{S} \otimes \tilde{S}) \tau \Delta. \quad (2.47)$$

Unlike the antipode, \tilde{S} does not satisfy eq. (2.32), but the equivalent equation for \tilde{S} defines the single-valued map (c.f. ref. [55]),

$$\mathbf{s} = \mu(\tilde{S} \otimes \text{id}) \Delta, \quad (2.48)$$

and hence $\mathcal{G}(\vec{a}; z) = \mathbf{s}(G(\vec{a}; z))$ is the single-valued version of $G(\vec{a}; z)$.

Let us quickly discuss some properties of the map \mathbf{s} before showing that the image under \mathbf{s} is indeed single-valued. \mathbf{s} is \mathbb{Q} -linear and preserves multiplication [1]

$$\mathbf{s}(a \cdot b) = \mathbf{s}(a) \cdot \mathbf{s}(b). \quad (2.49)$$

It is important to remark that \mathbf{s} is only linear with respect to rational numbers and that it can act non-trivially on transcendental periods. In particular, we have [55]

$$\mathbf{s}(i\pi) = 0 \quad \text{and} \quad \mathbf{s}(\zeta_n) = 2\zeta_n, \quad \text{for } n \text{ odd}. \quad (2.50)$$

Let $L_\Sigma^{SV} \subset L_\Sigma \bar{L}_\Sigma$ be the image of L_Σ under the map \mathbf{s} . Then L_Σ^{SV} is again graded by the weight and a coaction is given by the action of the coproduct of $L_\Sigma \bar{L}_\Sigma$ restricted to L_Σ^{SV} ,

$$\Delta : L_\Sigma^{SV} \rightarrow L_\Sigma^{SV} \otimes L_\Sigma \bar{L}_\Sigma. \quad (2.51)$$

Let us now turn to the functions $\mathcal{G}(\vec{a}; z)$ and show that they are indeed single-valued. Let $\mathcal{M}_\sigma \mathcal{G}(\vec{a}; z)$ denote the result of analytically continuing $\mathcal{G}(\vec{a}; z)$ along a small, counter-clockwise loop encircling only the singularity $\sigma \in \Sigma$. Then $\mathcal{G}(\vec{a}; z)$ is single-valued if

$$\text{Disc}_\sigma \mathcal{G}(\vec{a}; z) = \mathcal{M}_\sigma \mathcal{G}(\vec{a}; z) - \mathcal{G}(\vec{a}; z) = 0, \quad \forall \sigma \in \Sigma. \quad (2.52)$$

We will show this by induction over the weight of $\mathcal{G}(\vec{a}; z)$. At weight one we have

$$\mathcal{G}(a; z) = G(a; z) + \tilde{S}(G(a; z)) = \log \left| 1 - \frac{z}{a} \right|^2, \quad (2.53)$$

which is manifestly single-valued. Let us now assume that all \mathcal{G} up to weight n are single-valued and let $\mathcal{G}(\vec{a}; z)$ be a SVMPL of weight $n+1$. Then it follows from the induction hypothesis that

$$\Delta \text{Disc}_\sigma(\mathcal{G}(\vec{a}; z)) = (\text{Disc}_\sigma \otimes \text{id}) \Delta(\mathcal{G}(a; z)) = \text{Disc}_\sigma \mathcal{G}(\vec{a}; z) \otimes 1, \quad (2.54)$$

where we have used that the discontinuity operator only acts on the first factor of the coproduct. Then eq. (2.32) yields

$$0 = \mu(\text{id} \otimes S) \Delta \text{Disc}_\sigma(\mathcal{G}(\vec{a}; z)) = \text{Disc}_\sigma(\mathcal{G}(\vec{a}; z)) \cdot S(1) = \text{Disc}_\sigma(\mathcal{G}(\vec{a}; z)), \quad (2.55)$$

and hence $\mathcal{G}(\vec{a}; z)$ is single-valued.

Let us now show that $\mathcal{G}(a_1, \dots, a_n; z)$ fulfils the same holomorphic differential equation as $G(a_1, \dots, a_n; z)$, i.e. that

$$\partial_z \mathbf{s} = \mathbf{s} \partial_z. \quad (2.56)$$

This can easily be shown by using that derivatives only act on the second factor of the coproduct. Using the Leibniz rule for differentiation $\partial_z \mu = \mu(\partial_z \otimes \text{id} + \text{id} \otimes \partial_z)$, we find

$$\mathbf{s} \partial_z = \mu(\tilde{S} \otimes \text{id}) \Delta \partial_z = \mu(\tilde{S} \otimes \partial_z) \Delta = \partial_z \mathbf{s} - \mu(\partial_z \tilde{S} \otimes \text{id}) \Delta. \quad (2.57)$$

Since $\tilde{S}(G(\vec{a}; z))$ is always anti-holomorphic, we have $\partial_z \tilde{S} = 0$ and hence

$$\partial_z \mathcal{G}(a, \vec{b}; z) = \frac{1}{z-a} \mathcal{G}(\vec{b}; z). \quad (2.58)$$

For the same reason it is evident that the single-valued map \mathbf{s} does not commute with antiholomorphic derivatives, $\partial_{\bar{z}} \mathbf{s} \neq (\mathbf{s} \partial_z)^*$, and the behaviour of SVMPLs under antiholomorphic derivatives is encoded in \tilde{S} . Equivalently, complex conjugation acts non-trivially on SVMPLs. Every complex conjugated SVMPL can be expressed as a linear combination of regular SVMPLs

$$\mathcal{G}(\vec{a}; \bar{z}) = \sum_{\vec{b}} c_{\vec{a}, \vec{b}} \mathcal{G}(\vec{b}; z). \quad (2.59)$$

This behaviour is, again, encoded in the map \tilde{S} and we have

$$\bar{\mathbf{s}} = \mathbf{s} \tilde{S}, \quad (2.60)$$

where $\bar{\mathbf{s}}$ denotes the complex conjugate of \mathbf{s} . For a generic single-valued multiple polylogarithm of weight two, we find

$$\mathcal{G}(\vec{a}, \bar{b}; \bar{z}) = \bar{\mathbf{s}}(G(a, b; z)) = \mathcal{G}(b, a; z) + \mathcal{G}(b; a) \mathcal{G}(a; z) - \mathcal{G}(a; b) \mathcal{G}(b; z), \quad (2.61)$$

and similarly, in the case of antiholomorphic differentiation,

$$\partial_{\bar{z}} \mathcal{G}(a, b; z) = \frac{1}{\bar{z}-\bar{a}} \mathcal{G}(b; a) + \frac{1}{\bar{z}-\bar{b}} (\mathcal{G}(a; z) - \mathcal{G}(a; b)). \quad (2.62)$$

Let us conclude this section by commenting on functional relations among SVMPLs. While we could express all SVMPLs in terms of regular MPLs, solve functional relations on these and reexpress everything in terms of SVMPLs in the end, we can use the single-valued map to promote relations among ordinary MPLs to relations among SVMPLs. Since $\mathbf{s}G(\vec{a}; z) = \mathcal{G}(\vec{a}; z)$, single-valued MPLs fulfil essentially the same functional relations as their non-single-valued

analogues. Let us however stress again that some non-algebraic periods behave non-trivially under \mathbf{s} (c.f. (2.50)), which is essential for these relations to hold. Let us illustrate this at the following example. Applying \mathbf{s} to both sides of the relation

$$\begin{aligned} G\left(0, 1, 1; \frac{1}{z}\right) &= -G(0, 0, 0; z) + G(0, 0, 1; z) + G(0, 1, 0; z) \\ &\quad - G(0, 1, 1; z) + i\pi [G(0, 0; z) - G(0, 1; z)] \\ &\quad + \frac{\pi^2}{2} G(0; z) + \zeta_3 - \frac{i\pi^3}{6}, \end{aligned} \quad (2.63)$$

we get

$$\begin{aligned} \mathcal{G}\left(0, 1, 1; \frac{1}{z}\right) &= -\mathcal{G}(0, 0, 0; z) + \mathcal{G}(0, 0, 1; z) + \mathcal{G}(0, 1, 0; z) \\ &\quad - \mathcal{G}(0, 1, 1; z) + 2\zeta_3. \end{aligned} \quad (2.64)$$

Generalized Single-Valued Multiple Polylogarithms

As we will see later, the single-valued multiple polylogarithms introduced in the previous section can be used to describe all amplitudes in the high-energy limit of $\mathcal{N} = 4$ super Yang-Mills theory (SYM). They will however not be enough to describe amplitudes in the high-energy limit of more general Yang-Mills theories. In particular, we will encounter single-valued polylogarithms whose holomorphic derivatives depend on the complex conjugate of the argument z itself, as for example in

$$\partial_z G(-1, |z|^2) = \frac{1}{z + 1/\bar{z}}. \quad (2.65)$$

A broader class of single-valued multiple polylogarithms covering also SVMPLs has been studied in ref. [58], where a recursive algorithm for the construction of gSVMPLs in one complex variable with singularities at

$$z = \frac{\alpha \bar{z} + \beta}{\gamma \bar{z} + \delta}, \quad \alpha, \beta, \gamma, \delta \in \mathbb{C} \quad (2.66)$$

was introduced. For $\alpha = \gamma = 0$, i.e. in the case where all singularities are constant, these gSVMPLs coincide with the SVMPLs we have introduced in the previous section. In this section we will review the definition and the construction of the gSVMPLs introduced in [58]. There it was shown that the following conditions uniquely define the functions $\mathcal{G}(a_1, \dots, a_n; z)$:

1. The functions $\mathcal{G}(a_1, \dots, a_n; z)$ are single-valued.

2. They form a shuffle algebra.
3. They satisfy the holomorphic differential equation,

$$\partial_z \mathcal{G}(a_1, \dots, a_n; z) = \frac{1}{z - a_1} \mathcal{G}(a_2, \dots, a_n; z). \quad (2.67)$$

4. They vanish for $z = 0$, except if all a_i are 0, in which case we have

$$\mathcal{G}(\underbrace{0, \dots, 0}_{n \text{ times}}; z) = \frac{1}{n!} \log^n |z|^2. \quad (2.68)$$

5. The singularities in eq. (2.67) are antiholomorphic functions of z of the form,

$$a_i = \frac{\alpha \bar{z} + \beta}{\gamma \bar{z} + \delta}, \text{ for some } \alpha, \beta, \gamma, \delta \in \mathbb{C}. \quad (2.69)$$

Let us make a few observations that will be important for the algorithmic construction of these functions. Let f be a linear combination of gSVMPLs with singularities at most at $z = a_i$, with a_i of the form (2.69). Then there exist two single-valued functions F_1 and F_2 such that

$$\partial_z F_1 = f = \partial_{\bar{z}} F_2. \quad (2.70)$$

These are the single-valued holomorphic (antiholomorphic) primitives which we will denote by $\int_{SV} dz f$ ($\int_{SV} d\bar{z} f$). The single-valued holomorphic (antiholomorphic) primitive agrees with any other holomorphic (antiholomorphic) primitive up to a purely antiholomorphic (holomorphic) function and we have

$$\int_{SV} dz f = \int dz f + \delta(\bar{z}). \quad (2.71)$$

Let us also define the functions π_0 ($\bar{\pi}_0$) as the projections that map any function to its analogue modulo holomorphic (antiholomorphic) residues,

$$\begin{aligned} \pi_0 : f &\mapsto f - \sum_{z_0 \in \mathbb{C}} \frac{\text{Res}_{z=z_0} f}{z - z_0}, \\ \bar{\pi}_0 : f &\mapsto f - \sum_{\bar{z}_0 \in \mathbb{C}} \frac{\overline{\text{Res}_{\bar{z}=\bar{z}_0} f}}{\bar{z} - \bar{z}_0}, \end{aligned} \quad (2.72)$$

where we sum over all poles of f . Then we can recursively construct the gSVMPLs using the commutative diagram shown in fig. 2.1 [58].

$$\begin{array}{ccc}
& & F \\
& \nearrow \int_{SV} dz & \\
\pi_0(\partial_z F) & & \nwarrow \int_{SV} d\bar{z} \\
& \uparrow \pi_0 & \\
\partial_z F & & \partial_{\bar{z}} F \\
& \searrow \partial_{\bar{z}} & \nearrow \int_{SV} \\
& & \partial_z \partial_{\bar{z}} F
\end{array}$$

Figure 2.1: Commutative diagram from ref. [58] for the computation of single-valued primitives.

Let us sketch the process of computing the single-valued holomorphic primitive F of the single-valued function $f = \partial_z F$ of weight n assuming that we already know how to compute single-valued primitives of functions of lower weight. Then we can define

$$F_1(z, \bar{z}) = \int dz \pi_0(\partial_z F(z, \bar{z})) \quad (2.73)$$

and

$$\bar{F}_2(z, \bar{z}) = \int d\bar{z} \bar{\pi}_0(\partial_{\bar{z}} F(z, \bar{z})). \quad (2.74)$$

These two functions must be equal to the desired single-valued primitive up to purely (anti)holomorphic functions

$$F(z, \bar{z}) = F_1(z, \bar{z}) + \delta_1(\bar{z}) = \bar{F}_2(z, \bar{z}) + \delta_2(z), \quad (2.75)$$

and hence

$$F_1(z, \bar{z}) - \bar{F}_2(z, \bar{z}) = \delta_2(z) - \delta_1(\bar{z}). \quad (2.76)$$

This fixes the functions δ_1 and δ_2 up to a constant. This constant can be fixed by requiring that all gSVMPLs vanish for $z = 0$. We then recover the desired single-valued primitive F by adding back the previously subtracted residues,

$$\begin{aligned}
F &= \delta(\bar{z}) + \int_{SV} dz f \\
&= \delta(\bar{z}) + \int_{SV} dz \pi_0(f) + \sum_{z_0 \in \mathbb{C}} \text{Res}_{z=z_0} f \int_{SV} \frac{dz}{z - z_0} \\
&= \delta(\bar{z}) + \int_{SV} dz \pi_0(f) + \sum_{z_0 \in \mathbb{C}} \text{Res}_{z=z_0} f \mathcal{G}(z_0; z),
\end{aligned} \quad (2.77)$$

where $\delta(\bar{z})$ is any antiholomorphic rational function.

Let us illustrate this process explicitly by computing the function $F(z, \bar{z}) = \mathcal{G}_{-1/\bar{z}, 1}(z)$, where we introduced the more compact notation $\mathcal{G}_{\bar{a}}(z) \equiv \mathcal{G}(\bar{a}; z)$. From eq. (2.67), it follows that

$$\partial_z F(z, \bar{z}) = \partial_z \mathcal{G}_{-1/\bar{z}, 1}(z) = \frac{1}{z + 1/\bar{z}} \mathcal{G}_1(z) = \frac{1}{z + 1/\bar{z}} \mathcal{G}_1(z) \equiv f(z, \bar{z}). \quad (2.78)$$

Since the denominator in eq. (2.78) never vanishes, $\pi_0(f) = f$, and we get

$$F_1(z, \bar{z}) = \int_0^z \frac{dt}{t + 1/\bar{z}} \mathcal{G}_1(t) = G_1(\bar{z}) G_{-1/\bar{z}}(z) + G_{-1/\bar{z}, 1}(z). \quad (2.79)$$

As mentioned before, this holomorphic primitive differs from the desired single-valued primitive at most by a purely antiholomorphic function δ_1 , and we have

$$F(z, \bar{z}) = F_1(z, \bar{z}) + \delta_1(\bar{z}). \quad (2.80)$$

Following the second path in fig. 2.1, we first need to compute the antiholomorphic derivative

$$\partial_{\bar{z}} f(z, \bar{z}) = \frac{1}{(1 + |z|^2)^2} \mathcal{G}_1(z) + \frac{1}{(\bar{z} - 1)(z + 1/\bar{z})}. \quad (2.81)$$

Since per our assumption we already know how to compute single-valued primitives of functions of lower weight, we get

$$\begin{aligned} \overline{F}'_2(z, \bar{z}) &= \int_{SV} dz \partial_{\bar{z}} f(z, \bar{z}) \\ &= \frac{1}{\bar{z} + 1/z} \mathcal{G}_1(z) - \frac{1}{\bar{z}} \mathcal{G}_{-1/\bar{z}}(z) + \frac{1}{\bar{z} - 1} \mathcal{G}_{-1/\bar{z}}(z) \\ &\quad + \frac{1}{\bar{z} + 1} [\mathcal{G}_{-1/\bar{z}}(z) - \mathcal{G}_1(z)]. \end{aligned} \quad (2.82)$$

Next, we have to subtract all antiholomorphic residues from \overline{F}'_2 . The residue at the pole at $\bar{z} = 0$ vanishes and for $\bar{z} = \pm 1$, we have

$$\overline{\text{Res}}_{\bar{z}=\pm 1} \overline{F}'_2(z, \bar{z}) = \pm \log 2. \quad (2.83)$$

This gives us

$$\begin{aligned} \overline{\pi}_0(\overline{F}'_2(z, \bar{z})) &= \frac{1}{\bar{z} + 1/z} \mathcal{G}_1(z) - \frac{1}{\bar{z}} \mathcal{G}_{-1/\bar{z}}(z) + \frac{1}{\bar{z} - 1} [\mathcal{G}_{-1/\bar{z}}(z) - \log 2] \\ &\quad + \frac{1}{\bar{z} + 1} [\mathcal{G}_{-1/\bar{z}}(z) - \mathcal{G}_1(z) + \log 2], \end{aligned} \quad (2.84)$$

with its antiholomorphic primitive

$$\begin{aligned}\bar{F}_2(z, \bar{z}) &= \int_0^{\bar{z}} d\bar{t} \bar{\pi}_0(\bar{F}'_2(z, \bar{t})) \\ &= G_1(\bar{z}) G_{-1/\bar{z}}(z) + G_{-1/\bar{z},1}(z) - G_{-1,1}(\bar{z}) \\ &\quad + \log 2 G_{-1}(\bar{z}) - \log 2 G_1(\bar{z}).\end{aligned}\tag{2.85}$$

Just as for the holomorphic primitive F_1 there is as purely holomorphic function δ_2 such that

$$F(z, \bar{z}) = \bar{F}_2(z, \bar{z}) + \delta_2(z).\tag{2.86}$$

From the equations (2.80) and (2.86) we can now determine the functions δ_i up to a constant a from

$$\begin{aligned}\delta_1(\bar{z}) - \delta_2(z) &= \bar{F}_2(z, \bar{z}) - F_1(z, \bar{z}) \\ &= -G_{-1,1}(\bar{z}) + \log 2 G_{-1}(\bar{z}) - \log 2 G_1(\bar{z}),\end{aligned}\tag{2.87}$$

and the fact that the two functions are purely holomorphic or antiholomorphic respectively. Hence, we find

$$\begin{aligned}\delta_1(\bar{z}) &= -G_{-1,1}(\bar{z}) + \log 2 G_{-1}(\bar{z}) - \log 2 G_1(\bar{z}) + a, \\ \delta_2(z) &= a.\end{aligned}\tag{2.88}$$

As mentioned before, we can fix a by requiring that F vanish at the origin, which yields $a = 0$ and finally

$$\begin{aligned}F(z, \bar{z}) &= \mathcal{G}_{-1/\bar{z},1}(z) = G_1(\bar{z}) G_{-1/\bar{z}}(z) + G_{-1/\bar{z},1}(z) - G_{-1,1}(\bar{z}) \\ &\quad + \log 2 G_{-1}(\bar{z}) - \log 2 G_1(\bar{z}).\end{aligned}\tag{2.89}$$

2.3 Elliptic Multiple Polylogarithms

In this section we will introduce a class of elliptic multiple polylogarithms defined on the torus. We will mainly work with this representation of eMPLs because they are closely connected to a class of iterated integrals of modular forms, which will be of great use later on. An introduction to a class of eMPLs that is more closely related to Feynman integrals can be found in ref. [43].

A torus can be described by a point τ in the upper half plane \mathbb{H} as the parallelogram spanned by 1 and τ where we identify opposite sides (c.f. fig. 2.2),

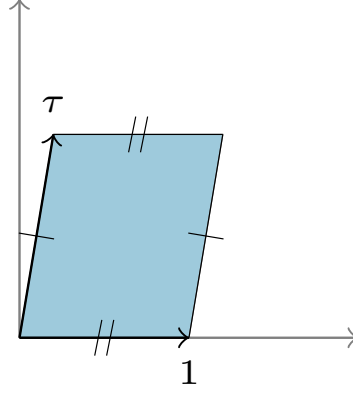


Figure 2.2: Diagram displaying the relation between the connection between a torus and a point $\tau \in \mathbb{H}$.

and two points τ, τ' define the same torus if they are related by a modular transformation

$$\tau \mapsto \tau' = \frac{a\tau + b}{c\tau + d}, \quad \gamma = \begin{pmatrix} a & b \\ c & d \end{pmatrix} \in SL(2, \mathbb{Z}). \quad (2.90)$$

Let us define elliptic multiple polylogarithms on the torus described by τ as [42, 50]

$$\tilde{\Gamma} \left(\begin{matrix} n_1 & \dots & n_k \\ z_1 & \dots & z_k \end{matrix}; z, \tau \right) = \int_0^z dw g^{(n_1)}(w - z_1, \tau) \tilde{\Gamma} \left(\begin{matrix} n_2 & \dots & n_k \\ z_2 & \dots & z_k \end{matrix}; w, \tau \right). \quad (2.91)$$

As opposed to regular multiple polylogarithms, the weight of an elliptic multiple polylogarithm does not correspond to the number of integrations but rather to the sum $\sum_i n_i$ and the number of integrations k is called the length. In the case where all $\binom{n_i}{z_i} = \binom{1}{0}$ we define

$$\tilde{\Gamma} \left(\underbrace{\binom{1}{0} \dots \binom{1}{0}}_{n \text{ times}}; z, \tau \right) = \frac{1}{n!} \tilde{\Gamma} \left(\binom{1}{0}; z, \tau \right)^n, \quad (2.92)$$

with

$$\begin{aligned} \tilde{\Gamma} \left(\binom{1}{0}; z, \tau \right) &= \log(1 - e^{2\pi iz}) - 2\pi iz \\ &+ \int_0^z dw \left(g^{(1)}(w, \tau) - \frac{2\pi i}{e^{2\pi iw} - 1} \right). \end{aligned} \quad (2.93)$$

Being defined as iterated integrals, they form, a shuffle algebra and we have, equivalently to regular MPLs,

$$\begin{aligned} \tilde{\Gamma}(A_1 \dots A_k; z, \tau) \tilde{\Gamma}(A_{k+1} \dots A_{k+l}; z, \tau) \\ = \sum_{\sigma \in \Sigma(k,l)} \tilde{\Gamma}(A_{\sigma(1)} \dots A_{\sigma(k+l)}; z, \tau), \end{aligned} \quad (2.94)$$

where $A_i = \binom{n_i}{z_i}$. We can use this property to regularize the integrals (2.91) with $(n_k, z_k) = (1, 0)$, for which this definition is divergent. Similarly to the relation (2.25) we can use the shuffle algebra to write all $\tilde{\Gamma}(A_1, \dots, A_k; z, \tau)$ with $A_i = \binom{1}{0}$ for $k-r < i \leq k$ as

$$\tilde{\Gamma}(A_1, \dots, A_k; z, \tau) = \sum_{i=0}^r c_i \tilde{\Gamma}\left(\binom{1}{0}; z, \tau\right)^i \tilde{\Gamma}(B_1^i, \dots, B_{n-i}^i; z, \tau), \quad (2.95)$$

such that all quantities on the r.h.s. are finite. The rather complicated form of (2.93) was chosen such that they both preserve the shuffle algebra as well as have a nice q -expansion, which we will get to later. The integration kernels $g^{(n)}(z, \tau)$ are the coefficients of the series expansion of the *Eisenstein-Kronecker series* [42, 59]

$$F(z, \alpha, \tau) = \frac{1}{\alpha} \sum_{n=0}^{\infty} g^{(n)}(z, \tau) \alpha^n = \frac{\theta_1'(0, \tau) \theta_1(z + \alpha, \tau)}{\theta_1(z, \tau) \theta_1(\alpha, \tau)}, \quad (2.96)$$

where θ_1 is the odd Jacobi theta function and $\theta_1'(z, \tau) = \partial_z \theta_1(z, \tau)$. The Eisenstein-Kronecker series is quasi periodic,

$$F(z+1, \alpha, \tau) = F(z, \alpha, \tau) \quad F(z+\tau, \alpha, \tau) = e^{-2\pi i \alpha} F(z, \alpha, \tau), \quad (2.97)$$

which translates to the coefficients $g^{(n)}(z, \tau)$ as

$$g^{(n)}(z+1, \tau) = g^{(n)}(z, \tau), \quad (2.98)$$

$$g^{(n)}(z+\tau, \tau) = \sum_{k=0}^n (-2\pi i)^k g^{(n-k)}(z, \tau). \quad (2.99)$$

Furthermore, they have definite parity

$$g^{(n)}(-z, \tau) = (-1)^n g^{(n)}(z, \tau) \quad (2.100)$$

and satisfy a Fay identity [50],

$$\begin{aligned}
g^{(n_1)}(z_1, \tau)g^{(n_2)}(z_2, \tau) &= (-1)^{n_2+1}g^{(n_1+n_2)}(z_1 - z_2, \tau) \\
&+ \sum_{m=0}^{n_2} \binom{n_1 + m - 1}{m - 1} g^{(n_2-m)}(z_2 - z_1, \tau)g^{(n_1+m)}(z_1, \tau) \\
&+ \sum_{m=0}^{n_1} \binom{n_2 + m - 1}{m - 1} g^{(n_1-m)}(z_1 - z_2, \tau)g^{(n_2+m)}(z_2, \tau),
\end{aligned} \tag{2.101}$$

which plays a role similar to partial fractioning when computing iterated integrals. $g^{(1)}(z, \tau)$ has a simple pole at every lattice point and the functions $g^{(n)}(z, \tau)$ with $n \geq 2$ are finite on the real axis and exhibit simple poles at all other lattice points through the appearance of $g^{(1)}$ through (2.99). The functions $\tilde{\Gamma}$ defined in eq. (2.91) therefore exhibit at most logarithmic singularities, as expected from a generalization of multiple polylogarithms on the torus. Since the $g^{(n)}$ are only quasi periodic, they are technically not well-defined functions on the torus. This is due to the fact that there exists no doubly periodic, purely holomorphic function with at most simple poles and one has to give up either holomorphicity or periodicity when defining eMPLs on the torus. We chose to give up periodicity in favour of holomorphicity, as this allows us to compute the total differential of the resulting elliptic multiple polylogarithms $\tilde{\Gamma}$. A periodic version Γ of eMPLs on the torus is often found in the mathematics- and string theory literature. These functions are defined as [42, 50]

$$\Gamma \left(\begin{matrix} n_1 & \dots & n_k \\ z_1 & \dots & z_k \end{matrix}; z, \tau \right) = \int_0^z dw f^{(n_1)}(w - z_1, \tau) \Gamma \left(\begin{matrix} n_2 & \dots & n_k \\ z_2 & \dots & z_k \end{matrix}; w, \tau \right), \tag{2.102}$$

where the $f^{(n)}$ are the coefficients of the series expansion of

$$\Omega(z, \alpha, \tau) = \frac{1}{\alpha} \sum_{n=0}^{\infty} f^{(n)}(z, \tau) \alpha^n = \exp \left[2\pi i \alpha \frac{\text{Im}z}{\text{Im}\tau} \right] F(z, \alpha, \tau). \tag{2.103}$$

From the additional exponential in this definition and the quasi-periodic behaviour of F in eq. (2.97), it is easy to see that Ω is indeed periodic,

$$\Omega(z + 1, \alpha, \tau) = \Omega(z, \alpha, \tau) \quad \Omega(z + \tau, \alpha, \tau) = \Omega(z, \alpha, \tau). \tag{2.104}$$

2.3.1 The Symbol of eMPLs

In this section, we introduce a symbol map for eMPLs through a recursion similar to eq. (2.40). For this purpose, we first need to know the total differential of elliptic multiple polylogarithms. The differential for the $\tilde{\Gamma}$ was recently

worked out in [52], and reads

$$\begin{aligned}
& d\tilde{\Gamma}(A_1 \dots A_k; z, \tau) \\
&= \sum_{j=1}^{k-1} (-1)^{n_j+1} \tilde{\Gamma}(A_1 \dots A_{j-1} \begin{smallmatrix} 0 \\ A_{j+2} \dots A_k \end{smallmatrix}; z, \tau) \omega_{j,j+1}^{(n_j+n_{j+1})} \\
&+ \sum_{j=1}^k \sum_{m=0}^{n_j+1} \binom{n_{j-1}+m-1}{n_{j-1}-1} \tilde{\Gamma}(A_1 \dots A_{j-1}^{[m]} A_{j+1} \dots A_k; z, \tau) \omega_{j,j-1}^{(n_j-m)} \\
&- \sum_{j=1}^k \sum_{m=0}^{n_j+1} \binom{n_{j+1}+m-1}{n_{j+1}-1} \tilde{\Gamma}(A_1 \dots A_{j-1} A_{j+1}^{[m]} \dots A_k; z, \tau) \omega_{j,j+1}^{(n_j-m)},
\end{aligned} \tag{2.105}$$

where we set $z_0 = z$, $z_{k+1} = 0$, $n_0 = n_{k+1} = 0$ and where we have introduced the shorthand

$$A_i^{[m]} \equiv \begin{pmatrix} n_i+m \\ z_i \end{pmatrix} \quad \text{with} \quad A_i^{[0]} \equiv A_i. \tag{2.106}$$

The $\omega_{ij}^{(n)}$ are differential one forms and are defined as

$$\begin{aligned}
\omega_{ij}^{(n)} &= d\tilde{\Gamma} \left(\begin{smallmatrix} n \\ z_i \end{smallmatrix}; z_j, \tau \right) - (-1)^n d\tilde{\Gamma} \left(\begin{smallmatrix} n \\ 0 \end{smallmatrix}; z_i, \tau \right) - \frac{nd\tau}{2\pi i} G_{n+1}(\tau) \\
&= (dz_j - dz_i) g^{(n)}(z_j - z_i, \tau) + \frac{nd\tau}{2\pi i} g^{(n+1)}(z_j - z_i, \tau)
\end{aligned} \tag{2.107}$$

for $n \geq 0$ and for $n = -1$ as

$$\omega_{ij}^{(-1)} = -\frac{d\tau}{2\pi i}. \tag{2.108}$$

The functions $G_{2m}(\tau)$ are so-called Eisenstein series and are defined as

$$G_{2m}(\tau) = \sum_{\substack{\alpha, \beta \in \mathbb{Z} \\ (\alpha, \beta) \neq (0,0)}} \frac{1}{(\alpha + \beta\tau)^{2m}}, \tag{2.109}$$

with $G_{2m+1}(\tau) = 0$. Note that the elliptic polylogarithms appearing in the total differential (2.105) are all of lower length than the original and the corresponding differential equation therefore has a trivial homogeneous part. This

allows us to define the symbol of eMPLs through the recursion

$$\begin{aligned}
& \mathcal{S}\left(\tilde{\Gamma}(A_1 \dots A_k; z, \tau)\right) \tag{2.110} \\
&= \sum_{j=1}^{k-1} (-1)^{n_j+1} \pi_k \left[\mathcal{S}\left(\tilde{\Gamma}(A_1 \dots A_{j-1} \underset{0}{A_{j+2}} \dots A_k; z)\right) \otimes \omega_{j,j+1}^{(n_j+n_{j+1})} \right] \\
&+ \sum_{j=1}^k \sum_{m=0}^{n_j+1} \\
&\times \left(\binom{n_{j-1}+m-1}{n_{j-1}-1} \pi_k \left[\mathcal{S}\left(\tilde{\Gamma}(A_1 \dots A_{j-1}^{[m]} A_{j+1} \dots A_k; z)\right) \otimes \omega_{j,j-1}^{(n_j-m)} \right] \right. \\
&\left. - \binom{n_{j+1}+m-1}{n_{j+1}-1} \pi_k \left[\mathcal{S}\left(\tilde{\Gamma}(A_1 \dots A_{j-1} A_{j+1}^{[m]} \dots A_k; z)\right) \otimes \omega_{j,j+1}^{(n_j-m)} \right] \right),
\end{aligned}$$

where we have dropped the explicit dependence of $\tilde{\Gamma}$ on τ on the r.h.s. for compactness. The functions π_k are projections onto tensors of length k . This is necessary because elliptic polylogarithms of weight zero can evaluate to rational numbers, such as $\tilde{\Gamma}\left(\begin{smallmatrix} 0 \\ 0 \end{smallmatrix}; 1, \tau\right) = 1$, in which case we can encounter tensor products of length smaller than k . Note that the entries of the symbol are now one-forms and not algebraic functions as before.

Let us quickly demonstrate the role of the projector π_k at a simple example. First we will need a genuine eMPL, i.e. an eMPL that does not evaluate to a number, otherwise the symbol map acts trivially on it, and we have for example $\mathcal{S}\left(\tilde{\Gamma}\left(\begin{smallmatrix} 0 \\ 0 \end{smallmatrix}; 1, \tau\right)\right) = 1$. The symbol of any such eMPL of length $k = 1$ will correspond directly to the combination of one-forms $\omega_{i,j}^{(n)}$ and we will therefore automatically get tensor products of the correct length. The first time the projector π_k in eq. (2.110) will be important is for eMPLs of length $k = 2$. Let us consider the simple example $\tilde{\Gamma}\left(\begin{smallmatrix} 0 \\ 0 \end{smallmatrix}; \frac{1}{3}; 1, \tau\right)$. Already for this simple example, writing out all terms in eq. (2.110) without evaluating the projector π_k will yield many terms that don't serve any purpose in demonstrating the effect of π_k . Let us therefore only consider the term from the first line of the r.h.s. of eq. (2.110),

$$\mathcal{S}\left(\tilde{\Gamma}\left(\begin{smallmatrix} 0 \\ 0 \end{smallmatrix}; \frac{1}{3}; 1, \tau\right)\right) = -\pi_2 \left[\mathcal{S}\left(\tilde{\Gamma}\left(\begin{smallmatrix} 0 \\ 0 \end{smallmatrix}; 1, \tau\right)\right) \otimes \omega_{1,2}^{(1)} \right] + \dots \tag{2.111}$$

where the dots correspond to the terms multiplying binomial coefficients. The tensor product acts on differential one-forms, and hence

$$\mathcal{S}\left(\tilde{\Gamma}\left(\begin{smallmatrix} 0 \\ 0 \end{smallmatrix}; 1, \tau\right)\right) \otimes \omega_{1,2}^{(1)} = 1 \otimes \omega_{1,2}^{(1)} = \otimes \omega_{1,2}^{(1)} \tag{2.112}$$

corresponds to a tensor product consisting of only a single factor, and we have highlighted the fact that eq. (2.112) corresponds to a symbol and not just the one-form $\omega_{1,2}^{(1)}$ by keeping the tensor symbol. Consequently we have

$$\pi_2 \left[\mathcal{S} \left(\tilde{\Gamma} \left(\begin{smallmatrix} 0 \\ 0 \end{smallmatrix}; 1, \tau \right) \right) \otimes \omega_{1,2}^{(1)} \right] = 0 \quad (2.113)$$

and the only terms surviving on the r.h.s. are tensor products of one-forms $\omega_{i_1, j_1}^{(n_1)} \otimes \omega_{i_2, j_2}^{(n_2)}$.

2.3.2 The Coaction of eMPLs

The symbol provides a powerful tool to analyse the structure of eMPLs. A lot of information is lost, however, when reducing a function to its symbol. To recover part of this information, we would like to have a coaction similar to the one we had in the MPL case, where we have already seen how a coaction can be used to find relations among MPLs. Such a coaction was introduced in the mathematics literature [60] for motivic periods as

$$\Delta^{\mathfrak{m}}([M, \gamma, \omega]^{\mathfrak{m}}) = \sum_i [M, \gamma, \omega_i]^{\mathfrak{m}} \otimes [M, \omega_i^{\vee}, \omega]^{\mathfrak{dr}}, \quad (2.114)$$

where γ is a contour of integration, M is the underlying geometric space, $[M, \gamma, \omega_i]^{\mathfrak{m}}$ is a motivic period, $[M, \omega_i^{\vee}, \omega]^{\mathfrak{dr}}$ is a de Rham period, ω_i are differential forms and ω_i^{\vee} are the corresponding canonical dual forms. For the purpose of this thesis we will follow ref. [52] and simplify the notation slightly to yield

$$\Delta([\gamma, \omega]) = \sum_i [\gamma, \omega_i] \otimes [\omega_i, \omega]. \quad (2.115)$$

A folklore conjecture states that motivic periods encode the same information as the corresponding integral. Hence, we can lift the coaction (2.115) defined for motivic periods to a coaction for elliptic multiple polylogarithms by identify the motivic period $[\gamma, \omega]$ with the corresponding integral

$$[\gamma, \omega] \cong \int_{\gamma} \omega. \quad (2.116)$$

We can then think of the periods $[\gamma, \omega_i]$ we sum over as a basis of master integrals to the integral family to which $[\gamma, \omega]$ belongs. For $[\gamma, \omega] = \tilde{\Gamma}(\vec{A}; z, \tau)$, the sum runs over all eMPLs appearing in the iterated total differential of $\tilde{\Gamma}(\vec{A}; z, \tau)$. As discontinuities act only on the first component of the coaction, the second component, namely the de Rham period $[\omega_i, \omega]$, should be unaffected

by contour deformations. In the polylogarithmic case, we achieved this by setting appearances of $i\pi$ to zero in the second factor of the coproduct, which allowed us to treat the de Rham period as the corresponding integral modulo $i\pi$. In the elliptic world, however, this fails because not all discontinuities are proportional to $i\pi$. The complete elliptic integral of the first kind,

$$K(\lambda) = \int_0^1 \frac{dt}{(1-t^2)(1-\lambda t^2)}, \quad (2.117)$$

for example, has the discontinuity

$$\text{Disc } K(\lambda) = \theta(\lambda - 1) \frac{2}{\sqrt{\lambda}} K\left(1 - \frac{1}{\lambda}\right). \quad (2.118)$$

Instead, we can associate to a de Rham period $[\omega_i, \omega]$ a symbol,

$$[\omega_i, \omega] \cong \mathcal{S}([\omega_i, \omega]) = [\xi_{i_1} | \dots | \xi_{i_k}], \quad (2.119)$$

as was shown in [60]. The ξ_i in eq. (2.119) are differential one-forms and we adopted the notation from [52]. A technical description of how to compute the symbols appearing on the r.h.s. of eq. (2.119) can be found in appendix A. We can then define the coaction Δ as the concatenation of the motivic coaction Δ^m and the symbol map,

$$\Delta = (\text{id} \otimes \mathcal{S})\Delta^m. \quad (2.120)$$

Let us comment at this point on the definition of the symbol map \mathcal{S} . The symbol is only defined for unipotent periods, while the motivic coaction is defined for arbitrary periods. Since only functions of lower length appear in the differential of eMPLs (and regular MPLs), this definition makes sense for all eMPLs (and MPLs), we might however run into trouble when acting with the symbol on certain linear combinations of (elliptic) multiple polylogarithms. In this case, we can make use of the fact that any such period x can be written as linear combinations

$$x = \sum_i s_i u_i, \quad (2.121)$$

where the u_i are unipotent periods and s_i are *semi-simple* periods [60]. Then we define the action of Δ on semi-simple periods, analogously to appearances of $i\pi$ in the definition of Δ_G , as

$$\Delta(s_i) = s_i \otimes 1. \quad (2.122)$$

While the only semi-simple periods we encountered in the MPL case were factors of $i\pi$, we can encounter semi-simple periods with non-trivial functional

dependence in the elliptic case. Consider the matrix

$$P = \begin{pmatrix} \omega_1 & \omega_2 \\ \eta_1 & \eta_2 \end{pmatrix}, \quad (2.123)$$

containing the periods ω_i and quasi-periods⁴ η_i of the elliptic curve, and assume without loss of generality that $\text{Im } \omega_2/\omega_1 > 0$. Then we can decompose P into a semi-simple matrix S and a unipotent matrix U ,

$$P = SU, \quad (2.124)$$

with

$$S = \begin{pmatrix} \omega_1 & 0 \\ \eta_1 & -i\pi/\omega_1 \end{pmatrix} \quad \text{and} \quad U = \begin{pmatrix} 1 & \tau \\ 0 & 1 \end{pmatrix}, \quad (2.125)$$

$\tau = \omega_2/\omega_1$, and where we have used the Legendre relation among the periods and quasi-periods. The matrix U clearly satisfies a unipotent differential equation

$$dU = AU, \quad \text{with} \quad A = \begin{pmatrix} 0 & d\tau \\ 0 & 0 \end{pmatrix}, \quad (2.126)$$

and hence τ is unipotent and we get

$$\Delta(\tau) = \tau \otimes 1 + 1 \otimes [d\tau]. \quad (2.127)$$

The objects appearing in S are semi-simple, so the coaction acts trivially on them,

$$\Delta(\omega_1) = \omega_1 \otimes 1 \quad \text{and} \quad \Delta(\eta_1) = \eta_1 \otimes 1. \quad (2.128)$$

The behaviour of the remaining (quasi-)period then follows and we have

$$\Delta(\omega_2) = \omega_2 \otimes 1 + \omega_1 \otimes [d\tau] \quad \text{and} \quad \Delta(\eta_2) = \eta_2 \otimes 1 + \eta_1 \otimes [d\tau]. \quad (2.129)$$

Note that while the coaction defined in this way shares all the algebraic properties of the coaction Δ_G , it commutes slightly differently with derivatives. In particular we have

$$\Delta(\partial_z x) = \sum_i \Delta(u_i) \partial_z s_i + s_i (\text{id} \otimes \partial_z) \Delta(u_i), \quad (2.130)$$

⁴Similarly to the periods ω_i of an elliptic curve we can define quasi periods η_i such that they fulfil the legendre relation $\omega_1 \eta_2 - \omega_2 \eta_1 = -i\pi$. Generally, the primitive $F(z)$ of an elliptic function $f(z)$ is not periodic but *quasi periodic*, and we have $F(z + \omega_i) = F(z) + C_i$, where the C_i are independent of z . The quasi-periods η_i are closely related to the mismatches C_i . For the Weierstrass \wp function, $f(z) = \wp(z)$ we have $\eta_i = \zeta_\wp(\omega_i/2)$, where ζ_\wp is the Weierstrass zeta function and we have $\zeta_\wp(z + \omega_i) = \zeta_\wp(z) + 2\eta_i$.

where we have decomposed x into semi-simple and unipotent parts according to eq. (2.121). The discontinuity operator still commutes with the coaction in the usual way and we have

$$\Delta(\text{Disc } x) = (\text{Disc} \otimes \text{id})\Delta(x). \quad (2.131)$$

2.4 Iterated Integrals of Modular Forms

In this section, we will introduce modular forms and a class of iterated integrals over them [44, 61] that is closely connected to the elliptic multiple polylogarithms $\tilde{\Gamma}$. In fact, every elliptic multiple polylogarithm $\tilde{\Gamma} \left(\begin{smallmatrix} n_1 & \dots & n_k \\ z_1 & \dots & z_k \end{smallmatrix}; z, \tau \right)$ evaluated at rational points can be expressed as iterated integrals of modular forms.

2.4.1 Modular Forms

Let us start this section with a quick review of modular forms. This review will only cover the essentials needed within the scope of this thesis and by no means covers the extent of research that has been done on this subject. See e.g. [62] for a more detailed review. As we have seen before, every $\tau \in \mathbb{H}$ defines a torus \mathbb{C}/Λ_τ and two points $\tau, \tau' \in \mathbb{H}$ define the same torus if they are related by a modular transformation. For our purpose, it is sufficient to define a *modular form of weight n* as a holomorphic function f from the extended upper half plane $\bar{\mathbb{H}} \equiv \mathbb{H} \cup \mathbb{Q} \cup \{i\infty\}$ to the complex numbers that behaves under modular transformations as

$$f\left(\frac{a\tau + b}{c\tau + d}\right) = (c\tau + d)^n f(\tau). \quad (2.132)$$

Often times we are not interested in functions that transform nicely under the action of the full modular group $SL(2, \mathbb{Z})$, but only under certain subgroups $\Gamma \subseteq SL(2, \mathbb{Z})$. In particular, we will be interested in functions that transform nicely under the *congruence subgroups of level N* ,

$$\begin{aligned} \Gamma_0(N) &= \left\{ \begin{pmatrix} a & b \\ c & d \end{pmatrix} \in SL(2, \mathbb{Z}) : c \equiv 0 \pmod{N} \right\} \\ \Gamma_1(N) &= \left\{ \begin{pmatrix} a & b \\ c & d \end{pmatrix} \in SL(2, \mathbb{Z}) : c \equiv 0 \pmod{N} \text{ and } a, d \equiv 1 \pmod{N} \right\} \\ \Gamma(N) &= \left\{ \begin{pmatrix} a & b \\ c & d \end{pmatrix} \in SL(2, \mathbb{Z}) : b, c \equiv 0 \pmod{N} \text{ and } a, d \equiv 1 \pmod{N} \right\}. \end{aligned} \quad (2.133)$$

We can further define for every congruence subgroup Γ the *vector space of all modular forms of weight n for Γ* , $\mathcal{M}_n(\Gamma)$. These vector spaces are always finite

dimensional and the prototypical examples of modular forms are the Eisenstein series $G_{2m}(\tau)$.

Every congruence subgroup of level N contains the matrix $\begin{pmatrix} 1 & N \\ 0 & 1 \end{pmatrix}$ which translates τ by N , $\tau \mapsto \tau + N$. Therefore, all modular forms in these subgroups are periodic with period N and allow for a q -expansion

$$f(\tau) = \sum_{m=0}^{\infty} a_m q_N^m, \quad (2.134)$$

where $q_N \equiv \exp(2\pi i\tau/N)$ and $q \equiv q_1$. Let us further mention that $SL(2, \mathbb{Z})$ acts separately on \mathbb{H} and $\mathbb{Q} \cup \{i\infty\}$ and the images of the latter under modular transformations play a special role in the mathematics literature. The elements of $\mathbb{Q} \cup \{i\infty\}$ are mapped onto distinct orbits under transformations from congruence subgroups Γ that are usually referred to as *cusps of Γ* and an element of $\mathcal{M}_n(\Gamma)$ that vanishes on all cusps is called a *cuspidal form of weight n for Γ* . We can then decompose the space of modular forms of weight n for Γ as

$$\mathcal{M}_n(\Gamma) = \mathcal{E}_n(\Gamma) \oplus \mathcal{S}_n(\Gamma), \quad (2.135)$$

where $\mathcal{S}_n(\Gamma)$ is the space of all cuspidal forms of weight n for Γ and $\mathcal{E}_n(\Gamma)$ is the *Eisenstein subspace of weight n for Γ* .

2.4.2 Iterated Integrals of Modular Forms

Similarly to the variations of polylogarithms we have seen before, we can also define iterated integrals of modular forms. Let $f_i(\tau)$ be modular forms, then we define [44, 45, 61]

$$I(f_{i_1}, \dots, f_{i_k}; \tau, \tau_0) = \int_{\tau_0}^{\tau} d\tau' f_{i_1}(\tau') I(f_{i_2}, \dots, f_{i_k}; \tau', \tau_0), \quad (2.136)$$

with $I(; \tau, \tau_0) \equiv 1$, $\tau, \tau_0 \in \bar{\mathbb{H}}$. and where the number of integrations k is called the *length* of the iterated integral I . While the underlying modular forms behave nicely under modular transformations, this nice behaviour does not carry over to their integrals. As iterated integrals, the functions defined in eq. (2.136) form a shuffle algebra

$$\begin{aligned} I(f_{i_1}, \dots, f_{i_k}; \tau, \tau_0) I(f_{i_{k+1}}, \dots, f_{i_{k+l}}; \tau, \tau_0) \\ = \sum_{\sigma \in \Sigma(k, l)} I(f_{i_{\sigma(1)}}, \dots, f_{i_{\sigma(k+l)}}; \tau, \tau_0), \end{aligned} \quad (2.137)$$

and hence the length is preserved under multiplications.

The total differential of iterated integrals of modular forms is unipotent and takes the form

$$\begin{aligned} dI(f_{i_1}, \dots, f_{i_k}; \tau, \tau_0) & \quad (2.138) \\ &= f_{i_1}(\tau)I(f_{i_2}, \dots, f_{i_k}; \tau, \tau_0) d\tau - f_{i_k}(\tau_0)I(f_{i_1}, \dots, f_{i_{k-1}}; \tau, \tau_0) d\tau_0. \end{aligned}$$

We can therefore define the symbol of iterated integrals of modular forms through the usual recursion as

$$\begin{aligned} \mathcal{S}(I(f_{i_1}, \dots, f_{i_k}; \tau, \tau_0)) &= \mathcal{S}(I(f_{i_2}, \dots, f_{i_k}; \tau, \tau_0)) \otimes f_{i_1}(\tau) d\tau \\ &\quad - \mathcal{S}(I(f_{i_1}, \dots, f_{i_{k-1}}; \tau, \tau_0)) \otimes f_{i_k}(\tau_0) d\tau_0. \end{aligned} \quad (2.139)$$

This recursion can be solved and we get the closed form

$$\begin{aligned} \mathcal{S}(I(f_{i_1}, \dots, f_{i_k}; \tau, \tau_0)) & \quad (2.140) \\ &= \sum_{m=0}^k (-1)^{k-m} \left(\hat{f}_{i_{m+1}}(\tau_0) \otimes \dots \otimes \hat{f}_{i_k}(\tau_0) \right) \sqcup \left(\hat{f}_{i_m}(\tau) \otimes \dots \otimes \hat{f}_{i_1}(\tau) \right), \end{aligned}$$

where we defined $\hat{f}_i(\tau) \equiv f_i(\tau) d\tau$ for compactness.

In the following we will choose the cusp at infinity, $\tau_0 = i\infty$, as the base point for iterated integrals of modular forms. As usual, all integrals with a different base point can be related to the ones starting from the cusp at infinity via path composition. If the modular forms f_i don't vanish at the cusp at infinity, the integral may diverge and need to be regularized. These divergences are captured by a power series in $\log q_0$ with $q_0 = \exp 2\pi i \tau_0 \rightarrow 0$ and we regularize the integral as [45, 61]

$$I(f_{i_1}, \dots, f_{i_k}; \tau) \equiv \lim_{\tau_0 \rightarrow i\infty} R[I(f_{i_1}, \dots, f_{i_k}; \tau, \tau_0)], \quad (2.141)$$

where R sets all appearances of $\log q_0$ to zero. This regularization preserves the shuffle algebra.

Since the space of modular forms is finite dimensional, we will assume without loss of generality that all modular forms f_i appearing in the iterated integrals are expressed in terms of basis elements and are thus linearly independent. Since the differential equation (2.138) is unipotent, we can define a coproduct for these iterated integrals as before. Let

$$J = \left(\int_{\gamma} \omega_1, \dots, \int_{\gamma} \omega_k \right)^{\top}, \quad (2.142)$$

with

$$\omega_j = [\hat{f}_{i_k}(\tau) | \dots | \hat{f}_{i_j}(\tau)], \quad (2.143)$$

and let

$$dJ = AJ. \quad (2.144)$$

Then it is easy to see from eq. (2.138) that $A_{ij} = \delta_{i,j+1} \hat{f}_{i_j}$ and we find the de Rham periods

$$\begin{aligned} \mathcal{S}([\omega_b, \omega_a]) &= \theta(b-a) [\hat{f}_{i_{b-1}}(\tau) | \dots | \hat{f}_{i_a}(\tau)] \\ &= \theta(b-a) \mathcal{S}(I(f_{i_b}, \dots, f_{i_{a-1}}; \tau)), \end{aligned} \quad (2.145)$$

where θ is the Heaviside step function. Then the coaction takes the closed form

$$\begin{aligned} \Delta(I(f_{i_1}, \dots, f_{i_k}; \tau)) \\ = \sum_{m=1}^{k+1} I(f_{i_m}, \dots, f_{i_k}; \tau) \otimes \mathcal{S}(I(f_{i_1}, \dots, f_{i_{m-1}}; \tau)). \end{aligned} \quad (2.146)$$

2.4.3 eMPLs Evaluated at Rational Points and IMFs

In this section we will demonstrate how to rewrite elliptic multiple polylogarithms on the torus as iterated integrals of modular forms. Let us start by defining what it means if an eMPL is evaluated at rational points. The generic elliptic multiple polylogarithm $\tilde{\Gamma} \left(\begin{smallmatrix} n_1 & \dots & n_k \\ z_1 & \dots & z_k \end{smallmatrix}; z, \tau \right)$ depends on $k+1$ variables $z_0 \equiv z, \dots, z_k$ as well as the parameter τ . We say that an elliptic multiple polylogarithm is evaluated at rational points if all

$$z_i = a_i + b_i \tau, \quad (2.147)$$

with $a_i, b_i \in \mathbb{Q}$. Any eMPL evaluated at rational points can be rewritten in terms of iterated integrals of modular forms and we will outline an algorithmic way to achieve this in the remainder of this section.

We will start with the coaction of an eMPL $\tilde{\Gamma} \left(\begin{smallmatrix} n_1 & \dots & n_k \\ z_1 & \dots & z_k \end{smallmatrix}; z, \tau \right)$ of length k . As we have seen in the previous chapter, the coaction of an eMPL is a linear combination of tensor products

$$\tilde{\Gamma} \left(\begin{smallmatrix} m_1, \dots, m_i \\ w_1, \dots, w_i \end{smallmatrix}; w, \tau \right) \otimes [g^{m_{i+1}}(w_{i+1}, \tau) \mathfrak{D}_{i+1} | \dots | g^{m_{i+1}}(w_k, \tau) \mathfrak{D}_k], \quad (2.148)$$

with $\mathfrak{D}_j \in \{dz_i, d\tau\}$. Note that the combined length of the eMPL in the first component and the de Rham period in the second component is equal to the length k of the original eMPL⁵. For eMPLs evaluated at rational points we have $dz_i = b_i d\tau$ and hence all differentials \mathfrak{D}_i are proportional to $d\tau$ and hence

⁵Treating eMPLs evaluating to numbers as the corresponding eMPLs

the coaction of an eMPL evaluated at rational points is a linear combination of terms of the form

$$\tilde{\Gamma}(w_1, \dots, w_i; w, \tau) \otimes \left[g^{(m_{i+1})}(w_{i+1}, \tau) d\tau \mid \dots \mid g^{(m_k)}(w_k, \tau) d\tau \right]. \quad (2.149)$$

We have said that any such eMPL can be written as iterated integrals of modular forms and hence its coaction must also be the coaction of an IMF. We must therefore be able to rewrite the differential forms appearing in the de Rham period of eq. (2.149) as modular forms. Let us at this point consider the integration kernels $g^{(n)}(z, \tau)$. As we have seen in the previous section, they can be related to the doubly periodic Eisenstein series $f^{(n)}(z, \tau)$, and for rational a, b we find

$$g^{(n)}(a + b\tau, \tau) = \sum_{k=0}^n \frac{(2\pi ib)^k}{k!} f^{(n-k)}(a + b\tau, \tau). \quad (2.150)$$

If z is a rational point then $f^{(n)}(z, \tau)$ is a modular form of weight n for a congruence group Γ [52]. In order to demonstrate this, let us first introduce a different notation for $f^{(n)}(z, \tau)$ evaluated at rational points. Due to the periodicity of f we can without loss of generality assume that $z = a + b\tau$ with

$$a = \frac{r}{N} \quad \text{and} \quad b = \frac{s}{N}, \quad (2.151)$$

for some $r, s, N \in \mathbb{N}$ and $r, s < N$. Then we define

$$h_{N,r,s}^{(n)}(\tau) \equiv f^{(n)}\left(\frac{r}{N} + \frac{s}{N}\tau, \tau\right). \quad (2.152)$$

The functions f behave nicely under modular transformations and we have [42]

$$f^{(n)}\left(\frac{z}{c\tau + d}, \frac{a\tau + b}{c\tau + d}\right) = (c\tau + d)^n f^{(n)}(z, \tau), \quad (2.153)$$

or equivalently

$$h_{N,r,s}^{(n)}\left(\frac{a\tau + b}{c\tau + d}\right) = (c\tau + d)^n h_{N,rd+sb,rc+sa}^{(n)}(\tau). \quad (2.154)$$

This suggests that the $h_{N,r,s}^{(n)}$ transform nicely under modular transformations for a group $\Gamma \subseteq SL(2, \mathbb{Z})$ if for all $\begin{pmatrix} a & b \\ c & d \end{pmatrix} \in \Gamma$ we have

$$(s, r) \begin{pmatrix} a & b \\ c & d \end{pmatrix} = (s, r) \pmod{N}. \quad (2.155)$$

In particular, $h_{N,r,s}^{(n)}$ is a modular form for $\Gamma(N)$ [52]. We can therefore rewrite the coaction of an eMPL evaluated at rational forms as linear combinations of

$$\tilde{\Gamma} \left(\begin{matrix} m_1, \dots, m_i \\ w_1, \dots, w_i \end{matrix}; w, \tau \right) \otimes \left[h_{N,r_{i+1},s_{i+1}}^{(n)}(\tau) d\tau \mid \dots \mid h_{N,r_k,s_k}^{(n)}(\tau) d\tau \right]. \quad (2.156)$$

Let us now demonstrate how to rewrite any eMPL evaluated at rational points as an iterated integral of modular forms. Note that the length of all appearing $\tilde{\Gamma}$ in the first argument of the tensor products (2.156) are either the original eMPL or of lower length. Collecting all appearing eMPLs in the coaction as well as all eMPLs appearing in their coaction etc. we get a list of eMPLs that is closed under taking the coaction. We can compute the representation of each of them in terms of iterated integrals of modular forms iteratively over their length. In the following, all iterated integrals of modular forms correspond to the integrals defined in eq. (2.141) where the modular forms $f_{i_j} = h_{N_j,r_j,s_j}^{(n_j)}$ correspond to Eisenstein series and where we write

$$I \left(\begin{matrix} n_1 & N_1 \\ r_1 & s_1 \end{matrix} \mid \dots \mid \begin{matrix} n_k & N_k \\ r_k & s_k \end{matrix}; \tau \right) \equiv I(h_{N_1,r_1,s_1}^{(n_1)}, \dots, h_{N_k,r_k,s_k}^{(n_k)}; \tau). \quad (2.157)$$

Let us now assume that we have a representation in terms of eMPLs of all lower-length eMPLs in the coaction of $f(\tau) = \tilde{\Gamma} \left(\begin{matrix} n_1 & \dots & n_k \\ z_1 & \dots & z_k \end{matrix}; z, \tau \right)$ evaluated at rational points. Similarly to finding relations among MPLs (c.f. sec. 2.2) we can use the coaction to rewrite eMPLs as IMFs. Let us start with the part consisting of tensors of the form $1 \otimes X_k$ where X_k is a symbol of length k . We replace the symbol in the second component by the corresponding iterated integral⁶ and multiply the two components to define

$$f_k(\tau) = \mu(\text{id} \otimes f) \Delta_{0,k} f(\tau) \quad (2.158)$$

where μ is the multiplication and $\Delta_{i,j}$ is the part of the coaction whose first entry is a eMPL of length i and the second entry is a symbol of length j , and

$$\int [f_{i_1} d\tau \mid \dots \mid f_{i_j} d\tau] = I(f_{i_j}, \dots, f_{i_1}, \tau) \quad (2.159)$$

is the iterated integral of modular forms with canonical base point defined in (2.141). Then $f_k(\tau)$ fixes all terms $1 \otimes X_k$ in the coaction of $f(\tau)$ and we have

$$\Delta_{0,k}(f(\tau) - f_k(\tau)) = 0. \quad (2.160)$$

Next we compute

$$f_{k-1}(\tau) = f_k(\tau) + \mu(\text{id}_I \otimes f) \Delta_{1,k-1}(f(\tau) - f_k(\tau)) \quad (2.161)$$

⁶Note the reversal of words in the definition of the symbol of de Rham periods.

where id_I replaces all eMPLs at rational points by their corresponding iterated integrals of modular forms, after which we have fixed all terms in $\Delta_{1,k-1}$ as well as $\Delta_{0,k}$,

$$\Delta_{0,k}(f(\tau) - f_{k-1}(\tau)) = \Delta_{1,k-1}(f(\tau) - f_{k-1}(\tau)) = 0. \quad (2.162)$$

After iterating this procedure we arrive at a point where the only term left to fix is the term

$$(f(\tau) - f_1(\tau)) \otimes 1 = \Delta(f(\tau) - f_1(\tau)). \quad (2.163)$$

We can infer from eq. (2.163) that $f(\tau) - f_1(\tau)$ is a constant and we have

$$f(\tau) = c + f_1(\tau). \quad (2.164)$$

All iterated integrals of modular forms in f_1 are defined with the canonical base point $\tau_0 = i\infty$ and hence vanish in the limit $\tau \rightarrow i\infty$. We can therefore compute the missing constant c as the value of $f(\tau)$ at the cusp at infinity,

$$c = \text{Cusp}f(\tau) \equiv \lim_{\tau \rightarrow i\infty} f(\tau). \quad (2.165)$$

Let us demonstrate this procedure at an example. Consider the eMPL $f(\tau) = \tilde{\Gamma}\left(\begin{smallmatrix} 0 & 1 \\ 0 & \tau/3 \end{smallmatrix}; \frac{1}{6}, \tau\right)$. We assume that we already know how to write the lower-length eMPLs appearing in the coaction in terms of iterated integrals of modular forms,

$$\tilde{\Gamma}\left(\begin{smallmatrix} 0 & 1 \\ 0 & \tau/3 \end{smallmatrix}; \frac{1}{6}, \tau\right) = \frac{1}{6}, \quad (2.166)$$

$$\tilde{\Gamma}\left(\begin{smallmatrix} 1 & 1 \\ \tau/3 & \tau/3 \end{smallmatrix}; \frac{1}{6}, \tau\right) = \frac{i\pi}{6} + \frac{i}{2\pi}I\left(\begin{smallmatrix} 2 & 6 \\ 0 & 2 \end{smallmatrix}; \tau\right) - \frac{i}{2\pi}I\left(\begin{smallmatrix} 2 & 6 \\ 1 & 4 \end{smallmatrix}; \tau\right), \quad (2.167)$$

$$\begin{aligned} \tilde{\Gamma}\left(\begin{smallmatrix} 2 & 1 \\ \tau/3 & \tau/3 \end{smallmatrix}; \frac{1}{6}, \tau\right) &= -\frac{\pi^2}{18} - \frac{1}{3}I\left(\begin{smallmatrix} 2 & 6 \\ 0 & 2 \end{smallmatrix}; \tau\right) + \frac{1}{3}I\left(\begin{smallmatrix} 2 & 6 \\ 1 & 4 \end{smallmatrix}; \tau\right) + \frac{2i}{3\pi}I\left(\begin{smallmatrix} 3 & 6 \\ 3 & 2 \end{smallmatrix}; \tau\right) \\ &+ \frac{i}{\pi}I\left(\begin{smallmatrix} 3 & 6 \\ 3 & 2 \end{smallmatrix}; \tau\right) - \frac{2i}{3\pi}I\left(\begin{smallmatrix} 3 & 6 \\ 0 & 1 \end{smallmatrix}; \tau\right) - \frac{2i}{3\pi}I\left(\begin{smallmatrix} 3 & 6 \\ 3 & 1 \end{smallmatrix}; \tau\right). \end{aligned} \quad (2.168)$$

The coaction of $f(\tau)$ is given as

$$\begin{aligned} \Delta f(\tau) &= f(\tau) \otimes 1 + \frac{i}{2\pi}\tilde{\Gamma}\left(\begin{smallmatrix} 0 & 1 \\ 0 & \tau/3 \end{smallmatrix}; \frac{1}{6}, \tau\right) \otimes [h_{6,0,2}^{(2)}] + \frac{i\pi}{9}\tilde{\Gamma}\left(\begin{smallmatrix} 0 & 1 \\ 0 & \tau/3 \end{smallmatrix}; \frac{1}{6}, \tau\right) \otimes [1] \\ &- \frac{1}{3}\tilde{\Gamma}\left(\begin{smallmatrix} 1 & 1 \\ \tau/3 & \tau/3 \end{smallmatrix}; \frac{1}{6}, \tau\right) \otimes [1] - \frac{i}{2\pi}\tilde{\Gamma}\left(\begin{smallmatrix} 2 & 1 \\ \tau/3 & \tau/3 \end{smallmatrix}; \frac{1}{6}, \tau\right) \otimes [1] - \frac{1}{3\pi^2}1 \otimes [h_{6,0,1}^{(3)}|1] \\ &+ \frac{1}{3\pi^2}1 \otimes [h_{6,3,2}^{(3)}|1] + \frac{1}{2\pi^2}1 \otimes [h_{6,5,2}^{(3)}|1] - \frac{1}{3\pi^2}1 \otimes [h_{6,3,1}^{(3)}|1], \end{aligned} \quad (2.169)$$

where we have dropped the explicit dependence of the $h_{N,r,s}^{(n)}$ on τ as well as the differential $d\tau$ in each entry of the symbols $[h_1 | \dots | h_j]$. Then $f_2(\tau)$ defined

in eq. (2.158) is given by

$$\begin{aligned} f_2(\tau) = & -\frac{1}{3\pi^2} I\left(\begin{smallmatrix} 0 & 0 \\ 0 & 0 \end{smallmatrix} \middle| \begin{smallmatrix} 3 & 6 \\ 0 & 1 \end{smallmatrix}; \tau\right) + \frac{1}{3\pi^2} I\left(\begin{smallmatrix} 0 & 0 \\ 0 & 0 \end{smallmatrix} \middle| \begin{smallmatrix} 3 & 6 \\ 3 & 2 \end{smallmatrix}; \tau\right) \\ & + \frac{1}{2\pi^2} I\left(\begin{smallmatrix} 0 & 0 \\ 0 & 0 \end{smallmatrix} \middle| \begin{smallmatrix} 3 & 6 \\ 5 & 2 \end{smallmatrix}; \tau\right) - \frac{1}{3\pi^2} I\left(\begin{smallmatrix} 0 & 0 \\ 0 & 0 \end{smallmatrix} \middle| \begin{smallmatrix} 3 & 6 \\ 3 & 1 \end{smallmatrix}; \tau\right). \end{aligned} \quad (2.170)$$

Then f_2 fixes all terms in the coaction that have no eMPL as the first factor of the tensor product, $\Delta_{0,2}(f(\tau) - f_2(\tau)) = 0$. Looking at the terms that have an eMPL of length 1 as the first factor of the tensor product and replacing all appearing eMPLs by IMFs, we find

$$(\text{id}_I \otimes \text{id})\Delta_{1,1}(f(\tau) - f_2(\tau)) = \frac{i}{12\pi} 1 \otimes [h_{6,0,2}^{(2)}] - \frac{i\pi}{108} 1 \otimes [1]. \quad (2.171)$$

Following the above algorithm we find

$$f_1(\tau) = f_2(\tau) + \frac{i}{12\pi} I\left(\begin{smallmatrix} 2 & 6 \\ 0 & 2 \end{smallmatrix}; \tau\right) - \frac{i\pi}{108} I\left(\begin{smallmatrix} 0 & 0 \\ 0 & 0 \end{smallmatrix}; \tau\right), \quad (2.172)$$

which should capture the entire dependence of $f(\tau)$ on τ . Indeed we have

$$f(\tau) = \text{Cusp}(f(\tau)) + f_1(\tau) = \frac{i\pi}{72} + f_1(\tau). \quad (2.173)$$

Let us quickly comment on the terms appearing in eq. (2.171). It appears that all τ dependent terms in the first factor of the coproduct have been cancelled and the only terms left are those containing the cusp values of the eMPLs appearing in the coaction of $f(\tau)$. One might wonder if this is generally true, and indeed it can easily be shown that this holds in general. Consider an eMPL $f(\tau) = \tilde{\Gamma}\left(\begin{smallmatrix} n_1 & \dots & n_k \\ z_1 & \dots & z_k \end{smallmatrix}; z, \tau\right)$ evaluated at rational points. Then the term $f_k(\tau)$ defined in eq. (2.158) captures all terms in the coaction $\Delta f(\tau)$ with a symbol of length k in the second factor. Now consider a term $\gamma_i \otimes X_{k-i}$ in the coaction of $f(\tau)$ where γ_i is an eMPL of length i and X_j is a symbol of length j . Let us assume that the τ -dependence in the first factor of $\Delta_{i,k-i}(f(\tau) - f_k)$ is not completely cancelled. Then, after rewriting γ_i in terms of IMFs, we must have a term

$$I(h_1 | \dots | h_i; \tau) \otimes [h_k | \dots | h_{i+1}] \subset \Delta_{i,k-i}(f(\tau) - f_k). \quad (2.174)$$

Following our algorithm this term will enter the final result as $I(h_1 | \dots | h_k; \tau)$. From the coaction for iterated integrals of modular forms we see that the coaction of this term will contain the term $1 \otimes [h_k | \dots | h_1]$ and must therefore already be part of $f_k(\tau)$. This tells us that we can simplify the algorithm outlined above. It is not necessary to compute all eMPLs appearing in the coproduct of $f(\tau)$ in terms of iterated integrals of modular forms. Instead we just need to compute their cusp values. Subsequently,

$$\text{id}_I f(\tau) = \mu(\text{Cusp} \otimes f)\Delta f(\tau) \quad (2.175)$$

gives the correct representation of $f(\tau)$ in terms of iterated integrals of modular forms.

This concludes our review of the special functions appearing in this work. We have defined all functions relevant for the description of scattering amplitudes and Feynman integrals appearing in the remainder of this thesis. We have also reviewed their function spaces and useful algebraic properties that will help us to perform the computations in the remainder of this thesis efficiently.

Chapter 3

The Multi-Regge Limit of Planar $\mathcal{N} = 4$ SYM

In this chapter, we will consider a special kinematical limit, called the multi-Regge limit, within the scope of $\mathcal{N} = 4$ supersymmetric Yang-Mills theory. The Regge limit $s \gg |t|$ was first considered in early QCD computations and it was shown that amplitudes in this limit were dominated by a gluon exchange in the t channel. The resummation [63–68] of large radiative corrections to parton-parton scattering in this limit in the Balitsky-Fadin-Kuraev-Lipatov (BFKL) theory gave rise to a description of strong interactions in this kinematical regime that, to leading accuracy, is valid to all orders in perturbation theory. This kinematical limit can be extended to amplitudes with higher multiplicities by assuming a strong rapidity ordering among the outgoing gluons. In these so-called multi-Regge kinematics (MRK), scattering processes are dominated by the t channel exchange of an effective particle called the Reggeon between the two initial partons which emits the other external gluons along its path. As we will see, we can completely describe the underlying geometry of scattering amplitudes in the multi-Regge limit of $\mathcal{N} = 4$ SYM allowing us to fully classify the functional space of the final result. The corresponding building-blocks describing parton scattering in MRK are multi-gluon amplitudes whose dependence on the rapidities of external particles is integrated out, reducing the problem to a two-dimensional one in terms of transverse momenta.

Scattering amplitudes in planar $\mathcal{N} = 4$ SYM in the euclidean region, where all Mandelstam invariants are negative, factorize to all orders in perturbation theory into certain building blocks describing the propagation of the Reggeon

and the emission of gluons along the t channel ladder after BFKL resummation. These building blocks are determined to all orders by four- and five-point amplitudes and scattering amplitudes in MRK in this region of phase-space are trivial [69–73]. Starting from six external gluons, amplitudes exhibit so-called Regge cuts that are not captured correctly by the Regge-factorized form. As a result, scattering amplitudes in the multi-Regge limit are no longer trivial after analytically continuing the energy components of a subset of the emitted gluons to a different Mandelstam region [69, 70]. This discontinuity is described to all orders by a dispersion integral closely related to the BFKL evolution equation, whose integrand can be written in a factorized form in Fourier-Mellin space.

In recent years, a lot of progress has been made in the computation of six-particle scattering in the multi-Regge limit of planar $\mathcal{N} = 4$ SYM, both at strong coupling [74, 75] and at weak coupling [33, 76–84]. It was found [33] that the six-point amplitude at leading logarithmic accuracy (LLA) can be described perturbatively in terms of single-valued harmonic polylogarithms [57]. Beyond six points, only two-loop amplitudes are known analytically to LLA [85, 86] and up to transcendental constants at next-to-leading logarithmic accuracy (NLLA) [87].

In this chapter we will study scattering amplitudes in the multi-Regge limit of planar $\mathcal{N} = 4$ SYM for any number N of external legs and for arbitrary helicity configurations. In particular, we will introduce a new computational formalism based on the single-valuedness of scattering amplitudes in this kinematical regime that will circumvent the computation of the multiple infinite sums usually required to evaluate Fourier-Mellin integrals. We foresee that this formalism can be applied to the computation of scattering amplitudes in MRK in planar $\mathcal{N} = 4$ SYM to all logarithmic accuracies as well as to the computation of certain scattering amplitudes beyond $\mathcal{N} = 4$ SYM. We will show that scattering amplitudes in MRK are naturally described by iterated integrals over Riemann spheres with marked points and are therefore functions on the configuration space $\mathfrak{M}_{0,n}$ of genus 0 curves with n marked points. Iterated integrals on $\mathfrak{M}_{0,n}$ can be expressed in terms of multiple polylogarithms with singularities when two of the marked points coincide [88].

In addition to developing a mathematical framework allowing us to compute scattering amplitudes efficiently, we show that scattering amplitudes in MRK in momentum space can be decomposed into certain building blocks that recur for different numbers of external particles. In particular we generalize the factorization of two-loop MHV amplitudes [85, 86] to higher loop orders and other helicity configurations. Then it will be possible to express an infinite number of scattering amplitudes as linear combinations of a finite number of

building blocks. In particular, at LLA, all ℓ -loop scattering amplitudes in the MHV configuration are determined by MHV amplitudes with up to $(\ell + 4)$ external legs.

3.1 Multi-Regge-Kinematics

Let us now define the multi-Regge limit in $\mathcal{N} = 4$ SYM and introduce some useful notation for the description of scattering amplitudes in this limit. We will be studying color-ordered scattering amplitudes of N gluons with all momenta outgoing. In multi-Regge kinematics (MRK), it is convenient to represent momenta in terms of lightcone coordinates with (complex) transverse momenta where we decompose a vector p into the parts

$$p^\pm \equiv p^0 \pm p^z, \quad \mathbf{p}_k \equiv p_{k\perp} = p_k^x + ip_k^y. \quad (3.1)$$

The scalar product in these coordinates is then given by

$$2p \cdot q = p^+ q^- + p^- q^+ - \mathbf{p}\bar{\mathbf{q}} - \bar{\mathbf{p}}\mathbf{q}. \quad (3.2)$$

Let us also without loss of generality choose the reference frame such that the momenta of the two initial gluons, p_1 and p_2 , are aligned with the z -axis and we have $p_2^z = p_2^0$ and hence $p_1^+ = p_2^- = \mathbf{p}_1 = \mathbf{p}_2 = 0$. The multi-Regge limit is defined as the limit where the produced gluons with momenta p_3, \dots, p_N are strongly ordered in rapidity, while their transverse components are all comparable. In lightcone coordinates, this reads

$$p_3^+ \gg p_4^+ \gg \dots p_{N-1}^+ \gg p_N^+, \quad |\mathbf{p}_3| \simeq \dots \simeq |\mathbf{p}_N|, \quad (3.3)$$

and the on-shell condition $p_i^2 = p_i^+ p_i^- - |\mathbf{p}_i|^2 = 0$ implies

$$p_N^- \gg p_{N-1}^- \gg \dots p_4^- \gg p_3^-. \quad (3.4)$$

This ordering also translates to the Lorentz invariants

$$s_{i(i+1)\dots j} \equiv (p_i + p_{i+1} + \dots + p_j)^2 = x_{(i-1)j}^2, \quad (3.5)$$

$$t_{i+1} \equiv q_i^2, \quad q_i \equiv -p_2 - \dots - p_{i+3} = x_{(i+3)1}. \quad (3.6)$$

Overall energy-momentum conservation dictates that the initial gluons are of the same order as the first and last produced gluon respectively,

$$p_1^- = -\sum_{i=3}^N p_i^- \simeq -p_N^-, \quad p_2^+ = -\sum_{i=3}^N p_i^+ \simeq -p_3^+, \quad 0 = \sum_{i=3}^N \mathbf{p}_i. \quad (3.7)$$

Then we find for the product of two vectors

$$\begin{aligned}
s_{12} &= 2p_1 \cdot p_2 \simeq p_3^+ p_N^- \\
s_{1i} &= 2p_1 \cdot p_i \simeq -p_i^+ p_N^- \\
s_{2i} &= 2p_2 \cdot p_i \simeq -p_3^+ p_i^- \\
s_{ij} &= 2p_i \cdot p_j \simeq p_i^+ p_j^-, \quad 3 \leq i < j \leq N,
\end{aligned} \tag{3.8}$$

where we used that $\mathbf{p}_i \simeq \mathbf{p}_j \simeq p_i^+ p_i^- + p_j^+ p_j^- \ll p_i^+ p_j^-$. Keeping only the leading terms in the kinematical invariants (3.5), we find that all invariants including the same number k of consecutive particles are of the same order and that they are larger than invariants involving $k - 1$ consecutive momenta. We further have, for the momentum transfers q_i (c.f. fig. 3.2), $q_i^+ \simeq p_{i+4}^+$, $q_i^- \simeq -p_{i+3}^-$ and therefore $-q_i^+ q_i^- \ll p_{i+3}^+ p_{i+3}^- \simeq |\mathbf{q}_i|^2$, which finally yields

$$\begin{aligned}
s_{12} \gg s_{3\dots N-1}, s_{4\dots N} \gg s_{3\dots N-2}, s_{4\dots N-1}, s_{5\dots N} \gg \dots \\
\dots \gg s_{34}, \dots, s_{N-1N} \gg -t_1, \dots, -t_{N-3}.
\end{aligned} \tag{3.9}$$

3.1.1 MRK in the Planar Limit

Let us now turn to planar $\mathcal{N} = 4$ SYM and investigate the effect of the rapidity-ordering in MRK on the conformally invariant cross-ratios (u_{1i}, u_{2i}, u_{3i}) introduced in eq. (1.29). As we have mentioned before, we can describe amplitudes in MRK as the emission of $N - 4$ particles from the t -channel exchange of a reggeon. As can be inferred from fig. 3.1, the cross-ratios can be related to the momenta q_i exchanged in the t -channel as [22, 23]

$$\begin{aligned}
u_{1i} &= 1 - \delta_i \frac{|\mathbf{k}_i + \mathbf{k}_{i+1}|^2}{|\mathbf{k}_{i+1}|^2} + \mathcal{O}(\delta_i^2), \\
u_{2i} &= \delta_i \frac{|\mathbf{q}_{i-1}|^2}{|\mathbf{q}_i|^2} + \mathcal{O}(\delta_i^2), \\
u_{3i} &= \delta_i \frac{|\mathbf{q}_{i+1}|^2 |\mathbf{k}_i|^2}{|\mathbf{q}_i|^2 |\mathbf{k}_{i+1}|^2} + \mathcal{O}(\delta_i^2),
\end{aligned} \tag{3.10}$$

where $k_i \equiv p_{i+3}$, $1 \leq i \leq N - 4$, denote the momenta of the gluons emitted along the t -channel ladder, and where the ratio $\delta_i \equiv k_{i+1}^+ / k_i^+$ corresponds to the separation in rapidity between the produced gluons. This ratio goes to zero as we approach the multi-Regge limit and the cross ratios in eq. (3.10) become trivial. We can however define the *reduced cross-ratios* [22, 23],

$$\begin{aligned}
\tilde{u}_{2i} &= \frac{u_{2i}}{1 - u_{1i}} = \frac{|\mathbf{q}_{i-1}|^2 |\mathbf{k}_{i+1}|^2}{|\mathbf{q}_i|^2 |\mathbf{k}_i + \mathbf{k}_{i+1}|^2} + \mathcal{O}(\delta_i), \\
\tilde{u}_{3i} &= \frac{u_{3i}}{1 - u_{1i}} = \frac{|\mathbf{q}_{i+1}|^2 |\mathbf{k}_i|^2}{|\mathbf{q}_i|^2 |\mathbf{k}_i + \mathbf{k}_{i+1}|^2} + \mathcal{O}(\delta_i),
\end{aligned} \tag{3.11}$$

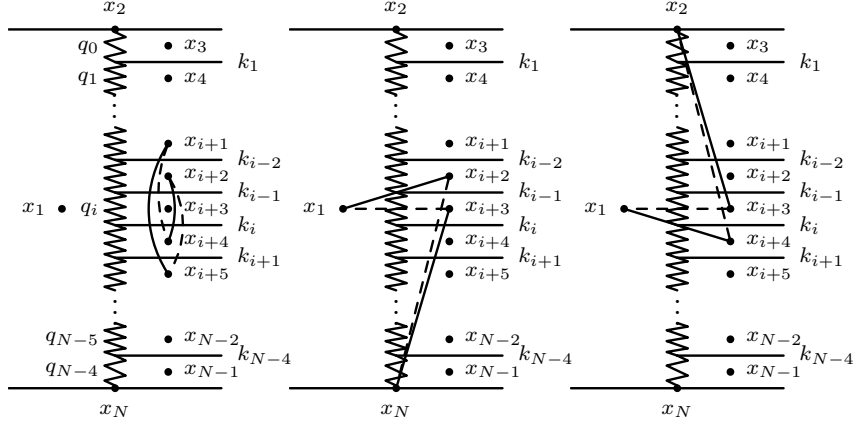


Figure 3.1: Connection between the three cross ratios u_{1i} (left) u_{2i} (middle) and u_{3i} (right) and the momentum transfers \mathbf{q}_i in t -channel reggeon exchange. Solid lines and dashed lines denote squared distances in the numerator and denominator, respectively.

which approach non-trivial values in the multi-Regge limit.

Let us now introduce transverse dual coordinates $\mathbf{x}_i \in \mathbb{C}\mathbb{P}^1$ as seen in fig. 3.2,

$$\mathbf{q}_i = \mathbf{x}_{i+2} - \mathbf{x}_1 \quad \text{and} \quad \mathbf{k}_i = \mathbf{x}_{i+2} - \mathbf{x}_{i+1}, \quad (3.12)$$

and relate them to the reduced cross-ratios \tilde{u}_{2i} and \tilde{u}_{3i} . These can be written as

$$\tilde{u}_{2i} \simeq |\xi_{2i}|^2 \quad \text{and} \quad \tilde{u}_{3i} \simeq |\xi_{3i}|^2, \quad (3.13)$$

with

$$\xi_{2i} = \frac{(\mathbf{x}_1 - \mathbf{x}_{i+1})(\mathbf{x}_{i+3} - \mathbf{x}_{i+2})}{(\mathbf{x}_1 - \mathbf{x}_{i+2})(\mathbf{x}_{i+3} - \mathbf{x}_{i+1})} \quad \text{and} \quad \xi_{3i} = \frac{(\mathbf{x}_1 - \mathbf{x}_{i+3})(\mathbf{x}_{i+2} - \mathbf{x}_{i+1})}{(\mathbf{x}_1 - \mathbf{x}_{i+2})(\mathbf{x}_{i+3} - \mathbf{x}_{i+1})}. \quad (3.14)$$

These cross-ratios are actually not independent and we have

$$\xi_i \equiv \xi_{2i} = 1 - \xi_{3i}. \quad (3.15)$$

Let us further introduce the cross-ratios

$$z_i \equiv 1 - \frac{1}{\xi_i} = \frac{(\mathbf{x}_1 - \mathbf{x}_{i+3})(\mathbf{x}_{i+2} - \mathbf{x}_{i+1})}{(\mathbf{x}_1 - \mathbf{x}_{i+1})(\mathbf{x}_{i+2} - \mathbf{x}_{i+3})} = -\frac{\mathbf{q}_{i+1} \mathbf{k}_i}{\mathbf{q}_{i-1} \mathbf{k}_{i+1}}. \quad (3.16)$$

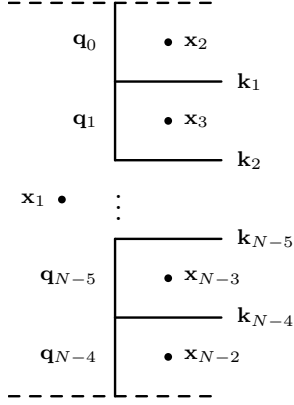


Figure 3.2: The t -channel ladder in transverse space with the corresponding dual coordinates. The dashed lines indicate the forward momenta that should be absent in this picture, as their transverse momentum is zero.

that will play an important role in the remainder of this chapter. They are related to the w_i that frequently appear in the literature via $w_i \equiv -z_i$.

Amplitudes in MRK are equipped with a natural \mathbb{Z}_2 symmetry, called *target-projectile symmetry* [22, 23], which corresponds to the mirror-symmetry of fig. 3.2 along the horizontal axis. It acts on the transverse dual coordinates via

$$\mathbf{x}_i \mapsto \begin{cases} \mathbf{x}_1, & \text{if } i = 1, \\ \mathbf{x}_{N-i}, & \text{if } 2 \leq i \leq N-2. \end{cases} \quad (3.17)$$

and on the cross ratios z_i as

$$z_i \mapsto 1/z_{N-4-i}. \quad (3.18)$$

3.1.2 Coordinate Systems on $\mathfrak{M}_{0,n}$

As we have seen, scattering amplitudes in the multi-Regge limit of $\mathcal{N} = 4$ SYM can be written in terms of the $n = N - 2$ transverse dual coordinates $\mathbf{x}_i \in \mathbb{CP}^1$ and can therefore be described by the configuration space $\text{Conf}_n(\mathbb{CP}^1)$. This space is isomorphic to the space of genus zero curves with n marked points, $\mathfrak{M}_{0,n}$. We will now discuss this space in more detail and review some choices of coordinates that are useful for the computation of scattering amplitudes in this limit. Geometrically, we can describe $\mathfrak{M}_{0,n}$ as the space of Riemann spheres

with n marked points. The Riemann sphere is symmetric under $SL(2, \mathbb{C})$ transformations and we will identify configurations of marked points that are related by such transformations. The space of $SL(2, \mathbb{C})$ transformations has dimension 3, and hence

$$\dim_{\mathbb{C}} \mathfrak{M}_{0,n} = n - 3. \quad (3.19)$$

We can find a basis of $\mathfrak{M}_{0,n}$ by using $SL(2, \mathbb{C})$ invariance to fix three of the points $\mathbf{x}_i \in \mathfrak{M}_{0,n}$ to concrete values. One such basis is given by the cross-ratios (3.16), which will play an important role in the description of the amplitude in so-called Fourier-Mellin space (c.f. sec. 3.2). We will therefore refer to these coordinates as *Fourier-Mellin coordinates*. While they are well suited for the description of scattering amplitudes in this space, they are not the optimal choice to express iterated integrals on $\mathfrak{M}_{0,n}$.

Let us now review some local coordinate systems called *simplicial coordinates*, studied in ref. [88], that allow for a nice description of scattering amplitudes in the multi-Regge limit. These coordinate systems can be obtained by setting three of the marked points on the Riemann sphere to 0, 1, and ∞ , e.g.

$$(\mathbf{x}_1, \dots, \mathbf{x}_n) \rightarrow (0, 1, \infty, t_1, \dots, t_{n-3}), \quad (3.20)$$

which gives

$$t_{i-3} = \frac{(\mathbf{x}_i - \mathbf{x}_1)(\mathbf{x}_2 - \mathbf{x}_3)}{(\mathbf{x}_i - \mathbf{x}_3)(\mathbf{x}_2 - \mathbf{x}_1)}, \quad 4 \leq i \leq n. \quad (3.21)$$

There are $6 \binom{n}{3} = n(n-1)(n-2)$ different sets of simplicial coordinates, and they are all equally well-suited to describe functions on $\mathfrak{M}_{0,n}$, as iterated integrals will only have singularities for $t_i \in \{0, 1, t_j\}$. There are, however, simplicial coordinates that transform nicely under the target-projectile symmetry of scattering amplitudes in MRK. These coordinates are given by fixing $(\mathbf{x}_1, \mathbf{x}_k, \mathbf{x}_{N-k})$, $2 \leq k \leq \lceil \frac{N-1}{2} \rceil$, or, for N even, $(\mathbf{x}_{N/2}, \mathbf{x}_k, \mathbf{x}_{N-k})$.

One set of these coordinates turns out to be particularly nice. When fixing the coordinates as

$$(\mathbf{x}_1, \dots, \mathbf{x}_{N-2}) \rightarrow (1, 0, \rho_1, \dots, \rho_{N-5}, \infty), \quad (3.22)$$

all two-loop MHV amplitudes at leading logarithmic accuracy in MRK factorise into sums of six-point amplitudes [85–87]. We will refer to these coordinates as *simplicial MRK coordinates*. They transform nicely under target-projectile symmetry,

$$(\rho_1, \dots, \rho_{N-5}) \mapsto (1/\rho_{N-5}, \dots, 1/\rho_1), \quad (3.23)$$

and are related to Fourier-Mellin coordinates as

$$z_i = \frac{(\rho_i - \rho_{i-1})(\rho_{i+1} - 1)}{(\rho_i - \rho_{i+1})(\rho_{i-1} - 1)}, \quad (3.24)$$

with $\rho_0 = 0$ and $\rho_{N-4} = \infty$.

Another class of simplicial coordinates that is well-suited for MRK is the class of all simplicial coordinates defined by

$$(\mathbf{x}_1, \dots, \mathbf{x}_{N-2}) \rightarrow (\infty, t_1^{(i)}, \dots, t_i^{(i)}, 0, 1, \dots, t_{N-5}^{(i)}). \quad (3.25)$$

These coordinates interpolate between Fourier-Mellin coordinates and simplicial coordinates, because $t_i^{(i)} = z_i$. These coordinates are not unique in the sense that there are other choices of coordinates with the property that $t_i^{(i)} = z_i$. We will refer to these coordinates as *simplicial coordinates based at z_i* .

3.2 The Ratio \mathcal{R}_N at Finite Coupling

Now that we have covered the kinematical dependence of scattering amplitudes in MRK in planar $\mathcal{N} = 4$ SYM, let us turn to a more concrete description of scattering amplitudes in this limit. The gluons going very forward are barely deflected and helicity must be conserved along their path. We will therefore label the BDS normalized ratio \mathcal{R} (c.f. (1.26)) only by the helicities $h_1 \dots h_{N-4}$ of the gluons produced along the ladder

$$e^{i\Phi_{h_1, \dots, h_{N-4}}} \mathcal{R}_{h_1, \dots, h_{N-4}} \equiv \left[\frac{A_N(-, +, h_1, \dots, h_{N-4}, +, -)}{A_N^{\text{BDS}}(-, +, \dots, +, -)} \right]_{\text{MRK}}. \quad (3.26)$$

The l.h.s. of eq. (3.26) is dual conformally invariant and tends to a phase, $e^{i\Phi}$, in the Euclidean region. This phase is immaterial for the remainder of this work and was made explicit such that $\mathcal{R} \rightarrow 1$ in the multi-Regge limit in the Euclidean region. After analytically continuing the final state momenta k_i of a consecutive set of particles $[p, q] \in \{1, \dots, N-4\}$ to a different *Mandelstam region*, the ratio \mathcal{R} will no longer be trivial due to the presence of a Regge cut (c.f. fig. 3.3) [23, 69, 70, 76–78, 86, 89, 90]. The function we obtain after analytic continuation of $q-p+1$ consecutive final state momenta is the same no matter the total number of external momenta. This means that we can reconstruct all other cases from the Mandelstam regions $[1, N-4]$ and we will therefore always consider that case.

By imposing a strong ordering in rapidity, the kinematical dependence on the longitudinal part factors into large logarithms $\log \tau_k$, with $\tau_k \equiv \sqrt{u_{2k} u_{3k}}$. It is

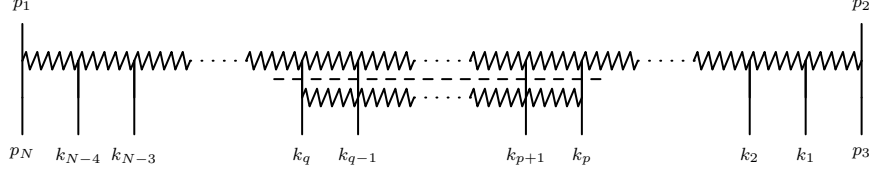


Figure 3.3: Diagrammatic representation of the Mandelstam region $[p, q]$. The discontinuity in the $(k_p + \dots + k_q)^2$ channel is indicated by the dashed line.

possible to resum these large logarithms to all orders in perturbation theory in Fourier-Mellin space where the amplitude is conjectured to factorize into three building blocks (c.f. fig. 3.4)

$$\omega(\nu_i, n_i) \equiv \omega_i = -a(E_i + aE_i^{(1)} + \mathcal{O}(a^2)), \quad (3.27)$$

$$\chi^\pm(\nu_i, n_i) \equiv \chi_i^\pm = \chi_{0,i}^\pm (1 + a\kappa_1^\pm + \mathcal{O}(a^2)), \quad (3.28)$$

$$C^\pm(\nu_i, n_i, \nu_j, n_j) \equiv C_{i,j}^\pm = C_{0,i,j}^\pm (1 + ac_{1,i,j}^\pm + \mathcal{O}(a^2)), \quad (3.29)$$

called the BFKL eigenvalue, impact factor and central emission block respectively. We will collectively refer to these objects as the *BFKL building blocks* and they are given explicitly in appendix C.

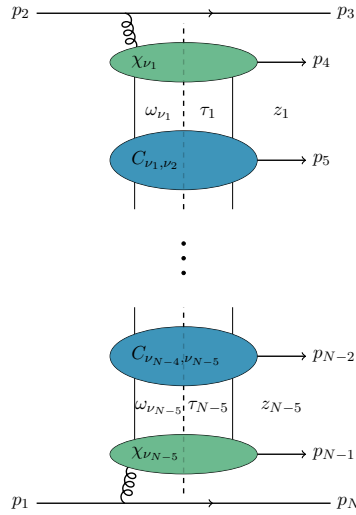


Figure 3.4: The structure of the N point amplitude in MRK.

Introducing the shorthand $\mathcal{R}_N \equiv \mathcal{R}_{h_1 \dots h_{N-4}}$, the conjectured factorized form of the remainder function reads

$$\mathcal{R}_N e^{i\delta_N} = 1 + a i\pi \mathcal{F}_{N-5} \left[\chi_1^{h_1} \left[\prod_{k=2}^{N-5} C_{k-1,k}^{h_k} \right] \chi_{N-5}^{-h_{N-4}} \prod_{k=1}^{N-5} e^{-L_k \omega_k} \right], \quad (3.30)$$

where a is the 't Hooft coupling and $L_k = \log \tau_k + i\pi$. The term δ_N is the so-called BDS phase,

$$\delta_N = \pi\Gamma \log \left| \frac{\rho_1}{(\rho_1 - 1)(\rho_{N-5} - 1)} \right|^2, \quad (3.31)$$

where

$$\Gamma \equiv \frac{\gamma_K}{8} = \frac{a}{2} - \frac{\zeta_2 a^2}{2} + \mathcal{O}(a^3) \quad (3.32)$$

is proportional to the cusp anomalous dimension γ_K known to all orders from integrability [91]. The BDS phase was introduced so that in the MHV configuration, the remainder R_N starts at two loops and the two-loop remainder is purely imaginary. The function \mathcal{F}_m in (3.30) denotes the m -fold inverse Fourier-Mellin transform,

$$\mathcal{F}_m \left[f(\{\nu_i, n_i\}) \right] \equiv \prod_{k=1}^m \sum_{n_k=-\infty}^{+\infty} \left(\frac{z_k}{\bar{z}_k} \right)^{n_k/2} \int_{-\infty}^{+\infty} \frac{d\nu_k}{2\pi} |z_k|^{2i\nu_k} f(\{\nu_i, n_i\}), \quad (3.33)$$

with the contour of integration given in fig. 3.5. The conjectural factorization in (3.30) reproduces the known Fourier-Mellin representation of the six-point MHV and NMHV amplitudes in MRK to LLA [69, 70, 86].

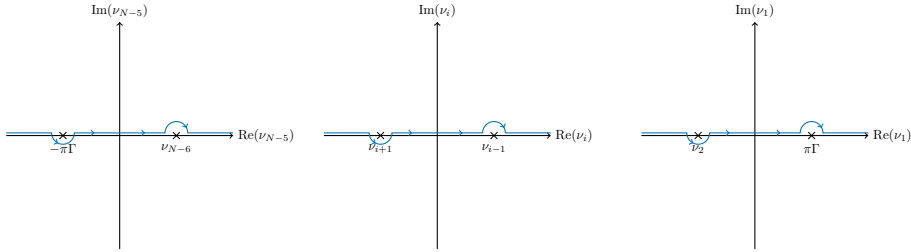


Figure 3.5: The initial integration contour for the N -gluon BFKL integral.

3.3 The Ratio \mathcal{R}_N at Weak Coupling

In the previous section we have introduced an all-order representation of the ratio \mathcal{R}_N in Fourier-Mellin space, we are however interested in a representation in

kinematical space. In order to achieve this, we would like to expand eq. (3.30) in the coupling a and solve the Fourier-Mellin integral on the r.h.s.. For small values of the coupling, the poles on the real axis in the contours in fig. 3.5 move towards one another and we would have pinched contours in the limit $a \rightarrow 0$. More precisely, the integral would develop a pinch singularity in the weak coupling limit when $n_{i-1} = n_i = 0$ for $i \in \{2, \dots, N-5\}$ for all integrands not proportional to a BFKL eigenvalue. These singularities can easily be regularized by deforming the contour of integration before approaching the weak coupling limit. In particular, we deform the contours from the initial contours given in fig. 3.5 that we will refer to as *Fourier-Mellin contours* to the contours given in fig. 3.6 which we will call *pinch-free contours*. An algorithmic way to perform these contour deformations is given in appendix F and explicit contour deformations for six, seven or eight external particles can be found in [3,4]. The contour deformations can be performed recursively over the number of external legs and the regularized integral can be written as the corresponding integral over pinch-free contours plus lower-point terms. Let us make this process a little more clear by considering the LLA and NLLA cases. For this purpose, we define $\mathcal{F}_{n,0} \equiv \mathcal{F}_n$ to denote the usual Fourier-Mellin transform defined with Fourier-Mellin contours and $\mathcal{F}_{0,n}$ to denote the corresponding Fourier-Mellin transform with pinch-free contours. This notation might seem arbitrary at this point but it is motivated by the algorithm described in appendix F.

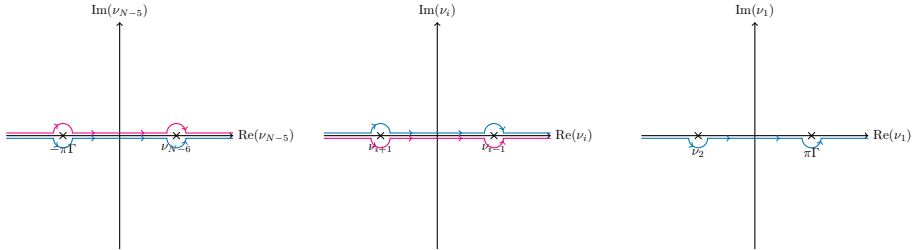


Figure 3.6: The integration contour for the N -gluon BFKL integral after contour deformation. The blue and red lines in the middle picture define the contour for even and odd i , respectively. Similarly, the blue and red lines in the last picture define the contour for odd and even N , respectively.

The one-loop amplitude is completely determined by the BDS amplitude, so we will start all our computations from two loops. At LLA, all two-loop (and higher loop) contributions contain at least one BFKL eigenvalue and hence the original integral

$$\mathcal{F}_{N-5} \left[\mathcal{I}_{N,LLA}^{(2)} \right] = \mathcal{F}_{N-5,0} \left[\mathcal{I}_{N,LLA}^{(2)} \right] \quad (3.34)$$

is finite. At NLLA, the two-loop contributions come without any insertion of the BFKL eigenvalue, and we need to regularize the Fourier-Mellin integral,

$$\begin{aligned} \mathcal{F}_{N-5} \left[\mathcal{I}_{N,\text{NLLA}}^{(2)} \right] &= \mathcal{F}_{N-5}^{\text{Reg}} \left[\mathcal{I}_{N,\text{NLLA}}^{(2)} \right] \\ &= \mathcal{F}_{0,N-5} \left[\mathcal{I}_{N,\text{NLLA}} \right] + P_{N,\text{NLLA}}^{(2)} + 2\pi i Q_{N,\text{NLLA}}^{(2)}, \end{aligned} \quad (3.35)$$

where P and Q correspond to the real- and imaginary parts of the lower-point functions introduced by the contour deformations. The explicit form of P and Q in the eight-particle case can be found in [4]. All higher-order NLLA contributions are finite and we keep the original contour. For explicit examples of P and Q we refer the reader to the aforementioned explicit examples in refs. [3, 4].

3.3.1 Perturbative Expansion of the Ratio \mathcal{R}_N

Now that we have regularized the integral (3.30), let us introduce some notation for the perturbative expansion of $\tilde{\mathcal{R}}_N \equiv \mathcal{R}_N e^{i\delta_N}$ that will prove useful in the following. At every loop order ℓ in MRK, the ratio $\tilde{\mathcal{R}}_N$ can be written as a polynomial in the logarithms $\log \tau_k$,

$$\begin{aligned} \tilde{\mathcal{R}}_{h_1, \dots, h_{N-4}} \left(\begin{matrix} \tau_1, \dots, \tau_{N-5} \\ z_1, \dots, z_{N-5} \end{matrix} \right) &= 1 + 2\pi i \sum_{\ell=1}^{\infty} \sum_{i_1, \dots, i_{N-5}=0}^{\ell-1} a^\ell \left(\prod_{k=1}^{N-5} \frac{1}{i_k!} \log^{i_k} \tau_k \right) \\ &\times \left(\tilde{g}_{h_1, \dots, h_{N-4}}^{(\ell; i_1, \dots, i_{N-5})}(z_1, \dots, z_{N-5}) + 2\pi i \tilde{h}_{h_1, \dots, h_{N-4}}^{(\ell; i_1, \dots, i_{N-5})}(z_1, \dots, z_{N-5}) \right), \end{aligned} \quad (3.36)$$

and we will refer to the imaginary- and real parts \tilde{g} and \tilde{h} of their coefficients as *perturbative coefficients*. In the following, we will often suppress the explicit kinematical dependence of the perturbative coefficients and write

$$\tilde{g}_{h_1, \dots, h_{N-4}}^{(\ell; i_1, \dots, i_{N-5})} \equiv \tilde{g}_{h_1, \dots, h_{N-4}}^{(\ell; i_1, \dots, i_{N-5})}(z_1, \dots, z_{N-5}), \quad (3.37)$$

$$\tilde{h}_{h_1, \dots, h_{N-4}}^{(\ell; i_1, \dots, i_{N-5})} \equiv \tilde{h}_{h_1, \dots, h_{N-4}}^{(\ell; i_1, \dots, i_{N-5})}(z_1, \dots, z_{N-5}). \quad (3.38)$$

At every loop order ℓ , the LLA perturbative coefficients are those with $\ell - 1 = \sum i_k$, the NLLA coefficients those with $\ell - 2 = \sum i_k$ etc.. The LLA ratio is purely imaginary, and hence

$$\tilde{h}_{h_1, \dots, h_{N-4}}^{(\ell; i_1, \dots, i_{N-5})} = 0 \quad \text{for } \ell - 1 = \sum_{k=1}^{N-5} i_k. \quad (3.39)$$

In the following we will limit ourselves to the computation of the $\tilde{\mathcal{R}}$ at LLA and NLLA. Expanding the r.h.s. of eq. (3.30), we can find a representation of the perturbative coefficients as Fourier-Mellin integrals. At LLA, i.e. for $\ell - 1 = \sum i_k$, we find

$$\tilde{g}_{h_1 \dots h_{N-4}}^{(\ell; i_1, \dots, i_{N-5})} = -\frac{1}{2} \mathcal{F}_{N-5} \left[\varpi_N \prod_{k=1}^{N-5} E_{\nu_k, n_k}^{i_k} \right], \quad (3.40)$$

where we have introduced the *vacuum ladder*

$$\varpi_N \equiv \chi_{0,1}^{h_1} \left[\prod_{i=2}^{N-5} C_{0, i-1, i}^{h_i} \right] \chi_{0, N-5}^{-h_{N-4}}. \quad (3.41)$$

This combination of leading-order impact factors and central emission blocks will appear in the description of all perturbative coefficients, and can be seen as the vacuum state where all other building blocks, like the E_i in eq. (3.40), play the role of insertions into the vacuum.

At NLLA, i.e. for $\ell - 2 = \sum i_k$, the situation becomes slightly more complicated, and it is helpful to introduce the *corrected perturbative coefficients*. Corrected perturbative coefficients are labelled by an additional leading index j in the superscript or subscript respectively, and we write

$$\begin{aligned} \tilde{g}_{h_1 \dots h_{N-4}}^{(\ell; i_1, \dots, i_{N-5})} &= \sum_{j=1}^{N-5} i_j \tilde{g}_{h_1 \dots h_{N-4}}^{j; (\ell; i_1, \dots, i_{N-5})} + \sum_{j=1}^{N-4} \tilde{g}_{j; h_1 \dots h_{N-4}}^{(\ell; i_1, \dots, i_{N-5})}, \\ \tilde{h}_{h_1 \dots h_{N-4}}^{(\ell; i_1, \dots, i_{N-5})} &= \sum_{j=1}^{N-5} \tilde{h}_{h_1 \dots h_{N-4}}^{j; (\ell; i_1, \dots, i_{N-5})} + \sum_{j=1}^{N-4} \tilde{h}_{j; h_1 \dots h_{N-4}}^{(\ell; i_1, \dots, i_{N-5})}. \end{aligned} \quad (3.42)$$

The additional upper indices represent insertions of corrections to BFKL eigenvalues and additional lower indices represent insertions of corrections to impact factors or central emission blocks into the vacuum ladder. In particular, we have

$$\begin{aligned} \tilde{g}_{h_1 \dots h_{N-4}}^{j; (\ell; i_1, \dots, i_{N-5})} &= \frac{1}{2} \mathcal{F}_{N-5} \left[\varpi_N E_j^{(1)} \prod_{k=1}^{N-5} E_k^{i_k - \delta_{kj}} \right], \\ \tilde{g}_{j; h_1 \dots h_{N-4}}^{(\ell; i_1, \dots, i_{N-5})} &= \frac{1}{2} \mathcal{F}_{N-5} \left[\varpi_N X_j \prod_{k=1}^{N-5} E_k^{i_k} \right], \end{aligned} \quad (3.43)$$

where

$$X_j = \begin{cases} \kappa_{1,1}^{h_1} & j = 1 \\ \kappa_{1, N-5}^{h_{N-4}} & j = N - 4 \\ \text{Re}(c_{1, j-1}^{h_j}) & 2 \leq j \leq N - 5 \end{cases}. \quad (3.44)$$

Similarly, for the real part, we find

$$\begin{aligned}\tilde{h}_{h_1 \dots h_{N-4}}^{j;(\ell; i_1, \dots, i_{N-5})} &= -\frac{1}{4} \mathcal{F}_{N-5} \left[\varpi_N E_j \prod_{k=1}^{N-5} E_k^{i_k} \right], \\ \tilde{h}_{j; h_1 \dots h_{N-4}}^{(\ell; i_1, \dots, i_{N-5})} &= \frac{1}{4\pi} \mathcal{F}_{N-5} \left[\varpi_N Y_j \prod_{k=1}^{N-5} E_k^{i_k} \right],\end{aligned}\tag{3.45}$$

where

$$Y_j = \begin{cases} 0 & j = 1, N-4 \\ \text{Im}(c_{1,j-1}^{h_j}) & 2 \leq j \leq N-5 \end{cases}.\tag{3.46}$$

It will also be useful to define the corrected perturbative coefficient corresponding to the correction to the entire vacuum ladder,

$$\begin{aligned}\tilde{g}_{\varpi; h_1 \dots h_{N-4}}^{(\ell; i_1, \dots, i_{N-5})} &= \sum_{j=1}^{N-4} \tilde{g}_{j; h_1 \dots h_{N-4}}^{(\ell; i_1, \dots, i_{N-5})} \\ \tilde{h}_{\varpi; h_1 \dots h_{N-4}}^{(\ell; i_1, \dots, i_{N-5})} &= \sum_{j=1}^{N-4} \tilde{h}_{j; h_1 \dots h_{N-4}}^{(\ell; i_1, \dots, i_{N-5})}.\end{aligned}\tag{3.47}$$

3.4 The Convolution-Formalism for MRK Amplitudes

In this section, we will discuss the computation of the perturbative coefficients that we have introduced in the last section. Traditionally, these computations are performed by closing the integration contour in the upper- or lower-half plane and summing the residues of the integrand [33, 76, 81, 83, 84, 86]. This works very well for the six-point amplitude, where the two-fold sums can be computed in terms of MPLs using standard techniques [31, 92–95], for more and more points, however, these computations quickly become unmanageable.

We will therefore introduce a new framework to perform computations of scattering amplitudes in the multi-Regge limit. The idea is to move away from explicitly computing Fourier-Mellin transformations and towards performing these computation directly in z -space using Fourier-Mellin convolutions

$$\mathcal{F}[F \cdot G] = \mathcal{F}[F] * \mathcal{F}[G] = f * g,\tag{3.48}$$

where the convolution defined as

$$(f * g)(z) = \frac{1}{\pi} \int \frac{d^2 w}{|w|^2} f(w) g\left(\frac{z}{w}\right).\tag{3.49}$$

Reading eq. (3.48) from right to left, we can insert BFKL building blocks into the integrand of a previously computed Fourier-Mellin transform. As a trade-off, we will have to perform integrals over the whole complex plane, which in itself poses a difficult task as well. Using the fact that scattering amplitudes in MRK are single-valued functions on $\mathfrak{M}_{0,N-2}$, we can make use of Stokes' theorem to greatly simplify these computations.

As is easy to see from eqs. (3.40), (3.43) and (3.45), all perturbative coefficients share a common basis, namely the vacuum ladder ϖ_N and only differ by the insertions of other building blocks into the integrand. In particular, at a fixed logarithmic order, two perturbative coefficients at different loop orders only differ by insertions of leading order BFKL eigenvalues E_k . This allows us to easily relate integrals at different loop orders through convolution integrals, and we have, for example,

$$g_{++}^{(\ell;\ell-1)} = -\frac{1}{2}\mathcal{F}[\chi^+ E^{\ell-1} \chi^-] = g_{++}^{(\ell-1;\ell-2)} * \mathcal{F}[E]. \quad (3.50)$$

Since the perturbative coefficients are single-valued functions in the cross-ratios z_i , the evaluation of the convolution integral can be simplified to a residue-computation as was shown in ref. [96]. Let $f(z)$ be a linear combination of single-valued polylogarithms whose coefficients are rational functions with singularities at $z = a_i$ and $z = \infty$. Then we can expand f around these singularities as

$$f(z) = \sum_{k,m,n} c_{k,m,n}^{a_i} \log^k \left| 1 - \frac{z}{a_i} \right|^2 (z - a_i)^m (\bar{z} - \bar{a}_i)^n, \quad z \rightarrow a_i, \quad (3.51)$$

$$f(z) = \sum_{k,m,n} c_{k,m,n}^\infty \log^k \frac{1}{|z|^2} \frac{1}{z^m} \frac{1}{\bar{z}^n}, \quad z \rightarrow \infty. \quad (3.52)$$

Let us define the holomorphic residue of f at $z = a$ as the coefficient of the simple holomorphic pole with no logarithmic singularities,

$$\text{Res}_{z=a} f(z) \equiv c_{0,-1,0}^a. \quad (3.53)$$

Then, if it exists, we can compute the integral of f over the whole complex plane as the sum of the holomorphic residues of its single-valued anti-holomorphic primitive F , i.e. if $\bar{\partial}F = f$, then [97]

$$\int \frac{d^2z}{\pi} f(z) = \text{Res}_{z=\infty} F(z) - \sum_i \text{Res}_{z=a_i} F(z). \quad (3.54)$$

Let us now show this procedure in detail at the example of the (already known [33, 81]) six-point MHV amplitude at LLA. We will compute the two-

loop perturbative coefficient

$$-2\tilde{g}_{++}^{(2;1)} = \mathcal{F}[\varpi_6 E] = \frac{1}{2}\mathcal{G}_{0,1}(z) + \frac{1}{2}\mathcal{G}_{1,0}(z) - \mathcal{G}_{1,1}(z) \quad (3.55)$$

from the Fourier-Mellin transform of the vacuum ladder

$$\mathcal{F}[\varpi_6] = \mathcal{G}_1(z) - \frac{1}{2}\mathcal{G}_0(z). \quad (3.56)$$

Apart from the Fourier-Mellin transform of the vacuum ladder, we also need the Fourier-Mellin transform of the BFKL eigenvalue,

$$\mathcal{E}(z_i) \equiv \mathcal{F}(E_i) = -\frac{z_i + \bar{z}_i}{2|1 - z_i|^2}. \quad (3.57)$$

The first step is to compute a single-valued anti-holomorphic primitive of

$$f(w) = \frac{1}{|w|^2} \mathcal{F}[\varpi_6](w) \mathcal{E}(z/w). \quad (3.58)$$

This is easily achieved after rewriting all appearing single-valued polylogarithms in terms of anti-holomorphic arguments,

$$\mathcal{G}_0(w) = \mathcal{G}_0(\bar{w}) \quad \text{and} \quad \mathcal{G}_1(w) = \mathcal{G}_1(\bar{w}). \quad (3.59)$$

Then we have

$$\begin{aligned} F(w) &= \int d\bar{w} f(w) = \frac{1}{2w(w-z)} \int d\bar{w} \left[\frac{1}{2}\mathcal{G}_0(\bar{w}) - \mathcal{G}_1(\bar{w}) \right] \frac{\bar{w}z + w\bar{z}}{\bar{w}(\bar{w} - \bar{z})} \\ &= \frac{1}{4(w-z)} [2\mathcal{G}_{0,z}(w) - 4\mathcal{G}_{1,z}(w) - \mathcal{G}_{0,0}(w) + 2\mathcal{G}_{1,0}(w) \\ &\quad - 4\mathcal{G}_1(w)\mathcal{G}_0(z) + 4\mathcal{G}_1(w)\mathcal{G}_1(z) + 2\mathcal{G}_0(z)\mathcal{G}_z(w) - 4\mathcal{G}_1(z)\mathcal{G}_z(w)] \\ &\quad + \frac{1}{4w} [-\mathcal{G}_{0,z}(w) + 2\mathcal{G}_{1,z}(w) + 2\mathcal{G}_1(w)\mathcal{G}_0(z) - 2\mathcal{G}_1(w)\mathcal{G}_1(z) \\ &\quad - \mathcal{G}_0(z)\mathcal{G}_z(w) + 2\mathcal{G}_1(z)\mathcal{G}_z(w)], \end{aligned} \quad (3.60)$$

where we have rewritten all single-valued polylogarithms in terms of holomorphic arguments using eqs. (3.59) and (2.61). The next step is to compute all residues of $F(w)$ and we can see that F has potential poles at 0, z and ∞ . Since for $w \rightarrow 0$ all polylogarithms either vanish or exhibit logarithmic singularities, the residue at $w = 0$ vanishes. At $w = z$, we have

$$\begin{aligned} \text{Res}_{w=z} F(w) &= -\frac{1}{4}\mathcal{G}_{0,0}(z) - \mathcal{G}_{0,1}(z) - \frac{1}{2}\mathcal{G}_{1,0}(z) + 2\mathcal{G}_{1,1}(z) - \mathcal{G}_{1,z}(z) \\ &= -\frac{1}{4}\mathcal{G}_{0,0}(z) - \frac{1}{2}\mathcal{G}_{1,0}(z) + \mathcal{G}_{1,1}(z). \end{aligned} \quad (3.61)$$

In order to compute the residue at $z = \infty$, we will need to replace $w \rightarrow \frac{1}{u}$, including the Jacobian, and compute the residue at $u = 0$, yielding

$$\text{Res}_{w=\infty} F(w) = \frac{1}{2} \mathcal{G}_{0,1}(z) - \frac{1}{4} \mathcal{G}_{0,0}(z). \quad (3.62)$$

Summing all residues according to eq. (3.54), we find

$$\begin{aligned} \mathcal{F}[\varpi_6 E] &= \text{Res}_{w=\infty} F(w) - \text{Res}_{w=z} F(w) \\ &= \frac{1}{2} \mathcal{G}_{0,1}(z) + \frac{1}{2} \mathcal{G}_{1,0}(z) - \mathcal{G}_{1,1}(z), \end{aligned} \quad (3.63)$$

which is indeed the correct answer.

Let us quickly comment on the Fourier-Mellin transform of the vacuum ladder. Since there is no insertion of BFKL eigenvalues, the integral $\mathcal{F}[\varpi_6]$ needs to be regularized and we have

$$\mathcal{F}[\varpi_6] = \mathcal{F}^{\text{Reg}}[\varpi_6] = \mathcal{F}_{0,1}[\varpi_6] + \frac{1}{8} \mathcal{G}_0(z) = \mathcal{G}_1(z) - \frac{1}{2} \mathcal{G}_0(z). \quad (3.64)$$

Then we should have performed the convolution on the Fourier-Mellin integral $\mathcal{F}_{0,1}[\varpi_6]$ only, to get

$$\mathcal{F}_{0,1}[\varpi_6 E] = \mathcal{F}_{0,1}[\varpi_6] * \mathcal{E}(z) = \left(\mathcal{F}[\varpi_6] - \frac{1}{8} \mathcal{G}_0(z) \right) * \mathcal{E}(z). \quad (3.65)$$

The reason why we got the correct result anyway is that

$$\mathcal{G}_0(z) * \mathcal{E}(z) = 0, \quad (3.66)$$

and that

$$\mathcal{F}[\varpi_6 E] = \mathcal{F}_{1,0}[\varpi_6 E] = \mathcal{F}_{0,1}[\varpi_6 E]. \quad (3.67)$$

This will not always be the case, as will be discussed in detail in section 3.4.2.

This procedure is not limited to the six-point case and allows us to compute (MHV) amplitudes of virtually any loop order provided we have a starting point for our recursion. At LLA, starting from

$$\tilde{g}_{+\dots+}^{(1;0,\dots,0)} = \frac{1}{4} \delta_N^{(1)}, \quad (3.68)$$

we can compute all MHV perturbative coefficients at any loop order by convolution with $\mathcal{E}_i \equiv \mathcal{E}(z_i)$. At NLLA the starting points will typically be the corrected perturbative coefficients

$$\tilde{g}_{\varpi;+\dots+}^{(2;0,\dots,0)}, \quad \tilde{h}_{\varpi;+\dots+}^{(2;0,\dots,0)} \quad \text{and} \quad \tilde{g}_{+\dots+}^{j;(3;0,\dots,i_j=1,\dots,0)}, \quad (3.69)$$

so that we will only ever have to perform convolutions with $\mathcal{E}(z_i)$. Let us stress that this formalism is not limited to performing convolutions with the building blocks \mathcal{E}_i . In fact, it is possible to insert any of the BFKL building blocks into the vacuum ladder. The reason why we choose to start off our recursion such that we only need to insert leading-order BFKL eigenvalues is that the starting points (3.69) are very easy to obtain.

Let us now extend this procedure to the computation of amplitudes in any helicity configuration. From

$$\mathcal{F} [\chi^+(\nu, n) F(\nu, n)] \longrightarrow \mathcal{F} [\chi^-(\nu, n) F(\nu, n)] \quad (3.70)$$

$$\begin{aligned} &= \mathcal{F} \left[\frac{\chi^-(\nu, n)}{\chi^+(\nu, n)} \right] * \mathcal{F} [\chi^+(\nu, n) F(\nu, n)] \quad (3.71) \\ &= \mathcal{H}(z) * \mathcal{F} [\chi^+(\nu, n) F(\nu, n)] , \end{aligned}$$

it is easy to see that we can flip the helicity of an impact factor χ by convolution with the *helicity flip kernel*

$$\begin{aligned} \mathcal{H}(z) &= \mathcal{F} \left[\frac{\chi_i^-}{\chi_i^+} \right] = \mathcal{H}^{(0)}(z_i) + a\mathcal{H}^{(1)}(z_i) + \mathcal{O}(a^2) \quad (3.72) \\ &= -\frac{z_i}{(1-z_i)^2} + \frac{a}{4} \left[\mathcal{G}_1(z_i) + \frac{z_i}{(1-z_i)} \mathcal{G}_0(z_i) + \frac{z_i}{(1-z_i)^2} \mathcal{G}_{0,0}(z_i) \right] \\ &\quad + \mathcal{O}(a^2) . \end{aligned}$$

The same kernel can also be used to flip the helicity of one of the central emission blocks, as can be inferred from the seven-point amplitude. Since MHV and $\overline{\text{MHV}}$ amplitudes are identical, we can relate a helicity flip on the central emission block to flipping the helicities of both impact factors:

$$\begin{aligned} g_{+++}^{(\ell; i_1, i_2)} &\longrightarrow g_{+-+}^{(\ell; i_1, i_2)} = \mathcal{H}(\bar{z}_1) * \mathcal{H}(z_2) * g_{---}^{(\ell; i_1, i_2)} \quad (3.73) \\ &= \mathcal{H}(\bar{z}_1) * \mathcal{H}(z_2) * g_{+++}^{(\ell; i_1, i_2)} . \end{aligned}$$

Let us comment on the leading-order helicity flip kernel $\mathcal{H}^{(0)}$. Let $f(z)$ be a pure function in z and let us convolute it with the leading order helicity flip kernel,

$$\mathcal{H}^{(0)}(z) * f(z) = - \int \frac{d^2 w}{\pi} \frac{z}{\bar{w}(w-z)^2} f(w) . \quad (3.74)$$

Computing the anti-holomorphic primitive, we find

$$\frac{z}{(w-z)^2} F(w) \equiv \int \frac{d\bar{w}}{\bar{w}} \frac{z}{(w-z)^2} f(w) . \quad (3.75)$$

Since the l.h.s. has a double pole in $w = z$, and assuming $f(w)$ is a linear combination of polylogarithms, there is no pole at infinity, and we have

$$\mathcal{H}^{(0)}(z) * f(z) = \text{Res}_{w=z} \frac{z F(w)}{(w-z)^2} = z \partial_z F(z). \quad (3.76)$$

We can therefore compute the leading-order helicity flip of any pure function by computing its single-valued anti-holomorphic primitive and taking a derivative.

We have seen how to efficiently compute higher loop scattering amplitudes in MRK given a certain lower-loop amplitude as a starting-point. It is, however, not clear yet how to find convenient starting points for Fourier-Mellin convolutions. In the next chapter we will introduce a property of perturbative coefficients called the *factorization theorem*, that will help us find some of these starting points and will reduce the number of necessary computations even further.

3.4.1 The Factorization Theorem for MRK Amplitudes

In this section we will show that two perturbative coefficients for different numbers of legs with the same pattern of insertions are closely related. More precisely, we will generalize the factorization of scattering amplitudes that was previously observed for the two-loop six-point case at LLA [85–87],

$$\tilde{\mathcal{R}}_{N,\text{MHV}}^{(2)} = 2\pi i a^2 \sum_{k=1}^{N-5} \log \tau_k \tilde{g}_{++}^{(2;1)}(\rho_k), \quad (3.77)$$

where we have expressed the result in terms of simplicial MRK coordinates. This implies

$$\begin{aligned} \tilde{g}_{+\dots+}^{(2;0,\dots,1,\dots,0)}(\rho_1, \dots, \rho_{N-5}) &= \tilde{g}_{++}^{(2;1)}(\rho_k) \\ &= \log |1 - \rho_k|^2 \log \left| 1 - \frac{1}{\rho_k} \right|^2, \end{aligned} \quad (3.78)$$

and it appears that we can drop all zero-indices $i_j = 0$ and the functional dependence on the corresponding simplicial MRK coordinate ρ_j . Let us now make this statement more precise. As a first step, we will limit ourselves to the leading-logarithmic case and introduce a graphical representation of the perturbative coefficients. As we have seen in fig. 3.2, we can naturally identify the faces of the diagram with the transverse dual coordinates \mathbf{x}_j and we can similarly label the same faces with the number i_j of insertions of BFKL eigen-

values E_{i_j} . Then, using simplicial MRK coordinates, and labelling outgoing lines with the helicity of the corresponding particle, we have

$$\tilde{g}_{h_1 \dots h_{N-4}}^{(\ell, i_1, \dots, i_{N-5})}(\rho_1, \dots, \rho_{N-5}) = 1 \cdot \begin{array}{c} \text{-----} \\ | \\ \hline 0 \\ \hline \rho_1 \quad i_1 \\ \hline h_1 \\ \hline \vdots \\ \hline h_2 \\ \hline \vdots \\ \hline h_{N-5} \\ \hline \rho_{N-5} \quad i_{N-5} \\ \hline h_{N-5} \\ \hline \infty \\ \hline \text{-----} \end{array}, \quad (3.79)$$

and the vacuum ladder corresponds to the diagram with all $i_j = 0$. Then the factorization theorem can be stated in the simple form

$$\begin{array}{c} \text{-----} \\ | \\ \hline \vdots \\ \hline \rho_c \quad i_c \\ \hline \rho_b \quad 0 \\ \hline h \\ \hline \rho_a \quad i_a \\ \hline \vdots \\ \hline \text{-----} \end{array} = \begin{array}{c} \text{-----} \\ | \\ \hline \rho_c \quad i_c \\ \hline h \\ \hline \rho_a \quad i_a \\ \hline \vdots \\ \hline \text{-----} \end{array}, \quad (3.80)$$

i.e. we delete those faces of the diagram that have no insertions and that are bounded by two external lines with the same helicities. Note that this only holds when at least one of the i_k is non-zero. In particular, this implies that we can delete all faces without the insertion of a BFKL eigenvalue in the MHV case,

$$\begin{aligned} \tilde{g}_{+\dots+}^{(\ell; 0, \dots, 0, i_{a_1}, 0, \dots, 0, i_{a_2}, 0, \dots, 0, i_{a_k}, 0, \dots, 0)}(\rho_1, \dots, \rho_{N-5}) \\ = \tilde{g}_{+\dots+}^{(\ell; i_{a_1}, i_{a_2}, \dots, i_{a_k})}(\rho_{i_{a_1}}, \rho_{i_{a_2}}, \dots, \rho_{i_{a_k}}). \end{aligned} \quad (3.81)$$

Beyond LLA we can have additional insertions into the vacuum ladder and will need to represent them graphically. At NLLA, we represent the correction to the BFKL eigenvalue with a double line at the base of the corresponding face and the correction to an impact factor or central emission block with a circle

around the corresponding vertex,

$$\tilde{g}_{h_1 \dots h_{N-4}}^{j;(\ell, i_1, \dots, i_{N-5})}(\rho_1, \dots, \rho_{N-5}) = \begin{array}{c} \text{---} \\ | \\ \text{---} h_1 \\ | \\ \text{---} h_{j-2} \\ | \\ \rho_{j-1} \quad i_{j-1} \\ | \\ \rho_j \quad i_j \\ | \\ h_{j-1} \\ | \\ h_j \\ | \\ \rho_{j+1} \quad i_{j+1} \\ | \\ h_{j+1} \\ | \\ \text{---} h_{N-4} \\ \text{---} \end{array}, \quad (3.82)$$

$$\tilde{g}_{j;h_1 \dots h_{N-4}}^{(\ell, i_1, \dots, i_{N-5})}(\rho_1, \dots, \rho_{N-5}) = \begin{array}{c} \text{---} \\ | \\ \text{---} h_1 \\ | \\ \text{---} h_{j-1} \\ | \\ \rho_{j-1} \quad i_{j-1} \\ | \\ \circ \quad \rho_j \quad i_j \\ | \\ h_j \\ | \\ h_{j+1} \\ | \\ \text{---} h_{N-4} \\ \text{---} \end{array}. \quad (3.83)$$

(3.84)

Then the factorization theorem is still essentially given by (3.80). In other words, we delete those faces of the diagram that have no insertions and that are bounded by two external lines with the same helicities that don't originate from a corrected vertex. Note that there is no conceptual difference in this regard between the imaginary- and the real part and we limit ourselves to defining the factorization for the imaginary parts. Replacing \tilde{g} by \tilde{h} in the definitions (3.82) and (3.83), all graphical equations will still be valid. A proof of the factorization theorem is given in appendix G.

Let us discuss the implications of the factorization theorem on the structure of scattering amplitudes in the multi-Regge limit of $\mathcal{N} = 4$ SYM. At LLA, and at ℓ loops, the sum of indices i_k is equal to $\ell - 1$ and hence we can have at most $\ell - 1$ non-zero indices. We can therefore only have a finite number of different perturbative coefficients at every loop order, generalizing the factorisation observed for the two-loop MHV amplitude in MRK to LLA [85–87]. Indeed, at two loops we find the factorization (3.77). At three loops the amplitude no longer factorizes completely into six-point terms and we find

$$\begin{aligned} \tilde{\mathcal{R}}_{++++}^{(3)} &= i\pi \sum_{i=1}^{N-5} \log^2 \tau_i \tilde{g}_{+++}^{(3;2)}(\rho_i) \\ &\quad + 2\pi i \sum_{1 \leq i < j \leq N-5} \log \tau_i \log \tau_j \tilde{g}_{++++}^{(3;1,1)}(\rho_i, \rho_j). \end{aligned} \quad (3.85)$$

At four loops, we will need to compute the eight-point perturbative coefficient $\tilde{g}_{++++}^{(4;1,1,1)}$ along with four-loop six- and seven-point perturbative coefficients.

Generally, all ℓ -loop MHV amplitudes at LLA are determined by the perturbative coefficients up to ℓ -loops with up to $(\ell + 4)$ external legs.

A similar statement can be made for amplitudes beyond LLA, but the number of perturbative coefficients that are needed to write the ℓ -loop amplitude for any number of particles grows quickly with the logarithmic order. At three loops, for example we find the factorization

$$\begin{aligned}
\frac{\tilde{\mathcal{R}}_{+\dots+}^{(3)}}{2\pi i} &= \log \tau_1 \tilde{g}_{1;+++}^{(3;1)}(\rho_1) + \log \tau_{N-5} \tilde{g}_{2;+++}^{(3;1)}(\rho_{N-5}) + \sum_{j=1}^{N-5} \log \tau_j \tilde{g}_{++}^{j;(3;1)}(\rho_j) \\
&+ \sum_{j=2}^{N-5} \left[\log \tau_{j-1} \tilde{g}_{2;+++}^{(3;1,0)}(\rho_{j-1}, \rho_j) + \log \tau_j \tilde{g}_{2;+++}^{(3;0,1)}(\rho_{j-1}, \rho_j) \right] \\
&+ \sum_{j=2}^{N-5} \left[\log \tau_{j-1} \tilde{g}_{3;+++}^{(3;1,0)}(\rho_{j-1}, \rho_{N-5}) + \log \tau_j \tilde{g}_{1;+++}^{(3;0,1)}(\rho_1, \rho_j) \right] \\
&+ \sum_{1 \leq i < j-1 \leq N-5} \log \tau_i \tilde{g}_{3;++++}^{(3;1,0,0)}(\rho_i, \rho_{j-1}, \rho_j) \\
&+ \sum_{1 \leq j < i \leq N-5} \log \tau_i \tilde{g}_{1;++++}^{(3;0,0,1)}(\rho_{j-1}, \rho_j, \rho_i) + 2\pi i (\tilde{g} \rightarrow \tilde{h})
\end{aligned} \tag{3.86}$$

In particular, we have to sum over all distributions of non-zero indices i_j relative to the corrected building blocks.

Beyond MHV we can no longer express all ℓ -loop amplitudes in terms of a finite number of perturbative coefficients, since the perturbative coefficients $\tilde{g}_{-+-+\dots}^{(\ell; i_1, \dots, i_{N-5})}$ don't have any neighbouring particles with equal helicities and will therefore not simplify to lower-point objects. It is nevertheless possible to obtain results for any number of external legs. In particular, for fixed k we can express all N^k MHV amplitudes in terms of a finite number of building blocks. At LLA we have, for example

$$\tilde{\mathcal{R}}_{-+-+\dots+}^{(2)} = 2\pi i \left[\log \tau_i \tilde{g}_{-+}^{(2;1)}(\rho_1) + \sum_{i=2}^{N-5} \log \tau_i \tilde{g}_{-++}^{(2;0,1)}(\rho_1, \rho_i) \right]. \tag{3.87}$$

3.4.2 Computing Scattering Amplitudes in MRK

Let us finish this section by outlining the strategy for computing scattering amplitudes at LLA and NLLA in the multi-Regge limit of planar $\mathcal{N} = 4$ SYM using convolutions. Fourier-Mellin convolutions allow us to exploit the single-valuedness of the perturbative coefficients to efficiently compute scattering amplitudes in MRK given a starting point for this recursion. A set of starting

points that is easily available are the perturbative coefficients

$$\tilde{g}_{+\dots+}^{(1;0,\dots,0)}, \quad \tilde{g}_{+\dots+}^{(2;0,\dots,0)}, \quad \tilde{h}_{+\dots+}^{(2;0,\dots,0)} \quad \text{and} \quad \tilde{g}_{++}^{1;(3;1)}. \quad (3.88)$$

Starting from these building blocks, all other perturbative coefficients can be computed using only convolutions with the building blocks $\mathcal{E}(z_i)$ and $\mathcal{H}(z_i)$ and using the factorization theorem. In addition, these building blocks can be easily obtained. The Fourier-Mellin transform of the vacuum ladder corresponds up to a factor to the BDS phase δ_N ,

$$\tilde{g}_{+\dots+}^{(1;0,\dots,0)} = \frac{1}{4}\delta_N^{(1)} = \frac{1}{4}\mathcal{G}_0(\rho_1) - \frac{1}{4}\mathcal{G}_1(\rho_1) - \frac{1}{4}\mathcal{G}_1(\rho_{N-5}). \quad (3.89)$$

The corrections to the vacuum ladder at NLLA can be determined from the two-loop MHV ratio $\mathcal{R}_N^{(2)}$ known for any number of particles at LLA [86] and NLLA [3, 87], and we have

$$\tilde{g}_{+\dots+}^{(2;0,\dots,0)} = \frac{\mathcal{R}_N^{(2)} - i\delta_N^{(2)}}{2\pi i} = \tilde{g}_{\overline{\omega};+\dots+}^{(2;0,\dots,0)}, \quad (3.90)$$

$$\tilde{h}_{+\dots+}^{(2;0,\dots,0)} = \frac{(i\delta_N^{(1)})^2}{2(2\pi i)^2} = \sum_{j=1}^{N-5} \tilde{h}_{+\dots+}^{j;(2;0,\dots,0)} + \tilde{h}_{\overline{\omega};+\dots+}^{(2;0,\dots,0)}. \quad (3.91)$$

The remaining starting point, $\tilde{g}_{++}^{1;(3;1)}$, corresponds to a six-point Fourier-Mellin integral that can easily be computed using available algorithms [31, 92–95]. In addition, many perturbative coefficients up to four loops have already been computed [1, 3, 4] and can be used as starting points as well.

Finally, let us comment on the regularization of Fourier-Mellin integrals with no insertions of BFKL eigenvalues and their effect on Fourier-Mellin convolutions. As we have already mentioned before, we still get the correct result when ignoring the regularization procedure at LLA when inserting a leading-order BFKL eigenvalue into the vacuum ladder. This statement does not generally extend to perturbative coefficients at higher logarithmic orders. The correct prescription is always to perform convolutions only on the well-defined Fourier-Mellin integrals appearing in the regularization procedure. At NLLA, the only integrals that need regularization are the two-loop perturbative coefficients and so we find, for convolutions with $\mathcal{E}(z_k)$,

$$\begin{aligned} \tilde{g}_{\overline{\omega};+\dots+}^{(3;\delta_{k,1},\dots,\delta_{k,3})} &= \mathcal{E}(z_k) * \left(\tilde{g}_{+\dots+}^{(2;0,\dots,0)} - P_{+\dots+}^{(2;0,\dots,0)} \right) + P_{+\dots+}^{(3;\delta_{k,1},\dots,\delta_{k,3})}, \\ \tilde{h}_{\overline{\omega};+\dots+}^{(3;\delta_{k,1},\dots,\delta_{k,3})} &= \mathcal{E}(z_k) * \left(\tilde{h}_{+\dots+}^{(2;0,\dots,0)} - Q_{+\dots+}^{(2;0,\dots,0)} \right) + Q_{+\dots+}^{(3;\delta_{k,1},\dots,\delta_{k,3})}. \end{aligned} \quad (3.92)$$

where P and Q are the corresponding coefficients from the perturbative expansion of the lower-point ratios introduced during the regularization procedure (3.35).

As we can infer from the algorithm outlined in appendix F, the Fourier-Mellin integrals with the two contour prescriptions are related by terms including lower-point ratios $\tilde{\mathcal{R}}$ and powers of $|z_i|$ only. Expanding these terms, it is easy to see that P and Q consist only of lower-point perturbative coefficients and powers of logarithms $\mathcal{G}_0(z_i)$. Recursively it can be shown that the only obstructions to Fourier-Mellin convolutions due to the regularization procedure can be reduced to the appearances of these logarithms and it can be shown [3, 4, 6] that we have, at NLLA,

$$P_{+\dots+}^{(3;\delta_{k,1},\dots,\delta_{k,3})} = \mathcal{E}(z_k) * P_{+\dots+}^{(2;0,\dots,0)}, \quad (3.93)$$

$$Q_{+\dots+}^{(3;\delta_{k,1},\dots,\delta_{k,3})} = \mathcal{E}(z_k) * \left(Q_{+\dots+}^{(2;0,\dots,0)} - \frac{1}{32} \mathcal{G}_0(z_k)^2 \right), \quad (3.94)$$

This implies that at NLLA we can perform convolutions directly on all perturbative coefficients with exception for the two-loop real part.

We have applied the convolution framework described above to compute perturbative coefficients \tilde{g} and \tilde{h} both at leading-logarithmic accuracy and at next-to-leading-logarithmic accuracy. In particular, we have computed all LLA perturbative coefficients required to describe all MHV amplitudes up to five loops for any number of external particles [1]. Beyond MHV we have computed all perturbative coefficients through four loops and up to eight external particles in all helicity configurations [1]. At NLLA we have computed all MHV perturbative coefficients required to write down all three-loop amplitudes for any number of external particles [3, 4]. Beyond MHV we have computed all amplitudes up to eight points and three loops in all helicity configurations [3, 4].

3.5 The Structure of Scattering Amplitudes

Let us finish this chapter by commenting on the structure of scattering amplitudes in the multi-Regge limit of $\mathcal{N} = 4$ SYM. For a formal analysis including proofs we refer the reader to our papers [1, 3, 4, 6]. It is believed that MHV and NMHV amplitudes in planar $\mathcal{N} = 4$ SYM can be written in terms of multiple polylogarithms [98] and that amplitudes beyond NMHV exhibit more general classes of special functions [99, 100]. Despite the lack of constraints on the possible function space of scattering amplitudes in general kinematics it was shown that the six-point amplitude expanded to LLA in the multi-Regge limit can be written in terms of polylogarithms to all orders in perturbation theory [81, 84]. This can prove to be valuable information on the structure of scattering amplitudes in general kinematics and it would be nice to have a similar statement for amplitudes with more external legs.

It can be shown [1, 3, 4, 6] that this is a universal property of scattering amplitudes in the multi-Regge limit of $\mathcal{N} = 4$ SYM that holds to all logarithmic accuracies and for any number of external legs. In particular, it is possible to show that scattering amplitudes in MRK can be written in terms of linear combinations of MPLs of uniform, maximally transcendental weight. The proof is performed using Fourier-Mellin convolutions to show that the insertion of elementary building blocks into the integrand raise the weight of an expression by a fixed amount.

Chapter 4

Transcendentality Properties of the BFKL Ladder

In the previous chapter we have studied the multi-Regge limit of scattering amplitudes in planar $\mathcal{N} = 4$ SYM. In particular, we have developed a computational framework that is especially well-suited for the computation of scattering amplitudes in this limit. In this section we will apply the convolution-formalism to the multi-Regge limit of scattering amplitudes in more general Yang-Mills theories and in particular in QCD.

As we have seen in the previous chapter, the multi-Regge limit naturally gives rise to large logarithms encoding the longitudinal part of the kinematical dependence and the scattering amplitude can be described by the t -channel exchange of an effective particle. Similarly, QCD scattering processes in the forward scattering limit $s \gg |t|$ are dominated by gluon exchanges in the t -channel. The BFKL resummation of logarithms $\log(s/|t|)$ in this limit can be achieved at LLA [63–65, 101] and at NLLA [66, 68].

The NLO corrections to the singlet eigenvalue of the BFKL equation had been previously approximated by Fadin and Lipatov [66] by acting with the NLO BFKL kernel on the leading-order eigenfunctions. This procedure, however is not consistent and it was already predicted by Fadin and Lipatov that the difference to the correct eigenvalue is due to terms related to the running of the coupling. Later, Chirilli and Kovchegov constructed the correct NLO eigenfunctions [102, 103] and found that the mismatch was indeed proportional to the beta function. In this chapter, we will show that these corrections to the

eigenfunctions can be eliminated by choosing the scale of the coupling to be the geometric mean of the transverse momenta at both ends of the BFKL ladder.

In ref. [104], it was shown that the BFKL ladder at LLA can be expressed in terms of SVMPLs (c.f. 2.2.2) on the moduli space $\mathfrak{M}_{0,4}$ of Riemann spheres with four marked points. We will extend this result and show that the analytic structure of the BFKL ladder at NLLA is described by the slightly larger class of gSVMPLs (c.f. 2.2.2). We will then use this property to develop techniques for the computation of the BFKL ladder in momentum space to any loop-order at LLA and NLLA and provide explicit results through five loops.

Finally, we will present necessary conditions for the BFKL ladder of a generic $SU(N)$ gauge theory with arbitrary matter content to have maximal transcendental weight. Solving these constraints, we find that the only theories satisfying them have a vanishing beta function and a matter content that can be arranged into supersymmetric multiplets. We also find that there is no theory capturing exactly the maximal transcendental part of QCD.

4.1 The BFKL Equation

Let us start by introducing the BFKL ladder and its connection to the BFKL equation. The BFKL ladder f is part of the total cross-section σ for parton scattering in the high-energy limit,

$$\sigma(s) \simeq \int \frac{d^2 q_1 d^2 q_2}{(2\pi)^2 q_1^2 q_2^2} \Phi_A(q_1) \Phi_B(q_2) f(q_1, q_2, \log(s/s_0)), \quad (4.1)$$

where $\Phi_{A/B}$ denote the impact factors, s is the center-of-mass energy and where we defined s_0 as the geometric mean of the transverse momenta q_1 and q_2 ,

$$s_0 \equiv \sqrt{q_1^2 q_2^2}. \quad (4.2)$$

The BFKL ladder can be written as

$$f(q_1, q_2, y) = \int_C \frac{d\omega}{2\pi i} e^{y\omega} f_\omega(q_1, q_2). \quad (4.3)$$

where the contour C is a straight vertical line such that all poles in ω are to the right of C . The function f_ω is a solution to the BFKL equation

$$\omega f_\omega(q_1, q_2) = \frac{1}{2} \delta^{(2)}(q_1 - q_2) + (\mathcal{K} \star f_\omega)(q_1, q_2). \quad (4.4)$$

and the integral operator \mathcal{K} acts as a convolution,

$$(\mathcal{K} \star f_\omega)(q_1, q_2) \equiv \int d^2k K(q_1, k) f_\omega(k, q_2), \quad (4.5)$$

where $K(q_1, q_2) = K(q_2, q_1)$ is the BFKL kernel. Due to the symmetry of the BFKL kernel, \mathcal{K} is hermitian and has real eigenvalues.

Solutions to the BFKL equation can be expressed in terms of a complete orthonormal set of eigenfunctions $\Phi_{\nu, n}$ of the BFKL integral operator,

$$(\mathcal{K} \star \Phi_{\nu n})(q) = \omega_{\nu n} \Phi_{\nu n}(q). \quad (4.6)$$

They are distinguished by a real number ν and an integer n and they are orthonormal and complete in the sense that

$$\begin{aligned} 2 \int d^2q \Phi_{\nu n}(q) \Phi_{\nu' n'}^*(q) &= \int_0^\infty dq^2 \int_0^{2\pi} d\theta \Phi_{\nu n}(q) \Phi_{\nu' n'}^*(q) \\ &= \delta(\nu - \nu') \delta_{nn'}, \end{aligned} \quad (4.7)$$

and

$$\sum_{n=-\infty}^{+\infty} \int_{-\infty}^{+\infty} d\nu \Phi_{\nu n}(q) \Phi_{\nu n}^*(q') = \frac{1}{2} \delta^{(2)}(q - q') = \delta(q^2 - q'^2) \delta(\theta - \theta'). \quad (4.8)$$

In conformally invariant theories, these eigenfunctions are completely fixed by symmetry constraints [105],

$$\varphi_{\nu n}(q) \equiv \Phi_{\nu n}^{CFT}(q) = \frac{1}{2\pi} (q^2)^{-1/2+i\nu} e^{in\theta}. \quad (4.9)$$

It is easy to check explicitly that the $\varphi_{\nu n}$ are complete and orthonormal.

Then the function

$$f_\omega(q_1, q_2) = \sum_{n=-\infty}^{+\infty} \int_{-\infty}^{+\infty} d\nu \frac{1}{\omega - \omega_{\nu n}} \Phi_{\nu n}(q_1) \Phi_{\nu n}^*(q_2) \quad (4.10)$$

is a solution to eq. (4.4), as can be easily verified using the completeness relation,

$$\begin{aligned} (\mathcal{K} \star f_\omega)(q_1, q_2) &= \sum_{n=-\infty}^{+\infty} \int_{-\infty}^{+\infty} d\nu \frac{1}{\omega - \omega_{\nu n}} (\mathcal{K} \star \Phi_{\nu n})(q_1) \Phi_{\nu n}^*(q_2) \\ &= \sum_{n=-\infty}^{+\infty} \int_{-\infty}^{+\infty} d\nu \frac{\omega_{\nu n}}{\omega - \omega_{\nu n}} \Phi_{\nu n}(q_1) \Phi_{\nu n}^*(q_2) \\ &= -\frac{1}{2} \delta^{(2)}(q_1 - q_2) + \omega f_\omega(q_1, q_2). \end{aligned} \quad (4.11)$$

Inserting f_ω into eq. (4.3), we arrive at

$$f(q_1, q_2, y) = \sum_{n=-\infty}^{+\infty} \int_{-\infty}^{+\infty} d\nu \Phi_{\nu n}(q_1) \Phi_{\nu n}^*(q_2) e^{y\omega_{\nu n}}. \quad (4.12)$$

In the following, we will focus on the perturbative expansion of the BFKL ladder in the renormalized strong coupling constant $\bar{\alpha}_\mu = N_C \alpha_S(\mu^2)/\pi$ evaluated at a scale μ^2 . The BFKL kernel, eigenvalue and eigenfunctions can each be expanded in $\bar{\alpha}_\mu$,

$$\begin{aligned} K(q_1, q_2) &= \bar{\alpha}_\mu \sum_{l=0}^{\infty} \bar{\alpha}_\mu^l K^{(l)}(q_1, q_2), \\ \omega_{\nu n} &= \bar{\alpha}_\mu \sum_{l=0}^{\infty} \bar{\alpha}_\mu^l \omega_{\nu n}^{(l)}, \\ \Phi_{\nu n}(q) &= \sum_{l=0}^{\infty} \bar{\alpha}_\mu^l \Phi_{\nu n}^{(l)}(q). \end{aligned} \quad (4.13)$$

The leading-order BFKL kernel $K^{(0)}$ [63–65, 101] gives the resummation at LLA, i.e. it captures all terms of $\mathcal{O}((\bar{\alpha}_\mu y)^n)$, the NLO kernel $K^{(1)}$ [66, 68] resums the terms at NLLA, i.e. of $\mathcal{O}(\bar{\alpha}_\mu (\bar{\alpha}_\mu y)^n)$, and so forth. The perturbative coefficients $\mathcal{K}^{(k)}$ of the BFKL integral operator are defined as the natural extension of the expansion of the BFKL kernel K . Note that the eigenfunctions are completely determined by conformal symmetry, and hence we expect their quantum corrections to be proportional to the beta function in order for them to vanish in conformal theories. Truncating the eigenvalues and eigenfunctions,

$$\omega_{\nu n}^{N^k LO} = \bar{\alpha}_\mu \sum_{l=0}^k \bar{\alpha}_\mu^l \omega_{\nu n}^{(l)} \quad \text{and} \quad \Phi_{\nu n}^{N^k LO}(q) = \sum_{l=0}^k \bar{\alpha}_\mu^l \Phi_{\nu n}^{(l)}(q), \quad (4.14)$$

we get eigenvalues and eigenfunctions of the truncated BFKL integral operator,

$$\left(\mathcal{K}^{N^k LO} \star \Phi_{\nu n}^{N^k LO} \right) (q) = \omega_{\nu n}^{N^k LO} \Phi_{\nu n}^{N^k LO}(q) + \mathcal{O}(\bar{\alpha}_\mu^{k+1}). \quad (4.15)$$

In the remainder of this chapter we will discuss the BFKL ladder at LLA, $f^{LL}(q_1, q_2, \eta_\mu)$, and at NLLA, $f^{NLL}(q_1, q_2, \eta_\mu)$, corresponding to the first two terms in the expansion of the BFKL ladder,

$$f(q_1, q_2, y) = f^{LL}(q_1, q_2, \eta_\mu) + \bar{\alpha}_\mu f^{NLL}(q_1, q_2, \eta_\mu) + \dots, \quad \eta_\mu = \bar{\alpha}_\mu y. \quad (4.16)$$

4.2 The BFKL ladder at leading logarithmic accuracy

Let us start by reviewing the BFKL ladder at LLA. Independently of the theory, the leading order BFKL kernel is conformally invariant and hence the leading-order eigenfunctions are given by eq. (4.9). The LO eigenvalue was computed in refs. [64, 65] and is given by

$$\chi_{\nu n} \equiv \omega_{\nu n}^{(0)} = -2\gamma_E - \psi\left(\frac{|n|+1}{2} + i\nu\right) - \psi\left(\frac{|n|+1}{2} - i\nu\right), \quad (4.17)$$

where $\gamma_E = -\Gamma'(1)$ is the Euler-Mascheroni constant and $\psi(z) = \frac{d}{dz} \log \Gamma(z)$ is the digamma function, and we have

$$(\mathcal{K}^{LO} \star \varphi_{\nu n})(q) = \chi_{\nu n} \varphi_{\nu n}(q). \quad (4.18)$$

Then, upon inserting the leading order eigenvalue and eigenfunctions into eq. (4.12), we find the BFKL ladder at LLA,

$$f^{LL}(q_1, q_2, \eta_\mu) = \sum_{n=-\infty}^{+\infty} \int_{-\infty}^{+\infty} d\nu e^{\eta_\mu \chi_{\nu n}} \varphi_{\nu n}(q_1) \varphi_{\nu n}^*(q_2), \quad (4.19)$$

and we define the perturbative coefficients f_k^{LL} through the expansion

$$f^{LL}(q_1, q_2, \eta_\mu) = \frac{1}{2} \delta^{(2)}(q_1 - q_2) + \frac{1}{2\pi \sqrt{q_1^2 q_2^2}} \sum_{k=1}^{\infty} \frac{\eta_\mu^k}{k!} f_k^{LL}(z). \quad (4.20)$$

The coefficients of powers of η_μ depend only on the variable

$$z \equiv \frac{\tilde{q}_1}{\tilde{q}_2}, \quad \text{with } \tilde{q}_k \equiv q_k^x + i q_k^y, \quad (4.21)$$

and can be written as a Fourier-Mellin transform

$$f_k^{LL}(z) = \mathcal{F}[\chi_{\nu n}^k] \equiv \sum_{n=-\infty}^{+\infty} \left(\frac{z}{\bar{z}}\right)^{n/2} \int_{-\infty}^{+\infty} \frac{d\nu}{2\pi} |z|^{2i\nu} \chi_{\nu n}^k. \quad (4.22)$$

The inverse of the Fourier-Mellin transform is given by

$$\mathcal{F}^{-1}[f(z)] = \int \frac{d^2 z}{\pi} z^{-1-i\nu-n/2} \bar{z}^{-1-i\nu+n/2} f(z). \quad (4.23)$$

In ref. [33] it was shown that the natural function space associated to Fourier-Mellin transforms of this type is the space of single-valued harmonic polylogarithms (SVHPLs) $\mathcal{G}(a_1, \dots, a_n; z)$, $a_i \in \{-1, 0, 1\}$, which form a subspace of the SVMPLs introduced in sec. 2.2.2.

A conjectural generating functional of the BFKL ladder at LLA was given in ref. [104] according to which all coefficients $f_k^{LL}(z)$ are given by a linear combination of SVHPLs with singularities at 0 and 1, including single-valued zeta values. Writing

$$f_k^{LL}(z) = \frac{|z|}{2\pi|1-z|^2} F_k(z), \quad (4.24)$$

the first few coefficients are given by [104],

$$\begin{aligned} F_1(z) &= 1, \\ F_2(z) &= 2\mathcal{G}_1(z) - \mathcal{G}_0(z), \\ F_3(z) &= 6\mathcal{G}_{1,1}(z) - 3\mathcal{G}_{0,1}(z) - 3\mathcal{G}_{1,0}(z) + \mathcal{G}_{0,0,0}(z), \\ F_4(z) &= 24\mathcal{G}_{1,1,1}(z) + 4\mathcal{G}_{0,0,1}(z) + 6\mathcal{G}_{0,1,0}(z) - 12\mathcal{G}_{0,1,1}(z) + 4\mathcal{G}_{1,0,0}(z) \\ &\quad - 12\mathcal{G}_{1,0,1}(z) - 12\mathcal{G}_{1,1,0}(z) - \mathcal{G}_{0,0,0}(z) + 8\zeta_3, \end{aligned} \quad (4.25)$$

where we used the shorthand $\mathcal{G}_{a_1, \dots, a_n}(z) \equiv \mathcal{G}(a_1, \dots, a_n; z)$. Generally, following the conjecture of ref. [104], all F_k are pure linear combinations of SVHPLs of uniform weight $(k-1)$ with singularities at most at $z=0$ or $z=1$.

Our goal is, to extend this analysis to NLLA and to analyse the analytic structure of the BFKL ladder at NLLA. We will start by deriving a consistent representation of the NLLA BFKL ladder as a Fourier-Mellin transform in the following section and by subsequently evaluating f^{NLL} perturbatively using Fourier-Mellin convolutions in section 4.4.

4.3 The BFKL ladder at next-to-leading logarithmic accuracy

4.3.1 Beyond the leading order: the Chirilli-Kovchegov procedure

The BFKL kernel in QCD was determined to NLO in ref. [66] and the corresponding corrections to the BFKL singlet eigenvalue, in the approximation where they are obtained by acting on the corrected BFKL kernel with the leading-order eigenfunctions, was computed in refs. [66, 106, 107]. In this approximation the NLO corrections to the BFKL eigenvalues, $\delta_{\nu n}$, are defined by the equation,

$$(\mathcal{K}^{NLO} \star \varphi_{\nu n})(q) \equiv \bar{\alpha}_S(q^2) \left(\chi_{\nu n} + \bar{\alpha}_S(q^2) \frac{\delta_{\nu n}}{4} \right) \varphi_{\nu n}(q) + \mathcal{O}(\bar{\alpha}_S^3(q^2)), \quad (4.26)$$

and are given by

$$\begin{aligned} \delta_{\nu n} &= 6\zeta_3 - \frac{1}{2}\beta_0 \chi_{\nu n}^2 + 4\gamma_K^{(2)} \chi_{\nu n} + \frac{i}{2}\beta_0 \partial_\nu \chi_{\nu n} + \partial_\nu^2 \chi_{\nu n} \\ &\quad - 2\Phi(n, \gamma) - 2\Phi(n, 1 - \gamma) - \frac{\Gamma(\gamma)\Gamma(1 - \gamma)}{2i\nu} [\psi(\gamma) - \psi(1 - \gamma)] \quad (4.27) \\ &\quad \times \left[\delta_{n0} \left(3 + \left(1 + \frac{N_f}{N_c^3} \right) \frac{2 + 3\gamma(1 - \gamma)}{(3 - 2\gamma)(1 + 2\gamma)} \right) \right. \\ &\quad \left. - \delta_{|n|2} \left(\left(1 + \frac{N_f}{N_c^3} \right) \frac{\gamma(1 - \gamma)}{2(3 - 2\gamma)(1 + 2\gamma)} \right) \right], \end{aligned}$$

where $\gamma = 1/2 + i\nu$, β_0 denotes the one-loop beta function and $\gamma_K^{(2)}$ the two-loop cusp anomalous dimension for QCD in the dimensional reduction (DRED)¹ scheme,

$$\beta_0 = \frac{11}{3} - \frac{2N_f}{3N_c}, \quad \gamma_K^{(2)} = \frac{1}{4} \left(\frac{64}{9} - \frac{10N_f}{9N_c} \right) - \frac{\zeta_2}{2}. \quad (4.28)$$

The functions $\Phi(n, \gamma)$ appearing in eq. (4.27) are defined as

$$\begin{aligned} \Phi(n, \gamma) &= \sum_{k=0}^{\infty} \frac{(-1)^{k+1}}{k + \gamma + |n|/2} \left(\psi'(k + |n| + 1) - \psi'(k + 1) \right. \\ &\quad \left. + (-1)^{k+1} [\beta'(k + |n| + 1) + \beta'(k + 1)] \right. \\ &\quad \left. - \frac{1}{k + \gamma + |n|/2} [\psi(k + |n| + 1) - \psi(k + 1)] \right), \quad (4.29) \end{aligned}$$

with

$$\beta'(z) = \frac{1}{4} \left[\psi' \left(\frac{1+z}{2} \right) - \psi' \left(\frac{z}{2} \right) \right]. \quad (4.30)$$

For $\mathcal{N} = 4$ SYM, the cusp anomalous dimension reads

$$\gamma_K^{(2)\mathcal{N}=4} = -\frac{1}{2} \zeta_2, \quad (4.31)$$

and we find the corrected BFKL eigenvalue

$$\delta_{\nu n}^{\mathcal{N}=4} = 6\zeta_3 + 4\gamma_K^{(2)\mathcal{N}=4} \chi_{\nu n} + \partial_\nu^2 \chi_{\nu n} - 2\Phi(n, \gamma) - 2\Phi(n, 1 - \gamma). \quad (4.32)$$

Since $\mathcal{N} = 4$ SYM is a conformal theory, the eigenfunctions are given to all orders by eq. (4.9) and hence $\delta_{\nu n}^{\mathcal{N}=4}$ is the correct NLO BFKL eigenvalue in $\mathcal{N} = 4$ SYM.

¹The DRED scheme is a regularization scheme similar to the dimensional regularisation introduced previously. It is primarily used in supersymmetric theories to preserve the number of degrees of freedom of the particles while still considering all momenta to be d dimensional.

As we have mentioned before, the NLO eigenvalue in eq. (4.27) was derived under the assumption that the eigenfunctions receive no perturbative corrections at NLO. This, of course, is not the case in non-conformal theories. Further, the BFKL eigenvalue must be real and independent of q^2 , which is not the case for the BFKL eigenvalue given above: the r.h.s. of eq. (4.26) contains the strong coupling constant evaluated at q^2 and the correction to the eigenvalue in eq. (4.27) contains the term $i\beta_0 \partial_\nu \chi_{\nu n}$, which is imaginary.

In refs. [102, 103], Chirilli and Kovchegov showed that it is possible to find the correct description of the BFKL eigenvalue by modifying the leading-order eigenfunctions with terms depending on the running coupling. We will now review this procedure and construct the eigenfunctions and corresponding eigenvalues at NLO for any value of n .

Our goal is to construct functions $\omega_{\nu n}^{(1)}$ and $\Phi_{\nu n}^{(1)}(q)$ such that

$$\begin{aligned} & \left[\mathcal{K}^{NLO} \star \left(\varphi_{\nu n} + \bar{\alpha}_\mu \Phi_{\nu n}^{(1)} \right) \right] (q) \\ &= \bar{\alpha}_\mu \left(\chi_{\nu n} + \bar{\alpha}_\mu \omega_{\nu n}^{(1)} \right) \left[\varphi_{\nu n}(q) + \bar{\alpha}_\mu \Phi_{\nu n}^{(1)}(q) \right] + \mathcal{O}(\bar{\alpha}_\mu^3). \end{aligned} \quad (4.33)$$

We start with an Ansatz for the NLO eigenvalue $\omega_{\nu n}^{(1)}$ by modifying $\delta_{\nu n}$ with an unknown function $c_{\nu n}$ as

$$\omega_{\nu n}^{(1)} = \frac{\delta_{\nu n}}{4} + c_{\nu n} = i \frac{\beta_0}{8} \partial_\nu \chi_{\nu n} + \Delta_{\nu n} + c_{\nu n}, \quad (4.34)$$

where $\Delta_{\nu n}$ contains all terms in eq. (4.27) that are symmetric under $\nu \rightarrow -\nu$, and we expect $\omega_{\nu n}^{(1)}$ to be symmetric as well. Inserting this parametrization into eq. (4.33) and using eq. (4.26) and the running of the coupling at NLO,

$$\bar{\alpha}_S(q^2) = \frac{\bar{\alpha}_S(\mu^2)}{1 + \frac{\beta_0}{4} \bar{\alpha}_S(\mu^2) \log \frac{q^2}{\mu^2}} = \bar{\alpha}_\mu \left[1 - \bar{\alpha}_\mu \frac{\beta_0}{4} \log \frac{q^2}{\mu^2} + \mathcal{O}(\bar{\alpha}_\mu^2) \right], \quad (4.35)$$

we find

$$\left(\mathcal{K}^{LO} \star \Phi_{\nu n}^{(1)} \right) (q) = \left(c_{\nu n} + \frac{\beta_0}{4} \chi_{\nu n} \log \frac{q^2}{\mu^2} \right) \varphi_{\nu n}(q) + \chi_{\nu n} \Phi_{\nu n}^{(1)}(q). \quad (4.36)$$

Following refs. [102, 103], eq. (4.36) must hold for all values of q and therefore $\Phi_{\nu n}^{(1)}$ must be proportional to $\varphi_{\nu n}$ and our Ansatz reads

$$\Phi_{\nu n}^{(1)}(q) = \left(a_{0,\nu n} + a_{1,\nu n} \log \frac{q^2}{\mu^2} + a_{2,\nu n} \log^2 \frac{q^2}{\mu^2} \right) \varphi_{\nu n}(q), \quad (4.37)$$

where $a_{j,\nu n}$ for $j = 0, 1, 2$ are complex coefficients. Inserting eq. (4.37) into (4.36), we find

$$\begin{aligned} a_{2,\nu n} &= i \frac{\beta_0}{8} \frac{\chi_{\nu n}}{\partial_\nu \chi_{\nu n}}, \\ c_{\nu n} &= -i a_{1,\nu n} \partial_\nu \chi_{\nu n} + i \frac{\beta_0}{8} \frac{\chi_{\nu n} \partial_\nu^2 \chi_{\nu n}}{\partial_\nu \chi_{\nu n}}. \end{aligned} \quad (4.38)$$

Note that for $n = 0$ we have $\partial_\nu \chi_{\nu n}|_{\nu=0} = 0$, and hence the previous equations only hold for $n \neq 0$. We can regularize this singularity for $n = 0$ by interpreting the eigenfunctions as distributions and introducing the principle value prescription

$$\int_{-\infty}^{+\infty} d\nu \left(P \frac{1}{\nu} \right) f(\nu) \equiv \lim_{\epsilon \rightarrow 0} \left(\int_{-\infty}^{-\epsilon} \frac{d\nu}{\nu} f(\nu) + \int_{\epsilon}^{+\infty} \frac{d\nu}{\nu} f(\nu) \right). \quad (4.39)$$

Then we have

$$\begin{aligned} a_{2,\nu n} &= i \frac{\beta_0}{8} P \frac{\chi_{\nu n}}{\partial_\nu \chi_{\nu n}}, \\ c_{\nu n} &= -i a_{1,\nu n} \partial_\nu \chi_{\nu n} + i \frac{\beta_0}{8} P \frac{\chi_{\nu n} \partial_\nu^2 \chi_{\nu n}}{\partial_\nu \chi_{\nu n}}. \end{aligned} \quad (4.40)$$

Note that for regular functions g_ν , we must have

$$P(g_\nu/\nu) \equiv g_\nu P \frac{1}{\nu} \quad \text{and} \quad P g_\nu \equiv g_\nu, \quad (4.41)$$

and hence it is natural to define the principal value for a function X_ν with a simple pole at $\nu = 0$ to be

$$P X_\nu \equiv \nu X_\nu P \frac{1}{\nu}. \quad (4.42)$$

This determines the eigenfunctions up to the coefficients $a_{0,\nu n}$ and $a_{1,\nu n}$ and we have

$$\Phi_{\nu n}^{(1)}(q) = \varphi_{\nu n}(q) \left(a_{0,\nu n} + a_{1,\nu n} \log \frac{q^2}{\mu^2} + i \frac{\beta_0}{8} P \frac{\chi_{\nu n}}{\partial_\nu \chi_{\nu n}} \log^2 \frac{q^2}{\mu^2} \right). \quad (4.43)$$

The free coefficients in eq. (4.43) can be further constrained by requiring that the $\Phi_{\nu n}(q)$ form a complete and orthonormal set of functions. Imposing completeness, we find that

$$\begin{aligned} \text{Re}[a_{1,\nu n}] &= \frac{\beta_0}{8} \partial_\nu P \frac{\chi_{\nu n}}{\partial_\nu \chi_{\nu n}}, \\ 2\text{Re}[a_{0,\nu n}] &= \partial_\nu \text{Im}[a_{1,\nu n}]. \end{aligned} \quad (4.44)$$

which then leaves us with

$$\begin{aligned} \Phi_{\nu n}(q) = \varphi_{\nu n}(q) & \left[1 + \bar{\alpha}_\mu \left(\frac{1}{2} \partial_\nu \text{Im}[a_{1,\nu n}] + i \text{Im}[a_{1,\nu n}] \log \frac{q^2}{\mu^2} \right. \right. \\ & \left. \left. + i \text{Im}[a_{0,\nu n}] + \frac{\beta_0}{8} \log \frac{q^2}{\mu^2} \partial_\nu P \frac{\chi_{\nu n}}{\partial_\nu \chi_{\nu n}} + i \frac{\beta_0}{8} \log^2 \frac{q^2}{\mu^2} P \frac{\chi_{\nu n}}{\partial_\nu \chi_{\nu n}} \right) \right]. \end{aligned} \quad (4.45)$$

The eigenfunctions given in (4.45) are already orthonormal, and hence we can not further constrain them. It is, however, possible to absorb the real parameter $\text{Im}[a_{0,\nu n}]$ into the definition of the phase of the eigenfunctions. Finally, the last parameter $\text{Im}[a_{1,\nu n}]$ can be eliminated through a shift in the integration parameter ν . Then the BFKL eigenfunctions through NLO can be defined as

$$\Phi_{\nu n}(q) = \varphi_{\nu n}(q) \left[1 + \bar{\alpha}_\mu \frac{\beta_0}{8} \log \frac{q^2}{\mu^2} \left(\partial_\nu P \frac{\chi_{\nu n}}{\partial_\nu \chi_{\nu n}} + i \log \frac{q^2}{\mu^2} P \frac{\chi_{\nu n}}{\partial_\nu \chi_{\nu n}} \right) \right], \quad (4.46)$$

with corresponding eigenvalues

$$\omega_{\nu n}^{(1)} = \Delta_{\nu n} = \frac{\delta_{\nu n}}{4} - i \frac{\beta_0}{8} \partial_\nu \chi_{\nu n}. \quad (4.47)$$

We see that the NLO BFKL eigenvalue is given by the real part of $\delta_{\nu n}$ and that the correction is proportional to β_0 . Therefore, the eigenvalue did not change for conformal theories and we still find the correct eigenvalues in the $\mathcal{N} = 4$ case. Similarly, we find that the corrections to the eigenfunctions are proportional to the beta function and we recover the correct eigenfunctions for conformal theories.

4.3.2 The BFKL ladder through NLLA

Let us now consider the BFKL ladder (4.12) through NLLA when using the full NLO eigenfunctions given in eq. (4.46) and the corresponding eigenvalues (4.47), and let us define the function

$$X_{\nu n}(x) = \partial_\nu P \frac{\chi_{\nu n}}{\partial_\nu \chi_{\nu n}} + i \log x P \frac{\chi_{\nu n}}{\partial_\nu \chi_{\nu n}}. \quad (4.48)$$

The the product of the two eigenfunctions through NLO reads

$$\begin{aligned} \Phi_{\nu n}(q_1) \Phi_{\nu n}^*(q_2) & = \varphi_{\nu n}(q_1) \varphi_{\nu n}^*(q_2) \\ & \times \left[1 + \bar{\alpha}_\mu \frac{\beta_0}{8} \log \frac{q_1^2 q_2^2}{\mu^4} \left(\partial_\nu P \frac{\chi_{\nu n}}{\partial_\nu \chi_{\nu n}} + i \log \frac{q_1^2}{q_2^2} P \frac{\chi_{\nu n}}{\partial_\nu \chi_{\nu n}} \right) \right] \\ & = \varphi_{\nu n}(q_1) \varphi_{\nu n}^*(q_2) \left[1 + \bar{\alpha}_\mu \frac{\beta_0}{4} \log \frac{s_0}{\mu^2} X_{\nu n}(q_1^2/q_2^2) \right], \end{aligned} \quad (4.49)$$

where s_0 is the geometric mean defined in eq. (4.2) and the BFKL ladder through NLLA takes the form

$$f(q_1, q_2, y) = \sum_{n=-\infty}^{+\infty} \int_{-\infty}^{+\infty} d\nu e^{y\omega_{\nu n}} \varphi_{\nu n}(q_1) \varphi_{\nu n}^*(q_2) \times \left(1 + \bar{\alpha}_\mu \frac{\beta_0}{4} \log \frac{s_0}{\mu^2} X_{\nu n}(q_1^2/q_2^2) + \mathcal{O}(\bar{\alpha}_\mu^2) \right). \quad (4.50)$$

Using integration by parts, we can simplify the the term including the function X , and we have

$$\begin{aligned} & e^{y\omega_{\nu n}} \varphi_{\nu n}(q_1) \varphi_{\nu n}^*(q_2) \partial_\nu P \frac{\chi_{\nu n}}{\partial_\nu \chi_{\nu n}} \\ &= -e^{y\omega_{\nu n}} \varphi_{\nu n}(q_1) \varphi_{\nu n}^*(q_2) \left(y \partial_\nu \omega_{\nu n} + i \log \frac{q_1^2}{q_2^2} \right) P \frac{\chi_{\nu n}}{\partial_\nu \chi_{\nu n}} \\ &= e^{y\omega_{\nu n}} \varphi_{\nu n}(q_1) \varphi_{\nu n}^*(q_2) \left(-y \bar{\alpha}_\mu \partial_\nu \chi_{\nu n} - i \log \frac{q_1^2}{q_2^2} + \mathcal{O}(\bar{\alpha}_\mu^2) \right) P \frac{\chi_{\nu n}}{\partial_\nu \chi_{\nu n}} \\ &= e^{y\omega_{\nu n}} \varphi_{\nu n}(q_1) \varphi_{\nu n}^*(q_2) \left(-i \log \frac{q_1^2}{q_2^2} P \frac{\chi_{\nu n}}{\partial_\nu \chi_{\nu n}} - y \bar{\alpha}_\mu \chi_{\nu n} + \mathcal{O}(\bar{\alpha}_\mu^2) \right), \end{aligned} \quad (4.51)$$

which yields

$$\begin{aligned} & e^{y\omega_{\nu n}} \varphi_{\nu n}(q_1) \varphi_{\nu n}^*(q_2) X_{\nu n}(q_1^2/q_2^2) \\ &= e^{y\omega_{\nu n}} \varphi_{\nu n}(q_1) \varphi_{\nu n}^*(q_2) (-y \bar{\alpha}_\mu \chi_{\nu n} + \mathcal{O}(\bar{\alpha}_\mu^2)). \end{aligned} \quad (4.52)$$

Then, in agreement with the result in refs. [102, 103], the BFKL ladder takes the form

$$f(q_1, q_2, y) = \sum_{n=-\infty}^{+\infty} \int_{-\infty}^{+\infty} d\nu e^{y\omega_{\nu n}} \varphi_{\nu n}(q_1) \varphi_{\nu n}^*(q_2) \times \left(1 - \bar{\alpha}_\mu^2 \frac{\beta_0}{4} \log \frac{s_0}{\mu^2} y \chi_{\nu n} + \mathcal{O}(\bar{\alpha}_\mu^3) \right). \quad (4.53)$$

Finally, the remaining correction to the product of leading-order eigenfunctions can be absorbed into the coupling constant. More precisely, through NLLA, the term is exactly cancelled by the running of the coupling when changing the scale of $\bar{\alpha}$ from μ to s_0 ,

$$\begin{aligned} & \exp y [\bar{\alpha}_S(s_0) \chi_{\nu n} + \bar{\alpha}_S(s_0)^2 \Delta_{\nu n} + \mathcal{O}(\bar{\alpha}_S^3)] \\ &= \exp y \left[\bar{\alpha}_\mu \left(1 - \bar{\alpha}_\mu \frac{\beta_0}{4} \log \frac{s_0}{\mu^2} \right) \chi_{\nu n} + \bar{\alpha}_\mu^2 \Delta_{\nu n} + \mathcal{O}(\bar{\alpha}_\mu^3) \right] \\ &= e^{y\omega_{\nu n}} \left(1 - \bar{\alpha}_\mu^2 \frac{\beta_0}{4} \log \frac{s_0}{\mu^2} y \chi_{\nu n} + \mathcal{O}(\bar{\alpha}_\mu^3) \right). \end{aligned} \quad (4.54)$$

This brings us to the final form of the BFKL ladder through NLLA,

$$f(q_1, q_2, y) = \sum_{n=-\infty}^{+\infty} \int_{-\infty}^{+\infty} d\nu \varphi_{\nu n}(q_1) \varphi_{\nu n}^*(q_2) e^{y \bar{\alpha}_S(s_0) [\chi_{\nu n} + \bar{\alpha}_S(s_0) \Delta_{\nu n}]}, \quad (4.55)$$

and we see that we can use the leading-order eigenfunctions $\varphi_{\nu n}$ when evaluating the coupling at $\mu^2 = s_0 = \sqrt{q_1^2 q_2^2}$.

4.4 Analytic results for the BFKL ladder at NLLA in QCD

4.4.1 Fourier-Mellin representation of the BFKL ladder at NLLA

In this section we will use the description of the BFKL ladder we have worked out in the previous section to obtain analytic results, i.e. we will evaluate the coupling at s_0 , allowing us to use the leading-order eigenfunctions. Expanding the BFKL ladder in $\eta_{s_0} = y \bar{\alpha}_S(s_0)$, we define

$$f^{NLL}(q_1, q_2, \eta_{s_0}) = \frac{1}{2\pi \sqrt{q_1^2 q_2^2}} \sum_{k=1}^{\infty} \frac{\eta_{s_0}^k}{k!} f_{k+1}^{NLL}(z), \quad (4.56)$$

where the perturbative coefficients are given by the Fourier-Mellin transform,

$$f_k^{NLL}(z) = \mathcal{F} [\Delta_{\nu n} \chi_{\nu n}^{k-2}] = \sum_{n=-\infty}^{+\infty} \left(\frac{z}{\bar{z}}\right)^{n/2} \int_{-\infty}^{+\infty} \frac{d\nu}{2\pi} |z|^{2i\nu} \Delta_{\nu n} \chi_{\nu n}^{k-2}. \quad (4.57)$$

In the following it will be useful to split the NLO eigenvalue $\Delta_{\nu n}$ into several terms,

$$\Delta_{\nu n} = \frac{1}{4} \delta_{\nu n}^{(1)} + \frac{1}{4} \delta_{\nu n}^{(2)} + \frac{1}{4} \delta_{\nu n}^{(3)} + \frac{3}{2} \zeta_3 + \gamma_K^{(2)} \chi_{\nu n} - \frac{1}{8} \beta_0 \chi_{\nu n}^2. \quad (4.58)$$

The terms that depend (up to constants in (ν, n)) only on the leading order eigenvalue $\chi_{\nu n}$ evaluate to the LLA coefficients that have already been computed in eq. (4.22). In the QCD case, the remaining terms are

$$\delta_{\nu n}^{(1)} = \partial_{\nu}^2 \chi_{\nu n}, \quad (4.59)$$

$$\delta_{\nu n}^{(2)} = -2\Phi(n, \gamma) - 2\Phi(n, 1 - \gamma), \quad (4.60)$$

$$\begin{aligned} \delta_{\nu n}^{(3)} &= -\frac{\Gamma(\frac{1}{2} + i\nu)\Gamma(\frac{1}{2} - i\nu)}{2i\nu} \left[\psi\left(\frac{1}{2} + i\nu\right) - \psi\left(\frac{1}{2} - i\nu\right) \right] \\ &\times \left[\delta_{n0} \left(3 + A \frac{2 + 3\gamma(1 - \gamma)}{(3 - 2\gamma)(1 + 2\gamma)} \right) - \delta_{|n|2} \left(A \frac{\gamma(1 - \gamma)}{2(3 - 2\gamma)(1 + 2\gamma)} \right) \right], \end{aligned} \quad (4.61)$$

with $A = (1 + N_f/N_c^3)$. Equivalently, we write the BFKL ladder as

$$f_k^{NLL}(z) = \frac{1}{4} C_k^{(1)}(z) + \frac{1}{4} C_k^{(2)}(z) + \frac{1}{4} C_k^{(3)}(z) + \frac{3}{2} \zeta_3 f_{k-2}^{LL}(z) + \gamma_K^{(2)} f_{k-1}^{LL}(z) - \frac{1}{8} \beta_0 f_k^{LL}(z), \quad (4.62)$$

where we set $f_0^{LL}(z) = \mathcal{F}[1] = \pi \delta^{(2)}(1-z)$. Then the terms $C_k^{(i)}$ correspond to the Fourier-Mellin transforms of the respective $\delta_{\nu n}^{(i)}$,

$$C_k^{(i)}(z) = \mathcal{F} \left[\delta_{\nu n}^{(i)} \chi_{\nu n}^{k-2} \right], \quad (4.63)$$

with $k \geq 2$, and all other terms are correspond to LLA perturbative coefficients. We will now turn to the computation of the missing terms $C_k^{(i)}$.

4.4.2 The contribution from $\delta_{\nu n}^{(3)}$

Let us start by discussing the term $C_k^{(3)} \equiv C_k^{(3,0)}(z) + C_k^{(3,2)}(z)$, where $C_k^{(3,i)}(z)$ is due to the term proportional to $\delta_{|n|i}$. The Kronecker deltas in these terms cause the Fourier-Mellin transform to reduce to an ordinary Mellin transform,

$$C_k^{(3)}(z) = - \int_{-\infty}^{+\infty} \frac{d\nu}{2\pi} |z|^{2i\nu} \frac{\Gamma(\frac{1}{2} + i\nu) \Gamma(\frac{1}{2} - i\nu)}{2i\nu} \left[\psi \left(\frac{1}{2} + i\nu \right) - \psi \left(\frac{1}{2} - i\nu \right) \right] \times \left[\chi_{\nu 0}^{k-2} A_0(\nu) + \left(\frac{z}{\bar{z}} + \frac{\bar{z}}{z} \right) \chi_{\nu 2}^{k-2} A_2(\nu) \right], \quad (4.64)$$

where we have introduced a shorthand for the rational pre factors

$$A_0(\nu) = 3 + A \frac{2 + 3\gamma(1-\gamma)}{(3-2\gamma)(1+2\gamma)}, \quad A_2(\nu) = -A \frac{\gamma(1-\gamma)}{2(3-2\gamma)(1+2\gamma)}. \quad (4.65)$$

The integral in eq. (4.64) can be computed summing all residues $\nu = i(\frac{1}{2} + m)$, $m \in \mathbb{N}$ in the upper half-plane and the resulting sum can always be performed using the techniques of ref. [31,93,108]. We find that the result can be expressed in terms of MPLs $G(a_1, \dots, a_n; |z|)$, with $a_k \in \{-i, 0, i\}$. Since there are no singularities on the positive real axis, it is easy to see that these functions are single-valued in z .

Further, the set of functions is closed under complex conjugation, and we can write them in terms of their real and imaginary parts, e.g.

$$G(0, i; |z|) \pm G(0, -i; |z|) = \begin{cases} \frac{1}{2} G(0, -1, |z|^2), \\ 2i \text{Ti}_2(|z|), \end{cases} \quad (4.66)$$

where $\text{Ti}_n(z)$ are the inverse tangent integrals,

$$\text{Ti}_n(z) = \text{Im Li}_n(iz) = -\text{Im} G(\vec{0}_{n-1}, 1; iz) = \text{Im} G(\vec{0}_{n-1}, i; z), \quad (4.67)$$

with $\vec{0}_n = \underbrace{(0, \dots, 0)}_{n \text{ times}}$.

We find that all $C_k^{(3)}$ can be written in terms of HPLs $G(b_1, \dots, b_n; |z|^2)$ with $b_i \in \{-1, 0\}$ and *generalised inverse tangent integrals*,

$$\text{Ti}_{m_1, \dots, m_k}(|z|) = \text{Im Li}_{m_1, \dots, m_k}(\sigma_1, \dots, \sigma_{k-1}, i \sigma_k |z|), \quad (4.68)$$

where $\sigma_j = \text{sign}(m_j)$, and where

$$\begin{aligned} \text{Li}_{m_1, \dots, m_k}(z_1, \dots, z_k) &= \sum_{0 < n_1 < n_2 < \dots < n_k} \frac{z_1^{n_1} \dots z_k^{n_k}}{n_1^{m_1} \dots n_k^{m_k}} \\ &= (-1)^k G\left(\underbrace{0, \dots, 0}_{m_k-1}, \frac{1}{z_k}, \dots, \underbrace{0, \dots, 0}_{m_1-1}, \frac{1}{z_1 \dots z_k}; 1\right). \end{aligned} \quad (4.69)$$

We find that neither $C_k^{(3,0)}$ nor $C_k^{(3,2)}$ are of uniform weight and they each contain functions of weight $0 \leq w \leq k$.

4.4.3 The contribution from $\delta_{\nu n}^{(1)}$

Next, let us consider the term $C_k^{(3)}$. The second derivative in $\delta_{\nu n}^{(1)}$ does not affect the evaluation of the Fourier-Mellin transform much, and the integral can easily be solved employing the same techniques as in the LLA case. The resulting double sums can be computed using the sum algorithms presented in refs. [31, 93] and evaluate to linear combinations of SVHPLs with singularities at most at 0 and 1. The integral can, however, also be solved recursively using the techniques we have previously introduced in chapter 3.

The derivative in the Fourier-Mellin integral can easily be taken care of using integration by parts. The only term in the definition of the Fourier-Mellin transform depending on ν_i is the term $|z_i|^{2i\nu_i}$, and so we have

$$\mathcal{F}_{N-5}[D_{\nu_i} X] = -\mathcal{G}_0(z_i) \mathcal{F}[X]. \quad (4.70)$$

Then the two-loop coefficient reads

$$C_2^{(1)}(z) = \mathcal{F}[\partial_{\nu}^2 \chi_{\nu n}] = -\mathcal{X}(z) \log^2 |z|^2 = -\frac{|z|}{\pi |1-z|^2} \mathcal{G}_{0,0}(z), \quad (4.71)$$

where we defined \mathcal{X} to be the Fourier-Mellin transform of the leading order BFKL eigenvalue χ ,

$$\mathcal{X}(z) \equiv \mathcal{F}[\chi_{\nu n}] = f_1^{LL}(z) = \frac{|z|}{2\pi|1-z|^2}. \quad (4.72)$$

Then we can compute higher-order results by using Fourier-Mellin convolutions to insert leading-order BFKL eigenvalues $\chi_{\nu n}$ into the integrand,

$$C_{k+1}^{(1)}(z) = \mathcal{X}(z) * C_k^{(1)}(z), \quad (4.73)$$

with $k \geq 2$. Since the $C_k^{(1)}(z)$ are single-valued functions, we can evaluate the convolution integrals using Stokes' theorem, as we have done in the previous chapter.

We find that the functions $C_k^{(1)}$ are, up to a global rational pre factor, pure combinations of SVMPLs of uniform weight k with singularities at most at $z = 0$ and $z = 1$. It can be shown that this property holds at every loop order [2].

4.4.4 The contribution from $\delta_{\nu n}^{(2)}$

Let us now consider the contribution $C_k^{(2)}$ arising from the Fourier-Mellin integral involving $\delta_{\nu n}^{(2)}$. After computing the two-loop contribution by evaluating the double-sum we obtain from closing the integration contour in the complex ν -plane, we find

$$C_2^{(2)}(z) = \mathcal{F}[\delta_{\nu n}^{(2)}] = C_2^{(2,1)}(z) + C_2^{(2,2)}(z), \quad (4.74)$$

with

$$\begin{aligned} C_2^{(2,1)}(z) &= \frac{|z|(z-\bar{z})}{2\pi|1+z|^2|1-z|^2} [\mathcal{G}_{1,0}(z) - \mathcal{G}_{0,1}(z)], \\ C_2^{(2,2)}(z) &= \frac{|z|(1-|z|^2)}{2\pi|1+z|^2|1-z|^2} [\mathcal{G}_{1,0}(z) + \mathcal{G}_{0,1}(z) - G_{-1,0}(|z|^2) - \zeta_2]. \end{aligned} \quad (4.75)$$

We see that unlike the previous terms we have considered, $C_2^{(2)}(z)$ can no longer be written as a pure function multiplying a global rational prefactor but we find two separate rational prefactors multiplying pure functions. Further, we see that $C_2^{(2,2)}$ contains not only SVHPLs, but also regular polylogarithms evaluated at $|z|^2$. Since those polylogarithms only have singularities at most at 0 and -1 , and their argument is positive-definite, they are still single-valued

functions of z . In fact, $C_k^{(2,1)}(z)$ and $C_k^{(2,2)}(z)$ can each be written as pure linear combinations of gSVMPLs (c.f. sec. 2.2.2) with a global rational prefactor. The gSVMPLs we need to consider in this work are the $\mathcal{G}(a_1, \dots, a_n; z)$ with $a_i \in \{-1, 0, 1, -1/\bar{z}\}$ that we have previously introduced in section 2.2.2.

Higher-order contributions from $\delta_{\nu n}^{(2)}$ can again be obtained through the recursion

$$C_{k+1}^{(2)}(z) = \mathcal{X}(z) * C_k^{(2)}(z). \quad (4.76)$$

Since $1 + |z|^2$ never vanishes $C_k^{(2)}$ only has isolated singularities, and because $C_k^{(2)}$ is composed of single-valued functions, we can perform the convolution integrals using Stokes' theorem, as we have described before. The single-valued primitives that we need to compute in the process can be computed using the algorithm described in sec. 2.2.2 and they evaluate naturally to gSVMPLs. The results can, at every [2] order, be written in the form

$$C_k^{(2)}(z) = \frac{|z|(z - \bar{z})}{2\pi|1 + z|^2|1 - z|^2} C_k^{(2,1)} + \frac{|z|(1 - |z|^2)}{2\pi|1 + z|^2|1 - z|^2} C_k^{(2,2)}, \quad (4.77)$$

where the functions $\mathcal{C}_k^{(2,i)}$ are pure combinations of gSVMPLs of uniform weight k . The explicit form of the contributions $C_k^{(2)}(z)$ through five loops can be found in [2].

4.5 Transcendental weight properties of the BFKL ladder at NLLA

4.5.1 Transcendental weight of the BFKL ladder in QCD

In the previous section we have computed the QCD BFKL ladder at NLLA through five loops in momentum space. We have found that the ℓ -loop BFKL ladder at NLLA in QCD can be expressed as single-valued combinations of HPLs with weights up to ℓ . In particular, we have found that the QCD BFKL ladder is not a maximally transcendental function, matching the analysis of the corresponding result in moment space [106, 107, 109]. There, it was further discovered that the anomalous dimension of the leading-twist operators controlling the Bjorken scaling violations in $\mathcal{N} = 4$ SYM was of uniform, maximal transcendental weight in moment space and that it corresponds exactly to maximal weight part of the corresponding anomalous dimension in QCD. We will now make a similar analysis of the transcendental properties of the BFKL

ladder in Momentum space. We will start by considering the QCD case and then generalise this analysis to theories with arbitrary matter content.

As the results from the previous section show, the various terms contributing to eq. (4.62) have the following transcendental weights: The functions f_k^{LL} have uniform transcendental weight $k - 1$, the functions $C_k^{(1)}$ and $C_k^{(2)}$ have uniform weight k and the function $C_k^{(3)}$ contains terms of transcendental weights $0 \leq w \leq k$. We see that terms with transcendental weight less than k in eq. (4.62) arise only in the following places:

1. The term $\beta_0 f_k^{LL}(z)$ involving the beta function has weight $k - 1$.
2. The contribution multiplying the cusp anomalous dimension in eq. (4.62), $\gamma_K^{(2)} f_{k-1}^{LL}(z)$, involves a range of weights $k - 2 \leq w \leq k$ and lower weight terms arise entirely because the cusp anomalous dimension in QCD is not of maximal weight.
3. Using the explicit results through five loops of section 4.4.2, we see that in QCD the functions $C_k^{(3)}$ involve terms of weight $0 \leq w \leq k$.

Similarly to what has been found in refs. [106, 107, 109] in moment space, the $\mathcal{N} = 4$ result is of maximal weight and is completely contained in the result for QCD. The exact relation between the two is different, however. In momentum space, the contribution $C_k^{(3)}$, which is absent in $\mathcal{N} = 4$, also contains terms of maximal weight, and therefore $\mathcal{N} = 4$ is not equal to the maximal weight part of QCD. This raises the question, if we can find another theory describing exactly the maximal weight part of QCD. We will tend to this question in the following section.

4.5.2 The BFKL ladder in generic gauge theories

Let us now generalize the previous analysis to the NLLA BFKL ladder in a generic $SU(N_c)$ gauge theory with scalar or fermionic matter in arbitrary representations. We will start from the BFKL eigenvalue at NLO in a generic theory [106] and we write, analogously to eq. (4.62),

$$\begin{aligned} \Delta_{\nu n} = & \frac{1}{4}\delta_{\nu n}^{(1)} + \frac{1}{4}\delta_{\nu n}^{(2)} + \frac{1}{4}\delta_{\nu n}^{(3)}(\tilde{N}_f, \tilde{N}_s) \\ & + \frac{3}{2}\zeta_3 + \gamma^{(2)}(\tilde{n}_f, \tilde{n}_s)\chi_{\nu n} - \frac{1}{8}\beta_0(\tilde{n}_f, \tilde{n}_s)\chi_{\nu n}^2. \end{aligned} \quad (4.78)$$

The quantities $\delta_{\nu n}^{(1)}$ and $\delta_{\nu n}^{(2)}$ are independent of the particle content of the theory and are therefore equal to the corresponding terms in QCD given in eq. (4.59)

and eq. (4.60). The one-loop beta function and two-loop cusp anomalous dimension only depend on the theory through one-loop corrections to the gluon propagator and are therefore independent of the details of the theory (e.g. Yukawa couplings or scalar potentials). In DRED, they are given by

$$\begin{aligned}\beta_0(\tilde{n}_f, \tilde{n}_s) &= \frac{11}{3} - \frac{2\tilde{n}_f}{3N_c} - \frac{\tilde{n}_s}{6N_c}, \\ \gamma^{(2)}(\tilde{n}_f, \tilde{n}_s) &= \frac{1}{4} \left(\frac{64}{9} - \frac{10\tilde{n}_f}{9N_c} - \frac{4\tilde{n}_s}{9N_c} \right) - \frac{\zeta_2}{2},\end{aligned}\tag{4.79}$$

where

$$\tilde{n}_f = \sum_R n_f^R T_R \quad \text{and} \quad \tilde{n}_s = \sum_R n_s^R T_R.\tag{4.80}$$

The sum in eq. (4.80) runs over all irreducible representations R of $SU(N_c)$, and n_f^R and n_s^R denote the number of Weyl fermions and real scalars transforming in the representation R . The index T_R of the representation is defined by the normalization of the infinitesimal generators T_R^a of the representation R through $\text{Tr}(T_R^a T_R^b) = T_R \delta^{ab}$. We normalize the structure constants of $SU(N_c)$ such that the index of the fundamental representation is $T_F = 1/2$. The contribution $\delta_{\nu n}^{(3)}$ arises through (scalar) QED-type diagrams [106] and only depends on the matter content of the theory,

$$\delta_{\nu n}^{(3)}(\tilde{N}_f, \tilde{N}_s) = \delta_{\nu n}^{(3,1)}(\tilde{N}_f, \tilde{N}_s) + \delta_{\nu n}^{(3,2)}(\tilde{N}_f, \tilde{N}_s),\tag{4.81}$$

with

$$\tilde{N}_x = \frac{1}{2} \sum_R n_x^R T_R (2C_R - N_c), \quad x = f, s.\tag{4.82}$$

C_R is the quadratic Casimir of the representation R and the functions $\delta_{\nu n}^{(3,i)}$ read

$$\begin{aligned}\delta_{\nu n}^{(3,1)}(\tilde{N}_f, \tilde{N}_s) &= \frac{f(\gamma)}{8} \left[\delta_{n0} \left(2\tilde{N}_s + 12\tilde{N}_f - 30N_c^2 \right) \right. \\ &\quad \left. + \delta_{|n|2} \left(N_c^2 - 2\tilde{N}_f + \tilde{N}_s \right) \right], \\ \delta_{\nu n}^{(3,2)}(\tilde{N}_f, \tilde{N}_s) &= \frac{f(\gamma)}{8} \left[\frac{(3\delta_{|n|2} - 2\delta_{n0})(2\gamma - 1)}{2(2\gamma - 3)(2\gamma + 1)} \left(N_c^2 - 2\tilde{N}_f + \tilde{N}_s \right) \right],\end{aligned}\tag{4.83}$$

where $\gamma = \frac{1}{2} + i\nu$ and

$$f(\gamma) = \frac{1}{4\pi^2(1 - 2\gamma)} \Gamma(1 - \gamma) \Gamma(\gamma) \left[\psi(1 - \gamma) - \psi(\gamma) \right].\tag{4.84}$$

We have computed the contributions arising from $\delta_{\nu n}^{(3)}(\tilde{N}_f, \tilde{N}_s)$ explicitly through five loops and have found that the Fourier-Mellin transforms $\mathcal{F} \left[\delta_{\nu n}^{(3,1)} \chi_{\nu n}^k \right]$ evaluate to functions of uniform weight $k + 2$ while $\mathcal{F} \left[\delta_{\nu n}^{(3,2)} \chi_{\nu n}^k \right]$ evaluates exclusively to lower-weight terms. While we have no proof that this holds to all loop orders, we believe that our explicit computations through five loops provide compelling evidence that this holds in general.

In a gauge theory that is minimally coupled to matter fields, the NLO BFKL eigenvalue is entirely determined by the gauge group and the matter content of the theory [106] and is independent of the details of the interactions among the matter-fields of the theory. Therefore, we can repeat the analysis of the transcendental properties of the BFKL ladder from the last section for a generic gauge theory with variable fermionic and scalar matter content. From our previous analysis of the appearing Fourier-Mellin integrals we can formulate a set of necessary and sufficient conditions for a theory such that its BFKL ladder at NLLA is of uniform transcendental weight in momentum space:

1. The one-loop beta function vanishes, i.e., we have

$$\frac{11}{3} - \frac{2\tilde{n}_f}{3N_c} - \frac{\tilde{n}_s}{6N_c} = 0. \quad (4.85)$$

2. The two-loop cusp anomalous dimension is proportional to ζ_2 . In DRED, this implies

$$\frac{16}{9} - \frac{5\tilde{n}_f}{18N_c} - \frac{\tilde{n}_s}{9N_c} = 0. \quad (4.86)$$

3. The contribution from $\delta_{\nu n}^{(3,2)}$ vanishes, which implies

$$2\tilde{N}_f = N_c^2 + \tilde{N}_s. \quad (4.87)$$

The equations (4.85), (4.86) and (4.87) can be interpreted as conditions on the matter content of a theory for its NLLA BFKL ladder to have maximal weight. Before we solve these conditions for a mix of adjoint and fundamental matter in the next section, let us make a quick observation that holds independently of the representations of the matter fields. If eq. (4.87) is satisfied, then not only the term $\delta_{\nu n}^{(3,2)}$ vanishes, but the term proportional to $\delta_{|n|2}$ in $\delta_{\nu n}^{(3,1)}$ vanishes as well,

$$\delta_{\nu n}^{(3,1)}(\tilde{N}_f, 2\tilde{N}_f - N_c^2) = 2f(\gamma) \delta_{n0} \left(\tilde{N}_f - 2N_c^2 \right). \quad (4.88)$$

This term, however, evaluates to functions of maximal transcendental weight, which leads us to conclude that there exists no theory such that the NLLA BFKL ladder corresponds exactly to the maximal weight part in QCD.

4.5.3 Theories with adjoint and fundamental matter

Let us now study the conditions (4.85), (4.86) and (4.87) in a theory containing only matter in the fundamental and adjoint representations. The indices and Casimir operators of the fundamental and adjoint representations are

$$T_A = C_A = N_c \quad \text{and} \quad C_F = T_F \frac{N_c^2 - 1}{N_c}, \quad (4.89)$$

and we have, for $x = s, f$,

$$\begin{aligned} \tilde{n}_x &= T_A n_x^A + T_F n_x^F, \\ \tilde{N}_x &= \frac{1}{2} T_A (2C_A - N_c) n_x^A + \frac{1}{2} T_F (2C_F - N_c) n_x^F. \end{aligned} \quad (4.90)$$

We are now going to solve the constraints given in eqs. (4.85), (4.86) and (4.87) for an arbitrary number N_c of colours².

Inserting eq. (4.90) into eq. (4.87), we find

$$T_F (2C_F - N_c) n_f^F + N_c^2 n_f^A = N_c^2 + \frac{1}{2} N_c^2 n_s^A + \frac{1}{2} T_F (2C_F - N_c) n_s^F. \quad (4.91)$$

If we want this equation to hold for any number of colours N_c , we find the relations

$$2 n_f^F = n_s^F \quad \text{and} \quad 2 n_f^A = 2 + n_s^A. \quad (4.92)$$

between the number of scalars and the number of fermions in the adjoint and fundamental representations. Plugging these relations into eqs. (4.85) and (4.86), we find a relation between the number of fermions in the adjoint and fundamental representations,

$$4 - n_f^A - T_F \frac{n_f^F}{N_c} = 0. \quad (4.93)$$

The relations (4.92) and (4.93) are necessary conditions for a gauge theory with fundamental and adjoint matter only to have a BFKL ladder at NLLA of uniform and maximal transcendental weight.

While the previous conditions are independent of the details of the interactions between matter-particles, it is worth pointing out that eq. (4.92) describes the spectrum of a gauge theory with \mathcal{N} supersymmetry generators and $n_F \equiv n_f^F$

²We have tried to find solutions by independently varying the parameters N_c, n_f^F, n_s^F, n_f^A and n_s^A between 0 and 35 and have not found any other solutions than the ones derived in this section. We therefore conjecture that these are the only solutions.

\mathcal{N}	4	2	1	1
n_A	0	0	0	2
n_F	0	$4N_c$	$6N_c$	$2N_c$

Table 4.1: The four solutions to the constraints in eq. (4.94) into eq. (4.85) and (4.86).

chiral multiplets³ in the fundamental representation and $n_A \equiv n_f^A - \mathcal{N}$ chiral multiplets in the adjoint representation. To make this more obvious, we can reformulate the constraint (4.92) as

$$\begin{aligned}
 n_f^A &= \mathcal{N} + n_A, \\
 n_f^F &= n_F, \\
 n_s^A &= 2(\mathcal{N} - 1) + 2n_A, \\
 n_s^F &= 2n_F.
 \end{aligned}
 \tag{4.94}$$

Let us stress again, that the reformulation in terms of supersymmetric matter multiplets is purely a matter of convenience and that our analysis is impervious to the details of the interactions between those particles and that the analysis applies equally to any other theory with the same matter content and interactions that break supersymmetry.

After inserting eq. (4.94) into eq. (4.93), we find

$$n_A + \frac{n_F}{2N_c} + \mathcal{N} = 4.
 \tag{4.95}$$

This equation has only four solutions for positive integers, shown in Table 4.1. For these theories, the NLO BFKL eigenvalue takes the form,

$$\Delta_{\nu n} = \frac{1}{4}\delta_{\nu n}^{(1)} + \frac{1}{4}\delta_{\nu n}^{(2)} + \frac{3}{2}\zeta_3 + \frac{\zeta_2}{2}\chi_{\nu n} + f(\gamma)(N_c^2 + 1)(n_f^A - 4)\delta_{n0}.
 \tag{4.96}$$

As we have seen, the matter content of the four solutions we found can be put into supersymmetric hypermultiplets for different numbers \mathcal{N} of supersymmetries. In particular, they correspond to the following supersymmetric theories: The solution $(\mathcal{N}, n_A, n_F) = (4, 0, 0)$ has the same field content as $\mathcal{N} = 4$ SYM which we already knew from previous considerations, has a maximally transcendental BFKL ladder. The solution $(\mathcal{N}, n_A, n_F) = (2, 0, 4N_c)$ corresponds

³We consider chiral multiplets in $\mathcal{N} = 1$ supersymmetry, consisting of a Weyl fermion and two real scalar on-shell degrees of freedom.

to $\mathcal{N} = 2$ superconformal QCD with $N_f = 2N_c$ hypermultiplets [110]. The solution $(\mathcal{N}, n_A, n_F) = (1, 0, 6N_c)$ has the matter content of $\mathcal{N} = 1$ super-QCD at the upper end of the conformal window. The lower end of the conformal window, $(\mathcal{N}, n_A, n_F) = (1, 0, 3N_c)$ does not solve the constraints we have found. The fourth solution we found, $(\mathcal{N}, n_A, n_F) = (1, 2, 2N_c)$, to the best of our knowledge, has no interpretation as any specific superconformal theory.

Chapter 5

The Banana Integral

In the previous chapters we have studied scattering amplitudes both in an especially nice theory as well as in a special kinematic regime, the multi-Regge limit, in which scattering amplitudes seem to be expressible in terms of the well-known multiple polylogarithms. More precisely, all amplitudes we have seen in the previous chapters are single-valued linear combinations of multiple polylogarithms of transverse cross-ratios. We have seen how a careful analysis of the function space constituting scattering amplitudes in this limit and a good understanding of the algebraic properties of this function space can facilitate the computation of scattering amplitudes. As a result, we have been able to develop a mathematical framework that is especially well-suited for the computation of scattering amplitudes in the multi-Regge limit and that allowed us to compute scattering amplitudes in MRK to unprecedented accuracies.

In this chapter we will loosen the constraint we have imposed on the kinematics of our calculations and consider scattering amplitudes in general kinematics. The computation we will perform is also not related to any specific theory but is defined for Feynman integrals in general and can be of use for precision calculations in any theory. In order to properly define the family of integrals we are computing, let us give a slightly more detailed review of the mathematical theory around the computation of Feynman integrals.

5.1 Integral Families and How to Compute Them

In this section we will give a short review of some computational techniques that are very useful when computing scattering amplitudes via Feynman integrals. In doing so, we will also lay the groundwork for the computation of the banana integral. We will demonstrate how all Feynman integrals can be expressed in terms of Feynman integrals involving only scalar propagators. Then we will show how we can relate different Feynman integrals in order to reduce the number of individual Feynman integrals that need to be computed. In particular, we will see that we can associate families of Feynman integrals to given Feynman graphs and that we can express all integrals in a family in terms of just a few Feynman integrals. Finally, we will consider the sunrise integral and apply the concepts we will introduce in this section.

5.1.1 Master Integrals and Differential Equations

As we have already seen in chapter 1, Feynman integrals can be represented by Feynman graphs, where each line corresponds to the propagation of a particle of the theory and every intersection corresponds to an interaction term among the connected particle lines. One simple example of such an integral is the scalar one-loop integral given in (1.9). In general, the appearing internal lines in a Feynman graph don't always have to correspond to scalar particles and a Feynman integral can involve the integration over Lorentz tensors.

The one-loop correction to the propagator of a Fermion, for example, can contain the term

$$\int \frac{d^d k}{\pi^{d/2}} \frac{k^\mu}{((k+p)^2 - m_1^2)(k^2 - m_2^2)}. \quad (5.1)$$

It was shown [111] that these types of integrals can be rewritten as linear combinations of integrals where the Lorentz structure is completely captured by other quantities. Indeed, it makes sense that the solved integral does not depend on the integration variable k , and hence the Lorentz structure of the expression can only be in the form of external momenta or other Lorentz tensors like the metric tensor $g^{\mu\nu}$. Consider, for example, the integral in eq. (5.1). The solved integral can only be a function of the external momentum p^μ and hence must be of the form

$$\int \frac{d^d k}{\pi^{d/2}} \frac{k^\mu}{((k+p)^2 - m_1^2)(k^2 - m_2^2)} = Ap^\mu. \quad (5.2)$$

Multiplying both sides with p_μ , we find

$$\int \frac{d^d k}{\pi^{d/2}} \frac{k \cdot p}{((k+p)^2 - m_1^2)(k^2 - m_2^2)} = Ap^2, \quad (5.3)$$

and hence

$$A = \frac{1}{p^2} \int \frac{d^d k}{\pi^{d/2}} \frac{k \cdot p}{((k+p)^2 - m_1^2)(k^2 - m_2^2)}. \quad (5.4)$$

As we can see, we have successfully replaced the integration over a vector-like integration kernel by the integration over a scalar at the cost of introducing an additional scalar product in the numerator. It is useful to rewrite the additional scalar products introduced in the numerator as inverse powers of scalar propagators. We have, for example,

$$\frac{k \cdot p}{k^2(k+p)^2} = \frac{1}{2} \frac{(k+p)^2}{k^2(k+p)^2} - \frac{1}{2} \frac{k^2}{k^2(k+p)^2} - \frac{1}{2} \frac{p^2}{k^2(k+p)^2}. \quad (5.5)$$

Then we can write all Feynman integrals as linear combinations of integrals of the form

$$\begin{aligned} \mathcal{I}(a_1, \dots, a_n) &\equiv \int \frac{d^d k_1}{\pi^{d/2}} \cdots \frac{d^d k_m}{\pi^{d/2}} \frac{1}{D_1^{a_1} \cdots D_n^{a_n}} \\ &\equiv \int \frac{d^d k_1}{\pi^{d/2}} \cdots \frac{d^d k_m}{\pi^{d/2}} I(a_1, \dots, a_n), \end{aligned} \quad (5.6)$$

with $a_i \in \mathbb{Z}$, $D_i = (q_i^2 - m_i^2)$ and where the q_i are linear combinations of loop momenta k_i and external momenta p_i .

When performing these integrals we can use the fact that integrals over surface terms vanish [112]. This allows us to relate different integrals of the form (5.6) using integration by parts (IBP) and setting integrals over surface terms to zero. For the integral $\mathcal{I}(a_1, a_2)$ with $D_1 = k^2$ and $D_2 = (k+p)^2$ for example, we find

$$\begin{aligned} 0 &= \int \frac{d^d k}{\pi^{d/2}} \partial^\mu k_\mu I(a_1, a_2) \\ &= \int \frac{d^d k}{\pi^{d/2}} dI(a_1, a_2) - 2a_1 k^2 I(a_1 + 1, a_2) - 2a_2 k \cdot (k+p) I(a_1, a_2) \\ &= (d - 2a_1 - a_2) \mathcal{I}(a_1, a_2) + a_2 p^2 \mathcal{I}(a_1, a_2 + 1) - a_1 \mathcal{I}(a_1 - 1, a_2 + 1), \end{aligned} \quad (5.7)$$

and

$$\begin{aligned}
0 &= \int \frac{d^d k}{\pi^{d/2}} \partial^\mu p_\mu I(a_1, a_2) \\
&= \int \frac{d^d k}{\pi^{d/2}} -2a_1 k \cdot p I(a_1 + 1, a_2) - 2a_2 p \cdot (k + p) I(a_1, a_2) \\
&= a_1 p^2 \mathcal{I}(a_1 + 1, a_2) - a_2 p^2 \mathcal{I}(a_1, a_2 + 1) + (a_1 - a_2) \mathcal{I}(a_1, a_2) \\
&\quad - a_1 \mathcal{I}(a_1 + 1, a_2 - 1) + a_2 \mathcal{I}(a_1 - 1, a_2 + 1),
\end{aligned} \tag{5.8}$$

where in the last lines we have expressed the appearing scalar products as denominators. The differential $\partial^\mu = \partial/\partial k_\mu$ in the previous equations acts on the loop momentum k and we have $\partial^\mu k_\mu = d$. These so-called *IBP relations* can be used to express the appearing integrals in terms of a set of basis integrals, or *master integrals*, which greatly reduces the number of integrals that need to be computed, often by orders of magnitude. In this case, for example, it is possible to reduce all integrals $\mathcal{I}(a_1, a_2)$ to a single master integral $\mathcal{I}(1, 1)$ [113].

Note that the scalar propagators of the original integral are not always enough to capture all possible scalar products among external momenta and loop momenta and it is often necessary to introduce additional factors D_i to form a basis. These additional factors will, however, only appear in the numerator, and only these cases must be considered when computing IBP relations. It is then enough to find a basis of master integrals for an integral family $\mathcal{I}(a_1, \dots, a_n)$ with the restriction that $a_i < 0$ for $i \geq k$ for some k .

Having found a basis of master integrals, we can find further relations among integrals by taking derivatives with respect to external quantities. Take, for example, the massive bubble integral family

$$\mathcal{I}(a_1, a_2) = \int \frac{d^d k}{\pi^{d/2}} \frac{1}{(k^2 - m^2)^{a_1} ((k + p)^2 - m^2)^{a_2}} \tag{5.9}$$

and let $\mathcal{I}(b_1, b_2)$ be a master integral. Taking the derivative of this integral with respect to m^2 , we find

$$\partial_{m^2} \mathcal{I}(b_1, b_2) = b_1 \mathcal{I}(b_1 + 1, b_2) + b_2 \mathcal{I}(b_1, b_2 + 1). \tag{5.10}$$

The integrals appearing on the r.h.s. generally aren't master integrals themselves, but they are still members of the same integral family and we can rewrite them in terms of master integrals. Doing this for all master integrals of the family, we find a closed linear system of differential equations that can be written as a matrix A multiplying the vector J containing all master integrals [32, 114–117],

$$\partial_{m^2} J = AJ. \tag{5.11}$$

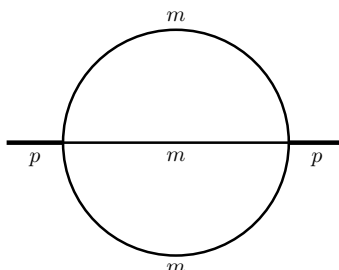


Figure 5.1: The two-loop sunrise graph with equal masses.

These differential equations can be used to solve master integrals and can further reduce the number of master integrals that need to be computed through direct integration.

5.1.2 The Sunrise Graph

In this section we will consider the sunrise graph and the family of Feynman integrals connected to it. The sunrise- and banana graph are the simplest Feynman graphs that can be drawn at two- or three loops respectively. The computation of the sunrise graph can be performed in an almost identical way as the computation of the banana graph and as such it makes sense to get accustomed to the calculation by considering this simpler example.

The Sunrise Family

The sunrise integral with all equal masses is the simplest example of a Feynman diagram that requires the introduction of elliptic integrals and this fact has been known for many years already [118, 119]. Consequently, the sunrise integral has been studied many times, and has been computed analytically in terms of many classes of functions generalizing elliptic integrals and multiple polylogarithms [35, 36, 45, 120–125]. As we will see in the following sections, some of these classes of functions are also suited to express the banana integral. For the remainder of this section we will review the sunrise integral family and the functions used to express its solution. These results are well-known and detailed reviews can be found in the literature (cf. e.g. ref. [120, 122]) so we will be brief in their description.

We will compute the Feynman integrals associated with the two-loop equal-mass sunrise graph depicted in fig. 5.1, i.e. solutions to all Feynman diagrams corresponding to the combination of scalar propagators given by the sunrise graph, raised to arbitrary powers. The corresponding integral family is given by

$$S_{a_1, \dots, a_5}(s, m^2; d) = \int \mathfrak{D}^d \ell_1 \mathfrak{D}^d \ell_2 \frac{(\ell_1 \cdot p)^{a_4} (\ell_2 \cdot p)^{a_5}}{[\ell_1^2 - m^2]^{a_1} [\ell_2^2 - m^2]^{a_2} [(\ell_1 - \ell_2)^2 - m^2]^{a_3}}, \quad (5.12)$$

with $s = -p^2$ and where we normalize the integration as

$$\int \mathfrak{D}^d \ell = \frac{1}{\Gamma(2 - \frac{d}{2})} \int \frac{d^d \ell}{i\pi^{d/2}}. \quad (5.13)$$

The scalar products appearing in the numerator are those we needed to add to the propagators of the sunrise graph in order to capture all appearing scalar products from IBP relations.

The sunrise integral family can be solved in terms of three master integrals, one of which is the tadpole integral $S_{1,1,0,0,0}(s, m^2; 2 - 2\epsilon)$. The remaining two master integrals obey a coupled system of differential equations and following ref. [122] we choose our master integrals to be

$$\begin{aligned} \mathcal{S}_1(\epsilon; t) &= s_1(t; 2 - 2\epsilon), \\ \mathcal{S}_2(\epsilon; t) &= \left[\frac{1}{3}(t^2 - 6t + 21) - 12\epsilon(t - 1) \right] s_1(t; 2 - 2\epsilon) \\ &\quad + 2(t - 1)(t - 9)s_2(t; 2 - 2\epsilon), \end{aligned} \quad (5.14)$$

where

$$\begin{aligned} s_1(t; 2 - 2\epsilon) &= S_{1,1,1,0,0}(s, m^2; 2 - 2\epsilon), \\ s_2(t; 2 - 2\epsilon) &= S_{2,1,1,0,0}(s, m^2; 2 - 2\epsilon). \end{aligned} \quad (5.15)$$

In order to reduce the number of scales in our computation, we defined the dimensionless ratio $t = s/m^2$ and will express all results in terms of t . We will also set $m = 1$ to simplify the computation even further. The dependence on the mass of the solution can later be recovered by dimensional analysis. The master integrals defined in eq. (5.14) fulfil the differential equation [122]

$$\partial_t \begin{pmatrix} \mathcal{S}_1(\epsilon; t) \\ \mathcal{S}_2(\epsilon; t) \end{pmatrix} = (B(t) - 2\epsilon D(t)) \begin{pmatrix} \mathcal{S}_1(\epsilon; t) \\ \mathcal{S}_2(\epsilon; t) \end{pmatrix} + \begin{pmatrix} 0 \\ -4 \end{pmatrix}, \quad (5.16)$$

where $B(t)$ and $D(t)$ are 2×2 matrices. In the following we are interested in finding a solution of the differential equation (5.16) in $d = 2$ dimensions. Since

the two master integrals defined in eq. (5.14) are finite and the matrices $B(t)$ and $D(t)$ are independent of ϵ we can compute the solution to the differential equation in $d = 2$ dimensions by setting $\epsilon \rightarrow 0$ in eq. (5.16). The matrix $B(t)$ is given by

$$B(t) = \begin{pmatrix} \frac{3+14t-t^2}{2t(t-1)(t-9)} & \frac{-3}{2t(t-1)(t-9)} \\ \frac{(t+3)(3+75t-15t^2+t^3)}{6t(t-1)(t-9)} & \frac{t^2-14t-3}{2t(t-1)(t-9)} \end{pmatrix}. \quad (5.17)$$

We can solve this differential equation in two steps. First, we try to find the fundamental solution matrix $\mathcal{W}_S(t)$ to the homogeneous differential equation, i.e. a 2×2 matrix whose columns form a basis to the solution space of the differential equation, $\partial_t \mathcal{W}_S(t) = B(t) \mathcal{W}_S(t)$. Then we try to find a vector $(T_1(t), T_2(t))^\top$ such that $(\mathcal{S}_1(t), \mathcal{S}_2(t))^\top = \mathcal{W}_S(t) (T_1(t), T_2(t))^\top$ solves the inhomogeneous differential equation. It is easy to see that this vector must obey the differential equation

$$\partial_t \begin{pmatrix} T_1(t) \\ T_2(t) \end{pmatrix} = \mathcal{W}_S(t)^{-1} \begin{pmatrix} 0 \\ -4 \end{pmatrix}. \quad (5.18)$$

The explicit solution $\mathcal{W}_S(t)$ of the homogeneous differential equation can be found in ref. [120, 122]. Before we get to the solution, let us note that it is possible to rewrite the homogeneous system of differential equations as a second order differential equation fulfilled by the first row of $\mathcal{W}_S(t)$. The corresponding differential equation was derived in [120] and reads

$$\mathcal{L}_t^{(2)} \Psi_i(t) = 0, \quad (5.19)$$

where

$$\mathcal{L}_t^{(2)} = \partial_t^2 + \left(\frac{1}{t-1} + \frac{1}{t} + \frac{1}{t-9} \right) \partial_t + \frac{1}{12(t-9)} + \frac{1}{4(t-1)} - \frac{1}{3t}. \quad (5.20)$$

This differential equation can be solved in terms of complete elliptic integrals of the first kind,

$$K(\lambda) = \int_0^1 \frac{dt}{\sqrt{(1-t^2)(1-\lambda t^2)}}, \quad (5.21)$$

and the solution space of this differential equation is spanned by the functions

$$\begin{aligned} \Psi_1(t) &= \frac{4}{[(3-\sqrt{t})(1+\sqrt{t})^3]^{1/2}} K \left(\frac{t_{14}(t)t_{23}(t)}{t_{13}(t)t_{24}(t)} \right), \\ \Psi_2(t) &= \frac{4i}{[(3-\sqrt{t})(1+\sqrt{t})^3]^{1/2}} K \left(\frac{t_{12}(t)t_{34}(t)}{t_{13}(t)t_{24}(t)} \right), \end{aligned} \quad (5.22)$$

where $t_{ij}(t) = t_i(t) - t_j(t)$ and where

$$t_1(t) = -4, \quad t_2(t) = -(1 + \sqrt{t})^2, \quad t_3(t) = -(1 - \sqrt{t})^2, \quad t_4(t) = 0. \quad (5.23)$$

The functions $\Psi_1(t)$ and $\Psi_2(t)$ are related to the maximal cut of the master integral $S_{1,1,1,0,0}(s, m^2; 2)$ [120] and are real-valued for $0 < t < 1$.

The Elliptic Curve Associated to the Sunrise Graph

The appearance of the complete elliptic integral K in the solution of the sunrise integral suggests that the geometry underlying the integral is somehow associated to an elliptic curve, and indeed, the sunrise integral has been computed in terms of eMPLs defined on an elliptic curve in ref. [126]. Loosely speaking, an elliptic curve can be defined as the solutions (x, y) of the polynomial equation $y^2 = (x - a_1) \cdots (x - a_4)$ where the a_i are complex constants. In the case of the sunrise integral, this elliptic curve is given by $a_i = t_i(t)$ where the $t_i(t)$ are given in eq. (5.23). Alternatively we can characterize the elliptic curve as a torus defined by the modular parameter (c.f. sec. 2.3)

$$\tau = \frac{\Psi_2(t)}{\Psi_1(t)}, \quad (5.24)$$

where the functions $\Psi_i(t)$ are the solutions to the homogeneous differential equation given in eq. (5.22).

The relation between t and τ can be inverted [127], and we find

$$t(\tau) = 9 \frac{\eta(\tau)^4 \eta(6\tau)^8}{\eta(2\tau)^8 \eta(3\tau)^4}, \quad (5.25)$$

where $\eta(\tau)$ denotes the Dedekind η -function,

$$\eta(\tau) = q^{1/24} \prod_{n=1}^{\infty} (1 - q^n), \quad q = e^{2\pi i \tau}. \quad (5.26)$$

The function $t(\tau)$ is invariant under modular transformations for $\Gamma_1(6)$,

$$t\left(\frac{a\tau + b}{c\tau + d}\right) = t(\tau), \quad \begin{pmatrix} a & b \\ c & d \end{pmatrix} \in \Gamma_1(6). \quad (5.27)$$

We see that the elliptic curves underlying the sunrise integral family are closely related to the congruence subgroup $\Gamma_1(6)$ (or $\Gamma_1(12)$, depending on whether the curve is defined through the Feynman parameter integral or its maximal cut) [35, 45].

Further, one can show that the function

$$f_{1,0}(\tau) \equiv \Psi_1(t(\tau)) \quad (5.28)$$

is a modular form of weight one (c.f. sec. 2.4) for $\Gamma_1(6)$ [45, 128]. As we have mentioned before, the space $\mathcal{M}_k(\Gamma)$ of modular forms of weight k for a congruence subspace Γ is finite-dimensional. A basis that is well-suited for the computation of the sunrise- and banana integral families was introduced in ref. [128] and we will now introduce that basis of the congruence subgroup $\Gamma_1(6)$.

Since $f_{1,0}(\tau)$ is a modular form of weight 1, all powers $f_{1,0}(\tau)^n$ will define a modular form of weight n . Further, since $t(\tau)$ is invariant under $\Gamma_1(6)$, multiplying a modular form by any (rational) function of $t(\tau)$ will preserve its modular properties under transformations in $\Gamma_1(6)$. Requiring that modular forms are holomorphic everywhere restricts the possible functions of $t(\tau)$ to polynomials. From the behaviour of $\Psi_1(t)$ for $t \rightarrow \infty$ we can further limit the maximal degree of the polynomial [128] and we find that a basis for $\mathcal{M}_n(\Gamma_1(6))$ is given by

$$f_{n,p}(\tau) = \Psi_1(t(\tau))^n t(\tau)^p, \quad 0 \leq p \leq n, \quad (5.29)$$

including $f_{0,0}(\tau) = 1$.

This basis is particularly well-suited for the computation of the sunrise- and banana integrals as we will demonstrate in the remainder of this section.

The Sunrise Integral and Modular Forms for $\Gamma_1(6)$

We have seen in a previous section that the homogeneous solution of the differential equation for the master integrals of the sunrise graph is given by the functions $\Psi_1(t)$ and $\Psi_2(t)$. In order to solve the inhomogeneous system, we need to find functions T_1 and T_2 such that equation (5.18) is fulfilled. Plugging in the fundamental solution matrix $\mathcal{W}_S(t)$, we find

$$\partial_t \begin{pmatrix} T_1(t) \\ T_2(t) \end{pmatrix} = -4 \begin{pmatrix} -\Psi_2(t) \\ \Psi_1(t) \end{pmatrix}. \quad (5.30)$$

Using the relation (5.25), we can rewrite this as a differential equation in the modular parameter τ . The Jacobian for this change of variables can be easily computed using eq. (5.24) and

$$\begin{aligned} \det \begin{pmatrix} \Psi_1(t) & \Psi_2(t) \\ \partial_t \Psi_1(t) & \partial_t \Psi_2(t) \end{pmatrix} &= \Psi_1(t) \partial_t \Psi_2(t) - \Psi_2(t) \partial_t \Psi_1(t) \\ &= -\frac{6\pi i}{t(t-1)(t-9)}, \end{aligned} \quad (5.31)$$

which ultimately yields

$$d\tau = -\frac{6\pi i dt}{t(t-1)(t-9)\Psi_1(t)^2}. \quad (5.32)$$

Changing variables from t to τ in equation (5.30),

$$\partial_\tau = -\frac{1}{6\pi i} t(\tau)(t(\tau)-1)(t(\tau)-9)\Psi_1(t(\tau))^2 \partial_t, \quad (5.33)$$

we can already guess that the functions $T_i(t)$ can be computed in terms of iterated integrals of the modular forms defined in eq. (5.29). In section 2.4 we have introduced the notion of iterated integrals of modular forms and have reviewed some of their basic properties. Let us now quickly fix the notation for iterated integrals over the modular forms defined in (5.29). We define

$$I_S\left(\begin{smallmatrix} n_1 & \dots & n_k \\ p_1 & \dots & p_k \end{smallmatrix}; \tau\right) \equiv I(f_{n_1, p_1}, \dots, f_{n_k, p_k}; \tau), \quad (5.34)$$

where $I(f_{i_1}, \dots, f_{i_k}; \tau)$ is the iterated integral over modular forms f_{i_j} with canonical basepoint $\tau_0 = i\infty$ defined in eq. (2.141) and where the $f_{n,p}$ correspond to the basis defined in equation (5.29). Note that the modular forms $f_{n,p}$ are normalized such that their Fourier coefficients are proportional to π^n . This allows us to define the weight of an iterated integral of modular forms $I_S\left(\begin{smallmatrix} n_1 & \dots & n_k \\ p_1 & \dots & p_k \end{smallmatrix}; \tau\right)$ as $\sum_{a=1}^k n_a$.

Using this notation, it is straight-forward to compute the functions $T_i(t)$ and we get, starting from equation (5.30),

$$\begin{aligned} \partial_\tau \begin{pmatrix} T_1(t(\tau)) \\ T_2(t(\tau)) \end{pmatrix} &= \frac{1}{24\pi^2} t(\tau)(t(\tau)-1)(t(\tau)-9)\Psi_1(t(\tau))^2 \begin{pmatrix} -\Psi_2(t) \\ \Psi_1(t) \end{pmatrix} \\ &= \frac{1}{24\pi^2} (f_{3,1}(\tau) - 10f_{3,2}(\tau) + 9f_{3,3}(\tau)) \begin{pmatrix} -\tau \\ 1 \end{pmatrix} \\ &= \frac{1}{24\pi^2} (f_{3,1}(\tau) - 10f_{3,2}(\tau) + 9f_{3,3}(\tau)) \begin{pmatrix} -I_S\left(\begin{smallmatrix} 0 \\ 0 \end{smallmatrix}; \tau\right) \\ 1 \end{pmatrix}, \end{aligned} \quad (5.35)$$

where we used that

$$\tau = \int_{i\infty}^{\tau} d\tau' f_{0,0}(\tau') = I_S\left(\begin{smallmatrix} 0 \\ 0 \end{smallmatrix}; \tau\right). \quad (5.36)$$

The initial condition for the differential equation have been computed in ref. [122] for $t \rightarrow 0$, which corresponds to $\tau \rightarrow i\infty$, and we have

$$\begin{aligned} T_1(t) &= \frac{\text{Cl}_2\left(\frac{\pi}{3}\right)}{2\pi} + \mathcal{O}(t), \\ T_2(t) &= \mathcal{O}(t), \end{aligned} \quad (5.37)$$

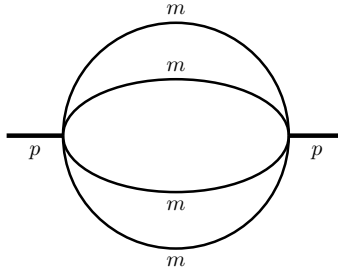


Figure 5.2: The three-loop equal-mass banana graph.

where

$$\text{Cl}_2(x) = \frac{i}{2} (\text{Li}_2(e^{-ix}) - \text{Li}_2(e^{ix})) \quad (5.38)$$

is the so-called Clausen function. Finally, this yields

$$\begin{aligned} T_1(t(\tau)) &= \frac{\text{Cl}_2\left(\frac{\pi}{3}\right)}{2\pi} - \frac{1}{24\pi^2} [I_S\left(\begin{smallmatrix} 3 & 0 \\ 1 & 0 \end{smallmatrix}; \tau\right) - 10I_S\left(\begin{smallmatrix} 3 & 0 \\ 2 & 0 \end{smallmatrix}; \tau\right) + 9I_S\left(\begin{smallmatrix} 3 & 0 \\ 3 & 0 \end{smallmatrix}; \tau\right)], \\ T_2(t(\tau)) &= \frac{1}{24\pi^2} [I_S\left(\begin{smallmatrix} 3 \\ 1 \end{smallmatrix}; \tau\right) - 10I_S\left(\begin{smallmatrix} 3 \\ 2 \end{smallmatrix}; \tau\right) + 9I_S\left(\begin{smallmatrix} 3 \\ 3 \end{smallmatrix}; \tau\right)]. \end{aligned} \quad (5.39)$$

We have seen how to compute solutions to a family of Feynman integrals by finding a basis of master integrals and how to compute these master integrals using differential equations. In particular, after analysing the elliptic curve underlying the integral and defining a suitable basis of modular forms, the computation of the inhomogeneous solution of the differential equation could be performed straight-forwardly in terms of iterated integrals of modular forms. In the next section we will consider the banana graph and compute the associated integrals in a similar fashion.

5.2 The Banana Graph

5.2.1 The Banana Family

In this section, we will compute the Feynman integrals associated with the three-loop equal-mass banana graph depicted in fig. 5.2. The corresponding

family of Feynman integrals is given by

$$I_{a_1, \dots, a_9}(s, m^2; d) = \int \prod_{i=1}^3 \mathfrak{D}^d k_i \quad (5.40)$$

$$\times \frac{(k_3^2)^{a_5} (k_1 \cdot p)^{a_6} (k_2 \cdot p)^{a_7} (k_3 \cdot p)^{a_8} (k_1 \cdot \ell_2)^{a_9}}{[k_1^2 - m^2]^{a_1} [k_2 - m^2]^{a_2} [(k_1 - \ell_3)^2 - m^2]^{a_3} [(k_2 - k_3 - p)^2 - m^2]^{a_4}},$$

with $a_i \in \mathbb{N}$ and $s = -p^2$. The scalar products appearing in the numerator are those we needed to add to the propagators of the banana graph in order to capture all appearing scalar products from IBP relations.

Let us quickly motivate why we are considering exactly this family of integrals. At every loop order ℓ , the simplest graph we can draw is the one connecting two vertices with $\ell + 1$ lines. For this reason, the so-called sunrise integral, the corresponding two-loop version of the banana graph, has been studied extensively and has been computed in various ways, both in the equal-mass case as well as the case where all masses are different. The sunrise graph is also the simplest elliptic Feynman integral and has been expressed in terms of virtually any description of elliptic integrals literature has to offer. A natural extension of this to three loops is to consider the banana graph. For arbitrary masses, the geometry of the integral can be very complicated and it is not easy to determine the function space containing the solved integral. In the equal-mass case, however, we will see that the underlying hypersurface of the integral is related to the hypersurface underlying the sunrise integral, which allows us to find a solution to the integral in terms of the elliptic integrals appearing in the sunrise case.

In order to reduce the number of parameters, we will again express all integrals as functions of the dimensionless ratio

$$x = \frac{4m^2}{s}, \quad (5.41)$$

and set $m = 1$. As before, the dependence on the mass m of the integral can be restored by analysing the mass-dimensions of each term.

Using integration by parts identities, we find that the class of integrals described in eq. (5.40) has four master integrals, namely a coupled system of three integrals,

$$\mathcal{I}_1(\epsilon; x) = (1 + 2\epsilon)(1 + 3\epsilon)I_{1,1,1,1,0,0,0,0,0}(4x, 1; 2 - 2\epsilon), \quad (5.42)$$

$$\mathcal{I}_2(\epsilon; x) = (1 + 2\epsilon)I_{2,1,1,1,0,0,0,0,0}(4x, 1; 2 - 2\epsilon), \quad (5.43)$$

$$\mathcal{I}_3(\epsilon; x) = I_{2,2,1,1,0,0,0,0,0}(4x, 1; 2 - 2\epsilon), \quad (5.44)$$

as well as the integral

$$\mathcal{I}_0(\epsilon; x) = I_{2,2,2,0,0,0,0,0}(4x, 1; 2 - 2\epsilon) = 1. \quad (5.45)$$

From simple power-counting of loop momenta k_i in the denominator, we see that the master integrals (5.42) can diverge for large momenta in $d = 4$ dimensions, and we will therefore compute them in $d = 2 - 2\epsilon$ dimensions. The coefficients of the Laurent series in ϵ in $d = 2 - 2\epsilon$ dimensions can then be related to the Laurent expansion in $d = 4 - 2\epsilon$ dimensions through dimensional shift identities [129–134]. In fact, in order to obtain the correct result of the master integrals in $d = 4 - 2\epsilon$ dimensions up to order $\mathcal{O}(\epsilon^0)$, it is sufficient to compute the integrals in $d = 2 - 2\epsilon$ dimensions up to the same order in ϵ .

5.2.2 The Coupled System of Differential Equations

As we have already mentioned above, the three integrals in equation (5.42) form a coupled system of differential equations. Taking a derivative with respect to the parameter x and rewriting the resulting integrals in terms of master integrals, we find that the integrals $\mathcal{I}_1, \mathcal{I}_2, \mathcal{I}_3$ fulfil the differential equation [135]

$$\partial_x \begin{pmatrix} \mathcal{I}_1(\epsilon; x) \\ \mathcal{I}_2(\epsilon; x) \\ \mathcal{I}_3(\epsilon; x) \end{pmatrix} = [B(x) + \epsilon D(x)] \begin{pmatrix} \mathcal{I}_1(\epsilon; x) \\ \mathcal{I}_2(\epsilon; x) \\ \mathcal{I}_3(\epsilon; x) \end{pmatrix} + \begin{pmatrix} 0 \\ 0 \\ \frac{1}{2(1-4x)} \end{pmatrix}, \quad (5.46)$$

where the matrices $B(x)$ and $D(x)$ are given by

$$B(x) = \begin{pmatrix} \frac{1}{x} & \frac{4}{x} & 0 \\ \frac{1}{4(1-x)} & \frac{1}{x} + \frac{2}{1-x} & \frac{3}{x} + \frac{3}{1-x} \\ \frac{1}{8(1-4x)} - \frac{1}{8(1-x)} & \frac{3}{2(1-4x)} - \frac{1}{1-x} & \frac{1}{x} + \frac{6}{1-4x} - \frac{3}{2(1-x)} \end{pmatrix}, \quad (5.47)$$

$$D(x) = \begin{pmatrix} \frac{3}{x} & \frac{12}{x} & 0 \\ \frac{1}{1-x} & \frac{2}{x} + \frac{6}{1-x} & \frac{6}{x} + \frac{6}{1-x} \\ \frac{1}{2(1-4x)} - \frac{1}{2(1-x)} & \frac{9}{2(1-4x)} - \frac{3}{1-x} & \frac{1}{x} + \frac{12}{1-4x} - \frac{3}{1-x} \end{pmatrix}. \quad (5.48)$$

Since the integrals \mathcal{I}_i are finite in $d = 2$ dimensions and we are only interested in the results up to $\mathcal{O}(\epsilon^0)$, we can set $\epsilon = 0$ and simplify the problem to the differential equation

$$\partial_x \begin{pmatrix} \mathcal{I}_1(x) \\ \mathcal{I}_2(x) \\ \mathcal{I}_3(x) \end{pmatrix} = B(x) \begin{pmatrix} \mathcal{I}_1(x) \\ \mathcal{I}_2(x) \\ \mathcal{I}_3(x) \end{pmatrix} + \begin{pmatrix} 0 \\ 0 \\ -\frac{1}{2(1-4x)} \end{pmatrix}. \quad (5.49)$$

As we have done for the sunrise integral, we will solve this differential equation in two steps. First, we will consider the homogeneous differential equation

$$\partial_x \begin{pmatrix} \mathcal{J}_1(x) \\ \mathcal{J}_2(x) \\ \mathcal{J}_3(x) \end{pmatrix} = B(x) \begin{pmatrix} \mathcal{J}_1(x) \\ \mathcal{J}_2(x) \\ \mathcal{J}_3(x) \end{pmatrix} \quad (5.50)$$

and find its fundamental solution matrix $\mathcal{W}(x)$. Then we will compute a vector $(M_1(x), M_2(x), M_3(x))^\top$ such that

$$\begin{pmatrix} \mathcal{I}_1(x) \\ \mathcal{I}_2(x) \\ \mathcal{I}_3(x) \end{pmatrix} = \mathcal{W}(x) \begin{pmatrix} M_1(x) \\ M_2(x) \\ M_3(x) \end{pmatrix} \quad (5.51)$$

solves the inhomogeneous differential equation (5.49). Plugging eq. (5.51) into both sides of eq. (5.49) we see that

$$\partial_x \begin{pmatrix} M_1(x) \\ M_2(x) \\ M_3(x) \end{pmatrix} = \mathcal{W}^{-1}(x) \begin{pmatrix} 0 \\ 0 \\ \frac{1}{2(1-4x)} \end{pmatrix}, \quad (5.52)$$

which we will use to compute $(M_1(x), M_2(x), M_3(x))^\top$. In the remainder of this section we will construct the fundamental solution matrix $\mathcal{W}(x)$ for the equal-mass banana graph.

5.2.3 The Fundamental Solution Matrix

It is generally a very demanding task to compute the fundamental solution matrix of a system of differential equations. Considering the differential equation for the banana graph, we are in luck, as there is a rather elegant way to obtain the fundamental solution matrix [135, 136], which we will review in the remainder of this section.

Let us explicitly label the different entries of the fundamental solution matrix as

$$\mathcal{W}(x) = \begin{pmatrix} H_1(x) & J_1(x) & I_1(x) \\ H_2(x) & J_2(x) & I_2(x) \\ H_3(x) & J_3(x) & I_3(x) \end{pmatrix}. \quad (5.53)$$

Then we can rewrite the system of first-order differential equations (5.50) as a single third-order differential equation

$$\mathcal{L}_x^{(3)} H_1(x) = \mathcal{L}_x^{(3)} J_1(x) = \mathcal{L}_x^{(3)} I_1(x) = 0, \quad (5.54)$$

that each element of the first row of $\mathcal{W}(x)$ must fulfil, and where we rewrote

$$\begin{aligned} H_2(x) &= \frac{1}{4}(x \partial_x - 1) H_1(x) \\ H_3(x) &= \frac{1}{12}(x^2(1-x) \partial_x^2 - x(1+x) \partial_x + 1) H_1(x), \end{aligned} \quad (5.55)$$

and equivalently for J_i and I_i . The differential operator $\mathcal{L}_x^{(3)}$ is given by [135, 136]

$$\mathcal{L}_x^{(3)} = \partial_x^3 + \frac{3(8x-5)}{2(x-1)(4x-1)} \partial_x^2 + \frac{4x^2-2x+1}{(x-1)(4x-1)x^2} \partial_x + \frac{1}{x^3(4x-1)}. \quad (5.56)$$

Given a solution for H_1 of the differential equation (5.54), we can easily compute H_2 and H_3 from equation (5.55). This might seem like a step in the wrong direction since there is no known algorithm to compute the solution of a generic third-order differential equation, it is however possible to write the differential operator $\mathcal{L}_x^{(3)}$ as the *symmetric square* of the second-order differential operator [137]

$$\mathcal{L}_x^{(2)} = \partial_x^2 + \frac{8x-5}{2(x-1)(4x-1)} \partial_x - \frac{2x-1}{4x^2(x-1)(4x-1)}. \quad (5.57)$$

For this work it is sufficient to think of the symmetric square of a differential operator \mathcal{L} as a higher-order differential operator that can be constructed from \mathcal{L} such that its solutions are given as products of the solutions of \mathcal{L} . The operator $\mathcal{L}_x^{(2)}$ given in eq. (5.57) is very closely related to the operator $\mathcal{L}_t^{(2)}$ we have seen in the previous section, allowing us to rewrite the functions in eq. (5.53) in terms of the functions (5.22). Upon defining

$$x(t) = \frac{-4t}{(t-1)(t-9)}, \quad (5.58)$$

we have

$$\begin{aligned} H_1(x(t)) &= -\frac{1}{3} t \Psi_1(t)^2, \\ J_1(x(t)) &= \frac{i}{3} t \Psi_1(t) (\Psi_1(t) + \Psi_2(t)), \\ I_1(x(t)) &= \frac{1}{3} t (\Psi_1(t) + \Psi_2(t)) (\Psi_1(t) + 3\Psi_2(t)). \end{aligned} \quad (5.59)$$

As expected, the solutions of $\mathcal{L}_x^{(3)}$ can be cast as sums of products of the solutions of $\mathcal{L}_t^{(2)}$.

We have seen that we can express the homogeneous solutions of the banana graph in terms of the homogeneous solutions of the sunrise graph. This begs the

question whether the functions spaces of the inhomogeneous solutions to the two integral families are as closely related as well. The solutions to the sunrise graph have previously been expressed in terms of elliptic polylogarithms [35, 36, 123–126, 138] as well as iterated integrals of modular forms [45, 52] and similar observations were made for the banana graph. More precisely it was shown in ref. [136] that the solution of the banana graph corresponds to elliptic trilogarithms and that it is closely related to integrals of modular forms relevant for the two-loop sunrise integral. In the remainder of this chapter we will make these observations manifest by computing the inhomogeneous solutions $M_i(x)$ in $d = 2$ dimensions in terms of these functions.

From the solutions defined in equation (5.59) we can obtain explicit representations of the remaining entries of the fundamental solution matrix $\mathcal{W}(x)$ through the relations given in equation (5.55). These solutions require us to take derivatives of the complete elliptic integral of the first kind K , which gives rise to the complete elliptic integral of the second kind,

$$E(\lambda) = \int_0^1 dt \sqrt{\frac{1 - \lambda t^2}{1 - t^2}}. \quad (5.60)$$

Explicit results for all entries of the fundamental solution matrix can be found in ref. [135].

From the previous analysis we can conclude that the functions $M_i(x)$ in eq. (5.52) can be expressed as integrals over products of complete elliptic integrals and this computation has been considered in [135]. We would nevertheless like to have a uniform description of the functions $M_i(x)$ and the functions in $\mathcal{W}(x)$ in terms of an appropriate class of functions. This is exactly the goal of this chapter. In the following section we will compute the inhomogeneous solution to the banana integral first in terms of the iterated integrals of modular forms we have introduced for the sunrise integral as we as in terms of the elliptic multiple polylogarithms that have been used to compute the sunrise integral [126].

5.3 The Equal-Mass Banana Graph and Modular Forms for $\Gamma_1(6)$

In the previous sections we have demonstrated how to use a suitable basis of iterated integrals of modular forms to compute the sunrise integral family. In this section we will show that the same class of functions is equally well-suited for the computation of the master integrals of the equal-mass banana graph in $d = 2$ dimensions. We start by relating the fundamental solution matrix $\mathcal{W}(x)$

to modular forms for $\Gamma_1(6)$ after which we will compute the missing functions $M_i(x)$ explicitly in terms of the iterated integrals of modular forms for $\Gamma_1(6)$ introduced in the previous section.

In eq. (5.59) we have expressed the first entries of the fundamental solution matrix $\mathcal{W}(x)$ in terms of the periods Ψ_1 and Ψ_2 of the elliptic curve underlying the equal-mass sunrise integral. Using the definition of the modular forms $f_{n,p}$ in eq. (5.29) as well as eq. (5.24), we can easily rewrite eq. (5.59) as

$$\begin{aligned} H_1(x(\tau)) &= -\frac{1}{3} f_{2,1}(\tau), \\ J_1(x(\tau)) &= \frac{i}{3} f_{2,1}(\tau) (1 + \tau), \\ I_1(x(\tau)) &= \frac{1}{3} f_{2,1}(\tau) (1 + \tau) (1 + 3\tau). \end{aligned} \tag{5.61}$$

where $x(\tau)$ can be obtained from equations (5.58) and (5.25),

$$x(\tau) = -4 \left(\frac{\eta(2\tau)\eta(6\tau)}{\eta(\tau)\eta(3\tau)} \right)^6. \tag{5.62}$$

We see that all first entries of $\mathcal{W}(x(\tau))$ are proportional to the modular form $f_{2,1}$ and that J_1 and I_1 are multiplied by polynomials in τ of degree 1 and 2 respectively. The other entries of \mathcal{W} also involve derivatives of Ψ_1 and Ψ_2 and can therefore not easily be rewritten in terms of modular forms for $\Gamma_1(6)$ and τ alone. After computing the inverse of \mathcal{W} and inserting it into the differential equation for the M_i in equation (5.61), we find that all appearances of derivatives of Ψ_i cancel out after using eq. (5.31), and we find

$$\begin{aligned} \partial_\tau \begin{pmatrix} M_1(x(\tau)) \\ M_2(x(\tau)) \\ M_3(x(\tau)) \end{pmatrix} & \\ &= \frac{f_{4,4}(\tau) - 10f_{4,3}(\tau) + 90f_{4,1}(\tau) - 81f_{4,0}(\tau)}{18i\pi^3} \begin{pmatrix} 3(1 + \tau)^2 \\ -2i(2 + 3\tau) \\ -1 \end{pmatrix} \\ &= \frac{f_{4,4}(\tau) - 10f_{4,3}(\tau) + 90f_{4,1}(\tau) - 81f_{4,0}(\tau)}{18i\pi^3} \begin{pmatrix} 3(1 + I_S(\frac{0}{0}; \tau))^2 \\ -2i(2 + 3I_S(\frac{0}{0}; \tau)) \\ -1 \end{pmatrix}, \end{aligned} \tag{5.63}$$

where we have used that the Jacobian for changing variables from x to τ , is given by

$$\partial_\tau = -\frac{2t(\tau)(t(\tau)^2 - 9)}{3\pi i (t(\tau) - 1)(t(\tau) - 9)} \Psi_1(t(\tau))^2 \partial_x. \tag{5.64}$$

Given the boundary conditions for $\tau \rightarrow i\infty$, or equivalently, for $x \rightarrow 0$, we can easily solve this differential equation in terms of the iterated integrals of modular forms I_S using direct integration. The boundary conditions can be extracted from the original Feynman integrals using Feynman parametrization by extracting the $\mathcal{O}(x^0)$ component and can be found in ref. [5]. While the computation is straight-forward, it is also very technical and we refer the reader to that paper for a detailed computation. The boundary terms are given by

$$\begin{aligned}\mathcal{I}_1(x) &= x \log(-x/4)^3 - 4x\zeta_3 + \mathcal{O}(x^2), \\ \mathcal{I}_2(x) &= \frac{3}{4}x \log(-x/4)^2 + \mathcal{O}(x^2), \\ \mathcal{I}_3(x) &= \frac{1}{2}x \log(-x/4) + \mathcal{O}(x^2).\end{aligned}\tag{5.65}$$

Then the result for the master integrals of the equal-mass banana integral family in $d = 2$ dimensions is given by

$$\begin{aligned}M_1(x(\tau)) &= -\frac{4\zeta_3}{\pi^2} - \frac{i}{6\pi^3} [81I_S(\frac{4}{0}; \tau) - 90I_S(\frac{4}{1}; \tau) + 10I_S(\frac{4}{3}; \tau) - I_S(\frac{4}{4}; \tau) \\ &\quad + 162I_S(\frac{4}{0} \frac{0}{0}; \tau) - 180I_S(\frac{4}{1} \frac{0}{0}; \tau) + 20I_S(\frac{4}{3} \frac{0}{0}; \tau) - 2I_S(\frac{4}{4} \frac{0}{0}; \tau) \\ &\quad + 162I_S(\frac{4}{0} \frac{0}{0} \frac{0}{0}; \tau) - 180I_S(\frac{4}{1} \frac{0}{0} \frac{0}{0}; \tau) + 20I_S(\frac{4}{3} \frac{0}{0} \frac{0}{0}; \tau) - 2I_S(\frac{4}{4} \frac{0}{0} \frac{0}{0}; \tau)],\end{aligned}\tag{5.66}$$

$$\begin{aligned}M_2(x(\tau)) &= -\frac{1}{9\pi^3} [162I_S(\frac{4}{0}; \tau) - 180I_S(\frac{4}{1}; \tau) + 20I_S(\frac{4}{3}; \tau) - 2I_S(\frac{4}{4}; \tau) \\ &\quad + 243I_S(\frac{4}{0} \frac{0}{0}; \tau) - 270I_S(\frac{4}{1} \frac{0}{0}; \tau) + 30I_S(\frac{4}{3} \frac{0}{0}; \tau) - 3I_S(\frac{4}{4} \frac{0}{0}; \tau)],\end{aligned}\tag{5.67}$$

$$\begin{aligned}M_3(x(\tau)) &= \\ &\quad \frac{i}{18\pi^3} [-81I_S(\frac{4}{0}; \tau) + 90I_S(\frac{4}{1}; \tau) - 10I_S(\frac{4}{3}; \tau) + I_S(\frac{4}{4}; \tau)].\end{aligned}\tag{5.68}$$

At this point we have successfully computed the inhomogeneous solution to the differential equation encoding the master integrals of the banana integral family in terms of iterated integrals of modular forms. The result however does not seem to have any particularly nice structure. Following ref. [38], however, it should be possible to write the solution in terms of combinations of iterated integrals of uniform length by splitting the fundamental solution matrix \mathcal{W} into the product of a semisimple matrix S and a unipotent matrix U ,

$$\mathcal{W} = SU.\tag{5.69}$$

Such a decomposition can be found in ref. [5] and we have

$$U = \begin{pmatrix} 1 & -\frac{i\Psi_1(t)+\Psi_2(t)}{\Psi_1(t)} & -\frac{(\Psi_1(t)+\Psi_2(t))(\Psi_1(t)+3\Psi_2(t))}{\Psi_1(t)^2} \\ 0 & 1 & -\frac{2i(2\Psi_1(t)+3\Psi_2(t))}{\Psi_1(t)} \\ 0 & 0 & 1 \end{pmatrix} \quad (5.70)$$

$$= \begin{pmatrix} 1 & -i(\tau+1) & -(\tau+1)(3\tau+1) \\ 0 & 1 & -2i(3\tau+2) \\ 0 & 0 & 1 \end{pmatrix}. \quad (5.71)$$

The semisimple matrix S is a rational function of the Ψ_i , their derivatives and explicit factors of t and does not contribute to the analysis done in this paper. Since the matrix is very complicated and does not serve any particular purpose for us, we are not showing it in this work explicitly. Then we can rotate the vector $(M_1, M_2, M_3)^\top$ using the matrix U to define

$$\begin{pmatrix} \tilde{M}_1 \\ \tilde{M}_2 \\ \tilde{M}_3 \end{pmatrix} \equiv U^{-1} \begin{pmatrix} M_1 \\ M_2 \\ M_3 \end{pmatrix} \quad (5.72)$$

and we have

$$\begin{aligned} \tilde{M}_1 &= -\frac{4\zeta_3}{\pi^2} - \frac{i}{3\pi^3} (81I_S\left(\begin{smallmatrix} 0 & 0 & 4 \\ 0 & 0 & 0 \end{smallmatrix}; \tau\right) - 90I_S\left(\begin{smallmatrix} 0 & 0 & 4 \\ 0 & 0 & 1 \end{smallmatrix}; \tau\right) \\ &\quad + 10I_S\left(\begin{smallmatrix} 0 & 0 & 4 \\ 0 & 0 & 3 \end{smallmatrix}; \tau\right) - I_S\left(\begin{smallmatrix} 0 & 0 & 4 \\ 0 & 0 & 4 \end{smallmatrix}; \tau\right)) \\ \tilde{M}_2 &= \frac{1}{3\pi^3} (81I_S\left(\begin{smallmatrix} 0 & 4 \\ 0 & 0 \end{smallmatrix}; \tau\right) - 90I_S\left(\begin{smallmatrix} 0 & 4 \\ 0 & 1 \end{smallmatrix}; \tau\right) + 10I_S\left(\begin{smallmatrix} 0 & 4 \\ 0 & 3 \end{smallmatrix}; \tau\right) - I_S\left(\begin{smallmatrix} 0 & 4 \\ 0 & 4 \end{smallmatrix}; \tau\right)) \\ \tilde{M}_3 &= \frac{i}{18\pi^3} (81I_S\left(\begin{smallmatrix} 4 \\ 0 \end{smallmatrix}; \tau\right) - 90I_S\left(\begin{smallmatrix} 4 \\ 1 \end{smallmatrix}; \tau\right) + 10I_S\left(\begin{smallmatrix} 4 \\ 3 \end{smallmatrix}; \tau\right) - I_S\left(\begin{smallmatrix} 4 \\ 4 \end{smallmatrix}; \tau\right)) \end{aligned} \quad (5.73)$$

As expected, the solutions \tilde{M}_i are all of uniform length $4-i$ and of weight 4. Let us further note that the structure of the individual solutions is very similar. Up to a global prefactor, the three solutions differ only by removing or adding integrations over the modular form $f_{0,0} = 1$ and are therefore derivatives of each other with respect to τ .

5.3.1 The Banana Integral and eMPLs

We have seen that the banana integral can be computed in terms of the same iterated integrals of modular forms as the sunrise integral. In the literature, the sunrise integral has also been computed in terms of elliptic multiple polylogarithms, so it is an obvious question if this can be achieved for the banana integral as well. Note that this is not a trivial question. While all eMPLs on the torus evaluated at rational points can be written as iterated integrals of

modular forms (c.f. sec. 2.4), the inverse is not generally true. In this section we will show that the banana integral can indeed be cast as a linear combination of the eMPLs defined on the torus associated to the sunrise integral. Since the homogeneous solution $\mathcal{W}(x)$ can be obtained from the homogeneous solutions of the sunrise integral, and since the sunrise integral has already been computed in terms of eMPLs [126], all that is left to show is that we can express the functions M_i in terms of eMPLs.

In section 2.4 we have seen how we can rewrite any elliptic multiple polylogarithm evaluated at rational points in terms of iterated integrals of modular forms by recursively reconstructing the corresponding function from its coaction. There we have also seen that a natural basis of modular forms for this endeavour is given by the Eisenstein forms $h_{N,r,s}^{(n)}$ defined in eq. (2.152). We will therefore start by rewriting the solution in eq. (5.73) in terms of iterated integrals of these modular forms. This can easily be done by finding the change of basis between the $f_{n,p}$ and the $h_{N,r,s}^{(n)}$. Then the transformation of the iterated integrals of modular forms follows directly from linearity of the integral,

$$I(\dots, f_1 + f_2, \dots, \tau) = I(\dots, f_1, \dots, \tau) + I(\dots, f_2, \dots, \tau). \quad (5.74)$$

Since all modular forms naturally have a q -expansion, we can find the change of basis by writing an ansatz for each basis element in terms of the second basis, expanding all modular forms to high orders and solving the resulting linear system. Note that all appearing modular forms in eq. (5.73) are of weight 4, so we only have to find a change of basis for the modular forms of weight $n = 4$. In ref. [52] a basis of Eisenstein forms of weight 4 for $\Gamma_1(6)$ has been computed which is given by

$$\begin{aligned} b_1 &= h_{6,0,1}^{(4)} + h_{6,1,1}^{(4)} + h_{6,2,1}^{(4)} + h_{6,3,1}^{(4)} + h_{6,4,1}^{(4)} + h_{6,5,1}^{(4)} \\ b_2 &= h_{6,1,2}^{(4)} + h_{6,3,2}^{(4)} + h_{6,5,2}^{(4)} \\ b_3 &= h_{6,1,0}^{(4)} \\ b_4 &= h_{6,1,3}^{(4)} + h_{6,4,3}^{(4)}. \end{aligned} \quad (5.75)$$

After performing the change of basis we find [5]

$$\begin{aligned}
\tilde{M}_1 &= \frac{36i}{\pi^3} \left(21 I\left(\begin{smallmatrix} 0 & 0 \\ 0 & 0 \end{smallmatrix} \middle| \begin{smallmatrix} 4 & 6 \\ 0 & 1 \end{smallmatrix}; \tau\right) - I\left(\begin{smallmatrix} 0 & 0 \\ 0 & 0 \end{smallmatrix} \middle| \begin{smallmatrix} 4 & 6 \\ 1 & 0 \end{smallmatrix}; \tau\right) + 21 I\left(\begin{smallmatrix} 0 & 0 \\ 0 & 0 \end{smallmatrix} \middle| \begin{smallmatrix} 4 & 6 \\ 1 & 1 \end{smallmatrix}; \tau\right) \\
&\quad + 3 I\left(\begin{smallmatrix} 0 & 0 \\ 0 & 0 \end{smallmatrix} \middle| \begin{smallmatrix} 4 & 6 \\ 1 & 2 \end{smallmatrix}; \tau\right) - 7 I\left(\begin{smallmatrix} 0 & 0 \\ 0 & 0 \end{smallmatrix} \middle| \begin{smallmatrix} 4 & 6 \\ 1 & 3 \end{smallmatrix}; \tau\right) + 21 I\left(\begin{smallmatrix} 0 & 0 \\ 0 & 0 \end{smallmatrix} \middle| \begin{smallmatrix} 4 & 6 \\ 2 & 1 \end{smallmatrix}; \tau\right) \\
&\quad + 21 I\left(\begin{smallmatrix} 0 & 0 \\ 0 & 0 \end{smallmatrix} \middle| \begin{smallmatrix} 4 & 6 \\ 3 & 1 \end{smallmatrix}; \tau\right) + 3 I\left(\begin{smallmatrix} 0 & 0 \\ 0 & 0 \end{smallmatrix} \middle| \begin{smallmatrix} 4 & 6 \\ 3 & 2 \end{smallmatrix}; \tau\right) + 21 I\left(\begin{smallmatrix} 0 & 0 \\ 0 & 0 \end{smallmatrix} \middle| \begin{smallmatrix} 4 & 6 \\ 4 & 1 \end{smallmatrix}; \tau\right) \\
&\quad - 7 I\left(\begin{smallmatrix} 0 & 0 \\ 0 & 0 \end{smallmatrix} \middle| \begin{smallmatrix} 4 & 6 \\ 4 & 3 \end{smallmatrix}; \tau\right) + 21 I\left(\begin{smallmatrix} 0 & 0 \\ 0 & 0 \end{smallmatrix} \middle| \begin{smallmatrix} 4 & 6 \\ 5 & 1 \end{smallmatrix}; \tau\right) + 3 I\left(\begin{smallmatrix} 0 & 0 \\ 0 & 0 \end{smallmatrix} \middle| \begin{smallmatrix} 4 & 6 \\ 5 & 2 \end{smallmatrix}; \tau\right) \right) \\
&\quad - \frac{4\zeta_3}{\pi^2}, \\
\tilde{M}_2 &= -\frac{36}{\pi^3} \left(21 I\left(\begin{smallmatrix} 0 & 0 \\ 0 & 0 \end{smallmatrix} \middle| \begin{smallmatrix} 4 & 6 \\ 0 & 1 \end{smallmatrix}; \tau\right) - I\left(\begin{smallmatrix} 0 & 0 \\ 0 & 0 \end{smallmatrix} \middle| \begin{smallmatrix} 4 & 6 \\ 1 & 0 \end{smallmatrix}; \tau\right) + 21 I\left(\begin{smallmatrix} 0 & 0 \\ 0 & 0 \end{smallmatrix} \middle| \begin{smallmatrix} 4 & 6 \\ 1 & 1 \end{smallmatrix}; \tau\right) \\
&\quad + 3 I\left(\begin{smallmatrix} 0 & 0 \\ 0 & 0 \end{smallmatrix} \middle| \begin{smallmatrix} 4 & 6 \\ 1 & 2 \end{smallmatrix}; \tau\right) - 7 I\left(\begin{smallmatrix} 0 & 0 \\ 0 & 0 \end{smallmatrix} \middle| \begin{smallmatrix} 4 & 6 \\ 1 & 3 \end{smallmatrix}; \tau\right) + 21 I\left(\begin{smallmatrix} 0 & 0 \\ 0 & 0 \end{smallmatrix} \middle| \begin{smallmatrix} 4 & 6 \\ 2 & 1 \end{smallmatrix}; \tau\right) \\
&\quad + 21 I\left(\begin{smallmatrix} 0 & 0 \\ 0 & 0 \end{smallmatrix} \middle| \begin{smallmatrix} 4 & 6 \\ 3 & 1 \end{smallmatrix}; \tau\right) + 3 I\left(\begin{smallmatrix} 0 & 0 \\ 0 & 0 \end{smallmatrix} \middle| \begin{smallmatrix} 4 & 6 \\ 3 & 2 \end{smallmatrix}; \tau\right) + 21 I\left(\begin{smallmatrix} 0 & 0 \\ 0 & 0 \end{smallmatrix} \middle| \begin{smallmatrix} 4 & 6 \\ 4 & 1 \end{smallmatrix}; \tau\right) \\
&\quad - 7 I\left(\begin{smallmatrix} 0 & 0 \\ 0 & 0 \end{smallmatrix} \middle| \begin{smallmatrix} 4 & 6 \\ 4 & 3 \end{smallmatrix}; \tau\right) + 21 I\left(\begin{smallmatrix} 0 & 0 \\ 0 & 0 \end{smallmatrix} \middle| \begin{smallmatrix} 4 & 6 \\ 5 & 1 \end{smallmatrix}; \tau\right) + 3 I\left(\begin{smallmatrix} 0 & 0 \\ 0 & 0 \end{smallmatrix} \middle| \begin{smallmatrix} 4 & 6 \\ 5 & 2 \end{smallmatrix}; \tau\right) \right), \\
\tilde{M}_3 &= -\frac{6i}{\pi^3} \left(21 I\left(\begin{smallmatrix} 4 & 6 \\ 0 & 1 \end{smallmatrix}; \tau\right) - I\left(\begin{smallmatrix} 4 & 6 \\ 1 & 0 \end{smallmatrix}; \tau\right) + 21 I\left(\begin{smallmatrix} 4 & 6 \\ 1 & 1 \end{smallmatrix}; \tau\right) + 3 I\left(\begin{smallmatrix} 4 & 6 \\ 1 & 2 \end{smallmatrix}; \tau\right) \\
&\quad - 7 I\left(\begin{smallmatrix} 4 & 6 \\ 1 & 3 \end{smallmatrix}; \tau\right) + 21 I\left(\begin{smallmatrix} 4 & 6 \\ 2 & 1 \end{smallmatrix}; \tau\right) + 21 I\left(\begin{smallmatrix} 4 & 6 \\ 3 & 1 \end{smallmatrix}; \tau\right) + 3 I\left(\begin{smallmatrix} 4 & 6 \\ 3 & 2 \end{smallmatrix}; \tau\right) \\
&\quad + 21 I\left(\begin{smallmatrix} 4 & 6 \\ 4 & 1 \end{smallmatrix}; \tau\right) - 7 I\left(\begin{smallmatrix} 4 & 6 \\ 4 & 3 \end{smallmatrix}; \tau\right) + 21 I\left(\begin{smallmatrix} 4 & 6 \\ 5 & 1 \end{smallmatrix}; \tau\right) + 3 I\left(\begin{smallmatrix} 4 & 6 \\ 5 & 2 \end{smallmatrix}; \tau\right) \right).
\end{aligned} \tag{5.76}$$

To rewrite this result in terms of eMPLs, we write a suitable Ansatz in terms of eMPLs $\tilde{\Gamma}$ evaluated at rational points, compute the corresponding expression in terms of iterated integrals of Eisenstein series and match the Ansatz with equation (5.76). In particular, we have computed all well defined $\tilde{\Gamma}$ of the form

$$\tilde{\Gamma} \left(\underbrace{\begin{smallmatrix} 0, \dots, 0 \\ 0, \dots, 0 \end{smallmatrix}}_{k\text{-times}} \begin{smallmatrix} 3-k \\ z_1 \end{smallmatrix}; z_0, \tau \right) \tag{5.77}$$

with $z_i = r_i/6 + s_i/N\tau$ for $r_i, s_i \in \{0, \dots, 5\}$ in terms of iterated integrals of Eisenstein series. After forming a suitable Ansatz for each of the \tilde{M}_i we have found that they can indeed be cast as linear combinations of eMPLs. One such solution is given in appendix H.

Conclusion and Outlook

Conclusion

In this thesis we have demonstrated that the computation of scattering amplitudes can be facilitated by first analysing the underlying geometry of the problem and identifying the class of functions they can be composed of. In particular, we have performed state of the art computations of scattering amplitudes both in the multi-Regge limit as well as in general kinematics.

We have started with the multi-Regge limit of $\mathcal{N} = 4$ supersymmetric Yang-Mills theory which served as a testing ground for our endeavour. In this limit, scattering amplitudes can be cast to all orders as a Fourier-Mellin transform of a combination of only three building blocks. We have used the mathematical properties of the Fourier-Mellin transform to develop an alternative way to perform computations in MRK. Instead of evaluating the Fourier-Mellin integral at every loop order, we computed higher-order results recursively from lower-order amplitudes. This allows us to both reuse the results we compute as well as to circumvent the tedious evaluation of Fourier-Mellin integrals by performing convolutions. We have shown that scattering amplitudes in this kinematical limit are single-valued polylogarithmic functions of the transverse external momenta and we were able to use this information to further reduce the complexity of the necessary computations. Due to the single-valuedness of the amplitude and good knowledge of the functional properties of polylogarithms we could evaluate the convolution integrals relating scattering amplitudes at different orders as a sum of residues. With this framework, it was possible to compute scattering amplitudes in the multi-Regge limit of $\mathcal{N} = 4$ SYM up to five loops and for up to nine external particles. We were further able to

prove that at every loop order, MHV scattering amplitudes in this limit for any number of external particles can be written as sums of a finite number of building-blocks. This finding, together with the convolution-framework allows us to compute virtually any scattering amplitude in the multi-Regge limit of $\mathcal{N} = 4$ SYM.

Next, we have extended the framework we have developed for the computation of scattering amplitudes in MRK to theories realised in nature. We have considered the BFKL ladder for dijet production in the forward scattering limit of QCD. This quantity can also be cast as a Fourier-Mellin transform to LLA and NLLA and therefore made a perfect candidate for us to test the framework we had previously developed in a more realistic setting and we found that the functional dependence on the transverse momenta is again captured by a class of single-valued polylogarithms. As a result, we were able to apply the same convolution-based computational framework to compute the BFKL ladder both at LLA and at NLLA and we were able to get results up to five-loop order. We were also able to generalize this computation to Yang-Mills theories with arbitrary matter content. This allowed us to investigate the transcendental properties of the BFKL ladder as a function of the matter content of the theory and we have identified four theories whose BFKL ladder was maximally transcendental.

Finally, we considered a family of Feynman integrals in general kinematics. More precisely, we considered the family of Feynman integrals corresponding to the equal-mass three-loop banana graph. In the case of generic masses, the geometry underlying these Feynman integrals is rather complicated and the resulting function-space of these integrals has not been well-studied. Luckily, in the equal-mass case, this geometry is closely related to the elliptic curve underlying the corresponding two-loop sunrise integrals. The function space of sunrise integrals has been studied for many years and is well-understood. We have used this understanding of the function space to compute the master integrals of the equal-mass banana family in terms of the functions arising from the sunrise integrals. We have defined a basis of modular forms that is well-suited for the computation of the banana integrals and were able to compute the solutions to the inhomogeneous differential equations among the master integrals analytically. To highlight the connection of the underlying geometry to the elliptic curve encountered for the sunrise integrals, we have then rewritten this result in terms of the elliptic multiple polylogarithms that have previously been defined for the sunrise integral.

Outlook

There are a few natural extensions of the work performed in this thesis. The recursive computation of scattering amplitudes in the multi-Regge limit of $\mathcal{N} = 4$ SYM using the convolution formalism constitutes a very systematic way to perform computations in this theory. Consequently, it should be possible to publish the code we have developed for the computation of these scattering amplitudes in the form of a MATHEMATICA package that automatically computes all necessary perturbative coefficients of a certain logarithmic accuracy, loop order and helicity configuration. Further, it would be interesting to see if scattering amplitudes in the multi-Regge limit can generally be expressed in terms of multiple polylogarithms. Many classes of Feynman graphs are known to evaluate to MPLs to all orders, and it would be interesting to see if these classes of Feynman graphs naturally arise when approaching the multi-Regge limit on a diagrammatic level.

In general kinematics, we can extend the analysis we have performed for the equal-mass banana graph. It appears that the banana integral with three different masses and one massless propagator can similarly be cast as an integral over an elliptic curve. This suggests that it should be possible to compute this integral using the same classes of functions we have considered in this work.

Acknowledgements

In this work I have presented the research that I have conducted during the last four years. This research, however, is not all that should be mentioned in this work, as there are many more contributions hidden from plain sight that should not go unnoticed.

First and foremost I would like to express my gratitude to my supervisor Claude for the opportunity to learn from him as well as for his guidance and support throughout the last four years, for sparking the right ideas in the face of stagnating progress and for his appreciation when progress was good.

I would like to thank my fellow PhD student, office mate and most importantly good friend Bram who accompanied me through the highs and lows of this journey for a very fruitful collaboration and for making it at absolute pleasure. I thank the friends I have made here for rounding off the days of work and for making me feel at home.

I extend my gratitude to the other (past and present) members of our group, Brenda, Liam, Lorenzo, Martin, Matteo, Samuel, Sophia and Zhengwen for helpful discussions during our group meetings and for many enjoyable encounters in between, to the many more co-workers at CP3, including administrative staff, for their help and without whom my breaks at the institute would not have been the same, and to my external collaborators, Falko, Georgios, James, Johannes, Stefan and Vittorio with whom working was very inspiring and a pleasure.

I express my great appreciation to my thesis committee for taking the time to read my manuscript, for their proposed improvements to it, and for seeing me off into the next chapter of my career.

I thank the European Research Council (ERC) for their support under the Horizon 2020 Research and Innovation Programme through the grant 637019 (MathAm).

Auch wenn der Weg, den ich in den letzten vier Jahren zurückgelegt habe fernab meiner Heimat verlief, hätte ich ihn ohne meine Familie und die Freunde, die ich dort machte nicht bewältigen können. Dafür möchte ich euch an dieser Stelle herzlichst danken.

Ich danke meinen Eltern Haiti und Kurt für ihre unendliche Geduld und Liebe. Ich bedanke mich dafür, dass ich stets einen sicheren Hafen habe, an den ich zurückkehren kann und dafür, dass sie mich stets bedingungslos unterstützen. Ich danke meiner Familie für ihren Zusammenhalt und für die vielen schönen Momente, die wir gemeinsam erlebt haben.

Ich danke meinen Freunden Eduard, Marc, Sven und vielen anderen dafür, dass sie mir wieder und wieder ein Stückchen Heimat nach Belgien gebracht haben und dafür, dass ich mich bei jedem Treffen so fühlen konnte, als wäre ich nie auch nur einen Tag von zu Hause weg gezogen. Ich bedanke mich bei Miyuki und Nico, dafür, dass sie mit mir am Start meiner Reise beiseite standen und mir damit den Weg ebneten und bei allen die sich Jahr für Jahr aufs Neue auf der Hütte zusammenfinden um gemeinsam die Welt für ein Wochenende zu vergessen.

Appendices

Appendix **A**

De Rham Periods and Symbols

In this chapter we will elaborate on the connection between the de Rham periods appearing in eq.(2.115) and words of one-forms, closely following the description in [52].

Let

$$I = \left(\int_{\gamma} \omega_1, \dots, \int_{\gamma} \omega_k \right)^{\top} \quad (\text{A.1})$$

be a vector of master integrals, i.e. integrals that form a complete and independent set with respect to IBP relations, and let I satisfy the linear, first order differential equation

$$dI = A I \quad \text{with} \quad A \equiv \sum_i A_i \xi_i, \quad (\text{A.2})$$

where the ξ_i are differential one-forms and $A_i \in \mathbb{Q}^{k \times k}$. Let us also assume without loss of generality that all ξ_i are independent. Let us further assume that the differential equation (A.2) has a non-trivial solution and hence $dA = A \wedge A$. If the matrix A is nilpotent, then we call the family of integrals (A.1) and the differential equation (A.2) unipotent. In that case, we can find a basis such that the matrix A is strictly upper triangular and the differential equation has a trivial homogeneous part, which is consistent with the differential of eMPLs in eq. (2.105). Let us now assume that the integrals in the vector I are such a basis. Then we can associate a symbol to a pair of differential forms $[\omega_i, \omega_j]$ as follows.

Consider the matrix

$$T_A = 1 + [A]^R + [A|A]^R + [A|A|A]^R + \dots, \quad (\text{A.3})$$

where the concatenation of matrices A corresponds to the ordinary matrix multiplication with concatenation of one-forms and where R reverses words of one-forms

$$[\xi_{i_1} | \dots | \xi_{i_k}]^R = [\xi_{i_k} | \dots | \xi_{i_1}]. \quad (\text{A.4})$$

Since the matrix A is nilpotent, only finitely many of the terms appearing in eq. (A.3) are non-zero. Furthermore, the matrix T_A is independent of the choice of contour γ defining the integrals in I . Then we define the symbol corresponding to a pair of differential forms $[\omega_i, \omega_j]$ as the corresponding matrix element of T_A ,

$$\mathcal{S}([\omega_i, \omega_j]) \equiv \langle \omega_i | T_A | \omega_j \rangle = (T_A)_{ji}. \quad (\text{A.5})$$

Let us illustrate this definition with a simple example. Consider the vector

$$I = \left(\int_{\gamma} \omega_1, \int_{\gamma} \omega_2, \int_{\gamma} \omega_3 \right)^{\top} = \left(\int_{\gamma} [\xi_1 | \xi_0], \int_{\gamma} [\xi_1], 1 \right)^{\top} \quad (\text{A.6})$$

for some contour γ and where $1 = \int_{\gamma} []$ is the integral over an empty word. Then I fulfils the differential equation (A.2) with

$$A = \begin{pmatrix} 0 & \xi_0 & 0 \\ 0 & 0 & \xi_1 \\ 0 & 0 & 0 \end{pmatrix}, \quad (\text{A.7})$$

and we have

$$[A|A]^R = \begin{pmatrix} 0 & 0 & [\xi_1 | \xi_0] \\ 0 & 0 & 0 \\ 0 & 0 & 0 \end{pmatrix} \quad \text{and} \quad [A|A|A]^R = 0, \quad (\text{A.8})$$

and hence

$$T_A = \begin{pmatrix} 1 & [\xi_0] & [\xi_1 | \xi_0] \\ 0 & 1 & [\xi_1] \\ 0 & 0 & 1 \end{pmatrix}. \quad (\text{A.9})$$

This gives us, for example, the symbol

$$\mathcal{S}([\omega_1, \omega_2]) = [\xi_0]. \quad (\text{A.10})$$

In general, the matrix T_A can be interpreted as the avatar of the fundamental solution of the differential equation A.2. More precisely, if γ is a path with end points x_0 and x and $I_0 \equiv I(x_0)$ are initial conditions, then

$$I(x) = \int_{\gamma} T_A I_0. \quad (\text{A.11})$$

A more extensive review of the properties of the symbol \mathcal{S} and the matrix T_A including a prove that it is indeed independent of the path γ can be found in [52].

Appendix **B**

MRK and the moduli space $\mathfrak{M}_{0,N-2}$

As we have mentioned in chapter 1, the possible divergences of gluon scattering amplitudes in $\mathcal{N} = 4$ SYM are encoded in cluster algebras and a set of coordinates that can be used to express the kinematical dependence of these amplitudes is given by the cluster in fig. 1.4. On the other hand, we have seen that scattering amplitudes in MRK in $\mathcal{N} = 4$ SYM can be written in terms of the $n = N - 2$ transverse dual coordinates $\mathbf{x}_i \in \mathbb{CP}^1$ and hence, the configuration space $\text{Conf}_n(\mathbb{CP}^1)$. In this section we will show that the two sets of variables are compatible with each other. The configuration space $\text{Conf}_n(\mathbb{CP}^1)$ containing the set of dual coordinates \mathbf{x}_i is isomorphic to the space of genus zero curves with n marked points,

$$\text{Conf}_n(\mathbb{CP}^1) \simeq \mathfrak{M}_{0,n}. \quad (\text{B.1})$$

Like the configuration space \mathbb{CP}^3 , this space can also be endowed with a cluster algebra. We will now show that the cluster algebra of scattering amplitudes in full kinematics reduces to a cluster algebra on $\mathfrak{M}_{0,n}$.

The multi-Regge limit of the cluster- \mathcal{X} coordinates in 1.4 has previously been computed [1] and it was found that the middle row vanishes, effectively splitting

the cluster algebra in two,

$$\begin{aligned}\mathcal{X}_{1j} &\rightarrow \frac{(\bar{\mathbf{x}}_2 - \bar{\mathbf{x}}_{j+2})(\bar{\mathbf{x}}_{j+3} - \bar{\mathbf{x}}_{j+4})}{(\bar{\mathbf{x}}_2 - \bar{\mathbf{x}}_{j+4})(\bar{\mathbf{x}}_{j+2} - \bar{\mathbf{x}}_{j+3})}, \\ \mathcal{X}_{2j} &\rightarrow 0, \\ \mathcal{X}_{3j} &\rightarrow \frac{(\mathbf{x}_1 - \mathbf{x}_{j+1})(\mathbf{x}_{j+2} - \mathbf{x}_{j+3})}{(\mathbf{x}_1 - \mathbf{x}_{j+3})(\mathbf{x}_{j+1} - \mathbf{x}_{j+2})}.\end{aligned}\tag{B.2}$$

The remaining two rows are given by $N - 5$ holomorphic or anti-holomorphic cross-ratios in \mathbb{CP}^1 , respectively. As such, the two separate clusters given by the \mathcal{X}_{1i} and \mathcal{X}_{3i} have the right size to be valid cluster algebras on $\text{Conf}_n(\mathbb{CP}^1)$ and have the singularity structure of $\mathfrak{M}_{0,n}$, i.e. they diverge only when two points $\mathbf{x}_i = \mathbf{x}_j$ coincide.

The separation of the cluster algebra attached to $\text{Conf}_n(\mathbb{CP}^3)$ according to eq. B.2 allows us to draw some interesting conclusions for scattering amplitudes in MRK. The cluster algebras formed out of the \mathcal{X}_{1i} (\mathcal{X}_{3i}) correspond to A_{N-5} Dynkin diagrams and are therefore referred to as A_{N-5} cluster algebras. Consequently, the cluster algebra associated to the scattering of N particles in planar $\mathcal{N} = 4$ SYM reduces to an $A_{N-5} \otimes A_{N-5}$ cluster algebra in the multi-Regge limit. It is remarkable that while the cluster algebra associated to general kinematics is infinite for $N \geq 8$, the A_{N-5} cluster algebra is finite for any number N [25, 28]. Scattering amplitudes in MRK therefore must have a very restricted singularity structure. They must be iterated integrals with poles at most where the cluster coordinates (B.2) diverge, i.e. when $\mathbf{x}_i = \mathbf{x}_j$. Indeed, the only singularities scattering amplitudes in MRK can have are singularities associated to external gluons becoming soft $\mathbf{k}_i \rightarrow 0$ and hence $\mathbf{x}_i \rightarrow \mathbf{x}_{i+1}$. It was further shown that iterated integrals on $\mathfrak{M}_{0,n}$ can be written as multiple polylogarithms [88]. Given that configurations in $\mathfrak{M}_{0,n}$ degenerate when two coordinates become equal, we can infer that scattering amplitudes in MRK in $\mathcal{N} = 4$ SYM are iterated integrals over words of differential one-forms $d\log(\mathbf{x}_i - \mathbf{x}_j)$ and their complex conjugates.

As we have just seen, the singularity structure of scattering amplitudes is not just constrained by the coordinates appearing in cluster algebras (i.e. $\mathbf{x}_i \rightarrow \mathbf{x}_j$) but also from physical considerations (i.e. $\mathbf{x}_i \rightarrow \mathbf{x}_{i+1}$). We will now use physical restrictions on the amplitude to show that the coefficients of the large resummed logarithms of scattering amplitudes in the multi-Regge limit of planar $\mathcal{N} = 4$ SYM are single-valued functions of the transverse momenta. In massless theories, scattering amplitudes can only exhibit branch cuts when Mandelstam invariants vanish or diverge [139], which puts strong constraints on the first letter in the word of one-forms describing the iterated integral. From this first entry condition, combined with the integrability condition for words

of one-forms, it can be shown that branch points in the Mandelstam region $[p, q]$ are given by products of cross-ratios that tend to 0, 1 or ∞ . The first letter must therefore either take the form $d \log U_{ijkl}$ or $d \log \left(1 - \prod_{ijkl} U_{ijkl}^{n_{ijkl}}\right)$.

Let us take a look at the $N(N-5)/2$ multiplicatively independent cross-ratios

$$\begin{aligned} u_{1i}, u_{2i}, u_{3i}, \quad 1 \leq i \leq N-5, \\ U_{ij} = U_{i j+1 j i+1}, \quad 2 \leq i \leq j-4 \leq N-5, \end{aligned} \quad (\text{B.3})$$

defined in eqs. (1.29) and (1.28). While we already know the behaviour of the former when approaching the multi-Regge limit, the latter haven't been studied yet. From the multi-soft limit, we can see that these cross-ratios tend to 1, and we define additional reduced cross-ratios

$$\tilde{U}_{ij} \equiv \frac{1 - U_{ij}}{\prod_{k=i-1}^{j-4} (1 - u_{1k})} \rightarrow \left| \frac{\mathbf{x}_i - \mathbf{x}_{j-1}}{\mathbf{x}_i - \mathbf{x}_{i+2}} \prod_{k=i+1}^{j-3} \frac{\mathbf{x}_k - \mathbf{x}_{k+1}}{\mathbf{x}_k - \mathbf{x}_{k+2}} \right|^2, \quad (\text{B.4})$$

which remain finite in the multi-Regge limit. Since all u_{1k} in the denominator tend to 1 at the same speed, we can conclude that the U_{ij} converge at different speeds.

Let us now take a look at entries of the form $d \log U_{ijkl}$. These vanish for all cross-ratios $U \rightarrow 1$, and so the only interesting quantities are $d \log u_{2i}$ and $d \log u_{3i}$. Since all divergent quantities from taking the multi-Regge limit are resummed and we are interested in the finite coefficients of these large logarithms, we can replace the cross-ratios u_{2i} and u_{3i} by their reduced versions \tilde{u}_{2i} and \tilde{u}_{3i} , which reduce to absolute squares of cross ratios.

Let us now turn to the entries of the form $d \log \left(1 - \prod_{ijkl} U_{ijkl}^{n_{ijkl}}\right)$, where it is sufficient to consider U_{ijkl} from the set of multiplicatively independent cross-ratios (B.3). If one of the cross ratios in the product vanishes in MRK, e.g. $\prod_{ijkl} U_{ijkl}^{n_{ijkl}} = u_{2i}^n * U$, we have

$$d \log(1 - u_{2i}^n U) \rightarrow \begin{cases} n d \log u_{2i} + d \log U, & \text{if } n < 0, \\ 0, & \text{if } n > 0, \end{cases} \quad (\text{B.5})$$

where all terms on the r.h.s. have already been covered. In the case where all of the factors tend to one we only need to keep the factor that converges the slowest. Then the one form $d \log \left(1 - \prod_{ijkl} U_{ijkl}^{n_{ijkl}}\right)$ converges, up to terms factoring into the large resummed logarithms, to a one-form including only squares of cross-ratios of \mathbf{x}_i (c.f. (B.4)).

We have seen that the first entries of the words contributing to the perturbative expansion of scattering amplitudes in MRK are squares of absolute values of

cross-ratios in the $A_{N-5} \times A_{N-5}$ cluster algebra described before. Therefore, the branch-points of these functions are given by absolute values and the functions must be single-valued when seen as functions of the complex transverse coordinates \mathbf{x}_i . Given that iterated integrals on $\mathfrak{M}_{0,n}$ evaluate to multiple polylogarithms and since the holomorphic and anti-holomorphic cross ratios are part of two separate copies of the A_5 cluster algebra, we can further infer that they can be written in terms of the single-valued multiple polylogarithms introduced in 2.2.2. Note that this is in agreement with the findings in ref. [33], where the six-point remainder function was computed in terms of SVMPLs with singularities for $z \in \{0, 1\}$.

Appendix **C**

The BFKL Building Blocks

In this section we give the explicit forms of the BFKL building blocks appearing in the Fourier-Mellin representation of scattering amplitudes in the multi-Regge limit of $\mathcal{N} = 4$ SYM through NLO. The impact factors can be found to all loop orders in ref. [82] and are given up to NLO by

$$\chi^+(\nu, n) = \frac{1}{\nu - \frac{i\pi}{2}} \left[1 - \frac{a}{4} \left(E^2 + \frac{3}{4}N^2 - NV + \frac{\pi^2}{3} \right) + \mathcal{O}(a^2) \right], \quad (\text{C.1})$$

$$\chi^-(\nu, n) = \frac{1}{\nu + \frac{i\pi}{2}} \left[1 - \frac{a}{4} \left(E^2 + \frac{3}{4}N^2 + NV + \frac{\pi^2}{3} \right) + \mathcal{O}(a^2) \right], \quad (\text{C.2})$$

$$-\omega(\nu, n) = aE - \frac{a^2}{4} (D^2E - 2VDE + 4\zeta_2E + 12\zeta_3) + \mathcal{O}(a^3). \quad (\text{C.3})$$

The central emission block is given through NLO by [3]

$$\begin{aligned}
C^+(\nu_1, n_1, \nu_2, n_2) = & \\
& \frac{-\Gamma(1 - i\nu_1 - \frac{n_1}{2})\Gamma(i\nu_2 + \frac{n_2}{2})\Gamma(i\nu_1 - i\nu_2 - \frac{n_1}{2} + \frac{n_2}{2})}{\Gamma(1 + i\nu_1 - \frac{n_1}{2})\Gamma(-i\nu_2 + \frac{n_2}{2})\Gamma(1 - i\nu_1 + i\nu_2 - \frac{n_1}{2} + \frac{n_2}{2})} \\
& \times \left[1 + a \left(\frac{1}{2} [DE_1 - DE_2 + E_1E_2 + \frac{1}{4}(N_1 + N_2)^2 + V_1V_2 \right. \right. \\
& \quad \left. \left. + (V_1 - V_2)(M - E_1 - E_2) + 2\zeta_2 + i\pi(V_2 - V_1 - E_1 - E_2) \right] \right. \\
& \quad \left. - \frac{1}{4}(E_1^2 + E_2^2 + N_1V_1 - N_2V_2) - \frac{3}{16}(N_1^2 + N_2^2) - \zeta_2 + \mathcal{O}(a^2) \right]. \tag{C.4}
\end{aligned}$$

The elementary building blocks appearing in the corrections of the impact factors and central emission block are defined as

$$\begin{aligned}
E(\nu, n) = & -\frac{1}{2} \frac{|n|}{\nu^2 + \frac{n^2}{4}} + \psi \left(1 + i\nu + \frac{|n|}{2} \right) \\
& + \psi \left(1 - i\nu + \frac{|n|}{2} \right) - 2\psi(1), \\
V(\nu, n) = & \frac{i\nu}{\nu^2 + \frac{n^2}{4}}, \quad N(\nu, n) = \frac{n}{\nu^2 + \frac{n^2}{4}}, \quad D_\nu = -i\partial/\partial\nu, \\
M(\nu_1, n_1, \nu_2, n_2) = & \psi(i(\nu_1 - \nu_2) - \frac{n_1 - n_2}{2}) \\
& + \psi(1 - i(\nu_1 - \nu_2) - \frac{n_1 - n_2}{2}) - 2\psi(1). \tag{C.5}
\end{aligned}$$

Appendix **D**

Soft Limits and the Contour of Integration

Due to the strong rapidity-ordering in MRK the external momenta are all well-separated and hence there are no collinear singularities. All soft singularities are associated with one of the momenta k_i , $1 \leq i \leq N - 4$ going to zero. Letting $\mathbf{k}_i \rightarrow 0$ in eq. (3.16), we can determine the corresponding behaviour of the Fourier-Mellin coordinates, and we find:

1. If $\mathbf{k}_1 \rightarrow 0$, $z_1 \rightarrow 0$.
2. If $\mathbf{k}_{N-4} \rightarrow 0$, $z_{N-5} \rightarrow \infty$.
3. If $\mathbf{k}_i \rightarrow 0$, for $2 \leq i \leq N - 5$, $z_i \rightarrow 0$ and $z_{i-1} \rightarrow \infty$, with $z_{i-1}z_i$ finite.

And equivalently, for simplicial MRK coordinates:

1. If $\mathbf{k}_1 \rightarrow 0$, $\rho_1 \rightarrow 0$.
2. If $\mathbf{k}_{N-4} \rightarrow 0$, $\rho_{N-5} \rightarrow \infty$.
3. If $\mathbf{k}_i \rightarrow 0$, for $2 \leq i \leq N - 5$, $\rho_{i-1} \rightarrow \rho_i$.

Under soft limits, amplitudes with different numbers of particles are closely related, and the ratio \mathcal{R}_N reduces to the ratio \mathcal{R}_{N-1} . More precisely, we have, for $2 \leq i \leq N - 5$,

$$\lim_{\mathbf{k}_i \rightarrow 0} \tilde{\mathcal{R}}_N = \tilde{\mathcal{R}}_{N-1}^{\{i\}}, \quad (\text{D.1})$$

where we have introduced the shorthand

$$\tilde{\mathcal{R}}_N \equiv (\mathcal{R}_{h_1 \dots h_{N-4}} e^{\delta_N}) \left(\begin{matrix} \tau_1, \dots, \tau_{N-5} \\ z_1, \dots, z_{N-5} \end{matrix} \right) \quad (\text{D.2})$$

and where the superscript in curly brackets encodes the kinematic dependence of the ratio $\tilde{\mathcal{R}}$ under soft limits,

$$\tilde{\mathcal{R}}_{N-1}^{\{1\}} \equiv |z_1|^{2\pi i \Gamma} (\mathcal{R}_{h_2 \dots h_{N-4}} e^{i\delta_{N-1}}) \left(\begin{matrix} \tau_2, \dots, \tau_{N-5} \\ z_2, \dots, z_{N-5} \end{matrix} \right), \quad (\text{D.3})$$

$$\tilde{\mathcal{R}}_{N-1}^{\{i\}} \equiv (\mathcal{R}_{h_1 \dots \hat{h}_i \dots h_{N-4}} e^{i\delta_{N-1}}) \left(\begin{matrix} \tau_1, \dots, \tau_{i-1}, \tau_i, \dots, \tau_{N-5} \\ z_1, \dots, -z_{i-1} z_i, \dots, z_{N-5} \end{matrix} \right), \quad (\text{D.4})$$

$$\tilde{\mathcal{R}}_{N-1}^{\{N-4\}} \equiv |z_{N-5}|^{-2\pi i \Gamma} (\mathcal{R}_{h_1 \dots h_{N-5}} e^{i\delta_{N-1}}) \left(\begin{matrix} \tau_1, \dots, \tau_{N-6} \\ z_1, \dots, z_{N-6} \end{matrix} \right). \quad (\text{D.5})$$

From these relations we can also infer the correct contour of integration for the Fourier-Mellin transform (3.33) and we find that for $i \in \{2, \dots, N-5\}$, the right hand side has poles at $\nu_1 = \pi\Gamma - i0^+$, $\nu_i = \nu_{i-1} + i0^+$, and $\nu_{N-5} = -\pi\Gamma + i0^+$ for $n_1 = 0$, $n_{i-1} = n_i$, and $n_{N-5} = 0$ respectively, where Γ was defined in eq. (3.32). This follows recursively in the number of external particles N , starting from the six-particle amplitude [3, 4, 6].

Appendix E

Symmetries and Soft Limits of Perturbative Coefficients

In the previous sections we have reviewed the soft-limits and symmetries of the ratio $\tilde{\mathcal{R}}$. Expanding both sides of these limits in the coupling a and in the large logarithms $\log \tau_k$, we can determine the behaviour of the perturbative coefficients \tilde{g} and \tilde{h} under soft limits and target-projectile symmetry. We will now give the behaviour of the perturbative coefficients at LLA and at NLLA under these limits. Under target-projectile symmetry, we have

$$\begin{aligned} \tilde{g}_{h_1, \dots, h_{N-4}}^{(\ell; i_1, \dots, i_{N-5})}(z_1, \dots, z_{N-5}) &= \tilde{g}_{-h_1, \dots, -h_{N-4}}^{(\ell; i_1, \dots, i_{N-5})}(\bar{z}_1, \dots, \bar{z}_{N-5}) \\ &= \tilde{g}_{-h_{N-4}, \dots, -h_1}^{(\ell; i_{N-5}, \dots, i_1)}\left(\frac{1}{z_{N-5}}, \dots, \frac{1}{z_1}\right). \end{aligned} \quad (\text{E.1})$$

and the same equation holds for \tilde{h} .

The behaviour of perturbative coefficients under soft limits is slightly more involved and we will consider the LLA and NLLA cases separately. Since the terms $|z_i|^{\pm 2\pi i \Gamma}$ don't contain any large logarithms $\log \tau_k$, we will find contributions from these exponentials that contribute exclusively to the soft limits of perturbative coefficients where all $i_j = 0$. It is therefore convenient to define

$$I = \sum_{j=1}^{N-5} i_j. \quad (\text{E.2})$$

Then the soft limits of LLA perturbative coefficients are

$$\begin{aligned}
& \lim_{k_1 \rightarrow 0} \tilde{g}_{h_1, \dots, h_{N-4}}^{(I+1; i_1, \dots, i_{N-5})}(z_1, \dots, z_{N-5}) \\
& \quad = \delta_{i_1 0} \tilde{g}_{h_2, \dots, h_{N-4}}^{(I+1; i_2, \dots, i_{N-5})}(z_2, \dots, z_{N-5}) + \frac{\delta_{I0}}{4} \mathcal{G}_0(z_1), \\
& \lim_{k_l \rightarrow 0} \tilde{g}_{h_1, \dots, h_{N-4}}^{(I+1; i_1, \dots, i_{N-5})}(z_1, \dots, z_{N-5}) \\
& \quad = \tilde{g}_{h_1, \dots, \tilde{h}_j, \dots, h_{N-4}}^{(I+1; i_1, \dots, i_{l-1}+i_l, \dots, i_{N-5})}(z_1, \dots, -z_{l-1}z_l, \dots, z_{N-5}), \\
& \lim_{k_{N-4} \rightarrow 0} \tilde{g}_{h_1, \dots, h_{N-4}}^{(I+1; i_1, \dots, i_{N-5})}(z_1, \dots, z_{N-5}) \\
& \quad = \delta_{i_{N-5} 0} \tilde{g}_{h_1, \dots, h_{N-5}}^{(I+1; i_1, \dots, i_{N-6})}(z_1, \dots, z_{N-6}) - \frac{\delta_{I0}}{4} \mathcal{G}_0(z_{N-5}).
\end{aligned} \tag{E.3}$$

At NLLA, we can similarly work out the behaviour of perturbative coefficients under soft limits. Similarly to the leading-logarithmic case, we find for the imaginary parts at NLLA

$$\begin{aligned}
& \lim_{k_1 \rightarrow 0} \tilde{g}_{h_1, \dots, h_{N-4}}^{(I+2; i_1, \dots, i_{N-5})}(z_1, \dots, z_{N-5}) \\
& \quad = \delta_{i_1 0} \tilde{g}_{h_2, \dots, h_{N-4}}^{(I+2; i_2, \dots, i_{N-5})}(z_2, \dots, z_{N-5}) + \frac{\delta_{I0}}{4} \mathcal{G}_0(z_1) \zeta_2, \\
& \lim_{k_l \rightarrow 0} \tilde{g}_{h_1, \dots, h_{N-4}}^{(I+2; i_1, \dots, i_{N-5})}(z_1, \dots, z_{N-5}) \\
& \quad = \tilde{g}_{h_1, \dots, \tilde{h}_j, \dots, h_{N-4}}^{(I+2; i_1, \dots, i_{l-1}+i_l, \dots, i_{N-5})}(z_1, \dots, -z_{l-1}z_l, \dots, z_{N-5}), \\
& \lim_{k_{N-4} \rightarrow 0} \tilde{g}_{h_1, \dots, h_{N-4}}^{(I+2; i_1, \dots, i_{N-5})}(z_1, \dots, z_{N-5}) \\
& \quad = \delta_{i_{N-5} 0} \tilde{g}_{h_1, \dots, h_{N-5}}^{(I+2; i_1, \dots, i_{N-6})}(z_1, \dots, z_{N-6}) - \frac{\delta_{I0}}{4} \mathcal{G}_0(z_{N-5}) \zeta_2.
\end{aligned} \tag{E.4}$$

In addition to the contributions we have found for the imaginary parts \tilde{g} , the real parts \tilde{h} also get contributions from the exponentials $|z_i|^{\pm 2\pi i \Gamma}$ when not all $i_j = 0$. Expanding the r.h.s. of equation (D.1) for $i \in \{1, N-4\}$, we also find contributions from lower order imaginary parts multiplying logarithms $\mathcal{G}_0(z_i)$.

More precisely, we find

$$\begin{aligned}
& \lim_{k_1 \rightarrow 0} \tilde{h}_{h_1, \dots, h_{N-4}}^{(I+2; i_1, \dots, i_{N-5})}(z_1, \dots, z_{N-5}) \\
&= \delta_{i_1 0} \tilde{h}_{h_2, \dots, h_{N-4}}^{(I+2; i_2, \dots, i_{N-5})}(z_2, \dots, z_{N-5}) + \frac{\delta_{I0}}{32} \mathcal{G}_0(z_1)^2 \\
&+ \frac{\delta_{i_1 0}}{4} \mathcal{G}_0(z_1) \tilde{g}_{h_2, \dots, h_{N-4}}^{(I+1; i_2, \dots, i_{N-5})}(z_2, \dots, z_{N-5}), \\
& \lim_{k_l \rightarrow 0} \tilde{h}_{h_1, \dots, h_{N-4}}^{(I+2; i_1, \dots, i_{N-5})}(z_1, \dots, z_{N-5}) \\
&= \tilde{h}_{h_1, \dots, \hat{h}_j, \dots, h_{N-4}}^{(I+2; i_1, \dots, i_{l-1}+i_l, \dots, i_{N-5})}(z_1, \dots, -z_{l-1}z_l, \dots, z_{N-5}), \\
& \lim_{k_{N-4} \rightarrow 0} \tilde{h}_{h_1, \dots, h_{N-4}}^{(I+2; i_1, \dots, i_{N-5})}(z_1, \dots, z_{N-5}) \\
&= \delta_{i_{N-5} 0} \tilde{h}_{h_1, \dots, h_{N-5}}^{(I+2; i_1, \dots, i_{N-6})}(z_1, \dots, z_{N-6}) + \frac{\delta_{I0}}{32} \mathcal{G}_0(z_{N-5})^2 \\
&- \frac{\delta_{i_{N-5} 0}}{4} \mathcal{G}_0(z_{N-5}) \tilde{g}_{h_1, \dots, h_{N-5}}^{(I+1; i_1, \dots, i_{N-6})}(z_1, \dots, z_{N-6}).
\end{aligned} \tag{E.5}$$

Appendix F

Deforming the Contour of Integration

In order to regularize the pinched singularities encountered when approaching the weak coupling limit, we will now define a prescription to deform the contours of integration such that the contours will not get pinched for small values of the coupling. In particular, we will subtract the residues at¹ $\nu_1 = \pi\Gamma$, at $\nu_{2i} = \nu_{2i+1}$, $1 \leq i \leq (N-6)/2$ and, for odd N , at $\nu_{N-5} = -\pi\Gamma$.

To perform the contour deformations, it is helpful to introduce a different set of building blocks that behave nicely when taking residues at the relevant poles,

$$\tilde{C}^h(\nu_1, n_1, \nu_2, n_2) = \frac{C^h(\nu_1, n_1, \nu_2, n_2)}{\chi^-(\nu_1, n_1)\chi^+(\nu_2, n_2)}, \quad (\text{F.1})$$

$$\tilde{\Phi}(\nu, n) = \chi^+(\nu, n)\chi^-(\nu, n), \quad (\text{F.2})$$

$$I^h(\nu, n) \equiv \frac{\chi^h(\nu, n)}{\chi^+(\nu, n)} = \begin{cases} 1, & h = + \\ H(\nu, n), & h = - \end{cases}, \quad (\text{F.3})$$

where

$$H(\nu, n) = \frac{\chi^-(\nu, n)}{\chi^+(\nu, n)}, \quad (\text{F.4})$$

is the helicity flip kernel in Fourier-Mellin space known to all orders from [82]. Then the chain of impact factors and central emission blocks in the integrand

¹Note that this choice of residues is not unique and we can also find a valid regularization by subtracting the residues at $\nu_{2i-1} = \nu_{2i}$, $1 \leq i \leq (N-6)/2$ and, for even N , at $\nu_{N-5} = -\pi\Gamma$

of eq. (3.30) reads

$$\chi_1^{h_1} \left[\prod_{k=2}^{N-5} C_{k-1,k}^{h_k} \right] \chi_{N-5}^{-h_{N-4}} = I_1^{h_1} \tilde{\Phi}_1 \left[\prod_{k=2}^{N-5} \tilde{C}_{k-1,k}^{h_k} \tilde{\Phi}_k \right] \bar{I}_{N-5}^{h_4}. \quad (\text{F.5})$$

The behaviour of these building blocks at $\nu_i = \pm\pi\Gamma$ and at $\nu_i = \nu_j$ was determined in [3, 6, 140], and is given by

$$\omega(\pm\pi\Gamma, 0) = 0, \quad (\text{F.6})$$

$$I(\nu, 0) = 1, \quad (\text{F.7})$$

$$\tilde{C}^h(\pi\Gamma, 0, \nu, n) = i\pi a I^h(\nu, n), \quad (\text{F.8})$$

$$\tilde{C}^h(\nu, n, -\pi\Gamma, 0) = -i\pi a \bar{I}^h(\nu, n), \quad (\text{F.9})$$

$$\text{Res}_{\nu_1=\nu_2} \tilde{C}^h(\nu_1, n, \nu_2, n) = \frac{(-1)^{n+1} i e^{i\pi\omega(\nu_2, n)}}{\tilde{\Phi}(\nu_2, n)}, \quad (\text{F.10})$$

$$\text{Res}_{\nu=\pm\pi\Gamma} \tilde{\Phi}(\nu, 0) = \pm \frac{1}{\pi a}. \quad (\text{F.11})$$

As we can see from eqs. (F.6-F.11) taking the residue at any of the previously described residues yields exactly the integrand for the lower-point ratio with the same kinematical dependence as when taking the corresponding soft limit.

We will now describe an algorithmic way to perform these contour deformations for any number of external legs. Our goal is, to deform the contours in fig. 3.5 to the ones displayed in fig. 3.6, where all contours are such that there will be no pinching when approaching the weak coupling limit. For this purpose, we will introduce the integral transform $\mathcal{F}_{n,m}$, whose aim is to interpolate between the two sets of contours. More precisely, we define $\mathcal{F}_{n,m}$ such that we integrate $\{\nu_1, \dots, \nu_n\}$ along the *Fourier-Mellin contours* 3.5 and $\{\nu_{n+1} \dots \nu_{n+m}\}$ along the *pinch-free contours* 3.6. Note that the Fourier-Mellin contours are always such that ν_i runs below ν_{i+1} , while in pinch-free contours ν_i alternately runs below or above ν_{i+1} , depending on whether i is even or odd. This means that only those $\mathcal{F}_{n,m}$ with odd m are valid contour prescriptions and we will only encounter those in the process. In this parlance, we are starting with the integral

$$\tilde{\mathcal{R}}_N = \mathcal{F}_{N-5} [\mathcal{I}_N] \equiv \mathcal{F}_{N-5,0} [\mathcal{I}_N], \quad (\text{F.12})$$

where \mathcal{I}_N is the integrand for the N -point dispersion integral in eq. (3.30), and it is our goal to rewrite this integral as $\mathcal{F}_{0,N-5} [\mathcal{I}_N]$. We will do this recursively over the number of external particles N and assume that we have a well-defined prescription for the dispersion integral of the $N - 1$ -point ratio function.

Let us also extend the shorthand for the kinematical dependence of the ratio $\tilde{\mathcal{R}}$ that we have introduced in (D.3) to the integrals $\mathcal{F}_{n,m}$. As we have already mentioned before, the integrand in the dispersion integral will reduce to a lower-point integrand when taking residues. Since the ratio is already defined as an integral $\mathcal{F}_{n,m}$, namely $\tilde{\mathcal{R}}_N = \mathcal{F}_{N-5,0}[\mathcal{I}_N]$, the prescription for the kinematical description extends naturally. In addition, we will need to iterate this description through the recursion

$$\mathcal{F}_{n,m}^{k_1,\dots,k_n} = \left(\mathcal{F}_{n,m}^{\{k_1\}} \right)^{\{k_2,\dots,k_{n-1}\}}. \quad (\text{F.13})$$

Then we have, for example,

$$\begin{aligned} \tilde{\mathcal{R}}_6^{\{3,1\}} &= \left(\tilde{\mathcal{R}}_{h_1 h_2 h_3 h_4} \left(\begin{array}{ccc} \tau_1 & \tau_2 & \tau_3 \\ z_1 & z_2 & z_3 \end{array} \right) \right)^{\{3,1\}} = \left(\tilde{\mathcal{R}}_{h_1 h_2 h_4} \left(\begin{array}{cc} \tau_1 & \tau_2 \tau_3 \\ z_1 & -z_2 z_3 \end{array} \right) \right)^{\{1\}} \\ &= |z_1|^{2\pi i \Gamma} \tilde{\mathcal{R}}_{h_2 h_4} \left(\begin{array}{cc} \tau_2 \tau_3 & \\ -z_2 z_3 & \end{array} \right). \end{aligned} \quad (\text{F.14})$$

With this at hand we can finally describe the contour deformations necessary for the regularization of the Fourier-Mellin integral at finite coupling. Starting from the ratio $\tilde{\mathcal{R}}_N = \mathcal{F}_{N-5,0} \equiv \mathcal{F}_{m,0}$ we will first change the contour of the ν_1 integral,

$$\mathcal{F}_{m,0} = \mathcal{F}_{m-1,1} + \mathcal{F}_{m-1,0}^{\{1\}}, \quad (\text{F.15})$$

where $\mathcal{F}_{m-1,0}^{\{1\}}$ is the residue we removed from the integration. $\mathcal{F}_{m-1,0}^{\{1\}}$ corresponds to an $m-1$ -fold Fourier-Mellin integral, and we have $\mathcal{F}_{m-1,0}^{\{1\}} = \tilde{\mathcal{R}}_{N-1}^{\{1\}}$. Removing the residue $\nu_2 = \nu_3$ from the m -fold Fourier-Mellin transform and leaving the lower-point terms untouched, we get

$$\mathcal{F}_{m,0} = \mathcal{F}_{m-1,1} + \mathcal{F}_{m-1,0}^{\{1\}} = \mathcal{F}_{m-3,3} + \mathcal{F}_{m-2,1}^{\{3\}} + \mathcal{F}_{m-1,0}^{\{1\}}. \quad (\text{F.16})$$

Note that the residue $\nu_2 = \nu_3$ couples the contour prescription in the ν_2 and ν_3 plane and hence fixes two contours at once. This ensures that we will only encounter those $\mathcal{F}_{n,m}$ with consistent contour prescriptions. Iterating this procedure until we find the desired integral $\mathcal{F}_{0,m}$, we have

$$\mathcal{F}_{m,0} = \mathcal{F}_{0,m} + \mathcal{F}_{m-1,0}^{\{1\}} + \sum_{i=1}^{\lfloor m/2 \rfloor} \mathcal{F}_{m-2i,2i-1}^{\{2i+1\}}. \quad (\text{F.17})$$

Since, by our assumption, we have already treated all lower-point cases $\tilde{\mathcal{R}}_{N-i}$, we will now rewrite all lower-point residues that we introduced in the process in terms of the $\tilde{\mathcal{R}}_{N-i}$. For this, we will need to deform the contours of the

lower-point integrals in eq. (F.17) back to Fourier-Mellin contours. This can be done recursively through the prescription

$$\mathcal{F}_{n,m}^{\{k_1, \dots, k_l\}} = \mathcal{F}_{n+2, m-2}^{\{k_1, \dots, k_l\}} - \mathcal{F}_{n+1, m-2}^{\{k_1, \dots, k_l, m\}}, \quad (\text{F.18})$$

where the recursion ends with

$$\mathcal{F}_{n,1}^{\{k_1, \dots, k_l\}} = \mathcal{F}_{n+1,0}^{\{k_1, \dots, k_l\}} - \mathcal{F}_{n,0}^{\{k_1, \dots, k_l, 1\}}, \quad (\text{F.19})$$

and where we set $\mathcal{F}_{0,0} = \tilde{\mathcal{R}}_5 = 1$. Note that this does not imply $\mathcal{F}_{0,0}^{\{k_1, \dots, k_l, 1\}} = 1$, because the bracket prescription for the kinematical dependence includes factors of $|z_i|^{2\pi i\Gamma}$. More precisely, we have

$$\begin{aligned} \mathcal{F}_{0,0}^{\{1\}} &= \tilde{\mathcal{R}}_5^{\{1\}} = (R_{h_1 h_2} \left(\frac{\tau_1}{z_1} \right))^{\{1\}} = |z_1|^{2\pi i\Gamma}, \\ \mathcal{F}_{0,0}^{\{3,1\}} &= \tilde{\mathcal{R}}_5^{\{3,1\}} = (R_{h_1 h_2 h_3} \left(\frac{\tau_1}{z_1}, \frac{\tau_2}{z_2} \right))^{\{3,1\}} \\ &= |z_2|^{-2\pi i\Gamma} (R_{h_1 h_2} \left(\frac{\tau_1}{z_1} \right))^{\{1\}} = |z_1|^{2\pi i\Gamma} |z_2|^{-2\pi i\Gamma}, \end{aligned} \quad (\text{F.20})$$

and no other combinations can show up. Following this prescription we find the same regularization in the 7- and 8-point cases that was introduced in refs. [1, 4]. Note that, while this prescription yields a valid regularization, it is customary in the literature to regularize $\tilde{\mathcal{R}}_6$ with a principle value prescription.

Appendix **G**

Proof of the Factorisation Theorem

G.1 Proof of the Factorization Theorem

In this section we will prove the factorisation theorem for LLA perturbative coefficients introduced in the previous section. The proof at LLA illustrates the basic strategy of the proof (also to higher logarithmic accuracies) and has the benefit of not being too technical. We will therefore start by proving the factorization theorem at LLA and consider the NLLA case afterwards. The proof is structured in two parts: We will first prove the factorisation of MHV amplitudes and later extend the proof to other helicity configurations. We stress again that the factorization holds for perturbative coefficients that have at least one index $i_j \neq 0$ and hence we will consider only such cases. The proof of factorization for MHV amplitudes relies on two claims that we are now going to prove.

Claim 1. *A perturbative coefficient corresponding to the Fourier-Mellin integral over the vacuum ladder with all equal helicities and with insertions that are independent of $\nu_1 \dots \nu_{i-1}$ and $n_1 \dots n_{i-1}$ only depends on $\rho_i, \dots, \rho_{N-5}$, i.e.*

$$\mathcal{F}_{N-5,0}[\varpi_N X(\nu_i, n_i, \dots, \nu_{N-5}, n_{N-5})] = f(\rho_i, \dots, \rho_{N-5}). \quad (\text{G.1})$$

Proof. Let us consider the MHV integral $\mathcal{F}_{N-5} [\varpi_N X(\nu_i, n_i, \dots, \nu_{N-5}, n_{N-5})]$ with $i > 1$, and let us focus on the ν_1 integration. This integral takes the form

$$\dots \int \frac{d\nu_1}{2\pi} \sum_{n_1=-\infty}^{+\infty} z_1^{i\nu_1+n_1/2} \bar{z}_1^{i\nu_1+n_1/2} z_2^{i\nu_2+n_2/2} \bar{z}_2^{i\nu_2+n_2/2} \quad (\text{G.2})$$

$$\times \chi^h(\nu_1, n_1) C^h(\nu_1, n_1, \nu_2, n_2) \dots,$$

where the dots contain only quantities that are independent of ν_1 and n_1 . Let us now show that this integral is independent of ρ_1 . From eq. (3.24), we can see that only z_1 and z_2 depend on ρ_1 , and hence we will ignore the dependence on z_j with $j > 2$. Due to the $z_1 \leftrightarrow \bar{z}_1$ symmetry of MHV amplitudes, we can consider only the purely holomorphic part $\bar{z}_1 \rightarrow 0$ with z_1 fixed, which corresponds to taking the residues at $i\nu_1 = n_1/2$ for $n_1 > 0$. Summing these residues we find

$$\mathcal{F}_{N-5,0} [\varpi_N X] \rightarrow \dots \chi^h(\nu_2, n_2) \underbrace{[(1-z_1)z_2]}_{=\rho_2}^{i\nu_2+n_2/2} \dots \quad (\text{G.3})$$

and we see that the integral does not depend on ρ_1 . Note that it is at this step that we require at least one of the indices i_j to be non-zero. In order for the ν_1 integration to yield the desired result we need the contour prescription to include the residue at $\nu_1 = \nu_2 = 0$, and hence we need to use Fourier-Mellin contours. As we can see, there is a new impact factor $\chi^h(\nu_2, n_2)$, which allows us to iterate this procedure for all further ν integrations without insertions. For two leading zeros without other insertions we find the same integral with z_1 replaced by ρ_2 , which yields

$$\dots \chi^h(\nu_3, n_3) \underbrace{[(1-\rho_2)z_3]}_{=\rho_3}^{i\nu_3+n_3/2} \dots \quad (\text{G.4})$$

Continuing this process, we see that

$$\mathcal{F}_{N-5,0} [\varpi_N X] (\rho_1, \dots, \rho_{N-5}) = f(\rho_i, \dots, \rho_{N-5}), \quad (\text{G.5})$$

for some function f .

□

It follows directly from claim 1 that for some f ,

$$\tilde{g}_{+\dots+}^{(\ell; 0, \dots, 0, i_1, \dots, i_{N-5})}(\rho_1, \dots, \rho_{N-5}) \equiv f(\rho_j, \dots, \rho_{N-5}). \quad (\text{G.6})$$

Taking the soft limits $k_j \rightarrow 0$ for $1 \leq j < l$ in the previous expression, we see that

$$\tilde{g}_{+\dots+}^{(\ell; 0, \dots, 0, i_1, \dots, i_{N-5})}(\rho_1, \dots, \rho_{N-5}) \equiv \tilde{g}_{+\dots+}^{(\ell; i_1, \dots, i_{N-5})}(\rho_k, \dots, \rho_{N-5}), \quad (\text{G.7})$$

and through target-projectile symmetry a similar equation holds for tailing zeros.

Claim 2. *If $f(\rho_1, \rho_{j_1}, \dots, \rho_{j_k})$ depends on a subset of simplicial MRK coordinates, then the convolution with some function $g(z_1)$ will depend on the same subset with ρ_1 added, i.e., we have*

$$g(z_1) * f(\rho_1, \rho_{j_1}, \dots, \rho_{j_k}) = F(\rho_1, \rho_{j_1}, \dots, \rho_{j_k}), \quad (\text{G.8})$$

for some function F .

The convolution in the r.h.s. of eq. (G.8) acts on z_1 and all simplicial MRK coordinates ρ_i are seen as functions of Fourier-Mellin coordinates z_i with the relation given in eq. (3.24).

Proof. Let us first change variables to simplicial coordinates based at z_1 and let us write $t_i \equiv t_i^{(1)}$. Then we have $z_1 = t_1$ and

$$\rho_1 = \frac{t_1}{t_{N-5}}, \quad \rho_2 = \frac{1-t_1}{1-t_{N-5}}, \quad \rho_i = \frac{t_{j_1-1}-t_1}{t_{j_1-1}-t_{N-5}}, \quad 2 < i < N-5. \quad (\text{G.9})$$

Let us first consider the case $j_1 \neq 2$. Then the convolution integral takes the form

$$\begin{aligned} g(z_1) * f(\rho_1, \rho_{j_1}, \dots, \rho_{j_k}) & \quad (\text{G.10}) \\ &= \frac{1}{\pi} \int \frac{d^2\tau}{|\tau|^2} g\left(\frac{t_1}{\tau}\right) f\left(\frac{\tau}{t_{N-5}}, \frac{t_{j_1-1}-\tau}{t_{j_1-1}-t_{N-5}}, \dots, \frac{t_{j_k-1}-\tau}{t_{j_k-1}-t_{N-5}}\right). \end{aligned}$$

After shifting the integration variable $\tau \rightarrow t_{N-5}\tau$ and defining $x_j = t_j/t_{N-5}$, we see that the explicit dependence on t_{N-5} drops out and that the integral can be written as a function \tilde{F} of the x_i only,

$$\begin{aligned} g(z_1) * f(\rho_1, \rho_{j_1}, \dots, \rho_{j_k}) &= \frac{1}{\pi} \int \frac{d^2\tau}{|\tau|^2} g\left(\frac{x_1}{\tau}\right) f\left(\tau, \frac{x_{j_1-1}-\tau}{x_{j_1-1}-1}, \dots, \frac{x_{j_k-1}-\tau}{x_{j_k-1}-1}\right) \\ &\equiv \tilde{F}(x_1, x_{j_1-1}, \dots, x_{j_k-1}). \end{aligned} \quad (\text{G.11})$$

Then, rewriting the integral in terms of simplicial MRK coordinates, we find

$$x_1 = \frac{t_1}{t_{N-5}} = \rho_1, \quad x_j = \frac{t_j}{t_{N-5}} = \frac{\rho_1 - \rho_{j+1}}{1 - \rho_{j+1}}, \quad j \geq 2, \quad (\text{G.12})$$

and hence that the integral depends on the same set of coordinates as before.

Let us now consider the case $j_1 = 2$. Then, after shifting the integration variable and defining $x_j = t_j/t_{N-5}$ the resulting function will still depend on t_{N-5} ,

$$g(z_1) * f(\rho_1, \rho_2, \rho_{j_2} \dots, \rho_{j_k}) = \tilde{F}(x_1, t_{N-5}, x_{j_2-1}, \dots, x_{j_k-1}). \quad (\text{G.13})$$

Upon verifying that t_{N-5} is only a function of ρ_1 and ρ_2 ,

$$t_{N-5} = \frac{1 - \rho_2}{\rho_1 - \rho_2}, \quad (\text{G.14})$$

we see that the integral depends, again, on the same set of coordinates as before.

□

Proof of the factorisation theorem for LLA amplitudes. We will now prove the factorization of LLA amplitudes using the properties of Fourier-Mellin integrals we have just shown. We start by considering the MHV case. In order to get a feeling for the structure of this proof, let us first argue that we can construct perturbative coefficients piece by piece by inserting BFKL eigenvalues $\mathcal{E}(z_1)$ and relabelling simplicial MRK coordinates. Let us demonstrate this at an easy example and construct the perturbative coefficient $\tilde{g}_{+\dots+}^{(4;0,2,0,0,1,0)}$. We start with the rightmost non-zero index, $i_5 = 1$, and add zero indices on both sides. From (G.7) and target-projectile symmetry it follows that

$$\tilde{g}_{+\dots+}^{(2;0,0,0,1,0)}(\rho_1, \dots, \rho_5) = \tilde{g}_{++}^{(2;1)}(\rho_4). \quad (\text{G.15})$$

In order to arrive at the desired perturbative coefficient, we need to insert two leading-order BFKL eigenvalues into the integrand, and we have

$$\tilde{g}_{+\dots+}^{(4;2,0,0,1,0)}(\rho_1, \dots, \rho_5) = \mathcal{E}(z_1) * \mathcal{E}(z_1) * \tilde{g}_{+\dots+}^{(2;0,0,0,1,0)}(\rho_1, \dots, \rho_5). \quad (\text{G.16})$$

Then all we need to do is add another zero to the left by relabelling the simplicial MRK coordinates in the previous expression (c.f. eqs. (G.7)) to find

$$\tilde{g}_{+\dots+}^{(4;0,2,0,0,1,0)}(\rho_1, \dots, \rho_6) = \tilde{g}_{+\dots+}^{(4;2,0,0,1,0)}(\rho_2, \dots, \rho_6). \quad (\text{G.17})$$

Then the factorization follows upon realizing that the perturbative coefficient on the r.h.s. of eq. (G.16) only depends on ρ_4 and following claim 2 the l.h.s. only depends on ρ_1 and ρ_4 . Let us now make this proof more rigorous.

We can prove the factorization theorem inductively over the number of external particles N . Let us assume that the factorization theorem holds for all perturbative coefficients up to $N - 1$ legs, and let us denote the perturbative

coefficient with N legs by $\tilde{g}_{+\dots+}^{(\ell; i_1, \dots, i_{N-5})}(\rho_1, \dots, \rho_{N-5})$. Let us also label all non-zero indices in (i_2, \dots, i_{N-5}) by i_{a_1}, \dots, i_{a_k} , $2 \leq a_j \leq N-5$. If $i_1 = 0$, then Claim 1 implies that we can drop the first index. The resulting function is an $(N-1)$ -point amplitude, where, by the induction hypothesis, eq. (3.81) applies, and we have

$$\begin{aligned} \tilde{g}_{+\dots+}^{(\ell; 0, i_2, \dots, i_{N-5})}(\rho_1, \dots, \rho_{N-5}) &= \tilde{g}_{+\dots+}^{(\ell; i_2, \dots, i_{N-5})}(\rho_2, \dots, \rho_{N-5}) \\ &= \tilde{g}_{+\dots+}^{(\ell; i_{a_1}, \dots, i_{a_k})}(\rho_{a_1}, \dots, \rho_{a_k}), \end{aligned} \quad (\text{G.18})$$

in agreement with eq. (3.80).

Let us now consider the case $i_1 \neq 0$. Then we can write the perturbative coefficient as the convolution of BFKL eigenvalues $\mathcal{E}(z_1)$ with the corresponding perturbative coefficient with $i_1 = 0$,

$$\begin{aligned} g_{+\dots+}^{(i_1, i_2, \dots, i_{N-5})}(\rho_1, \dots, \rho_{N-5}) &= \mathcal{E}(z_1)^{*i_1} * g_{+\dots+}^{(0, i_2, \dots, i_{N-5})}(\rho_2, \dots, \rho_{N-5}) \\ &= \mathcal{E}(z_1)^{*i_1} * g_{+\dots+}^{(i_{a_1}, \dots, i_{a_k})}(\rho_{a_1}, \dots, \rho_{a_k}), \end{aligned} \quad (\text{G.19})$$

where in the last equality we have used that factorization holds for the perturbative coefficient with $i_1 = 0$. The convolution in the last line only adds a ρ_1 dependence according to claim 2, which proves the factorization for MHV amplitudes.

Let us now extend the previous proof to other helicity configurations. We will again proceed by induction over the number of external legs or equivalently, the number of indices i_j . Let us assume that the factorization theorem (3.80) holds for up to k indices and let us consider a perturbative coefficient with $k+1$ indices. If the first two helicities are not equal, we can write the perturbative coefficient as the convolution of a helicity flip operator with a perturbative coefficient whose first two indices are equal,

$$g_{-+h_3 \dots h_{k+2}}^{(\ell; i_1 \dots i_{k+1})}(\rho_1, \dots, \rho_{k+1}) = \mathcal{H}^{(0)}(z_1) * g_{++h_3 \dots h_{k+2}}^{(\ell; i_1 \dots i_{k+1})}(\rho_1, \dots, \rho_{k+1}). \quad (\text{G.20})$$

Then it follows from claim 2 that the factorization theorem holds when the first two helicities are different if it holds when the first two helicities are equal. Let us now assume that the first two helicities are indeed equal.

If $i_1 \neq 0$ we can use Fourier-Mellin convolutions to reduce the value of i_1 to zero,

$$g_{++h_3 \dots h_{k+2}}^{(\ell; i_1 \dots i_{k+1})}(\rho_1, \dots, \rho_{k+1}) = \mathcal{E}(z_1)^{*i_1} * g_{++h_3 \dots h_{k+2}}^{(\ell-i_1; 0, i_2 \dots i_{k+1})}(\rho_1, \dots, \rho_{k+1}). \quad (\text{G.21})$$

Then it follows from claim 1 and soft limits that we can delete the index $i_1 = 0$. Since the resulting perturbative coefficient has only k indices i_j it follows from

the induction hypothesis that the factorization theorem holds. To complete the proof we need to perform the convolution integrals that we introduced to reduce the index i_1 to zero. Since these convolutions only act on z_1 , the factorization theorem for LLA amplitudes follows upon using claim 2. \square

Proof of the factorisation theorem for NLLA amplitudes. In this section we will prove the factorization of NLLA amplitudes in analogy to the proof at LLA. We will start with the MHV case and then generalize the proof to other helicity configurations. In the following, the same things often hold for both \tilde{g} and \tilde{h} with the same indices and we will state equations that hold for either of the two by using $\eta \in \{\tilde{g}, \tilde{h}\}$. Similarly to the LLA case, it follows from claim 1 that we can drop leading indices $i_1, \dots, i_j = 0$ as long as there are no insertions depending on ν_k , $k \leq j$. More precisely, for $j \geq k$, we have

$$\begin{aligned} \eta_{+\dots+}^{j;(\ell;0,\dots,0,i_k,\dots,i_{N-5})}(\rho_1, \dots, \rho_{N-5}) &\equiv \eta_{+\dots+}^{j-k+1;(\ell;i_k,\dots,i_{N-5})}(\rho_k, \dots, \rho_{N-5}), \\ \eta_{j+1;+\dots+}^{(\ell;0,\dots,0,i_k,\dots,i_{N-5})}(\rho_1, \dots, \rho_{N-5}) &\equiv \eta_{j-k+2;+\dots+}^{(\ell;i_k,\dots,i_{N-5})}(\rho_k, \dots, \rho_{N-5}). \end{aligned} \quad (\text{G.22})$$

The proof at LLA relied on the fact that we could recursively build up all perturbative coefficients using only convolutions acting on the variable z_1 . At NLLA, there is an exception to this rule: The correction to a central emission block $C_{1,12}^+$ is a function of ν_1 and ν_2 and will therefore be a function of z_1 and z_2 . Technically, we could still construct any such corrected perturbative coefficient by adding 0 indices and convolutions acting on z_1 only if we started this process from a corrected central emission block. Then we would have, for example,

$$\eta_{3;+\dots+}^{(\ell+1;1,i_1,i_2)} = \mathcal{E}(z_1) * \eta_{3;+\dots+}^{(\ell;0,i_1,i_2)} = \mathcal{E}(z_1) * \eta_{2;+\dots+}^{(\ell;i_1,i_2)}(\rho_2, \rho_3). \quad (\text{G.23})$$

The problem is, however, that we need at least one insertion of a BFKL eigenvalue in the integrand if we want to work with Fourier-Mellin contours, and hence the previous equation fails for $i_1 = i_2 = 0$. Subsequently, the observations made in LLA proof only allow us to show the desired factorization up to zeros 'trapped' between a corrected central emission block without any BFKL insertions and the closest BFKL insertion,

$$\eta_{j;+\dots+}^{(\ell;\dots,i_{j-2},0,\dots,0,i_k \neq 0,\dots)}(\dots, \rho_{j-1}, \dots, \rho_k, \dots). \quad (\text{G.24})$$

Let us now consider the N -point corrected perturbative coefficient $\eta_{2;+\dots+}^{(i+2;0,\dots,0,i)}$, $i > 0$. If we can show that

$$\eta_{2;+\dots+}^{(i+2;0,\dots,0,i)}(\rho_1, \dots, \rho_{N-5}) = \eta_{2;+\dots+}^{(i+2;0,0,i)}(\rho_1, \rho_2, \rho_{N-5}), \quad (\text{G.25})$$

then factorization for all MHV NLLA corrected perturbative coefficients follows. In order to prove this, let us have a closer look at the correction to the central emission block,

$$\begin{aligned} c_{1,12}^+ &= \left(\frac{1}{2} [DE_1 - DE_2 + E_1E_2 + \frac{1}{4}(N_1 + N_2)^2 + V_1V_2 + 2\zeta_2 \right. \\ &\quad \left. + (V_1 - V_2)(M_{12} - E_1 - E_2) + i\pi(V_2 - V_1 - E_1 - E_2)] \right) \quad (\text{G.26}) \\ &\quad - \frac{1}{4}(E_1^2 + E_2^2 + N_1V_1 - N_2V_2) - \frac{3}{16}(N_1^2 + N_2^2) - \zeta_2. \end{aligned}$$

As is easy to see, the correction to the central emission block $c_{1,12}^+$ is mostly made up of building blocks that only depend on one ν_i and whose Fourier-Mellin transform therefore depends only on one variable. For these contributions, the previous arguments hold, and we have

$$\mathcal{F}_{N-5}[\varpi_N B_j^2 E_{N-5}^i] = \mathcal{F}_{N-5}[\varpi_N B_j^2 E_{N-5}^i](\rho_j, \rho_{N-5}), \quad (\text{G.27})$$

$$\mathcal{F}_{N-5}[\varpi_N B_1 B_2 E_{N-5}^i] = \mathcal{F}_{N-5}[\varpi_N B_1 B_2 E_{N-5}^i](\rho_1, \rho_2, \rho_{N-5}), \quad (\text{G.28})$$

for B_i depending only on ν_i and n_i . The only terms posing a problem are the ones including the building block M_{12} .

We will now investigate the building block M_{12} and then show that the Fourier-Mellin transform $\mathcal{F}_{N-5}[\varpi_N M_{12} V_j E_{N-5}^i]$ for $j \in \{1, 2\}$ is a function of only ρ_1, ρ_2 and ρ_{N-5} . From equations (C.4) and (C.5), it is easy to verify that

$$M_{12} = \frac{D_{\nu_1} C_{0,12}^+}{C_{0,12}^+} + F_1, \quad (\text{G.29})$$

where we have introduced the new building-block

$$F(\nu, n) = -2\psi(1) + \psi\left(1 + i\nu - \frac{n}{2}\right) + \psi\left(1 - i\nu - \frac{n}{2}\right). \quad (\text{G.30})$$

$$(\text{G.31})$$

Using integration by parts we can then rewrite the integral as

$$\mathcal{F}_{N-5} \left[\varpi_N \frac{D_1 C_{0,12}^+}{C_{0,12}^+} E_{N-5}^i \right] \quad (\text{G.32})$$

$$= \mathcal{F}_{N-5} [D_1 \varpi_N E_{N-5}^i] - \mathcal{F}_{N-5} \left[\varpi_N \frac{D_1 \chi_{0,1} 1^+}{\chi_{0,1}^+} \right] \quad (\text{G.33})$$

$$= \mathcal{F}_{N-5} [D_1 \varpi_N E_{N-5}^i] + i \mathcal{F}_{N-5} [\varpi_N \chi_{0,1}^+] \quad (\text{G.34})$$

$$= \mathcal{F}_{N-5} [D_1 \varpi_N E_{N-5}^i] + \mathcal{F}_{N-5} [\varpi_N V_1] - \frac{1}{2} \mathcal{F}_{N-5} [\varpi_N N_1]. \quad (\text{G.35})$$

the derivative can be treated as before (c.f. eq. (4.70)). In particular, for $i = 1$, we have

$$\mathcal{G}_0(z_1) = \mathcal{G}_0(\rho_1) - \mathcal{G}_0(\rho_2) + \mathcal{G}_1(\rho_2) - \mathcal{G}_{\rho_2}(\rho_1). \quad (\text{G.36})$$

We already know that all terms in eq. (G.25) that do not contain the building block M_{12} evaluate to functions of ρ_1, ρ_2 and ρ_{N-5} only. Let us now show that the same is true for the terms

$$f_1 = \mathcal{F}_{N-5}[\varpi_N M_{12} V_1 E_{N-5}^i] \quad \text{and} \quad f_2 = \mathcal{F}_{N-5}[\varpi_N M_{12} V_2 E_{N-5}^i]. \quad (\text{G.37})$$

Treating M_{12} as before, we find, for $j \in \{1, 2\}$

$$\begin{aligned} f_j &= \mathcal{F}_{N-5}[D_1 \varpi_N E_{N-5}^i] * \mathcal{F}[V_j] + \mathcal{F}[\varpi_N V_1 E_{N-5}^i] * \mathcal{F}[V_j] \\ &\quad - \frac{1}{2} \mathcal{F}[\varpi_N N_1 E_{N-5}^i] * \mathcal{F}[V_j] + \frac{1}{2} \mathcal{F}[\varpi_N F_1 E_{N-5}^i] * \mathcal{F}[V_j]. \end{aligned} \quad (\text{G.38})$$

The last three terms take the form (G.27) and hence have the correct functional dependence. For $j = 1$, we know that

$$\mathcal{F}_{N-5}[D_1 \varpi_N E_{N-5}^i] = \mathcal{G}_0(z_1) \mathcal{F}_{N-5}[\varpi_N E_{N-5}^i]. \quad (\text{G.39})$$

The logarithm can be expressed in terms of ρ_1 and ρ_2 (c.f. eq. (G.36)) only and the second factor corresponds to the LLA perturbative coefficient $\tilde{g}_{++}^{(i+1;i)}(\rho_{N-5})$. Therefore, the function in eq. G.39 only depends on ρ_1, ρ_2 and ρ_{N-5} . Following Claim 2, convoluting the product of the two with a function of z_1 must therefore also be a function of ρ_1, ρ_2 and ρ_{N-5} only. V_2 is independent of ν_1 and we can write

$$\begin{aligned} \mathcal{F}_{N-5}[D_1 \varpi_N E_{N-5}^i] * \mathcal{F}[V_2] &= \mathcal{F}_{N-5}[D_1 \varpi_N V_2 E_{N-5}^i] \\ &= \mathcal{G}_0(z_1) \mathcal{F}_{N-5}[\varpi_N V_2 E_{N-5}^i]. \end{aligned} \quad (\text{G.40})$$

We know already that $\mathcal{F}_{N-5}[\varpi_N V_2 E_{N-5}^i]$ is a function of ρ_2 and ρ_{N-5} only and $\mathcal{G}_0(z_1)$ only depends on ρ_1 and ρ_2 . This shows that f_2 must also be a function of ρ_1, ρ_2 and ρ_{N-5} .

Therefore, $\eta_{2;+\dots+}^{(i+2;0,\dots,0,i)}(\rho_1, \dots, \rho_{N-5})$ must be a function of ρ_1, ρ_2 and ρ_{N-5} only. From the soft limits $\rho_i \rightarrow 0$ for $3 \leq i \leq N-6$, we can immediately see that eq. (G.25) holds. Then the factorization of NLLA perturbative coefficients follows recursively like in the LLA case.

We will now extend the proof of factorization at NLLA to the non-MHV case and we will again proceed by induction over the number of indices i_j . For this proof there is no conceptual difference between insertions of leading-order

BFKL eigenvalues and next-to leading-order BFKL eigenvalues. Their Fourier-Mellin transformations are both functions of only one variable and they both only appear as insertions into faces with non-zero index i_j . For perturbative coefficients with a corrected BFKL eigenvalue the LLA proof holds and we will therefore only explicitly consider corrections to the BFKL ladder. Let us first consider the perturbative coefficient $\eta_{j;h_1\dots h_n}^{(\ell;i_1,\dots,i_{n-1})}$ for $j > 2$. For these perturbative coefficients we can proceed as in the LLA case. If the first helicities are not equal we can factor out a leading order helicity flip kernel and only consider the case with two equal helicities $\eta_{j;+ + h_3\dots h_n}^{(\ell;i_1,\dots,i_{n-1})}$ and the induction step holds as in the LLA proof.

Let us now consider a corrected perturbative coefficient with a corrected impact factor, $\eta_{1;h_1\dots h_n}^{(\ell;i_1,\dots,i_{n-1})}$. We can factor out the Fourier-Mellin transform of the correction to the impact factor $\kappa_1^{h_1}(\nu_1, n_1)$ to find

$$\eta_{1;h_1\dots h_n}^{(\ell;i_1,\dots,i_{n-1})} = \mathcal{F}[\kappa_1^{h_1}](z_1) * \eta_{h_1\dots h_n}^{(\ell-1;i_1,\dots,i_{n-1})}. \quad (\text{G.41})$$

The perturbative coefficient on the r.h.s. of eq. (G.41) is a LLA perturbative coefficient for which we have already shown that it factorizes. Then Factorization for the NLLA perturbative coefficient on the l.h.s. follows from claim 2.

All that is left to show is that factorization holds for corrected perturbative coefficients $\eta_{2;h_1\dots h_n}^{(\ell;i_1,\dots,i_{n-1})}$. If one of the indices i_1 or i_2 is non-zero then let us consider the corresponding perturbative coefficient under target-projectile symmetry, $\eta_{n-1;h_n\dots h_1}^{(\ell;i_{n-1},\dots,i_1)}$. We can use the recursion from the LLA proof to show that factorization holds for $\eta_{n-1;h_n\dots h_1}^{(\ell;i_{n-1},\dots,i_1)}$ where the recursion starts from $\eta_{2;h_2 h_1}^{(\ell';i_2,i_1)}$. We will therefore consider the case where $i_1 = i_2 = 0$. We know that factorization holds for the LLA perturbative coefficient

$$\eta_0 = \eta_{h_1\dots h_n}^{(\ell-1;0,0,i_3,\dots,i_{n-1})}, \quad (\text{G.42})$$

so it is enough to show that $\eta_{2;h_1\dots h_n}^{(\ell-1;0,0,i_3,\dots,i_{n-1})}$ has the same functional dependence with ρ_1 and ρ_2 added.

Let us again consider the terms in $c_{1,12}^{h_2}$ that are independent of M_{12} . We can group those terms into three categories: Terms with two insertions that depend on ν_1 , terms with two insertions depending on ν_2 and those with one insertion each. From claim 2 it follows directly that

$$\eta_{h_1\dots h_n}^{(\ell-1;0,0,i_3,\dots,i_{n-1})} * \mathcal{F}[B_1(\nu_1, n_1)] * \mathcal{F}[B_2(\nu_1, n_1)] \quad (\text{G.43})$$

depends on the same set of simplicial MRK coordinates as η_0 with ρ_1 added. If $h_1 = h_2$ we have

$$\begin{aligned} & \eta_{h_1 \dots h_n}^{(\ell-1; 0, 0, i_3, \dots, i_{n-1})} * \mathcal{F}[B_1(\nu_2, n_2)] * \mathcal{F}[B_2(\nu_2, n_2)] \\ &= \eta_{h_2 \dots h_n}^{(\ell-1; 0, 0, i_3, \dots, i_{n-1})} * \mathcal{F}[B_1(\nu_2, n_2)] * \mathcal{F}[B_2(\nu_2, n_2)]. \end{aligned} \quad (\text{G.44})$$

Upon relabelling of all indices $i_j \rightarrow i'_{j-1}$, $\rho_j \rightarrow \rho'_{j-1}$, the term on the r.h.s. corresponds to a convolution in z'_1 and hence introduces at most a dependence on $\rho'_1 = \rho_2$. Iterating the two cases, we find that

$$\eta_{h_1 \dots h_n}^{(\ell-1; 0, 0, i_3, \dots, i_{n-1})} * \mathcal{F}[B_1(\nu_1, n_1)] * \mathcal{F}[B_2(\nu_2, n_2)] \quad (\text{G.45})$$

introduces both ρ_1 and ρ_2 . If the first two helicities are not equal we can factor out a leading-order helicity flip to get

$$\begin{aligned} & \eta_{h_1 h_2 \dots h_n}^{(\ell-1; 0, 0, i_3, \dots, i_{n-1})} * \mathcal{F}[B_1(\nu_1, n_1)] * \mathcal{F}[B_2(\nu_1, n_1)] \\ &= \left(\mathcal{H}_1^{(0)} * \eta_{h_2 h_2 \dots h_n}^{(\ell-1; 0, 0, i_3, \dots, i_{n-1})} \right) * \mathcal{F}[B_1(\nu_2, n_2)] * \mathcal{F}[B_2(\nu_2, n_2)] \\ &= \mathcal{H}_1^{(0)} * \left(\eta_{h_2 h_2 \dots h_n}^{(\ell-1; 0, 0, i_3, \dots, i_{n-1})} * \mathcal{F}[B_1(\nu_2, n_2)] * \mathcal{F}[B_2(\nu_2, n_2)] \right). \end{aligned} \quad (\text{G.46})$$

Then the previous arguments hold for the term in brackets in the last line and the helicity flip adds at most ρ_1 .

The terms involving the building block M_{12} can be treated similarly. As in the MHV case, we can replace M by a sum of building blocks depending only on ν_1 or ν_2 as well as a term corresponding to a total derivative. Except for the relation

$$i\chi_{0,1}^+ = V_1 - \frac{1}{2}N_1, \quad (\text{G.47})$$

the previous considerations were independent of the helicity configuration and other insertions depending only on (ν_j, n_j) for $j > 2$. Therefore, after realizing that

$$i\chi_{0,1}^- = V_1 + \frac{1}{2}N_1, \quad (\text{G.48})$$

we find that the insertions $M_{12} * V_i$ for $i = 1, 2$ only add a dependence on ρ_1 and ρ_2 .

We have shown that $\eta_{2; h_1 \dots h_n}^{(\ell; i_1, \dots, i_{n-1})}$ has the same functional dependence as the corresponding LLA coefficient $\eta_{h_1 \dots h_n}^{(\ell-1; i_1, \dots, i_{n-1})}$ with ρ_1 and ρ_2 added. This is exactly the functional dependence that we expect according to factorization. With this as additional starting point of the recursion introduced at LLA, the factorization of corrected perturbative coefficients at NLLA follows inductively. \square

Appendix H

The Banana Integral in Terms of eMPLs

In this chapter we present the solution $(\tilde{M}_1, \tilde{M}_2, \tilde{M}_3)^\top$ to the banana graph in terms of iterated integrals of modular forms that was computed in chapter 5. The solution is given as

$$\begin{aligned}
C_k \tilde{M}_k^{(0)} = & -\frac{13319}{96\pi^2} \Gamma_{AS}^k \left(\begin{smallmatrix} 0 & 3 \\ 1 & 0 \end{smallmatrix} \right) + \frac{2679}{160\pi^2} \Gamma_{AS}^k \left(\begin{smallmatrix} 0 & 5 \\ 1 & 4 \end{smallmatrix} \right) - \frac{77}{10\pi^2} \Gamma_{AS}^k \left(\begin{smallmatrix} 0 & 3 \\ 2 & 0 \end{smallmatrix} \right) \quad (\text{H.1}) \\
& - \frac{2911}{15\pi^2} \Gamma_{AS}^k \left(\begin{smallmatrix} 0 & 0 \\ 3 & 2 \end{smallmatrix} \right) + \frac{20261}{1440\pi^2} \Gamma_{AS}^k \left(\begin{smallmatrix} 0 & 1 \\ 3 & 4 \end{smallmatrix} \right) + \frac{577}{60\pi^2} \Gamma_{AS}^k \left(\begin{smallmatrix} 0 & 2 \\ 3 & 5 \end{smallmatrix} \right) \\
& - \frac{22841}{120\pi^2} \Gamma_{AS}^k \left(\begin{smallmatrix} 0 & 4 \\ 3 & 1 \end{smallmatrix} \right) + \frac{1639}{180\pi^2} \Gamma_{AS}^k \left(\begin{smallmatrix} 0 & 4 \\ 3 & 5 \end{smallmatrix} \right) - \frac{755827}{7200\pi^2} \Gamma_{AS}^k \left(\begin{smallmatrix} 0 & 5 \\ 3 & 0 \end{smallmatrix} \right) \\
& - \frac{1371547}{2160\pi^2} \Gamma_{AS}^k \left(\begin{smallmatrix} 0 & 5 \\ 3 & 2 \end{smallmatrix} \right) + \frac{969431}{720\pi^2} \Gamma_{AS}^k \left(\begin{smallmatrix} 0 & 5 \\ 3 & 3 \end{smallmatrix} \right) - \frac{1011209}{2160\pi^2} \Gamma_{AS}^k \left(\begin{smallmatrix} 0 & 5 \\ 3 & 5 \end{smallmatrix} \right) \\
& + \frac{77}{20\pi^2} \Gamma_{AS}^k \left(\begin{smallmatrix} 0 & 3 \\ 4 & 0 \end{smallmatrix} \right) - \frac{70291}{480\pi^2} \Gamma_{AS}^k \left(\begin{smallmatrix} 0 & 3 \\ 5 & 0 \end{smallmatrix} \right) + \frac{2679}{160\pi^2} \Gamma_{AS}^k \left(\begin{smallmatrix} 0 & 5 \\ 5 & 4 \end{smallmatrix} \right) \\
& - \frac{10409}{90\pi^2} \Gamma_{AS}^k \left(\begin{smallmatrix} 1 & 0 \\ 0 & 3 \end{smallmatrix} \right) + \frac{2197}{300\pi^2} \Gamma_{AS}^k \left(\begin{smallmatrix} 1 & 5 \\ 0 & 5 \end{smallmatrix} \right) - \frac{893}{120\pi^2} \Gamma_{AS}^k \left(\begin{smallmatrix} 1 & 0 \\ 1 & 3 \end{smallmatrix} \right) \\
& + \frac{665}{6\pi^2} \Gamma_{AS}^k \left(\begin{smallmatrix} 1 & 3 \\ 1 & 0 \end{smallmatrix} \right) - \frac{57739}{288\pi^2} \Gamma_{AS}^k \left(\begin{smallmatrix} 1 & 0 \\ 2 & 1 \end{smallmatrix} \right) + \frac{36031}{1440\pi^2} \Gamma_{AS}^k \left(\begin{smallmatrix} 1 & 0 \\ 2 & 5 \end{smallmatrix} \right) \\
& - \frac{140}{3\pi^2} \Gamma_{AS}^k \left(\begin{smallmatrix} 1 & 3 \\ 2 & 0 \end{smallmatrix} \right) + \frac{14}{5\pi^2} \Gamma_{AS}^k \left(\begin{smallmatrix} 1 & 3 \\ 2 & 3 \end{smallmatrix} \right) + \frac{22867}{360\pi^2} \Gamma_{AS}^k \left(\begin{smallmatrix} 1 & 3 \\ 3 & 0 \end{smallmatrix} \right)
\end{aligned}$$

$$\begin{aligned}
& -\frac{2069}{40\pi^2}\Gamma_{\text{AS}}^k\left(\begin{smallmatrix} 1 & 4 \\ 3 & 3 \end{smallmatrix}\right) - \frac{1427}{40\pi^2}\Gamma_{\text{AS}}^k\left(\begin{smallmatrix} 1 & 0 \\ 4 & 3 \end{smallmatrix}\right) + \frac{847}{40\pi^2}\Gamma_{\text{AS}}^k\left(\begin{smallmatrix} 1 & 0 \\ 4 & 4 \end{smallmatrix}\right) \\
& + \frac{7343}{60\pi^2}\Gamma_{\text{AS}}^k\left(\begin{smallmatrix} 1 & 3 \\ 4 & 0 \end{smallmatrix}\right) - \frac{1579}{120\pi^2}\Gamma_{\text{AS}}^k\left(\begin{smallmatrix} 1 & 0 \\ 5 & 3 \end{smallmatrix}\right) - \frac{55}{8\pi^2}\Gamma_{\text{AS}}^k\left(\begin{smallmatrix} 1 & 0 \\ 5 & 4 \end{smallmatrix}\right) \\
& + \frac{6207}{40\pi^2}\Gamma_{\text{AS}}^k\left(\begin{smallmatrix} 2 & 0 \\ 0 & 3 \end{smallmatrix}\right) - \frac{386267}{720\pi^2}\Gamma_{\text{AS}}^k\left(\begin{smallmatrix} 2 & 0 \\ 0 & 4 \end{smallmatrix}\right) - \frac{2197}{40\pi^2}\Gamma_{\text{AS}}^k\left(\begin{smallmatrix} 2 & 0 \\ 0 & 0 \end{smallmatrix}\right) \\
& - \frac{386267}{360\pi^2}\Gamma_{\text{AS}}^k\left(\begin{smallmatrix} 2 & 4 \\ 0 & 2 \end{smallmatrix}\right) + \frac{386267}{360\pi^2}\Gamma_{\text{AS}}^k\left(\begin{smallmatrix} 2 & 4 \\ 0 & 4 \end{smallmatrix}\right) - \frac{72913}{360\pi^2}\Gamma_{\text{AS}}^k\left(\begin{smallmatrix} 2 & 3 \\ 3 & 0 \end{smallmatrix}\right) \\
& + \frac{1481}{20\pi^2}\Gamma_{\text{AS}}^k\left(\begin{smallmatrix} 2 & 3 \\ 3 & 3 \end{smallmatrix}\right) + \frac{665}{12\pi^2}\Gamma_{\text{AS}}^k\left(\begin{smallmatrix} 2 & 3 \\ 4 & 0 \end{smallmatrix}\right) + \frac{893}{60\pi^2}\Gamma_{\text{AS}}^k\left(\begin{smallmatrix} 2 & 0 \\ 5 & 3 \end{smallmatrix}\right) \\
& - \frac{1367}{30\pi^2}\Gamma_{\text{AS}}^k\left(\begin{smallmatrix} 3 & 0 \\ 3 & 5 \end{smallmatrix}\right) - \frac{188113}{10800\pi^2}\Gamma_{\text{AS}}^k\left(\begin{smallmatrix} 3 & 2 \\ 3 & 0 \end{smallmatrix}\right) + \frac{105}{2\pi^2}\Gamma_{\text{AS}}^k\left(\begin{smallmatrix} 3 & 3 \\ 3 & 1 \end{smallmatrix}\right) \\
& + \frac{263}{3\pi^2}\Gamma_{\text{AS}}^k\left(\begin{smallmatrix} 3 & 3 \\ 3 & 2 \end{smallmatrix}\right) + \frac{1582769}{10800\pi^2}\Gamma_{\text{AS}}^k\left(\begin{smallmatrix} 3 & 4 \\ 3 & 0 \end{smallmatrix}\right) - \frac{1555}{8\pi^2}\Gamma_{\text{AS}}^k\left(\begin{smallmatrix} 3 & 5 \\ 3 & 0 \end{smallmatrix}\right) \\
& + \frac{77}{10\pi^2}\Gamma_{\text{AS}}^k\left(\begin{smallmatrix} 3 & 3 \\ 4 & 0 \end{smallmatrix}\right) + \frac{203}{30\pi^2}\Gamma_{\text{AS}}^k\left(\begin{smallmatrix} 3 & 0 \\ 5 & 3 \end{smallmatrix}\right) - \frac{21}{2\pi^2}\Gamma_{\text{AS}}^k\left(\begin{smallmatrix} 3 & 3 \\ 5 & 3 \end{smallmatrix}\right) \\
& + \frac{14}{5\pi^2}\Gamma_{\text{AS}}^k\left(\begin{smallmatrix} 3 & 3 \\ 5 & 4 \end{smallmatrix}\right) + \frac{8141}{120\pi^2}\Gamma_{\text{AS}}^k\left(\begin{smallmatrix} 4 & 0 \\ 1 & 3 \end{smallmatrix}\right) + \frac{1271}{24\pi^2}\Gamma_{\text{AS}}^k\left(\begin{smallmatrix} 4 & 3 \\ 1 & 0 \end{smallmatrix}\right) \\
& - \frac{1271}{24\pi^2}\Gamma_{\text{AS}}^k\left(\begin{smallmatrix} 4 & 3 \\ 1 & 3 \end{smallmatrix}\right) - \frac{386267}{720\pi^2}\Gamma_{\text{AS}}^k\left(\begin{smallmatrix} 4 & 0 \\ 2 & 2 \end{smallmatrix}\right) + \frac{386267}{720\pi^2}\Gamma_{\text{AS}}^k\left(\begin{smallmatrix} 4 & 2 \\ 2 & 0 \end{smallmatrix}\right) \\
& + \frac{386267}{720\pi^2}\Gamma_{\text{AS}}^k\left(\begin{smallmatrix} 4 & 2 \\ 2 & 2 \end{smallmatrix}\right) - \frac{665}{6\pi^2}\Gamma_{\text{AS}}^k\left(\begin{smallmatrix} 4 & 3 \\ 2 & 0 \end{smallmatrix}\right) - \frac{386267}{720\pi^2}\Gamma_{\text{AS}}^k\left(\begin{smallmatrix} 4 & 4 \\ 2 & 0 \end{smallmatrix}\right) \\
& - \frac{31277}{360\pi^2}\Gamma_{\text{AS}}^k\left(\begin{smallmatrix} 4 & 3 \\ 3 & 0 \end{smallmatrix}\right) - \frac{147}{5\pi^2}\Gamma_{\text{AS}}^k\left(\begin{smallmatrix} 4 & 3 \\ 3 & 3 \end{smallmatrix}\right) - \frac{386267}{360\pi^2}\Gamma_{\text{AS}}^k\left(\begin{smallmatrix} 4 & 2 \\ 4 & 0 \end{smallmatrix}\right) \\
& + \frac{386267}{720\pi^2}\Gamma_{\text{AS}}^k\left(\begin{smallmatrix} 4 & 4 \\ 4 & 0 \end{smallmatrix}\right) - \frac{253}{180\pi^2}\Gamma_{\text{AS}}^k\left(\begin{smallmatrix} 4 & 0 \\ 5 & 3 \end{smallmatrix}\right) - \frac{1111}{10\pi^2}\Gamma_{\text{AS}}^k\left(\begin{smallmatrix} 4 & 3 \\ 5 & 0 \end{smallmatrix}\right) \\
& - \frac{41}{12\pi^2}\Gamma_{\text{AS}}^k\left(\begin{smallmatrix} 4 & 3 \\ 5 & 2 \end{smallmatrix}\right) + \frac{221}{60\pi^2}\Gamma_{\text{AS}}^k\left(\begin{smallmatrix} 4 & 3 \\ 5 & 3 \end{smallmatrix}\right) + \frac{48}{5\pi^2}\Gamma_{\text{AS}}^k\left(\begin{smallmatrix} 5 & 0 \\ 1 & 1 \end{smallmatrix}\right) \\
& + \frac{519}{40\pi^2}\Gamma_{\text{AS}}^k\left(\begin{smallmatrix} 5 & 0 \\ 1 & 3 \end{smallmatrix}\right) - \frac{77}{2\pi^2}\Gamma_{\text{AS}}^k\left(\begin{smallmatrix} 5 & 3 \\ 1 & 3 \end{smallmatrix}\right) + \frac{70}{\pi^2}\Gamma_{\text{AS}}^k\left(\begin{smallmatrix} 5 & 4 \\ 1 & 0 \end{smallmatrix}\right) \\
& + \frac{168}{5\pi^2}\Gamma_{\text{AS}}^k\left(\begin{smallmatrix} 5 & 5 \\ 1 & 0 \end{smallmatrix}\right) - \frac{1045553}{720\pi^2}\Gamma_{\text{AS}}^k\left(\begin{smallmatrix} 5 & 0 \\ 2 & 2 \end{smallmatrix}\right) + \frac{231407}{270\pi^2}\Gamma_{\text{AS}}^k\left(\begin{smallmatrix} 5 & 0 \\ 2 & 3 \end{smallmatrix}\right) \\
& + \frac{1127}{60\pi^2}\Gamma_{\text{AS}}^k\left(\begin{smallmatrix} 5 & 3 \\ 2 & 0 \end{smallmatrix}\right) + \frac{518}{5\pi^2}\Gamma_{\text{AS}}^k\left(\begin{smallmatrix} 5 & 3 \\ 2 & 3 \end{smallmatrix}\right) + \frac{2069}{40\pi^2}\Gamma_{\text{AS}}^k\left(\begin{smallmatrix} 5 & 0 \\ 3 & 3 \end{smallmatrix}\right) \\
& - \frac{9379}{360\pi^2}\Gamma_{\text{AS}}^k\left(\begin{smallmatrix} 5 & 3 \\ 3 & 0 \end{smallmatrix}\right) - \frac{126}{5\pi^2}\Gamma_{\text{AS}}^k\left(\begin{smallmatrix} 5 & 4 \\ 3 & 0 \end{smallmatrix}\right) + \frac{126}{5\pi^2}\Gamma_{\text{AS}}^k\left(\begin{smallmatrix} 5 & 5 \\ 3 & 0 \end{smallmatrix}\right) \\
& - \frac{21637}{160\pi^2}\Gamma_{\text{AS}}^k\left(\begin{smallmatrix} 5 & 0 \\ 4 & 1 \end{smallmatrix}\right) - \frac{1579}{160\pi^2}\Gamma_{\text{AS}}^k\left(\begin{smallmatrix} 5 & 0 \\ 4 & 5 \end{smallmatrix}\right) + \frac{518}{5\pi^2}\Gamma_{\text{AS}}^k\left(\begin{smallmatrix} 5 & 1 \\ 4 & 1 \end{smallmatrix}\right)
\end{aligned}$$

$$\begin{aligned}
& + \frac{223}{10\pi^2} \Gamma_{\text{AS}}^k \left(\begin{smallmatrix} 5 & 3 \\ 4 & 0 \end{smallmatrix} \right) + \frac{24}{5\pi^2} \Gamma_{\text{AS}}^k \left(\begin{smallmatrix} 5 & 4 \\ 4 & 0 \end{smallmatrix} \right) + \frac{14}{5\pi^2} \Gamma_{\text{AS}}^k \left(\begin{smallmatrix} 5 & 4 \\ 4 & 5 \end{smallmatrix} \right) \\
& - \frac{208783}{144\pi^2} \Gamma_{\text{AS}}^k \left(\begin{smallmatrix} 5 & 0 \\ 5 & 1 \end{smallmatrix} \right) + \frac{1078601}{2160\pi^2} \Gamma_{\text{AS}}^k \left(\begin{smallmatrix} 5 & 0 \\ 5 & 3 \end{smallmatrix} \right) - \frac{141}{10\pi^2} \Gamma_{\text{AS}}^k \left(\begin{smallmatrix} 5 & 0 \\ 5 & 5 \end{smallmatrix} \right) \\
& - \frac{37841}{2700\pi^2} \Gamma_{\text{AS}}^k \left(\begin{smallmatrix} 5 & 2 \\ 5 & 0 \end{smallmatrix} \right) + \frac{321817}{2700\pi^2} \Gamma_{\text{AS}}^k \left(\begin{smallmatrix} 5 & 3 \\ 5 & 0 \end{smallmatrix} \right) - \frac{136121}{2700\pi^2} \Gamma_{\text{AS}}^k \left(\begin{smallmatrix} 5 & 4 \\ 5 & 0 \end{smallmatrix} \right) \\
& + \frac{12277}{300\pi^2} \Gamma_{\text{AS}}^k \left(\begin{smallmatrix} 5 & 5 \\ 5 & 0 \end{smallmatrix} \right)
\end{aligned}$$

where Γ_{AS}^k are antisymmetric combinations

$$\Gamma_{\text{AS}}^k \left(\begin{smallmatrix} r_1, r_2 \\ s_1, s_2 \end{smallmatrix} \right) = \tilde{\Gamma} \left(\underbrace{\begin{smallmatrix} 0 & \dots & 0 & k \\ 0 & \dots & 0 & z_1 \end{smallmatrix}}_{(3-k)\text{-times}}; z_2, \tau \right) - \tilde{\Gamma} \left(\underbrace{\begin{smallmatrix} 0 & \dots & 0 & k \\ 0 & \dots & 0 & -z_1 \end{smallmatrix}}_{(3-k)\text{-times}}; z_2, \tau \right) \quad (\text{H.2})$$

with $z_i = r_i/6 + \tau s_i/6$, and where the prefactors C_k are given by

$$C_1 = 12\pi^2 \qquad C_2 = 6\pi \qquad C_3 = 1. \quad (\text{H.3})$$

Bibliography

- [1] Vittorio Del Duca, Stefan Druc, James Drummond, Claude Duhr, Falko Dulat, Robin Marzucca, Georgios Papathanasiou, and Bram Verbeek, “Multi-Regge kinematics and the moduli space of Riemann spheres with marked points”, *JHEP*, vol. 08, pp. 152, 2016.
- [2] Vittorio Del Duca, Claude Duhr, Robin Marzucca, and Bram Verbeek, “The analytic structure and the transcendental weight of the BFKL ladder at NLL accuracy”, *arXiv.org*, May 2017.
- [3] Vittorio Del Duca, Stefan Druc, James Drummond, Claude Duhr, Falko Dulat, Robin Marzucca, Georgios Papathanasiou, and Bram Verbeek, “The seven-gluon amplitude in multi-Regge kinematics beyond leading logarithmic accuracy”, *JHEP*, vol. 06, pp. 116, 2018.
- [4] Robin Marzucca and Bram Verbeek, “The Multi-Regge Limit of the Eight-Particle Amplitude Beyond Leading Logarithmic Accuracy”, 2018.
- [5] Johannes Broedel, Claude Duhr, Falko Dulat, Robin Marzucca, Brenda Penante, and Lorenzo Tancredi, “An analytic solution for the equal-mass banana graph”, 2019.
- [6] Vittorio Del Duca, Stefan Druc, James M Drummond, Claude Duhr, Falko Dulat, Robin Marzucca, Georgios Papathanasiou, and Bram Verbeek, “In Preparation”.
- [7] Vittorio Del Duca, Stefan Druc, James Drummond, Claude Duhr, Falko Dulat, Robin Marzucca, Georgios Papathanasiou, and Bram Verbeek, “Multi-Loop Amplitudes in the High-Energy Limit in $N = 4$ SYM”, *PoS*, vol. LL2018, pp. 026, 2018.

-
- [8] Vittorio Del Duca, Stefan Druc, James Drummond, Claude Duhr, Falko Dulat, Robin Marzucca, Georgios Papathanasiou, and Bram Verbeek, “Amplitudes in the Multi-Regge Limit of $\mathcal{N}=4$ SYM”, in *Diffraction and Low-x 2018 (Diffflowx2018) Reggio Calabria, Italy, August 26-September 1, 2018*, 2018.
- [9] Niklas Beisert, Aleksander Garus, and Matteo Rosso, “Yangian Symmetry and Integrability of Planar $\mathcal{N}=4$ Supersymmetric Yang-Mills Theory”, *Phys. Rev. Lett.*, vol. 118, no. 14, pp. 141603, 2017.
- [10] Marcus T. Grisaru, Martin Rocek, and Warren Siegel, “Zero Three Loop beta Function in $\mathcal{N}=4$ Superyang-Mills Theory”, *Phys. Rev. Lett.*, vol. 45, pp. 1063–1066, 1980.
- [11] Paul S. Howe, K. S. Stelle, and P. K. Townsend, “The Relaxed Hypermultiplet: An Unconstrained $\mathcal{N}=2$ Superfield Theory”, *Nucl. Phys.*, vol. B214, pp. 519–531, 1983.
- [12] Stanley Mandelstam, “Light Cone Superspace and the Ultraviolet Finiteness of the $\mathcal{N}=4$ Model”, *Nucl. Phys.*, vol. B213, pp. 149–168, 1983.
- [13] Gerard 't Hooft and M. J. G. Veltman, “Scalar One Loop Integrals”, *Nucl. Phys.*, vol. B153, pp. 365–401, 1979.
- [14] J. M. Drummond, J. Henn, V. A. Smirnov, and E. Sokatchev, “Magic identities for conformal four-point integrals”, *JHEP*, vol. 01, pp. 064, 2007.
- [15] Zvi Bern, Michael Czakon, Lance J. Dixon, David A. Kosower, and Vladimir A. Smirnov, “The Four-Loop Planar Amplitude and Cusp Anomalous Dimension in Maximally Supersymmetric Yang-Mills Theory”, *Phys. Rev.*, vol. D75, pp. 085010, 2007.
- [16] Z. Bern, J. J. M. Carrasco, Henrik Johansson, and D. A. Kosower, “Maximally supersymmetric planar Yang-Mills amplitudes at five loops”, *Phys. Rev.*, vol. D76, pp. 125020, 2007.
- [17] Luis F. Alday and Juan Martin Maldacena, “Gluon scattering amplitudes at strong coupling”, *JHEP*, vol. 06, pp. 064, 2007.
- [18] J. M. Drummond, G. P. Korchemsky, and E. Sokatchev, “Conformal properties of four-gluon planar amplitudes and Wilson loops”, *Nucl. Phys.*, vol. B795, pp. 385–408, 2008.

-
- [19] Andreas Brandhuber, Paul Heslop, and Gabriele Travaglini, “MHV amplitudes in N=4 super Yang-Mills and Wilson loops”, *Nucl. Phys.*, vol. B794, pp. 231–243, 2008.
- [20] C. Anastasiou, Z. Bern, Lance J. Dixon, and D. A. Kosower, “Planar amplitudes in maximally supersymmetric Yang-Mills theory”, *Phys. Rev. Lett.*, vol. 91, pp. 251602, 2003.
- [21] Zvi Bern, Lance J. Dixon, and Vladimir A. Smirnov, “Iteration of planar amplitudes in maximally supersymmetric Yang-Mills theory at three loops and beyond”, *Phys. Rev.*, vol. D72, pp. 085001, 2005.
- [22] J. Bartels, V. Schomerus, and M. Sprenger, “Multi-Regge Limit of the n-Gluon Bubble Ansatz”, *JHEP*, vol. 11, pp. 145, 2012.
- [23] J. Bartels, V. Schomerus, and M. Sprenger, “The Bethe roots of Regge cuts in strongly coupled $\mathcal{N} = 4$ SYM theory”, *JHEP*, vol. 07, pp. 098, 2015.
- [24] Andrew Hodges, “Eliminating spurious poles from gauge-theoretic amplitudes”, *JHEP*, vol. 05, pp. 135, 2013.
- [25] John Golden, Alexander B. Goncharov, Marcus Spradlin, Cristian Vergu, and Anastasia Volovich, “Motivic Amplitudes and Cluster Coordinates”, *JHEP*, vol. 01, pp. 091, 2014.
- [26] S. Fomin and A. Zelevinsky, “Cluster algebras. i: Foundations”, *J. Am. Math. Soc.*, vol. 15, no. 2, pp. 497–529, 2002.
- [27] S. Fomin and A. Zelevinsky, “Cluster algebras. ii: Finite type classification”, *Invent. Math.*, vol. 154, no. 1, pp. 63–121, 2003.
- [28] J. S. Scott, “Grassmannians and cluster algebras”, *Adv. in Appl. Math.*, vol. 28, no. 2, pp. 119–144, 2002.
- [29] M. Gekhtman, M. Shapiro, and A. Vainshtein, “Cluster algebras and poisson geometry”, *Mosc. Math. J.*, vol. 3, no. 3, pp. 899–934, 2003.
- [30] B. Keller, “Cluster algebras, quiver representations and triangulated categories”, in *Triangulated Categories*. Cambridge University Press, 2003.
- [31] J. A. M. Vermaseren, “Harmonic sums, Mellin transforms and integrals”, *Int. J. Mod. Phys.*, vol. A14, pp. 2037–2076, 1999.
- [32] T. Gehrmann and E. Remiddi, “Two loop master integrals for gamma* —j 3 jets: The Planar topologies”, *Nucl. Phys.*, vol. B601, pp. 248–286, 2001.

-
- [33] Lance J. Dixon, Claude Duhr, and Jeffrey Pennington, “Single-valued harmonic polylogarithms and the multi-Regge limit”, *JHEP*, vol. 1210, pp. 074, 2012.
- [34] Simon Caron-Huot, Lance J. Dixon, Falko Dulat, Matt von Hippel, Andrew J. McLeod, and Georgios Papathanasiou, “Six-Gluon Amplitudes in Planar $\mathcal{N} = 4$ Super-Yang-Mills Theory at Six and Seven Loops”, *Submitted to: J. High Energy Phys.*, 2019.
- [35] Spencer Bloch and Pierre Vanhove, “The elliptic dilogarithm for the sunset graph”, *J. Number Theor.*, vol. 148, pp. 328–364, 2015.
- [36] Luise Adams, Christian Bogner, and Stefan Weinzierl, “The two-loop sunrise graph in two space-time dimensions with arbitrary masses in terms of elliptic dilogarithms”, *J. Math. Phys.*, vol. 55, no. 10, pp. 102301, 2014.
- [37] Ettore Remiddi and Lorenzo Tancredi, “An Elliptic Generalization of Multiple Polylogarithms”, *Nucl. Phys.*, vol. B925, pp. 212–251, 2017.
- [38] Johannes Broedel, Claude Duhr, Falko Dulat, Brenda Penante, and Lorenzo Tancredi, “Elliptic Feynman integrals and pure functions”, *JHEP*, vol. 01, pp. 023, 2019.
- [39] Jacob L. Bourjaily, Yang-Hui He, Andrew J. McLeod, Matt Von Hippel, and Matthias Wilhelm, “Traintracks through Calabi-Yau Manifolds: Scattering Amplitudes beyond Elliptic Polylogarithms”, *Phys. Rev. Lett.*, vol. 121, no. 7, pp. 071603, 2018.
- [40] Alexander B. Goncharov, “Multiple polylogarithms, cyclotomy and modular complexes”, *Math. Res. Lett.*, vol. 5, pp. 497–516, 1998.
- [41] A. B. Goncharov, “Multiple polylogarithms and mixed Tate motives”, , 2001.
- [42] Francis Brown and Andrey Levin, “Multiple Elliptic Polylogarithms”, 2011.
- [43] Johannes Broedel, Claude Duhr, Falko Dulat, and Lorenzo Tancredi, “Elliptic polylogarithms and iterated integrals on elliptic curves. Part I: general formalism”, *JHEP*, vol. 05, pp. 093, 2018.
- [44] Yuri I. Manin, “Iterated integrals of modular forms and noncommutative modular symbols”, *Progr. Math.*, vol. 253, pp. 565–597, 2005.

-
- [45] Luise Adams and Stefan Weinzierl, “Feynman integrals and iterated integrals of modular forms”, *Commun. Num. Theor. Phys.*, vol. 12, pp. 193–251, 2018.
- [46] Jens Vollinga and Stefan Weinzierl, “Numerical evaluation of multiple polylogarithms”, *Comput. Phys. Commun.*, vol. 167, pp. 177, 2005.
- [47] Erik Panzer, “Algorithms for the symbolic integration of hyperlogarithms with applications to Feynman integrals”, *Comput. Phys. Commun.*, vol. 188, pp. 148–166, 2015.
- [48] Erik Panzer, *Feynman integrals and hyperlogarithms*, PhD thesis, Humboldt U., Berlin, Inst. Math., 2015.
- [49] Claude Duhr and Falko Dulat, “PolyLogTools - Polylogs for the masses”, 2019.
- [50] Johannes Broedel, Carlos R. Mafra, Nils Matthes, and Oliver Schlotterer, “Elliptic multiple zeta values and one-loop superstring amplitudes”, *JHEP*, vol. 07, pp. 112, 2015.
- [51] Johannes Broedel, Nils Matthes, and Oliver Schlotterer, “Relations between elliptic multiple zeta values and a special derivation algebra”, *J. Phys.*, vol. A49, no. 15, pp. 155203, 2016.
- [52] Johannes Broedel, Claude Duhr, Falko Dulat, Brenda Penante, and Lorenzo Tancredi, “Elliptic symbol calculus: from elliptic polylogarithms to iterated integrals of Eisenstein series”, *JHEP*, vol. 08, pp. 014, 2018.
- [53] Kuo-Tsai Chen, “Iterated path integrals”, *Bull. Am. Math. Soc.*, vol. 83, pp. 831–879, 1977.
- [54] Claude Duhr, “Mathematical aspects of scattering amplitudes”, in *Theoretical Advanced Study Institute in Elementary Particle Physics: Journeys Through the Precision Frontier: Amplitudes for Colliders (TASI 2014) Boulder, Colorado, June 2-27, 2014*, 2014.
- [55] Francis Brown, “Single-valued periods and multiple zeta values”, , 2013.
- [56] Francis C. S. Brown, “Notes on motivic periods”, , 2015.
- [57] Francis C. S. Brown, “Single-valued multiple polylogarithms in one variable”, *C. R. Acad. Sci. Paris, Ser. I*, vol. 338, pp. 527, 2004.
- [58] Oliver Schnetz, “Numbers and Functions in Quantum Field Theory”, *J. Phys.*, vol. hep-th, 2016.

- [59] Leopold Kronecker, “Zur Theorie der elliptischen Funktionen”, *Mathematische Werke*, vol. IV, pp. 313, 1881.
- [60] Francis Brown, “Notes on Motivic Periods”, *arXiv.org*, 2015.
- [61] Francis Brown, “Multiple modular values and the relative completion of the fundamental group of $\mathcal{M}_{1,1}$ ”, 2014.
- [62] Don Zagier, “Elliptic Modular Forms and Their Applications”, in *The 1-2-3 of Modular Forms*. 2008, Springer.
- [63] E. A. Kuraev, L. N. Lipatov, and Victor S. Fadin, “Multi-Reggeon processes in the Yang-Mills theory”, *Sov. Phys. JETP*, vol. 44, pp. 443, 1976.
- [64] E. A. Kuraev, L. N. Lipatov, and Victor S. Fadin, “The Pomernanchuk singularity in nonabelian gauge theories”, *Sov. Phys. JETP*, vol. 45, pp. 199, 1977.
- [65] I. I. Balitsky and L. N. Lipatov, “The Pomernanchuk singularity in quantum chromodynamics”, *Sov. J. Nucl. Phys.*, vol. 28, pp. 822, 1978.
- [66] Victor S. Fadin and L. N. Lipatov, “BFKL pomeron in the next-to-leading approximation”, *Phys. Lett.*, vol. B429, pp. 127, 1998.
- [67] G. Camici and M. Ciafaloni, “Irreducible part of the next-to-leading BFKL kernel”, *Phys. Lett.*, vol. B412, pp. 396, 1997.
- [68] Marcello Ciafaloni and Gianni Camici, “Energy scale(s) and next-to-leading BFKL equation”, *Phys. Lett.*, vol. B430, pp. 349, 1998.
- [69] J. Bartels, L. N. Lipatov, and Agustin Sabio Vera, “BFKL Pomeron, Reggeized gluons and Bern-Dixon-Smirnov amplitudes”, *Phys. Rev.*, vol. D80, pp. 045002, 2009.
- [70] J. Bartels, L. N. Lipatov, and Agustin Sabio Vera, “N=4 supersymmetric Yang Mills scattering amplitudes at high energies: The Regge cut contribution”, *Eur. Phys. J.*, vol. C65, pp. 587–605, 2010.
- [71] Richard C. Brower, Horatiu Nastase, Howard J. Schnitzer, and Chung-I. Tan, “Implications of multi-Regge limits for the Bern-Dixon-Smirnov conjecture”, *Nucl. Phys.*, vol. B814, pp. 293–326, 2009.
- [72] Richard C. Brower, Horatiu Nastase, Howard J. Schnitzer, and Chung-I Tan, “Analyticity for Multi-Regge Limits of the Bern-Dixon-Smirnov Amplitudes”, *Nucl. Phys.*, vol. B822, pp. 301–347, 2009.

-
- [73] V. Del Duca, C. Duhr, and E. W. N. Glover, “Iterated amplitudes in the high-energy limit”, *JHEP*, vol. 12, pp. 097, 2008.
- [74] J. Bartels, J. Kotanski, and V. Schomerus, “Excited Hexagon Wilson Loops for Strongly Coupled N=4 SYM”, *JHEP*, vol. 01, pp. 096, 2011.
- [75] J. Bartels, J. Kotanski, V. Schomerus, and M. Sprenger, “The Excited Hexagon Reloaded”, , 2013.
- [76] L. N. Lipatov and A. Prygarin, “BFKL approach and six-particle MHV amplitude in N=4 super Yang-Mills”, *Phys. Rev.*, vol. D83, pp. 125001, 2011.
- [77] L. N. Lipatov and A. Prygarin, “Mandelstam cuts and light-like Wilson loops in N=4 SUSY”, *Phys. Rev.*, vol. D83, pp. 045020, 2011.
- [78] Lev Lipatov, Alexander Prygarin, and Howard J. Schnitzer, “The Multi-Regge limit of NMHV Amplitudes in N=4 SYM Theory”, *JHEP*, vol. 01, pp. 068, 2013.
- [79] Lance J. Dixon, James M. Drummond, and Johannes M. Henn, “Bootstrapping the three-loop hexagon”, *JHEP*, vol. 11, pp. 023, 2011.
- [80] Lance J. Dixon, James M. Drummond, Claude Duhr, and Jeffrey Pennington, “The four-loop remainder function and multi-Regge behavior at NNLLA in planar N = 4 super-Yang-Mills theory”, *JHEP*, vol. 06, pp. 116, 2014.
- [81] Jeffrey Pennington, “The six-point remainder function to all loop orders in the multi-Regge limit”, *JHEP*, vol. 1301, pp. 059, 2013.
- [82] Benjamin Basso, Simon Caron-Huot, and Amit Sever, “Adjoint BFKL at finite coupling: a short-cut from the collinear limit”, *JHEP*, vol. 01, pp. 027, 2015.
- [83] J. M. Drummond and G. Papathanasiou, “Hexagon OPE Resummation and Multi-Regge Kinematics”, *JHEP*, vol. 02, pp. 185, 2016.
- [84] Johannes Broedel and Martin Sprenger, “Six-point remainder function in multi-Regge-kinematics: an efficient approach in momentum space”, *JHEP*, vol. 05, pp. 055, 2016.
- [85] Alexander Prygarin, Marcus Spradlin, Cristian Vergu, and Anastasia Volovich, “All Two-Loop MHV Amplitudes in Multi-Regge Kinematics From Applied Symbology”, *Phys. Rev.*, vol. D85, pp. 085019, 2012.

-
- [86] J. Bartels, A. Kormilitzin, L. N. Lipatov, and A. Prygarin, “BFKL approach and $2 \rightarrow 5$ maximally helicity violating amplitude in $\mathcal{N} = 4$ super-Yang-Mills theory”, *Phys. Rev.*, vol. D86, pp. 065026, 2012.
- [87] Till Bargheer, Georgios Papathanasiou, and Volker Schomerus, “The Two-Loop Symbol of all Multi-Regge Regions”, *JHEP*, vol. 05, pp. 012, 2016.
- [88] Francis C.S. Brown, “Multiple zeta values and periods of moduli spaces $\mathcal{M}_{0,n}(\mathbb{R})$ ”, *Annales Sci.Ecole Norm.Sup.*, vol. 42, pp. 371, 2009.
- [89] Jochen Bartels, Andrey Kormilitzin, and Lev Lipatov, “Analytic structure of the $n = 7$ scattering amplitude in $\mathcal{N} = 4$ SYM theory in the multi-Regge kinematics: Conformal Regge pole contribution”, *Phys. Rev.*, vol. D89, no. 6, pp. 065002, 2014.
- [90] Jochen Bartels, Andrey Kormilitzin, and Lev N. Lipatov, “Analytic structure of the $n = 7$ scattering amplitude in $\mathcal{N} = 4$ theory in multi-Regge kinematics: Conformal Regge cut contribution”, *Phys. Rev.*, vol. D91, no. 4, pp. 045005, 2015.
- [91] Niklas Beisert, Burkhard Eden, and Matthias Staudacher, “Transcendentality and Crossing”, *J. Stat. Mech.*, vol. 0701, pp. P01021, 2007.
- [92] E. Remiddi and J.A.M. Vermaseren, “Harmonic polylogarithms”, *Int.J.Mod.Phys.*, vol. A15, pp. 725, 2000.
- [93] Sven Moch, Peter Uwer, and Stefan Weinzierl, “Nested sums, expansion of transcendental functions and multiscale multiloop integrals”, *J. Math. Phys.*, vol. 43, pp. 3363–3386, 2002.
- [94] Stefan Weinzierl, “Symbolic expansion of transcendental functions”, *Comput. Phys. Commun.*, vol. 145, pp. 357–370, 2002.
- [95] S. Moch and P. Uwer, “XSummer: Transcendental functions and symbolic summation in form”, *Comput. Phys. Commun.*, vol. 174, pp. 759–770, 2006.
- [96] Oliver Schnetz, “Graphical functions and single-valued multiple polylogarithms”, *Commun. Num. Theor. Phys.*, vol. 08, pp. 589–675, 2014.
- [97] Oliver Schnetz, “Graphical functions and single-valued multiple polylogarithms”, *arXiv.org*, February 2013.

-
- [98] Nima Arkani-Hamed, Jacob L. Bourjaily, Freddy Cachazo, Alexander B. Goncharov, Alexander Postnikov, and Jaroslav Trnka, *Scattering Amplitudes and the Positive Grassmannian*, Cambridge University Press, 2012.
- [99] Simon Caron-Huot and Kasper J. Larsen, “Uniqueness of two-loop master contours”, *JHEP*, vol. 10, pp. 026, 2012.
- [100] Dhritiman Nandan, Miguel F. Paulos, Marcus Spradlin, and Anastasia Volovich, “Star Integrals, Convolutions and Simplices”, *JHEP*, vol. 05, pp. 105, 2013.
- [101] Victor S Fadin, E A Kuraev, and L N Lipatov, “On the Pomeranchuk Singularity in Asymptotically Free Theories”, *Phys. Lett.*, vol. B60, no. 1, pp. 50–52, 1975.
- [102] Giovanni A Chirilli and Yuri V Kovchegov, “Solution of the NLO BFKL Equation and a Strategy for Solving the All-Order BFKL Equation”, *J. Phys.*, vol. 06, no. 6, pp. 055, 2013.
- [103] Giovanni A Chirilli and Yuri V Kovchegov, “ $\gamma^*\gamma^*$ Cross Section at NLO and Properties of the BFKL Evolution at Higher Orders”, *J. Phys.*, vol. 05, pp. 099, 2014.
- [104] Vittorio Del Duca, Lance J. Dixon, Claude Duhr, and Jeffrey Pennington, “The BFKL equation, Mueller-Navelet jets and single-valued harmonic polylogarithms”, *JHEP*, vol. 02, pp. 086, 2014.
- [105] L N Lipatov, “The Bare Pomeron in Quantum Chromodynamics”, *Sov. Phys. JETP*, vol. 63, pp. 904–912, 1986.
- [106] A V Kotikov and L N Lipatov, “NLO corrections to the BFKL equation in QCD and in supersymmetric gauge theories”, *J. Phys.*, vol. B582, no. 1-3, pp. 19–43, 2000.
- [107] A V Kotikov and L N Lipatov, “DGLAP and BFKL equations in the N=4 supersymmetric gauge theory”, *J. Phys.*, vol. B661, pp. 19–61, 2003.
- [108] Stefan Weinzierl, “Expansion around half-integer values, binomial sums and inverse binomial sums”, *J. Phys.*, vol. 45, pp. 2656–2673, 2004.
- [109] A V Kotikov, L N Lipatov, and V N Velizhanin, “Anomalous dimensions of Wilson operators in N=4 SYM theory”, *J. Phys.*, vol. B557, no. 1-2, pp. 114–120, 2003.

-
- [110] Abhijit Gadde, Elli Pomoni, and Leonardo Rastelli, “The Veneziano Limit of $N = 2$ Superconformal QCD: Towards the String Dual of $N = 2$ $SU(N(c))$ SYM with $N(f) = 2 N(c)$ ”, *J. Phys.*, vol. hep-th, 2009.
- [111] G. Passarino and M. J. G. Veltman, “One Loop Corrections for $e^+ e^-$ Annihilation Into $\mu^+ \mu^-$ in the Weinberg Model”, *Nucl. Phys.*, vol. B160, pp. 151–207, 1979.
- [112] Vladimir A. Smirnov, “Evaluating Feynman integrals”, *Springer Tracts Mod. Phys.*, vol. 211, pp. 1–244, 2004.
- [113] V. A. Smirnov, *Feynman integral calculus*, 2006.
- [114] A. V. Kotikov, “Differential equations method: New technique for massive Feynman diagrams calculation”, *Phys. Lett.*, vol. B254, pp. 158–164, 1991.
- [115] A. V. Kotikov, “Differential equations method: The Calculation of vertex type Feynman diagrams”, *Phys. Lett.*, vol. B259, pp. 314–322, 1991.
- [116] A. V. Kotikov, “Differential equation method: The Calculation of N point Feynman diagrams”, *Phys. Lett.*, vol. B267, pp. 123–127, 1991.
- [117] T. Gehrmann and E. Remiddi, “Differential equations for two loop four point functions”, *Nucl. Phys.*, vol. B580, pp. 485–518, 2000.
- [118] A. Sabry, “Fourth order spectral functions for the electron propagator”, *Nucl. Phys.*, vol. 33, no. 17, pp. 401–430, 1962.
- [119] David J. Broadhurst, “The Master Two Loop Diagram With Masses”, *Z. Phys.*, vol. C47, pp. 115–124, 1990.
- [120] S. Laporta and E. Remiddi, “Analytic treatment of the two loop equal mass sunrise graph”, *Nucl. Phys.*, vol. B704, pp. 349–386, 2005.
- [121] Ettore Remiddi and Lorenzo Tancredi, “Schouten identities for Feynman graph amplitudes; The Master Integrals for the two-loop massive sunrise graph”, *Nucl. Phys.*, vol. B880, pp. 343–377, 2014.
- [122] Ettore Remiddi and Lorenzo Tancredi, “Differential equations and dispersion relations for Feynman amplitudes. The two-loop massive sunrise and the kite integral”, *Nucl. Phys.*, vol. B907, pp. 400–444, 2016.
- [123] Luise Adams, Christian Bogner, and Stefan Weinzierl, “The iterated structure of the all-order result for the two-loop sunrise integral”, *J. Math. Phys.*, vol. 57, no. 3, pp. 032304, 2016.

- [124] Luise Adams, Christian Bogner, and Stefan Weinzierl, “The two-loop sunrise graph with arbitrary masses”, *J.Math.Phys.*, vol. 54, pp. 052303, 2013.
- [125] Luise Adams, Christian Bogner, and Stefan Weinzierl, “The two-loop sunrise integral around four space-time dimensions and generalisations of the Clausen and Glaisher functions towards the elliptic case”, *J. Math. Phys.*, vol. 56, no. 7, pp. 072303, 2015.
- [126] Johannes Broedel, Claude Duhr, Falko Dulat, and Lorenzo Tancredi, “Elliptic polylogarithms and iterated integrals on elliptic curves II: an application to the sunrise integral”, 2017.
- [127] R. S. Maier, “On Rationally Parametrized Modular Equations”, *ArXiv Mathematics e-prints*, November 2006.
- [128] Johannes Broedel, Claude Duhr, Falko Dulat, Brenda Penante, and Lorenzo Tancredi, “From modular forms to differential equations for Feynman integrals”, in *KMPB Conference: Elliptic Integrals, Elliptic Functions and Modular Forms in Quantum Field Theory Zeuthen, Germany, October 23-26, 2017*, 2018.
- [129] O. V. Tarasov, “Connection between Feynman integrals having different values of the space-time dimension”, *Phys. Rev.*, vol. D54, pp. 6479–6490, 1996.
- [130] Vladimir A. Smirnov and O. L. Veretin, “Analytical results for dimensionally regularized massless on-shell double boxes with arbitrary indices and numerators”, *Nucl. Phys.*, vol. B566, pp. 469–485, 2000.
- [131] C. Anastasiou, E. W. Nigel Glover, and C. Oleari, “The two-loop scalar and tensor pentabox graph with light-like legs”, *Nucl. Phys.*, vol. B575, pp. 416–436, 2000, [Erratum: *Nucl. Phys.*B585,763(2000)].
- [132] C. Anastasiou, T. Gehrmann, C. Oleari, E. Remiddi, and J. B. Tausk, “The Tensor reduction and master integrals of the two loop massless crossed box with lightlike legs”, *Nucl. Phys.*, vol. B580, pp. 577–601, 2000.
- [133] C. Anastasiou, J. B. Tausk, and M. E. Tejeda-Yeomans, “The On-shell massless planar double box diagram with an irreducible numerator”, *Nucl. Phys. Proc. Suppl.*, vol. 89, pp. 262–267, 2000.
- [134] R. N. Lee, “Space-time dimensionality D as complex variable: Calculating loop integrals using dimensional recurrence relation and analytical properties with respect to D ”, *Nucl. Phys.*, vol. B830, pp. 474–492, 2010.

-
- [135] Amedeo Primo and Lorenzo Tancredi, “Maximal cuts and differential equations for Feynman integrals. An application to the three-loop massive banana graph”, *Nucl. Phys.*, vol. B921, pp. 316–356, 2017.
- [136] Spencer Bloch, Matt Kerr, and Pierre Vanhove, “A Feynman integral via higher normal functions”, *Compos. Math.*, vol. 151, pp. 2329–2375, 2015.
- [137] G. Joyce, “On the simple cubic lattice Green function”, *Transactions of the Royal Society of London, Mathematical and Physical Sciences*, vol. 1973, pp. 583–610, 273.
- [138] Luise Adams, Christian Bogner, and Stefan Weinzierl, “The two-loop sunrise graph with arbitrary masses”, *J. Math. Phys.*, vol. 54, pp. 052303, 2013.
- [139] Davide Gaiotto, Juan Maldacena, Amit Sever, and Pedro Vieira, “Pulling the straps of polygons”, *JHEP*, vol. 12, pp. 011, 2011.
- [140] Simon Caron-Huot, “When does the gluon reggeize?”, *JHEP*, vol. 05, pp. 093, 2015.